NASA CR- 152,391
v. 4

3 1176 00161 6755

NASA CR-152391

NASA-CR-152391-VOL-4
19810014500

ANALYSIS OF WIND TUNNEL TEST RESULTS FOR A 9.39-PER CENT SCALE MODEL OF A VSTOL FIGHTER/ATTACK AIRCRAFT

VOLUME IV - RALS R104 AERODYNAMIC CHARACTERISTICS AND COMPARISONS WITH E205 CONFIGURATION AERODYNAMIC CHARACTERISTICS

DR. J. R. LUMMUS
G. T. JOYCE
C. D. O'MALLEY

Prepared under Contract NAS2-10344
by
General Dynamics
Fort Worth Division
for
Ames Research Center

NATIONAL AERONAUTICS AND SPACE ADMINISTRATION

1. Report No.
NASA CR-152391

2. Government Accession No.

3. Recipient's Catalog No.

4. Title and Subtitle
Analysis of Wind Tunnel Test Results for a 9.39-percent Scale Model of a VSTOL Fighter/Attack Aircraft

5. Report Date
October, 1980

6. Performing Organization Code

7. Author(s)
Dr. J. R. Lummus, G. T. Joyce, C. D. O'Malley

8. Performing Organization Report No.

9. Performing Organization Name and Address
General Dynamics/Fort Worth Division
P. O. Box 748
Fort Worth, Texas 76101

10. Work Unit No.

11. Contract or Grant No.
NAS2-10344

12. Sponsoring Agency Name and Address
NASA, AMES Research Center,
Moffett Field, Ca 94035

13. Type of Report and Period Covered
Contractor Final Report
Sept. 10, 1979-Feb. 10, 1981

14. Sponsoring Agency Code

15. Supplementary Notes
AMES Research Center Technical Monitor W. P. Nelms
(415) 965-5880

16. Abstract

The results of a series of NASA AMES wind tunnel tests of a General Dynamics vectored-engine-over wing, Navy VSTOL fighter/attack configuration have been analyzed to (1) assess prediction method capabilities, (2) evaluate geometry variations such as multiple canard longitudinal locations and strake shapes, and (3) evaluate the effects of configuration changes associated with varying the propulsive lift system from a jet-diffuser ejector to a Remote Augmentation Lift System (RALS). Configuration modification and additional testing and analysis are recommended to adequately evaluate the configuration potential.

This document is presented in four volumes - Volume I - Study Overview, Volume II - Evaluation of Prediction Methodologies, Volume III - Effects of Configuration Variations from Baseline E205 Configuration on Aerodynamic Characteristics, and Volume IV - RALS R104 Aerodynamic Characteristics and Comparisons with E205 Configuration Aerodynamic Characteristics.

17. Key Words (Suggested by Author(s))
CANARD, STRAKE, AERODYNAMIC
PREDICTION METHODS

18. Distribution Statement

19. Security Classif. (of this report)
UNCLASSIFIED

20. Security Classif. (of this page)
UNCLASSIFIED

21. No. of Pages

22. Price*

N81-23033 #

VOLUME IV - RALS R104 AERODYANMIC
CHARACTERISTICS AND COMPARISONS WITH
E205 CONFIGURATION AERODYNAMIC CHARACTERISTICS

TABLE OF CONTENTS

LIST OF FIGURES

LIST OF FIGURES (CONT'D.)

LIST OF FIGURES (CONT'D.)

LIST OF FIGURES (CONT'D.)

LIST OF FIGURES (CONT'D.)

LIST OF FIGURES (CONT'D.)

LIST OF FIGURES (CONT'D.)

LIST OF FIGURES (CONT'D.)

LIST OF FIGURES (CONT'D.)

LIST OF FIGURES (CONT'D.)

LIST OF FIGURES (CONT'D.)

LIST OF FIGURES (CONT'D.)

LIST OF FIGURES (CONT'D.)

LIST OF FIGURES (CONT'D.)

LIST OF SYMBOLS

a. English Symbols

A	axial force, lb (N)
a.c.	aerodynamic center, %$\bar{c}$
AR	aspect ratio
b	span, in. (m)
$\bar{c}$, MAC	mean aerodynamic chord, in. (m)
C_A	axial force coefficient
$C_{A_{ejector}}$	axial force coefficient due to ejector
C_D	drag coefficient
$C_{D_{AERO}}$	aero-only drag coefficient (no thrust increments included)
$C_{D_{min}}$	minimum drag coefficient
C_{D_E}	equivalent drag coefficient
$C_{D_{RAM}}$	ram-drag coefficient (engine inlet)
C_{D_t}	total drag coefficient
C_L	lift coefficient
$C_{L_{buffet}}$	buffet-onset lift coefficient
C_{L_E}	equivalent lift coefficient
$C_{L_{max}}$	maximum lift coefficient
$C_{L_{aero}}$	aero-only lift coefficient (no thrust increments included)
C_{L_t}	total lift coefficient
C_l	rolling moment coefficient

C_{l_β}	rolling moment derivative due to sideslip, 1/deg
C_{m_E}	equivalent pitching moment coefficient
$C_{m_{x_{\bar{c}}}}$	pitching moment coefficient about x percent $\bar{c}$
C_{m_o}	zero lift pitching moment coefficient
C_{m_t}	total pitching moment coefficient
C_N	normal force coefficient
C_n	yawing moment coefficient
C_{n_β}	yawing moment derivative due to sideslip, 1/deg
C_T	thrust coefficient, $\frac{T}{qS_{REF}}$
C_Y	side force coefficient
C_{Y_β}	side force derivative due to sideslip, 1/deg
CMU, C	ideal thrust coefficient, $\dot{w}\ Vj/gqS_{REF}$
D	drag, lb(N)
e	span efficiency factor
ESF	engine scale factor, $\frac{T}{T_{ESF = 1.0}}$
IGE	in ground effect
L	lift, lb(N)
L_Γ	lift due to supercirculation, lb(N)
l	rolling moment, ft lb (Nm)
M	Mach number
m	pitching moment, ft lb(Nm)
NPR	nozzle pressure ratio, $\frac{\text{Total Pressure}}{P}$

LIST OF SYMBOLS (Continued)

N	normal force, lb(kg)
n	yawing moment, ft lb (Nm)
OGE	out of ground effect
P	freestream static pressure, lb/ft^2 $(\frac{N}{m^2})$
P_o	freestream total pressure, lb/ft^2, $(\frac{N}{m^2})$
q	freestream dynamic pressure, lb/ft^2 $(\frac{N}{m^2})$
S_C	canard exposed area, ft^2 (m^2)
S_{ref}	reference area, $ft^2 (m^2)$ (usually equal to S_W)
STOL	short takeoff or landing
S_W	area of trapezoidal wing extended to centerline, $ft^2 (m^2)$
S_{V_T}	exposed area of vertical tail, $ft^2 (m^2)$
T	thrust, lb(N)
V_∞	freestream velocity, ft/sec, knots (m/sec)
V_j	jet velocity based on isentropic expansion from nozzle camber total pressure to freestream static pressure, ft/sec (m/sec)
VSTOL	vertical or short takeoff or landing
VTOL	vertical takeoff or landing
VEO-Wing	vectored engine over wing
$\dot{w}$	weight flow, lb/sec (kg/sec)
X_{cp}	action point of circulation lift relative to leading edge of MAC

LIST OF SYMBOLS (Continued)

b. Greek Symbols

α	alpha	angle of attack, deg
β,	beta	angle of sideslip, deg
Γ		supercirculation
γ		flight path angle, deg
δ_C, δ_i		canard deflection (positive, leading-edge up), deg
δ_{TF}, δ_F		VEO-Wing nozzle and outboard flaperon deflection, deg; except for aileron action the flaperons and VEO-Wing nozzle flaps always deflect together.
θ		pitch attitude angle, deg
θ_J		jet thrust deflection out of VEO-Wing nozzles when deflected, $_{TE}$, deg
Λ_{LE}		leading-edge sweep angle, deg
λ		taper ratio, $\frac{\text{tip chord}}{\text{root chord}}$
ϕ		ejector measured thrust/isentropic supply thrust (where isentropic supply thrust is the thrust which would be obtained from supplied air at the nozzle exit of pressures and flow rates expanded at isentropically to ambient pressure)

LIST OF SYMBOLS (Continued)

c. Model Symbols

B_1	VSTOL ejector configuration E-205 basic fuselage with fuselage strake that blends the fuselage to the inboard section to the wing.
B_2	VSTOL RALS configuration R-104 basic fuselage
C_1	All moveable nacelle-mounted horizontal canard of VSTOL ejector configuration E-205 in the mid-location
C_2	Horizontal canard in VSTOL E-205 or RALS R104 fwd-location
C_3	Horizontal canard in VSTOL E-205 or RALS R104 aft-location
N	VSTOL ejector configuration E-205 or RALS R104 VEO-wing nacelle
S_1	Baseline strake on E205 configuration
S_2	High sweep strake on E205 configuration
S_3	Low sweep strake on E205 configuration
V	All moveable vertical tail of VSTOL ejector configuration E-205 or RALS R104
W_1	VSTOL ejector configuration E-205 wing with linear elements between SS 96.496 and SS 223.695
W_2	VSTOL RALS configuration R-104 wing with linear elements between SS 87.231 and SS 214.430

SUMMARY

The longitudinal and lateral-directional aerodynamic characteristics of the RALS R104 wind tunnel model are summarized in this volume along with comparisons for the E205 configuration.

The RALS R104 wind tunnel model is really a "representation" of the RALS R104 airplane configuration. The RALS R104 wind tunnel model affords the opportunity to examine the effects of changing the nacelle spacing (by reducing the strake area between nacelles as well as the fuselage cross sectional area distribution aft of the nose and canopy), i.e., both planform and cross sectional area changes, while maintaining the same exposed lifting surfaces as the E205 configuration. In fact, as noted in Volume I, the E205 wings, canard, vertical tail, nose, canopy and nacelles are used in conjunction with the new fuselage section aft of the E205 nose-and-canopy section to simulate the RALS airplane configuration.

The trends observed in the aerodynamic characteristics from the component buildup of the R104 configuration model were found to be very similar to those indicated for the E205 configuration. However, in general, the E205 configuration performed somewhat better than the R104 model. The wider, flat strake arrangement of the E205 configuration acts as a more effective lifting surface inducing a substantially higher upwash on the E205 canard and wing which in turn results in the E205 wing and canard each performing better alone (and in the presence of each other) than with the narrow strake arrangement on the R104. This improved canard/wing performance coupled with the lower transonic and supersonic minimum drag of the E205 configuration (resulting from a lower maximum fuselage cross-sectional area) results better trimmed drag polars for the E205 configuration at most flight conditions.

The lateral-directional characteristics of the two configurations were also found to be very similar at most flight conditions.

Both configurations were found to suffer from the same primary deficiency - the inability to trim to α's > 8° at low speeds, power-off. Part of the problem stems from early wing stall because no leading edge protection was afforded during the current testing which should be alleviated with future testing.

1.0 RALS R104 AERODYNAMIC CHARACTERISTICS

1.1 Component Buildup

Figures 1-1 through 1-14 provide the lift, drag, and pitching moment characteristics for the component buildup of the R104 configuration for Mach numbers from .2 to 2.0. This is a very valuable data base because (1) it is very complete and should become an excellent test-case-package for future computational prediction methods, and (2) it provides some insight into the mutual interference of the components, especially the wing and canard.

Figure 1-1 compares the component-buildup variation of minimum drag with Mach number for the R104 configuration. Its The biggest increment in minimum drag is produced by the wing followed by the canard.

Lift, drag, and pitching moment increments for various components have been plotted as a function of angle of attack for Mach numbers from .6 to 1.2 and are compared in Section 2.1 with those of the E205 configuration in Figures 2-1 through 2-11.

The mutual interference effects of the canard and the wing are of primary interest for this type of configuration. The interference effects of the canard on the wing and vice-versa can be observed from the incremental (1) wing-alone data, (2) wing in the presence of the canard, and (3) the canard-alone data. Subsonically, the canard is theoretically supposed to be in an upwash field produced by the wing which has the effect of increasing the local angle of attack of the canard (relative to canard-alone) and increasing the magnitude of the local velocity vector, thereby increasing the canard lift and drag. Supersonically the canard is unaffected by the wing since disturbances are propogated only downstream and not upstream as in subsonic flow. At all speeds, the canard induces a downwash field on the wing inboard of the canard span resulting in a reduced local wing angle of attack on this inboard section and a reduction in the magnitude of the local velocity vector thereby reducing the lift and drag over this portion of the wing. Outboard of the canard span, the tip vortex from the canard produces an upwash on the wing resulting in a higher alpha and local velocity.

Enough experimental data is available to confirm the expected effects of the canard on the wing; unfortunately this is not the case for the influence of the wing on the canard.

While the canard and wing alone each exhibit the expected lift slopes and aerodynamic centers, the wing in the presence of the canard exhibits less lift and a forward aerodynamic center shift produced by the net detrimental effect of the canard on the wing. The forward a.c. shift is a result of this reduced lift on the wing (and probably increased lift on the canard). This effect is noted in both the lift, drag, and moment curves as well as the increment plots at all Mach numbers and for alphas up to 15° (at larger alphas (> 15°) the interference pattern is less clear).

Figures 2-1 through 2-10 allow a comparison of the R104 increments due to the canard alone (no wing) with what appears to be the increment due to the canard in the presence of the wing. However, the latter increment is somewhat deceiving because it is really the increment due to the canard in the presence of the wing <u>plus</u> the incremental effect of the canard on the wing, i.e., the increment is the net sum of the increased lift on the canard due to the wing plus the loss on the wing caused by the canard. Thus a canard balance is required to isolate the canard increments in the presence of the wing as this piece of the mutual interference is not available from the present data. (Note that these increments for R104 are presented in Section 2.0 to avoid duplication in data presentation.)

1.2 Aerodynamic Center

The aerodynamic center variation with Mach number for the baseline R104 configuration model is presented in Figure 1-15 . This variation is similar to that observed with the E205 configuration as shown in Section 2.0. The addition of the canard to the baseline R104 wing body shifts the a.c. forward approximately 20 percent subsonically and approximately 5 percent at supersonic speeds.

1.3 Canard Effectiveness

Figures 1-16 through 1-30 illustrate the effects of R104 canard deflection on lift, drag, and pitching moment for various canard longitudinal locations, wing trailing edge flap deflections and Mach number ranging from .2 to 2.0.

The canard effectiveness observed for the R104 configuration is basically the same as that discussed for the E205 configuration in Volume III. The moment produced by the canard deflection deteriorates rapidly at the subsonic and transonic Mach numbers for negative canard deflections for alpha > 20° with and without the flaps deflected; however with higher flap deflections (25°) and Mach = .9, the alpha for flap-moment deterioration is reduced to from 12° to 16°. Supersonically the canard moment does not deteriorate with alpha. Subsonically, a large part of whatever moment is being produced at high alphas by the canard is probably from the drag vectors from the canard.

Figures 1-31 through 1-37 illustrate the effects of varying the longitudinal canard location relative to the baseline location at Mach numbers from .2 to 1.2. The effects of canard longitudinal movement are about the same as observed for the E205 configuration. The primary effects of canard location are the change in the moment increment produced by the canard and the change in a.c. The forward canard movement causes a more positive canard moment increment and a more forward a.c. as expected. However the $\left|\frac{\Delta a.c.}{LT/\bar{c}}\right|$ for forward or aft canard movement from the baseline mid position is approximately constant. In general, the mid location produces larger lift increments and

less drag than either the fore or aft positions but the real test of which canard position is best for a given Mach number and c.g. can best be determined by examining the trimmed polars for each canard position as shown in Section 1.6.

Figures 1-38 through 1-43 illustrate the variation in lift, drag, and pitching moment increments between the canard on and the canard off (in the presence of the wing) for Mach numbers from .6 to 2.0. These increments include the loads and moments on the canard plus the influence of the canard on the wing (as noted in the previous section, a separate canard balance is required to isolate the canard loads and moments in the presence of the wing). As the canard deflection is varied from positive to a negative deflection, the detrimental downwash on the wing is apparently reduced at M = .6 and .9 because the lift and moment increments continue to increase at high alphas as δ_C becomes more negative. Supersonically, the incremental lift and moment variations are much more linear because the wing does not influence the canard supersonically.

1.4 Wing Trailing Edge Flap Effectiveness

The wing trailing edge flap effectiveness for the R104 configuration was determined by examining the lift, drag, and pitching moment curves of Figures 1-44 through 1-55 for Mach numbers from .6 to 2.0; these curves represent variations in canard and flap deflections. The lift, drag, and pitching moment curves are also presented in Figures 1-56 through 1-58 comparing the flap performance with the canard removed. The lift, drag, and pitching moment increments due to deflecting the wing trailing-edge flaps (relative to zero wing trailing-edge flap deflection) in and out of the presence of the canard (at various canard deflections) were obtained from the curves above and are shown in Figures 1-59 through 1-67. The canard presence or incidence has a negligible effect on the trailing-edge flap increments at all Mach numbers.

1.5 Canard Leading Edge Flap Effect

The canard leading-edge flaps were tested at a deflection of 15 degrees for a limited range of canard deflections and at Mach numbers from .6 to 1.2 in Figure 1-68 through 1-70. At the low alphas, deflecting the canard leading-edge produces an adverse effect (Figure 1-68); however, as the local angle of attack is increased, the untrimmed drag polar becomes more favorable. The real value of canard leading-edge flap must be determined on the basis of what it does for the trimmed drag polars as discussed in Section 1.6.

1.6 Trimmed Aerodynamics

Trimmed lift and drag polars for the R104 configuration were plotted in Figures 1-71 through 1-81 for Mach numbers from .6 to 2.0. Three methods were used for trimming (1) trimming with varying canard deflections at a constant trailing-edge flap deflection, (2) trimming with the optimum canard and wing trailing-edge flap combination (which yields the envelope lift curves shown in these figures), and (3) trimming with the wing trailing-edge flap alone and the canard undeflected.

Figure 1-74 compares the M = .6, .9, and 1.2 trimmed lift curves and drag polars obtained by trimming with the wing trailing-edge flaps only (with canard undeflected) and with the optimum envelope obtained from trimming with both canard and wing trailing-edge flap. There is virtually no difference in the drag polars obtained with the two trim methods. However, the trimmed lift curves do differ somewhat; the difference probably lies partly with a lack of flap-deflection data to determine a very accurate trimmed envelope. The data is so limited at M = 1.2 that only a small portion of the envelope trimmed lift curve can be determined with any confidence. It does appear that the complexity of using both the canard and the flap is not justified at these Mach numbers and that trimming with the wing trailing-edge flap alone is acceptable. At M = 1.6, 1.8, and 2.0 (compare Figures 1-75, 1-76, and 1-77) for C_L's greater than approximately .1 to .15 (depending on Mach number), trimming with the optimum canard/wing trailing edge flap combination does yield a substantially better trimmed polar. However, since the airplane is not designed for supersonic combat maneuvering, the complexity of moving both surfaces at these speeds would not be required. Figure 1-78 therefore, summarizes the M = 1.6, 1.8, and 2.0 trimmed lift and drag obtained by trimming with the canard alone.

Figures 1-79, 1-80, and 1-81 demonstrate the effects of deflecting the canard leading-edge flap on the M = .6, .9, and 1.2 trimmed lift curves and drag polars obtained by varying canard deflection with a fixed wing trailing-edge flap deflection. Although the data is quite limited, transonically the canard leading-edge flap saves about 55 counts of trimmed drag while it costs about 55 counts supersonically.

1.7 Lateral-Directional Characteristics

The lateral-directional characteristics of the R104 baseline wind tunnel model configuration are presented in Figures 1-82 through 1-97.

At M = .2 (Figure 1-82), the vehicle exhibits positive, directional stability. As angle of attack is increased this stability level increases slightly, then decreases to become unstable near an angle of attack of 21 degrees. With the vertical tail removed, the wing-body-canard characteristics are unstable but become slightly more stable with increasing angle of attack. The difference between these two curves is the tail contribution to directional stability. The sidewash gradient as a function of angle of attack was derived from the low speed test data as shown in Figure 1-83. The sidewash gradient is small until the wing loses effectiveness; then, the average gradient increases rapidly until it approaches 1.0 at large angles of attack. This is evident from this figure as well as from Figure 1-82. The gradient is nonlinear with sideslip angle as well. At small sideslip angles ($|\beta| < 2°$) and large angles of attack, the gradient is on the order of that at small angles of attack. However, past $|\beta| = 2°$ the gradient is very steep indicating that at these angles of attack and sideslip, the flow

at the vertical tail is very destabilizing. Although sidewash data is not available with the canards off, the shape of directional stability as a function of angle of attack at high angles of attack indicates that the canard is the disturbing element.

The effects of canard location on dihedral effect and directional stability are shown in Figure 1-84 for Mach number = .2. The location of the canard has a profound and detrimental effect on the vertical tail effectiveness. The directional stability with the canard off is also indicated in Figure 1-84. The canard introduces an effect that destroys much of the effectiveness of the vertical tail. Apparently any location of the canard other than the mid location is detrimental to the vertical effectiveness. The dihedral effect in the same figure shows that the forward canard location is the worst location; this is also true for the directional stability.

As the speed is increased to the transonic ranges, the directional stability characteristics for the baseline canard location remain approximately the same but the angle of attack for instability decreases. Figures 1-85, 1-86, and 1-87 indicate the variations of the directional stability at Mach = 0.6, 0.9, and 1.2. The angle of attack for instability decreases from 17 degrees at Mach = 0.6 to 15 degrees at Mach = 0.9. At M = 1.2, the angle of attack for instability ($C_{n\beta} = 0$) is beyond the alphas tested. The directional stability characteristics at supersonic speed are shown in Figure 1-88 and 1-89. The angle of attack for zero staiblity decreases from the trasonic value to near 6° - 8° at M = 1.6 and 2.0.

The configuration buildup for the forward canard location is shown in Figures 1-90 and 1-91 for Mach = .9 and 1.2. Shifting the canard forward from C_1 to C_2 reduces the angle of attack for instability at all Mach numbers. The effects of shifting canard location forward or aft of the baseline midlocation are compared in Figures 1-92 through 1-94 for Mach numbers of .9, 1.6, and 2.0. At Mach 2.0, the directional stability does not deteriorate for the aft canard location as occurred at the lower Mach numbers. Sufficient data was not obtained to explain this trend.

The directional control effectiveness is presented in Figures 1-95 through 1-97 for M = .2, .9, 1.2. The level of control remains approximately constant with deflection up to $\delta_{VT} = 15°$ indicating the control characteristics are linear in that region. This is true for all the Mach numbers tested. The vertical control effectiveness remains constant up to near 30 degrees where only a slight reduction occurs.

2.0 COMPARISONS OF E205 AND R104 AERODYNAMICS

The longitudinal and lateral-directional aerodynamic characteristics of the E205 and R104 wind tunnel models are compared in this section. To obtain meaningful comparisons, the aerodynamic coefficients of the R104 model are re-referenced to the E205 wing area and mean geometric chord (mgc) except as noted.

2.1 Component Build-Up

Lift, drag, and pitching moment increments for several components of the E205 and R104 configuration models are compared in Figures 2-1 through 2-10 for Mach = .2, .6, .9, and 1.2, 1.6, 1.8 and 2.0. Although not all of the components are available at each Mach number, those discussed include the following: the vertical tail, the wing alone (canard removed), the wing in the presence of the canard, the canard alone (no wing), and the canard in the presence of the wing.

At all Mach numbers, the increments due to the vertical tail are virtually identical for the E205 and R104 configurations.

For the "wing alone", the E205 configuration exhibits higher lift and drag increments, and a more nose down moment at all Mach numbers indicating that the wing is performing more effectively and is therefore experiencing a more favorable body interference with the E205 configuration, i.e. the wide, flat strake area of the E205 is effectively acting as a lifting surface.

When the wing is placed in the presence of the canard, the wing suffers a substantial lift loss resulting in more nose-up moment and reduced drag for both the E205 and R104 configurations. The data is limited to showing the magnitude of this change only for the R104 at M = .2 but comparisons with the E205 and R104 "wing in presence of the canard" are available at M = 1.6, 1.8, and 2.0 (Figures 2-6 through 2-10) and indicate that the E205 wing continues to preform better than the R104 wing with about the same differences noted for the wing-alone case.

The "canard-alone" increments are available only for the R104 at low speed but comparisons of E205 and R104 increments are available at M = 1.6, 1.8, and 2.0. These comparisons indicate that the canard on the E205 configuration performs more effectively than on the R104. The wide, flat body of the E205 configuration probably induces a higher upwash field on the canard and hence a higher effective canard alpha than the more narrow R104 strake/fuselage arrangement. The fact that the canard moment increment is more positive than that of the R104 is explained by the fact that the moment arm from the c.g. to the mgc of the canard on the R104 is enough larger than that of the E205 to produce a more nose-up moment with a smaller canard lift increment. The supersonic drag increment of the "canard-alone" is higher for the E205 as expected with the higher lift increment.

The increments due to the canard in the presence of the wing plus the influence of the canard on the wing are available for the E205 at M = .2 (Figure 2-1) while comparisons between the E205 and R104 increments are shown in Figures 2-2 through 2-10 for Mach numbers from .6 to 2.0. As noted above, a separate balance would be required to isolate the canard loads in the presence of the wing.

Subsonically, the increments due to the canard-plus wing-interference indicate a higher net loading for the E205 configuration, probably a combination of higher canard loads (influenced by a better performing wing even with wing alone) and less negative interference on the wing. The same trends are indicated supersonically, although the differences are not nearly so pronounced as noted in the subsonic cases.

Figure 2-11 compares the untrimmed (power off) minimum drag variation with Mach number for the E205 and R104 configurations. The R104 has about the same minimum drag at subsonic Mach numbers but the transonic drag rise is more severe; the probable unfavorable fuselage shape resulting from using the E205 nose, the much narrower channel between the nacelles and fuselage causing higher interference drag, and the larger maximum cross sectional area of the R104 model results in substantially higher supersonic minimum drag than obtained with the E205 model.

2.2 Aerodynamic Center

A comparison of the aerodynamic center location for the E205 and R104 configurations is presented in Figure 2-12. Subsonically, the two vehicles are very similar, differing in a.c. by approximately 1 percent. An extra data point was obtained at Mach = 0.95 and 1.1 for the R104 vehicle with canard off giving more definition to this curve transonically. The a.c. appears to be farther aft transonically (wing body) for the R104 than the E205. However, at supersonic speeds, the a.c. is 2-5 percent farther forward. The addition of the canard tempers the transonic a.c. shift for the R104 making it very similar to the E205. The addition of the canard makes approximately the same a.c. shift for both vehicle.

2.3 Wing Trailing-Edge Flap Effectiveness

The lift, drag, and pitching moment increments due to the deflected wing trailing-edge flaps ($S_{TE} = 10^{\circ}$ and 25°) in the presence of the undeflected canard were compared across the Mach number ranges tested for the R104 and E205 models. These comparisons showed that there was virtually no difference in flap effectiveness on the two configurations.

2.4 Trimmed Characteristics

Comparisons between the E205 and R104 wind tunnel model (unpowered) trimmed drag polars are shown in Figures 2-13 through 2-23 for Mach numbers from .6 to 2.0 . The M = .6, .9, and 1.2 trimmed drag polars represent the envelope polars obtained by trimming with optimum canard and wing trailing-edge flap deflections. At M = 1.6 and 2.0 the trimmed comparisons were obtained by varying the canard deflections with zero and ten degrees of wing trailing-edge flap deflection. Comparisons are made at each Mach number on a common-reference-area basis (E205) and on the individual-reference-area basis. Comparison on a common reference area basis affords the ability to measure which configuration may perform better with a given thrust while the comparisons on the individual-reference area basis affords the ability to measure which configuration is aerodynamically more efficient. (In this case, the reference areas are very close, E205 = 384 ft^2, R104 = 357 ft^2, so that there are only small changes in the polars.) At the transonic Mach numbers, the E205 has a better trimmed drag polar than the R104 for C_L's > .35 so for combat maneuvering the E205 looks superior; the R104 appears slightly superior for transonic cruise at the lower C_L's. At M = 1.2 the E205 is superior at all C_L's primarily because of the large differences in C_{Dmin}; however, the E205 would still yield a superior polar even if the C_{Dmin}'s were the same because it has a better polar shape.

The supersonic, untrimmed minimum drag of the R104 model is higher than that of the E205. The trimmed minimum drag however is less for the R104 at some supersonic Mach numbers primarily because of the differences in C_{mo} and a.c. of the two configurations (even though the canard, wing, and trailing-edge flap effectiveness are about the same on the two configurations).

At M = 1.6, the E205 has a lower minimum trimmed drag and a better polar shape than the R104 configuration when trimming with the canard and zero wing trailing-edge flap deflection. When trimming with the canard and 10° of wing trailing-edge flap deflection, the R104 has a lower minimum trimmed drag but a worse polar shape than the E205; using a combination of canard and flap yields a better envelope polar shape for C_L's < .5 for the R104 but the requirement to maneuver at much higher C_L's would be required to show a benefit for using trailing-edge flap deflections with the E205.

For M = 2.0, the R104 has a lower minimum trimmed drag but a worse polar shape than E205. Using the wing trailing-edge flap indicates that a better envelope polar can be obtained at M = 2.0 for both the E205 and R104 models.

2.5 Lateral-Directional Characteristics

The lateral-directional derivatives for the E205 and R104 configurations are compared in Figures 2-24 through 2-29. The coefficients for the R104 have been adjusted to account for the difference in reference area and span. There is only a slight difference between the directional stability for the two configurations at any Mach number except at Mach = 1.2. Apparently there is a more favorable flow at the vertical tail at M = 1.2 for the R104 than for the E205. This is not as evident at any other Mach number. There is a slight improvement at M = 2.0 but it is not of the same order of magnitude as at Mach = 1.2. The dihedral effects are similar at all subsonic speeds. At the supersonic speeds, the E205 seems to have some less dihedral effect than the R104 although the trends with angle of attack are similar.

II

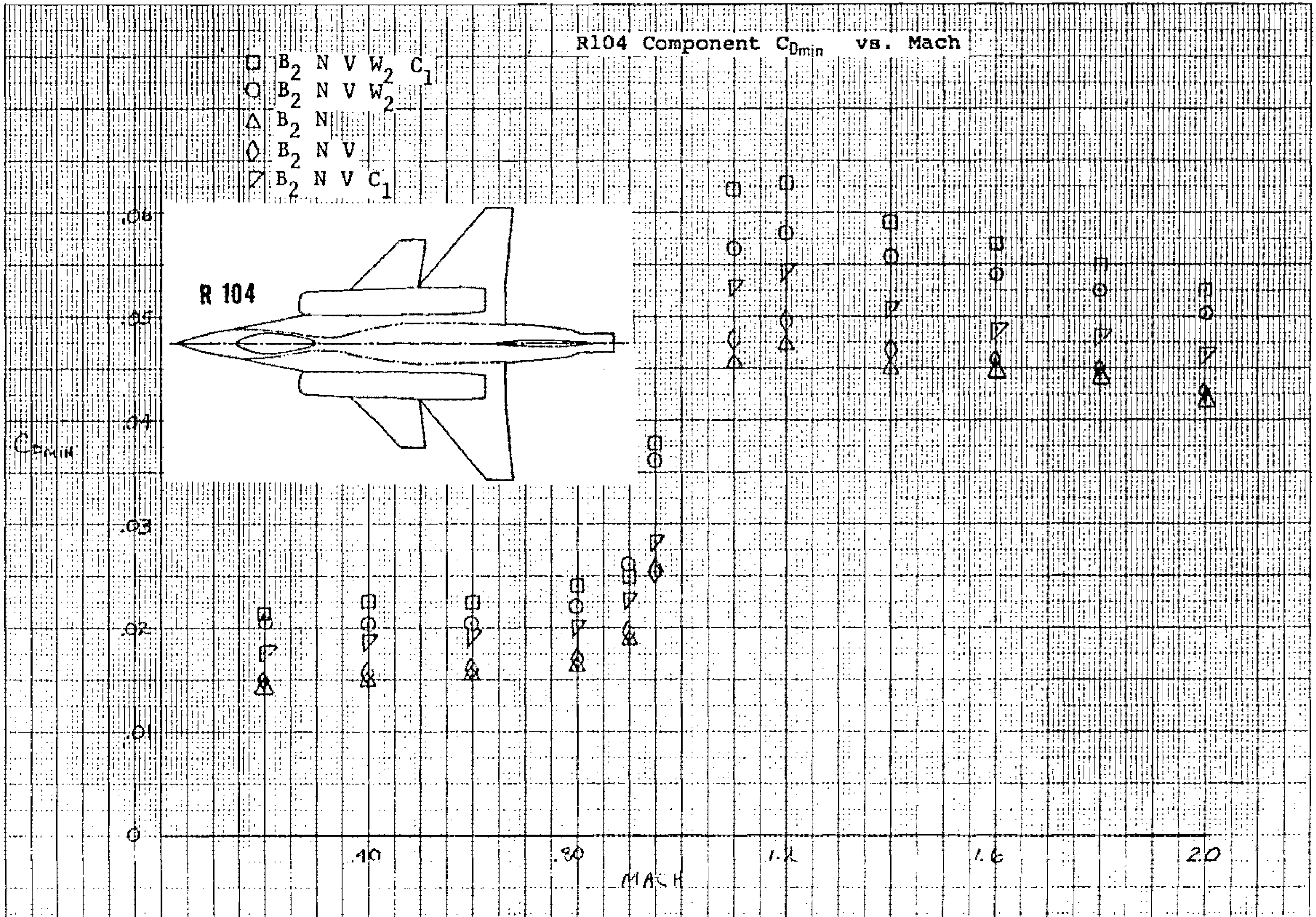

Figure 1-1 R104 Component Buildup Comparison of $C_{D_{MIN}}$ vs. Mach Number

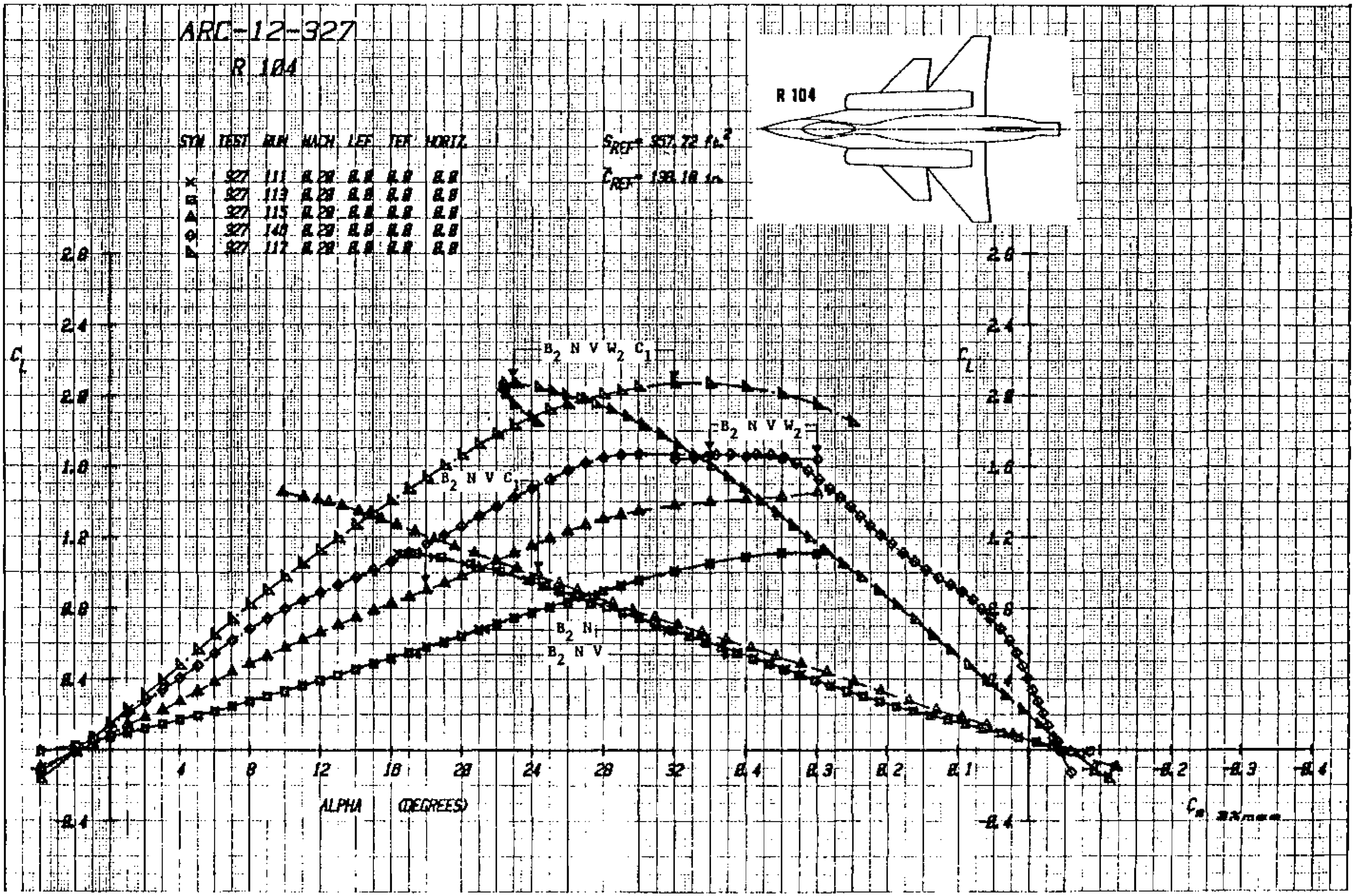

Figure 1-2a Effect of Component Buildup on Lift and Moment, Mach = .2

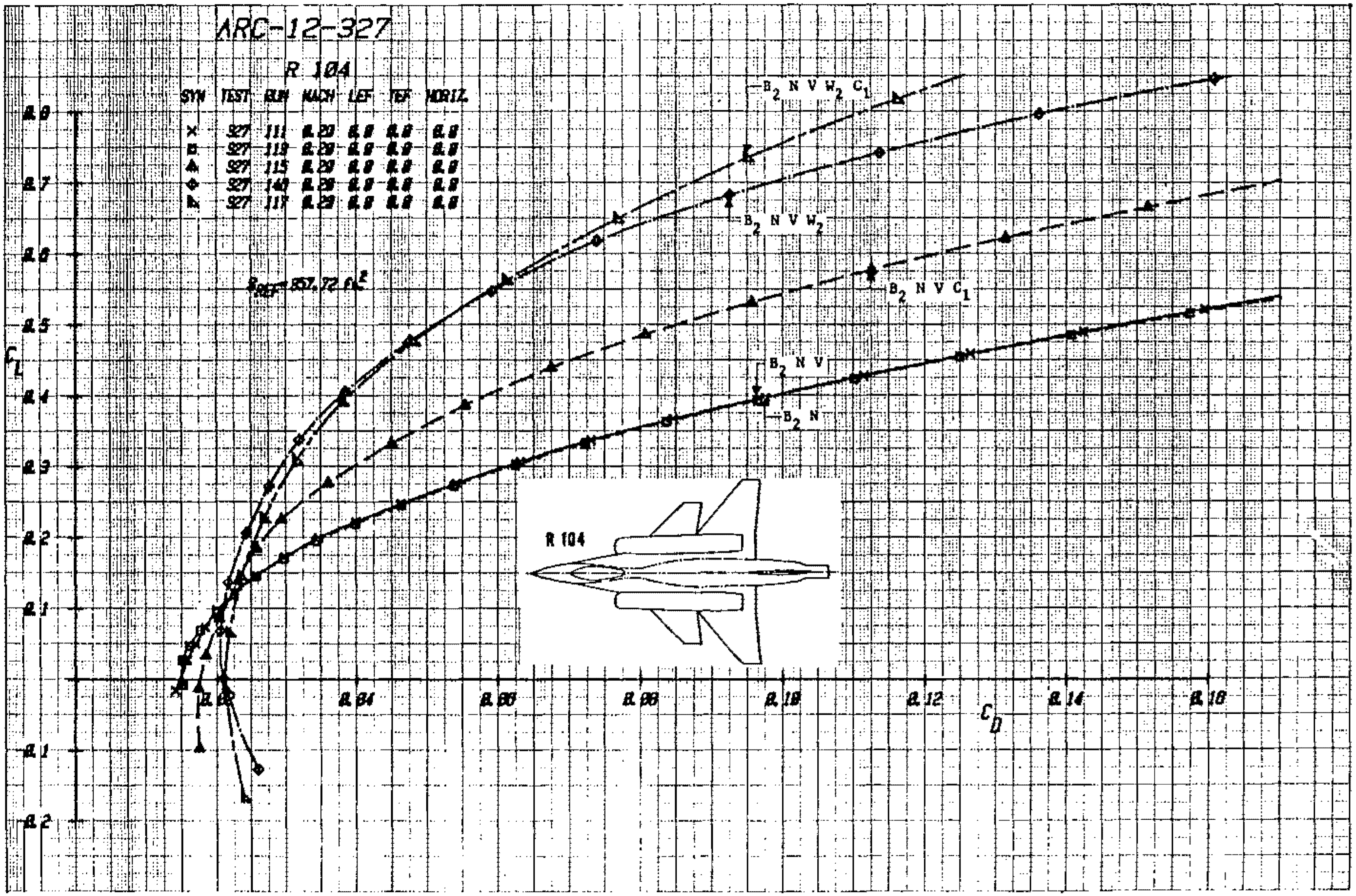

Figure1-2b Effect of Component Buildup on Drag, (Expanded Drag Scale), Mach = .2

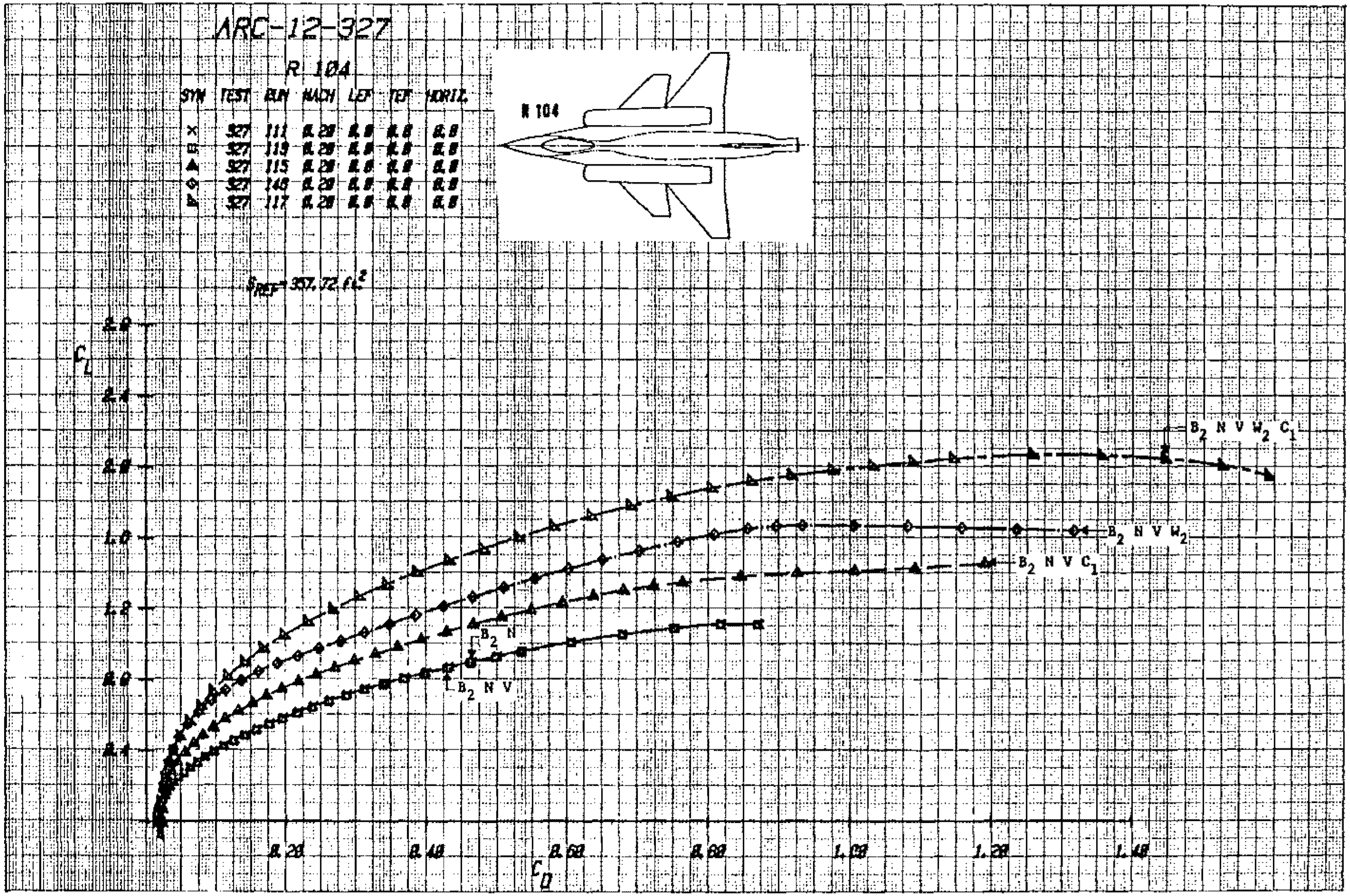

Figure 1-2c Effect of Component Buildup on Drag, Mach = .2

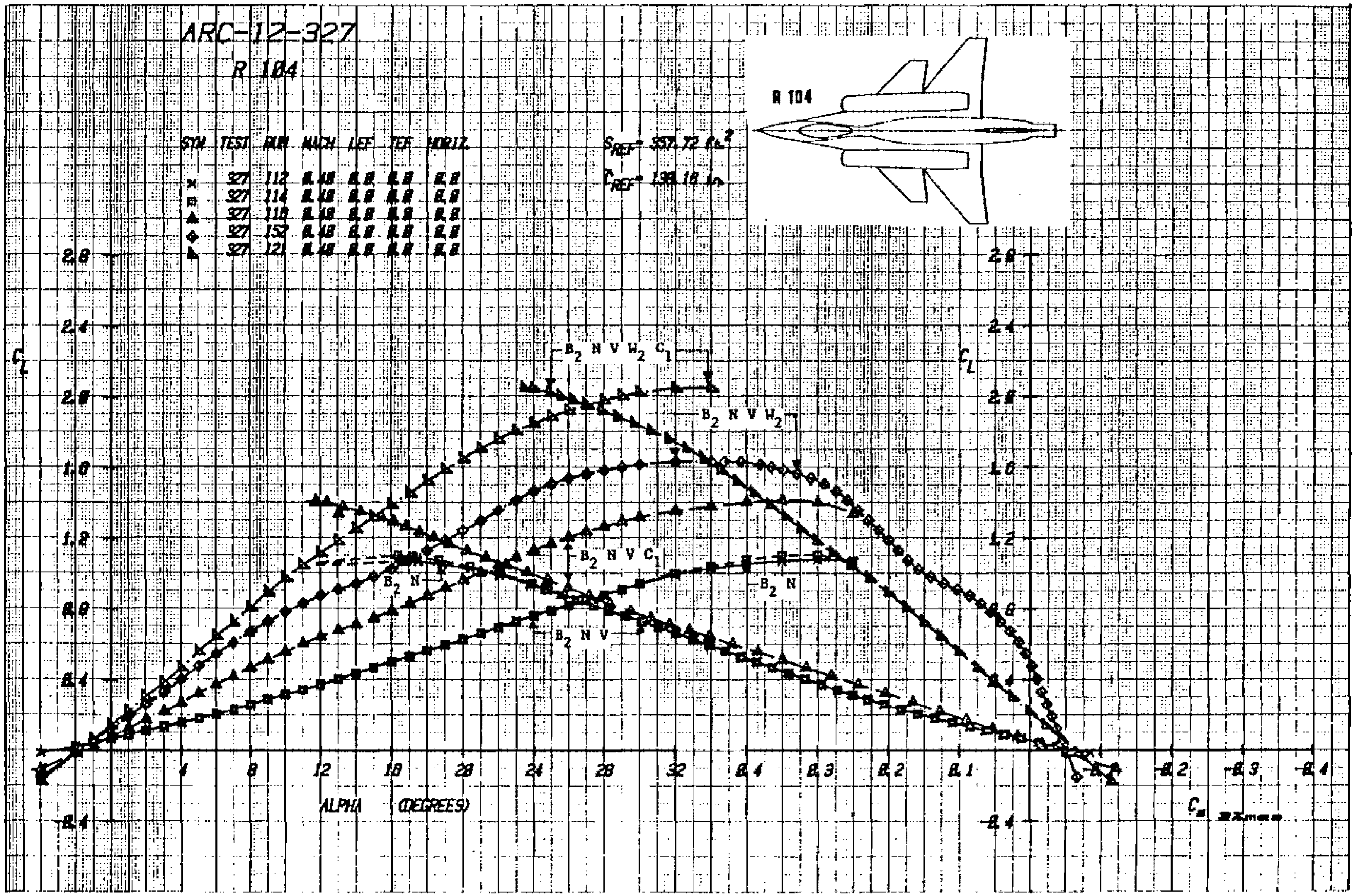

Figure 1-3a Effect of Component Buildup on Lift and Moment, Mach = .4

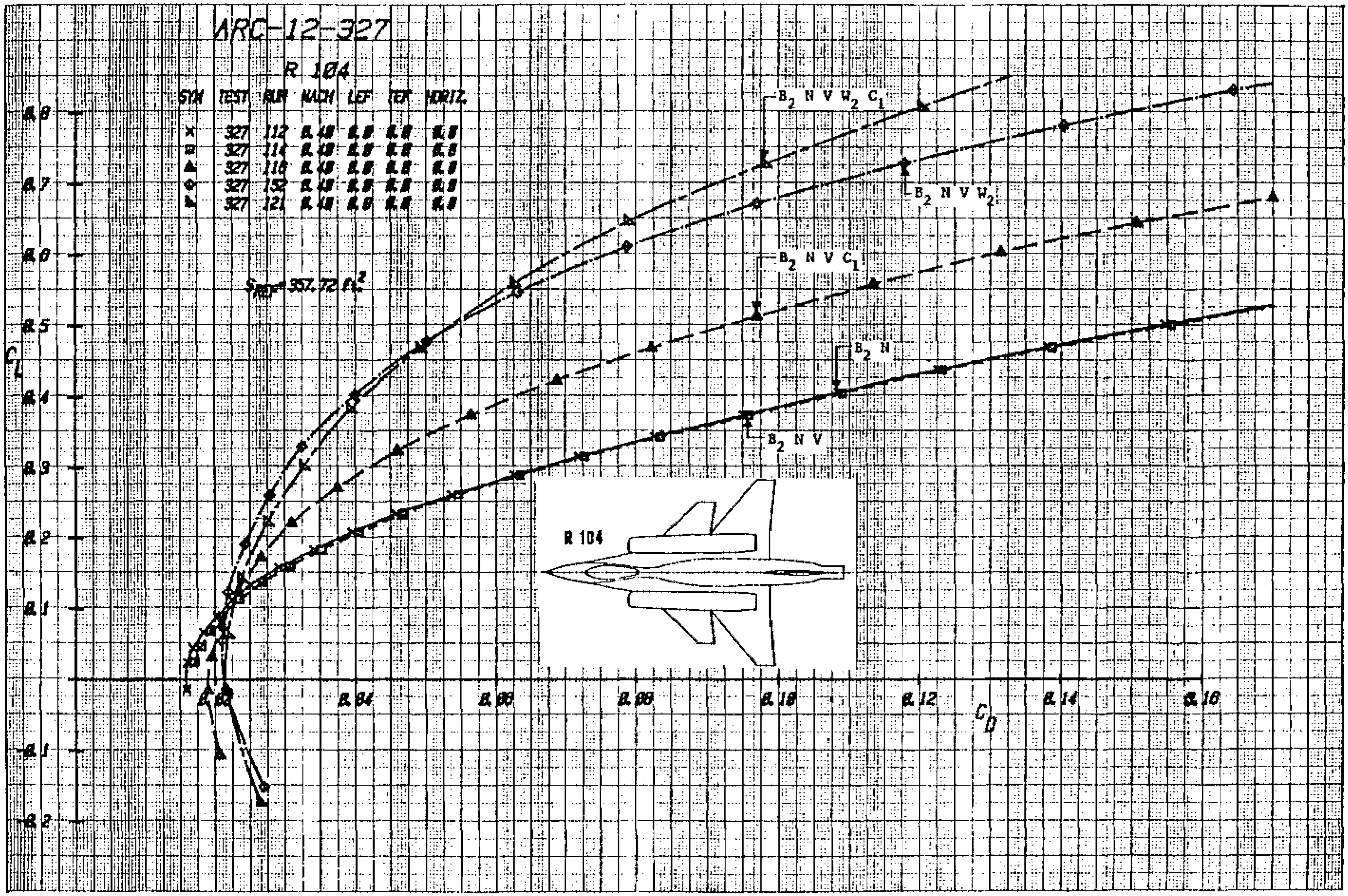

Figure 1-3b Effect of Component Buildup on Drag, (Expanded Drag Scale), Mach = .4

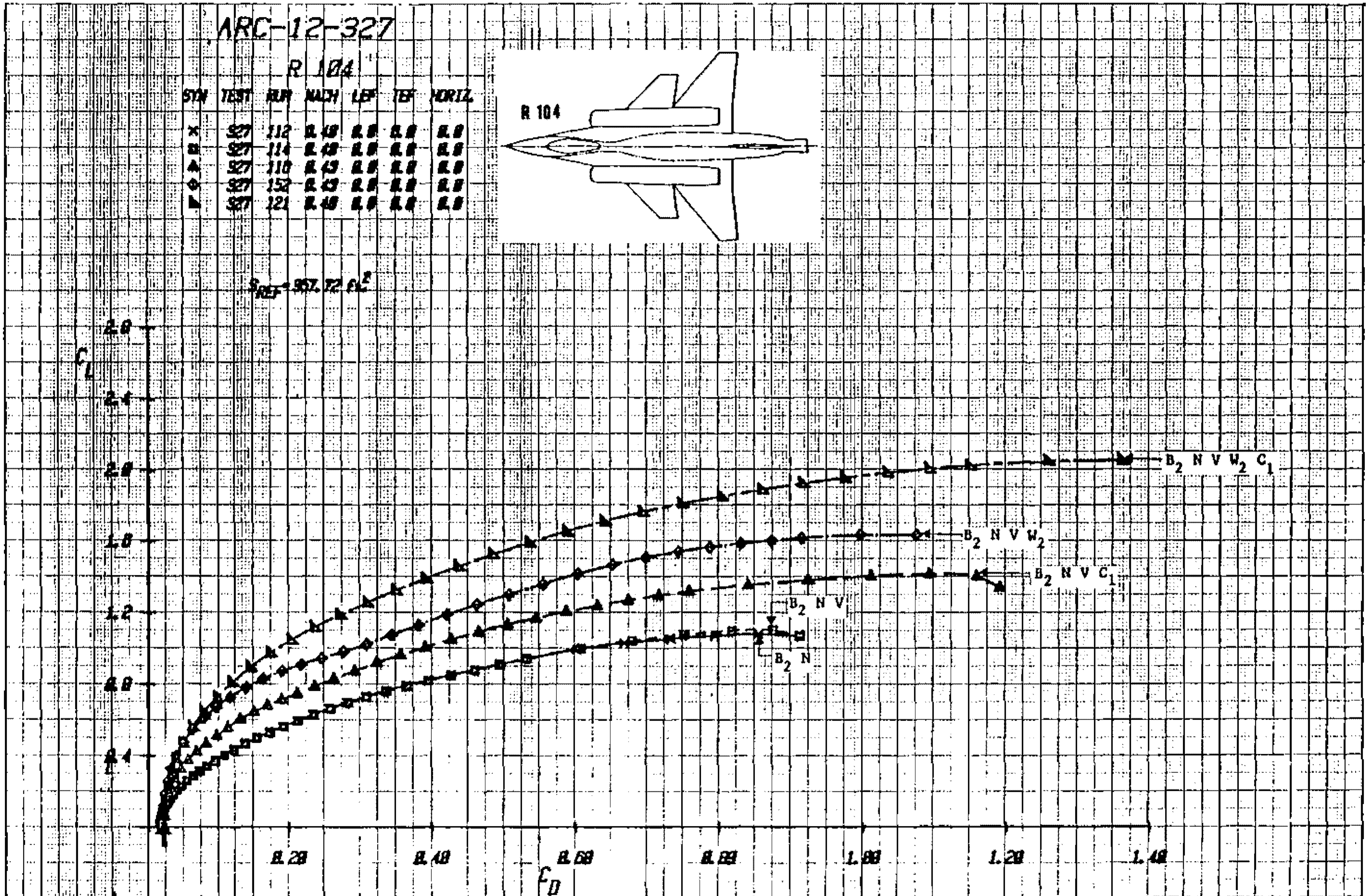

Figure 1-3c Effect of Component Buildup on Drag, Mach = .4

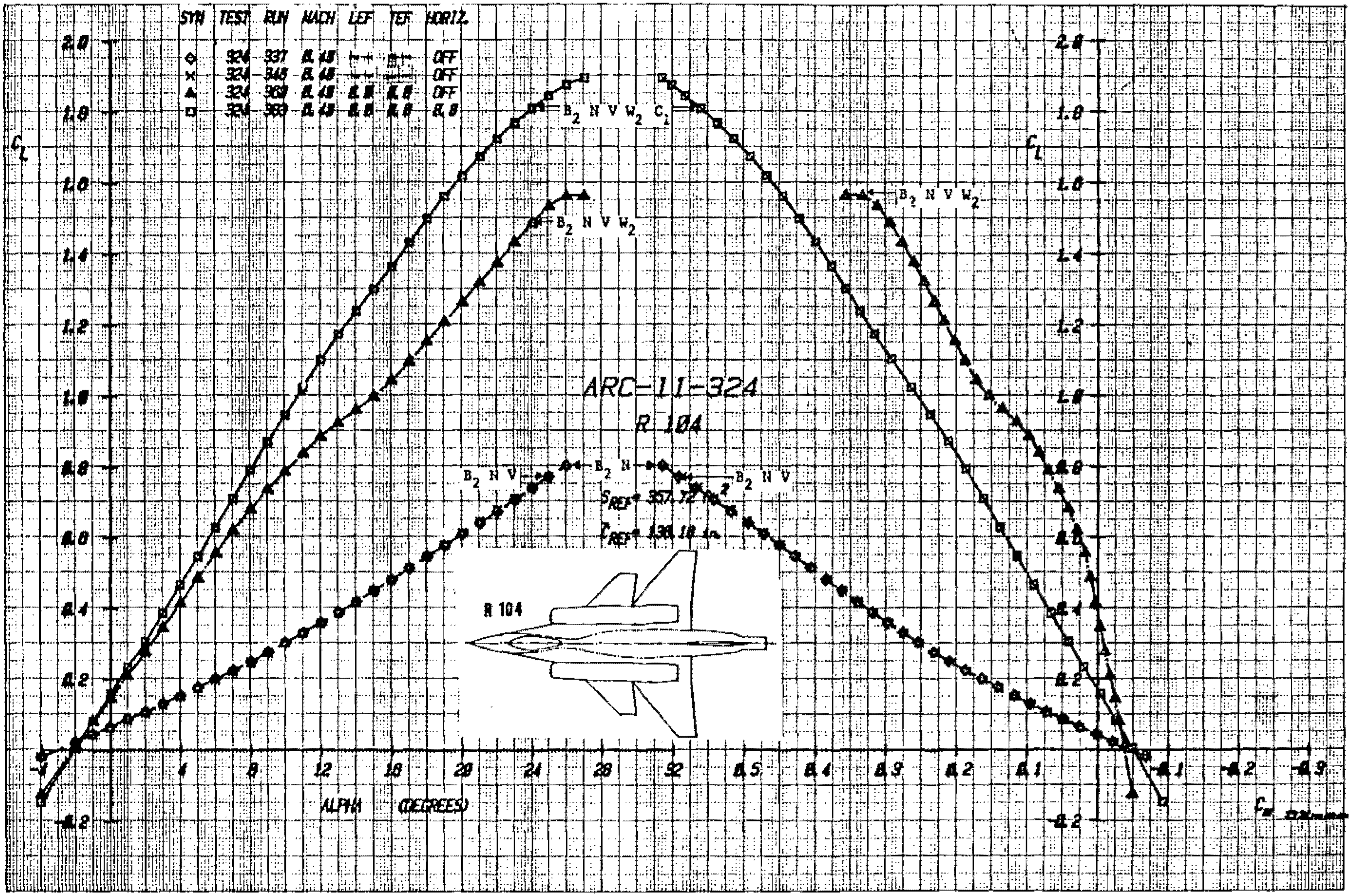

Figure1-4a Effect of Component Buildup on Lift and Moment, Mach = .4

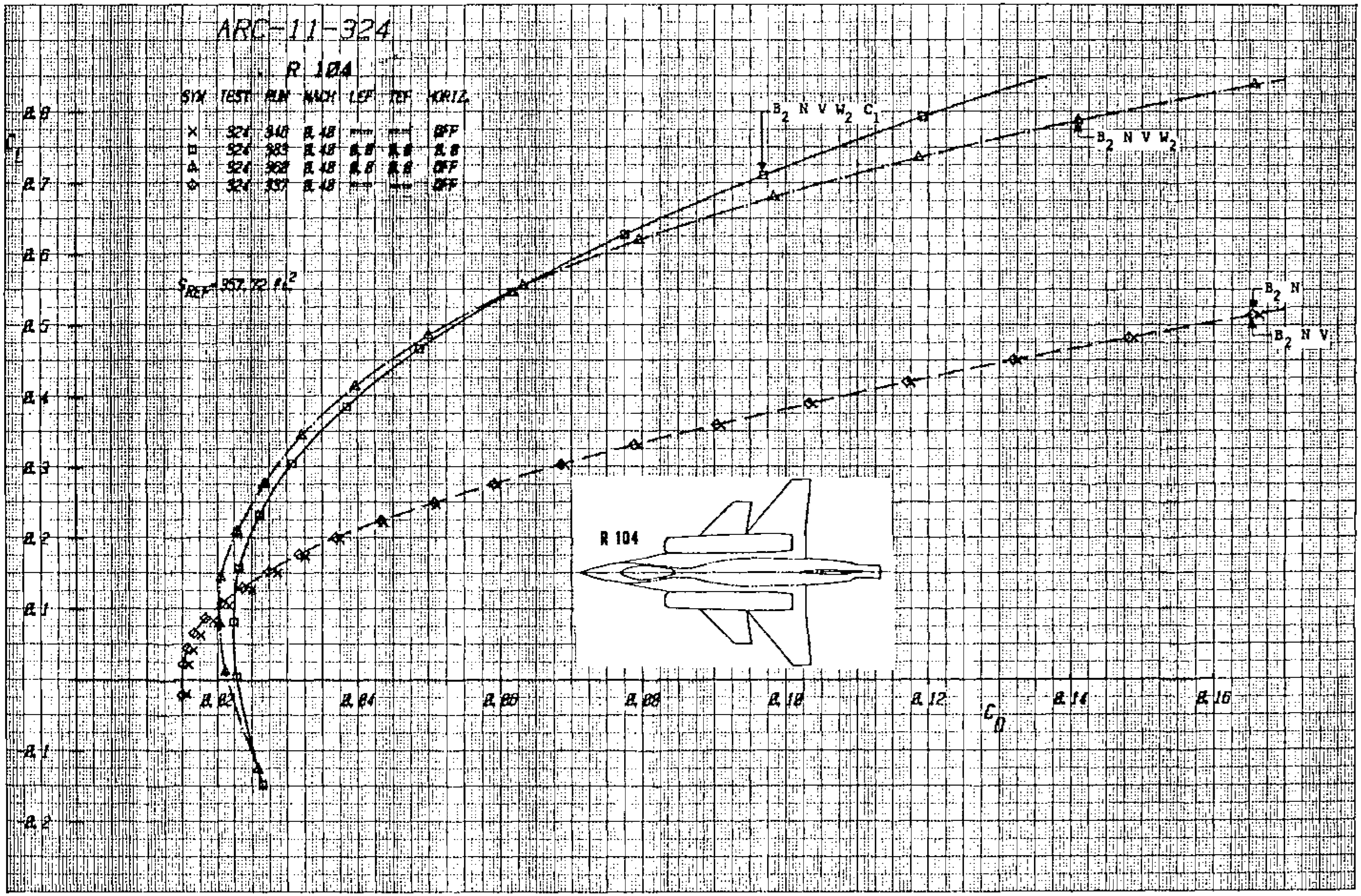

Figure 1-4b Effect of Component Buildup on Drag, Mach = .4

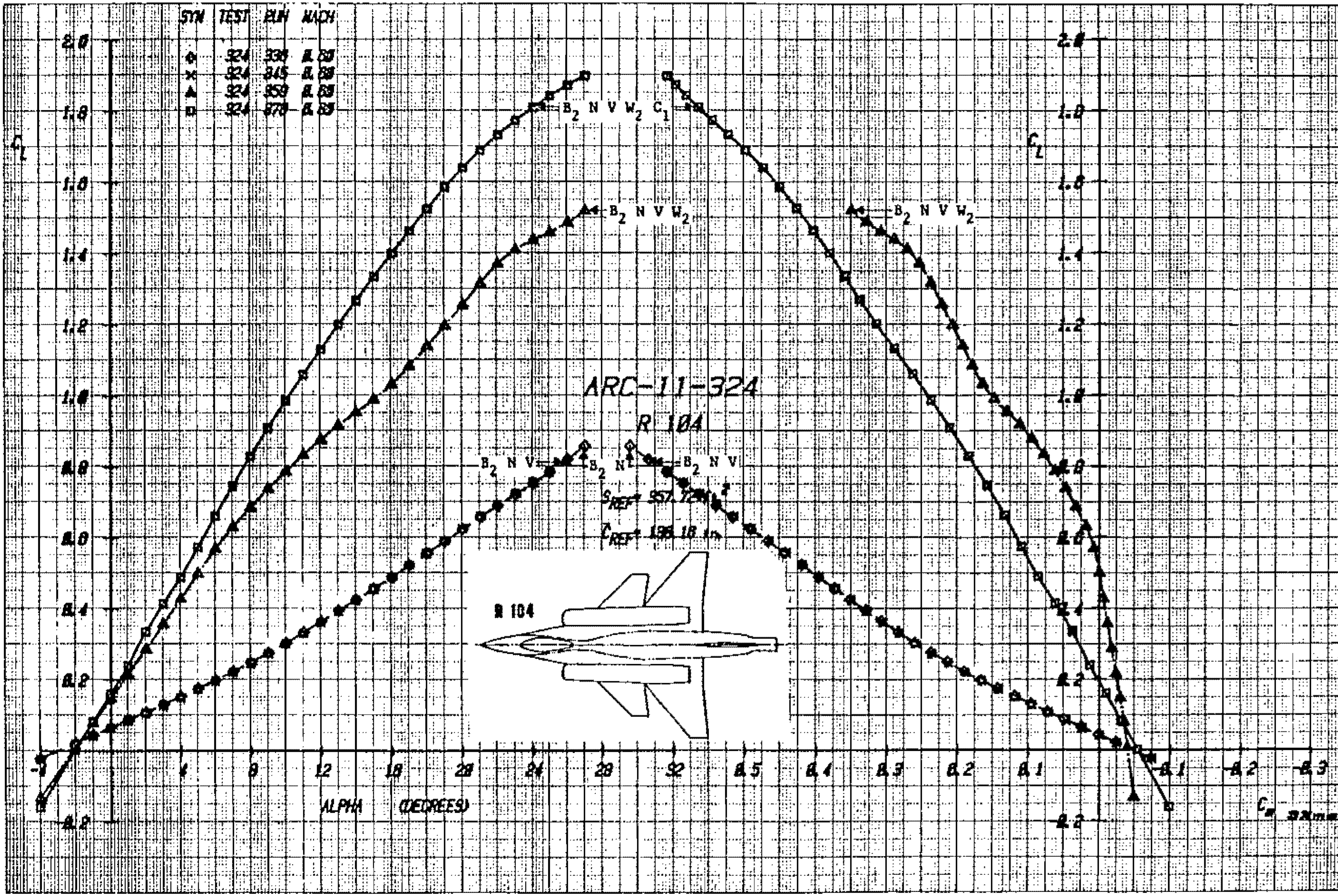

Figure 1-5a Effect of Component Buildup on Lift and Moment, Mach = .6

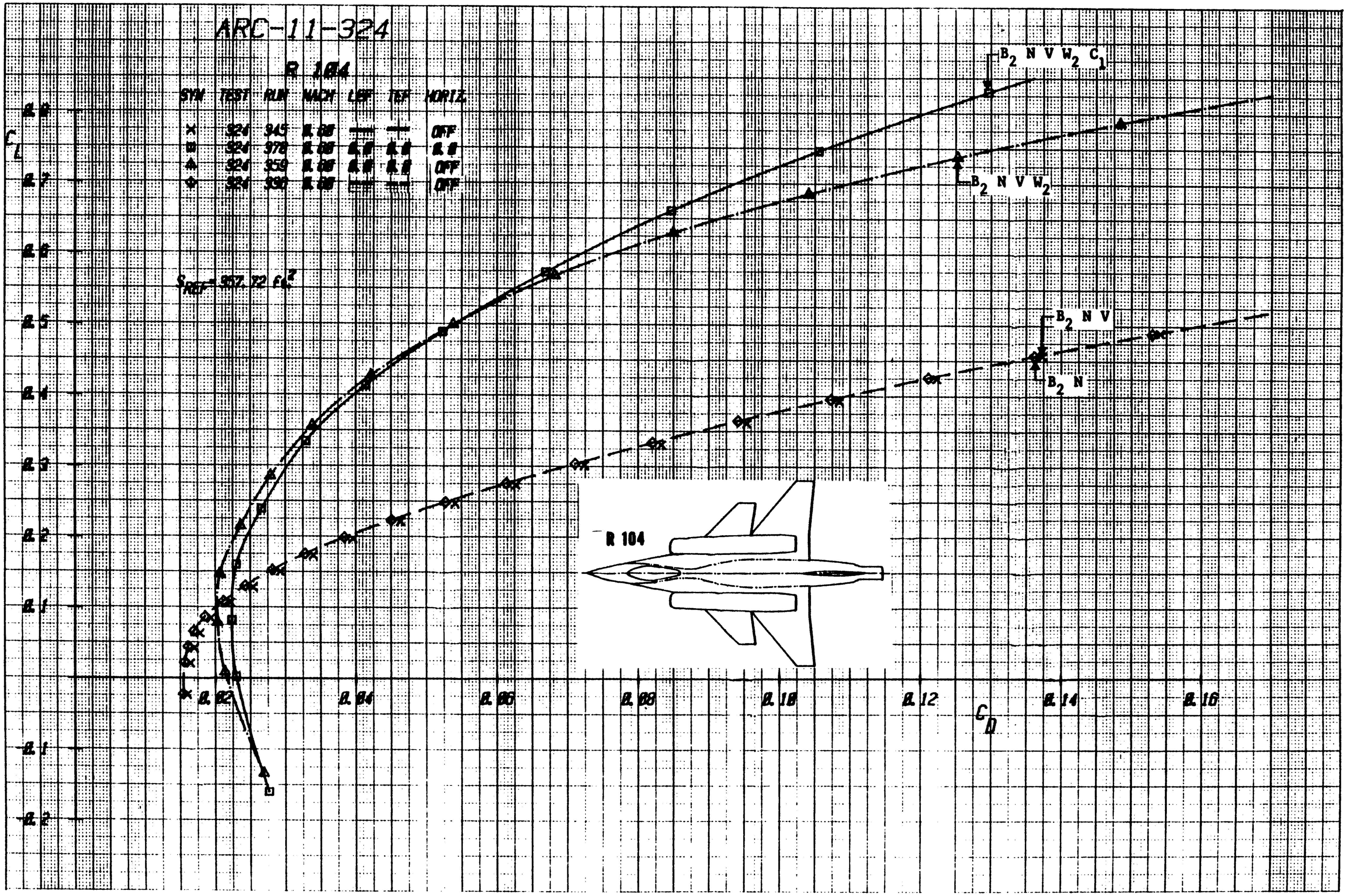

Figure1-5b Effect of Component Buildup on Drag, Mach = .6

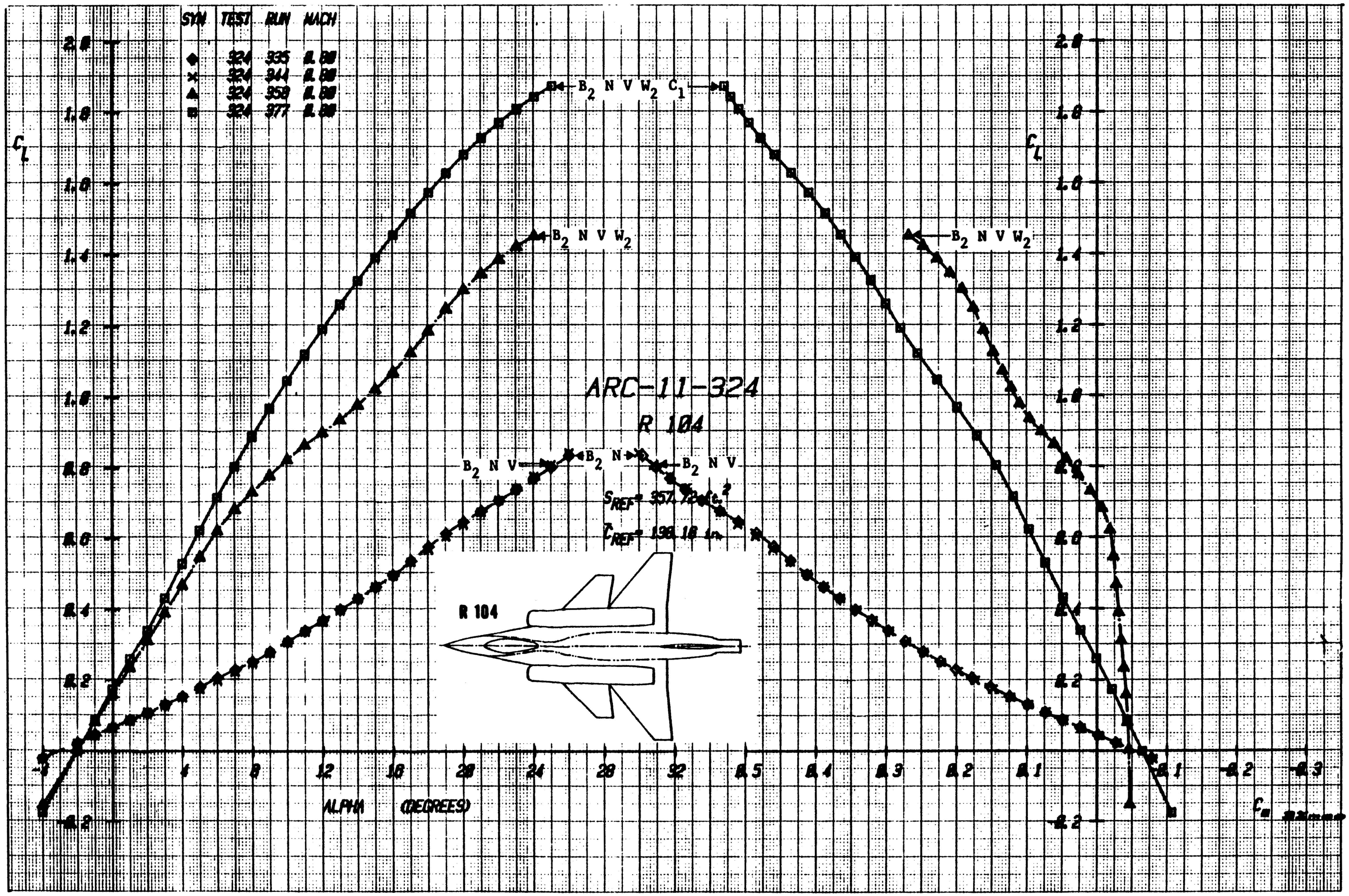

Figure 1-6a Effect of Component Buildup on Lift and Moment, Mach = .8

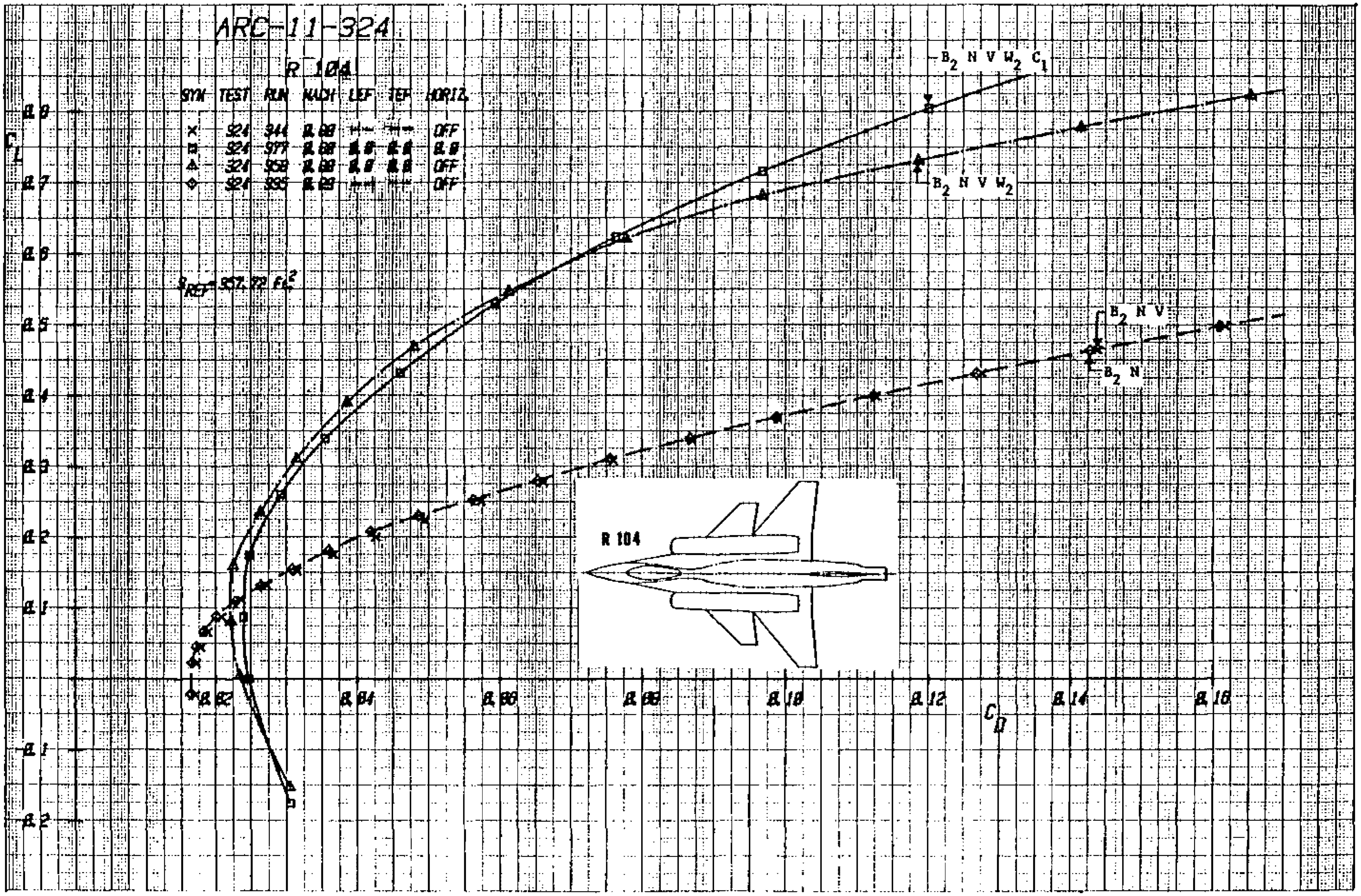

Figure 1-6b Effect of Component Buildup on Drag, Mach = .8

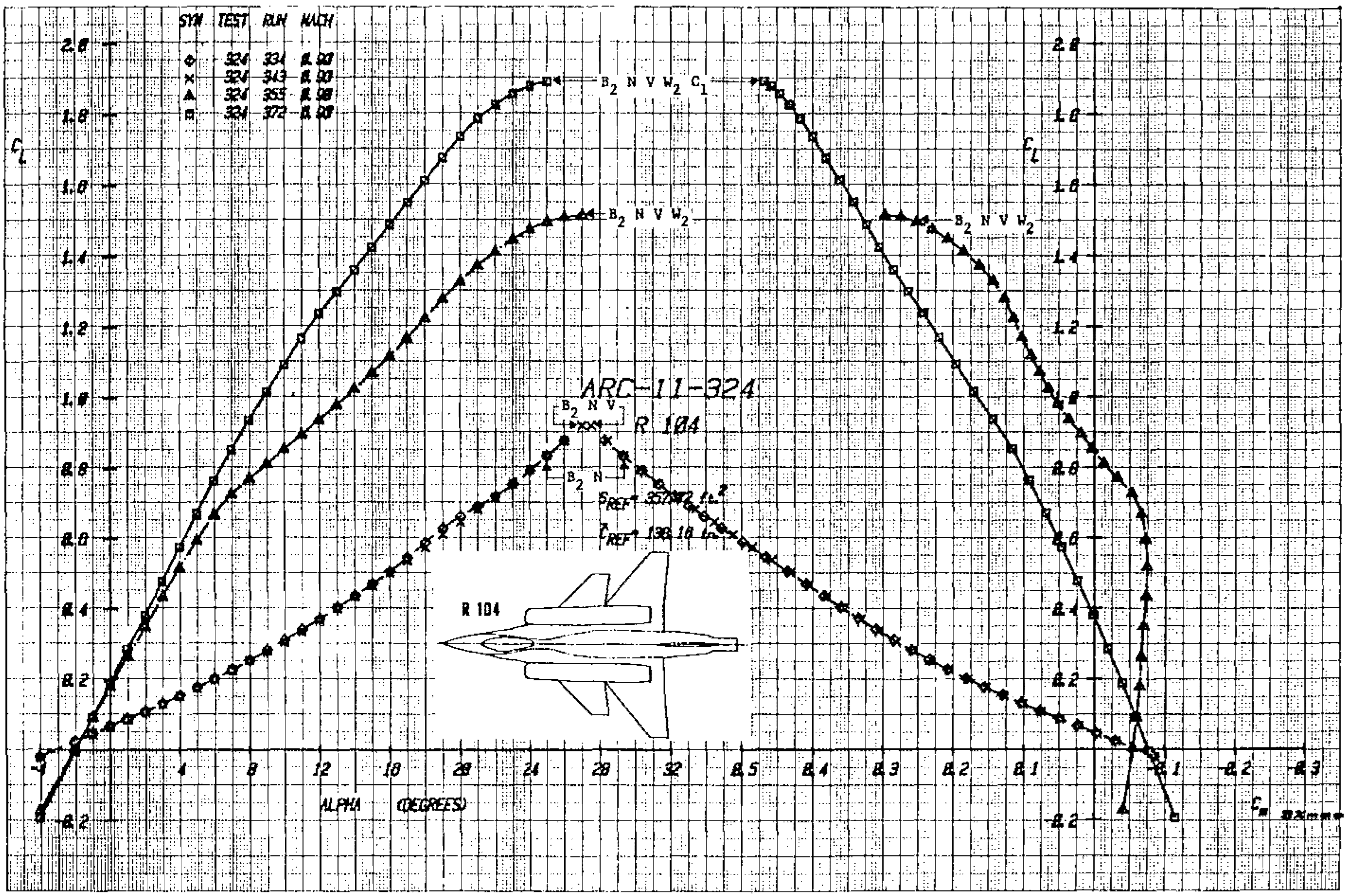

Figure 1-7a Effect of Component Buildup on Lift and Moment, Mach = .9

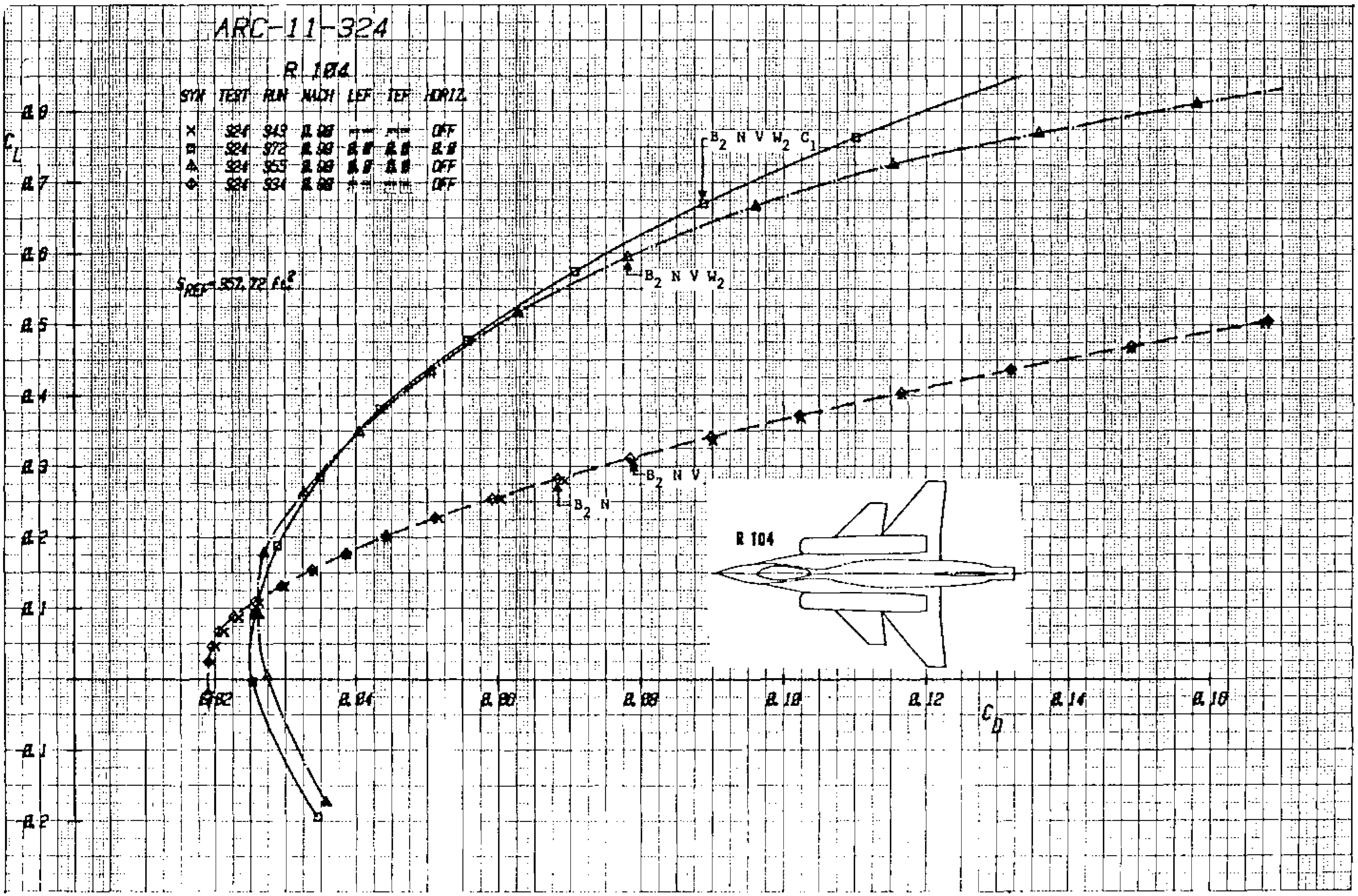

Figure 1-7b Effect of Component Buildup on Drag, Mach = .9

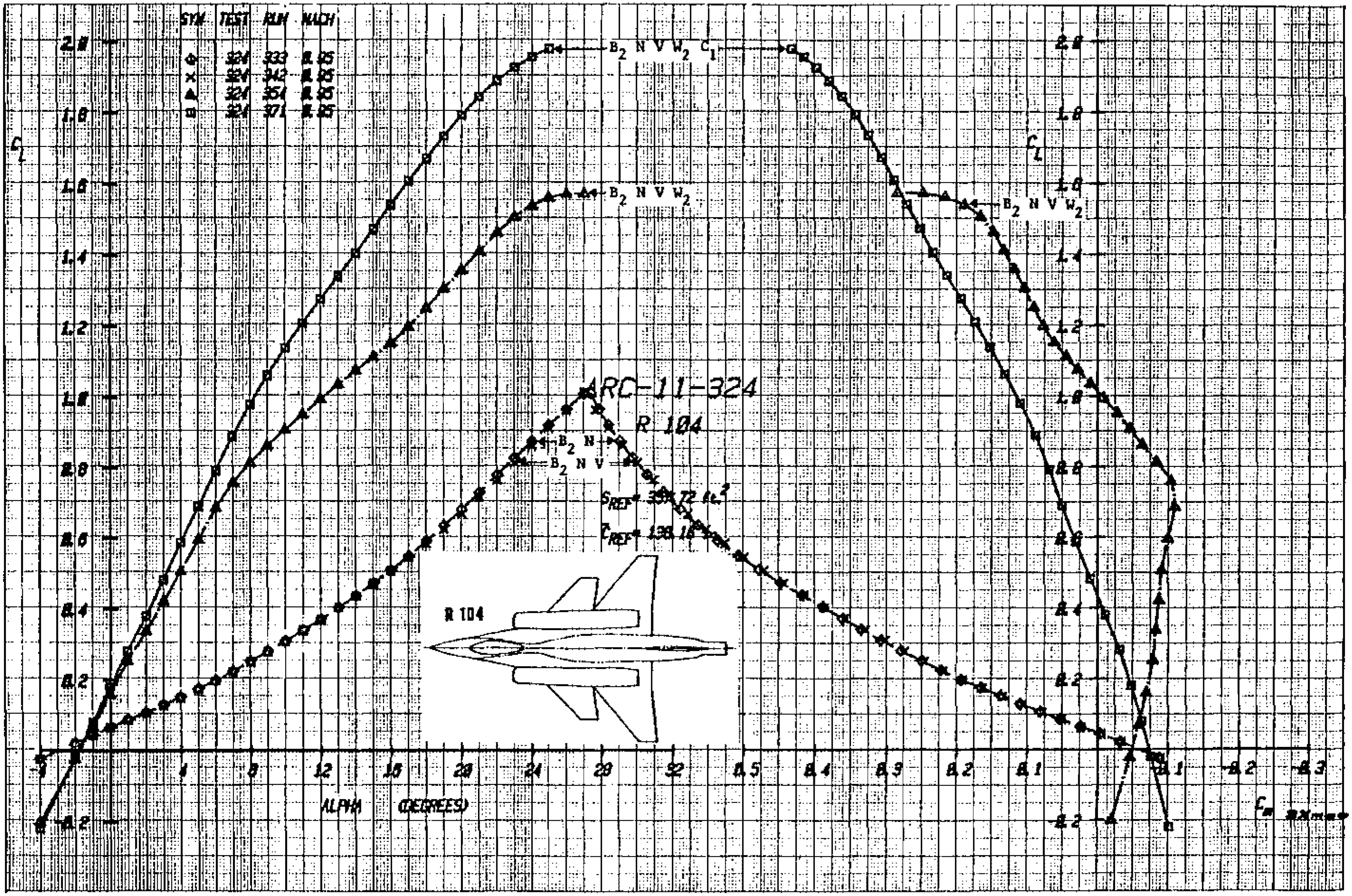

Figure 1-8a Effect of Component Buildup on Lift and Moment, Mach = .95

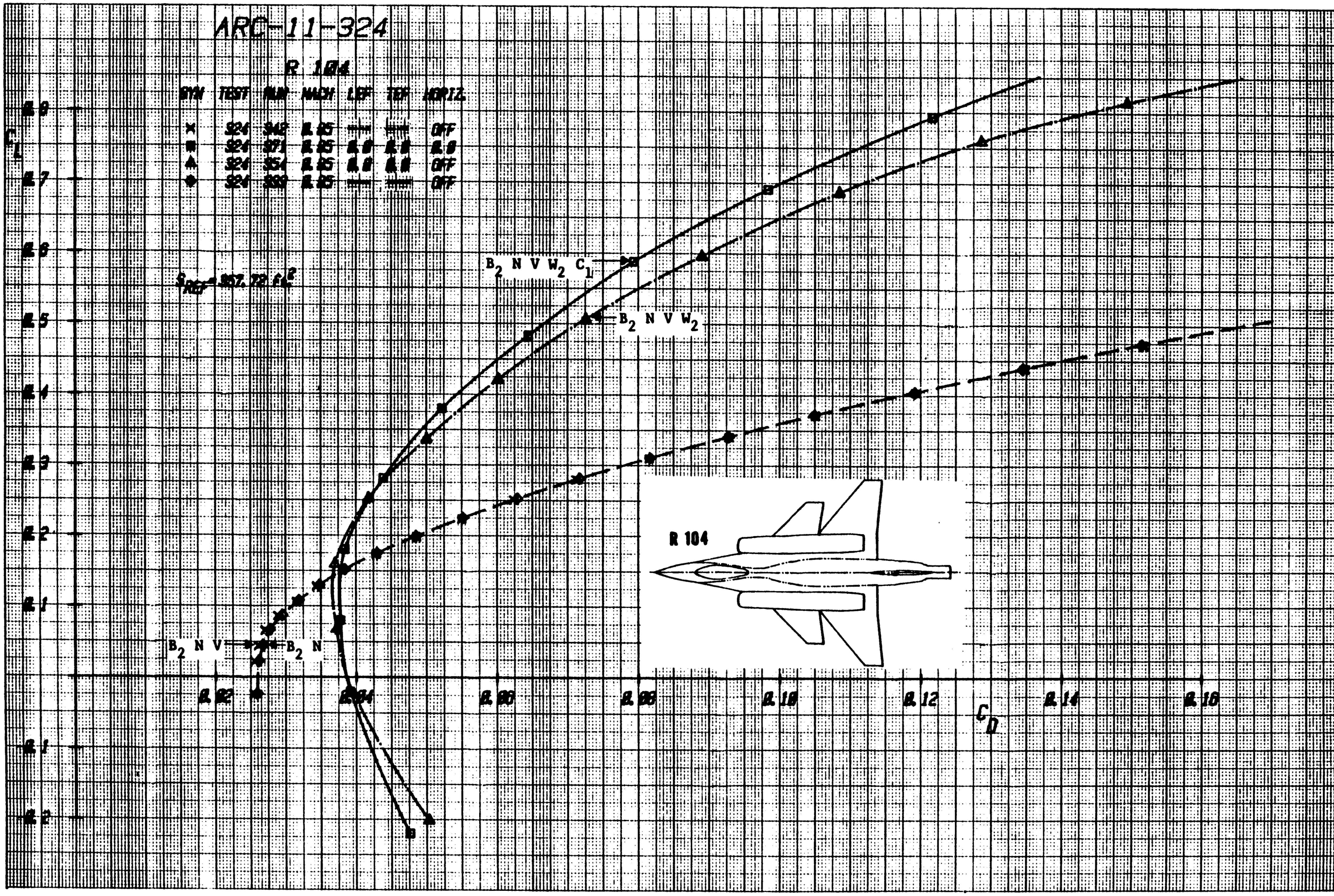

Figure 1-8b Effect of Component Buildup on Drag, Mach = .95

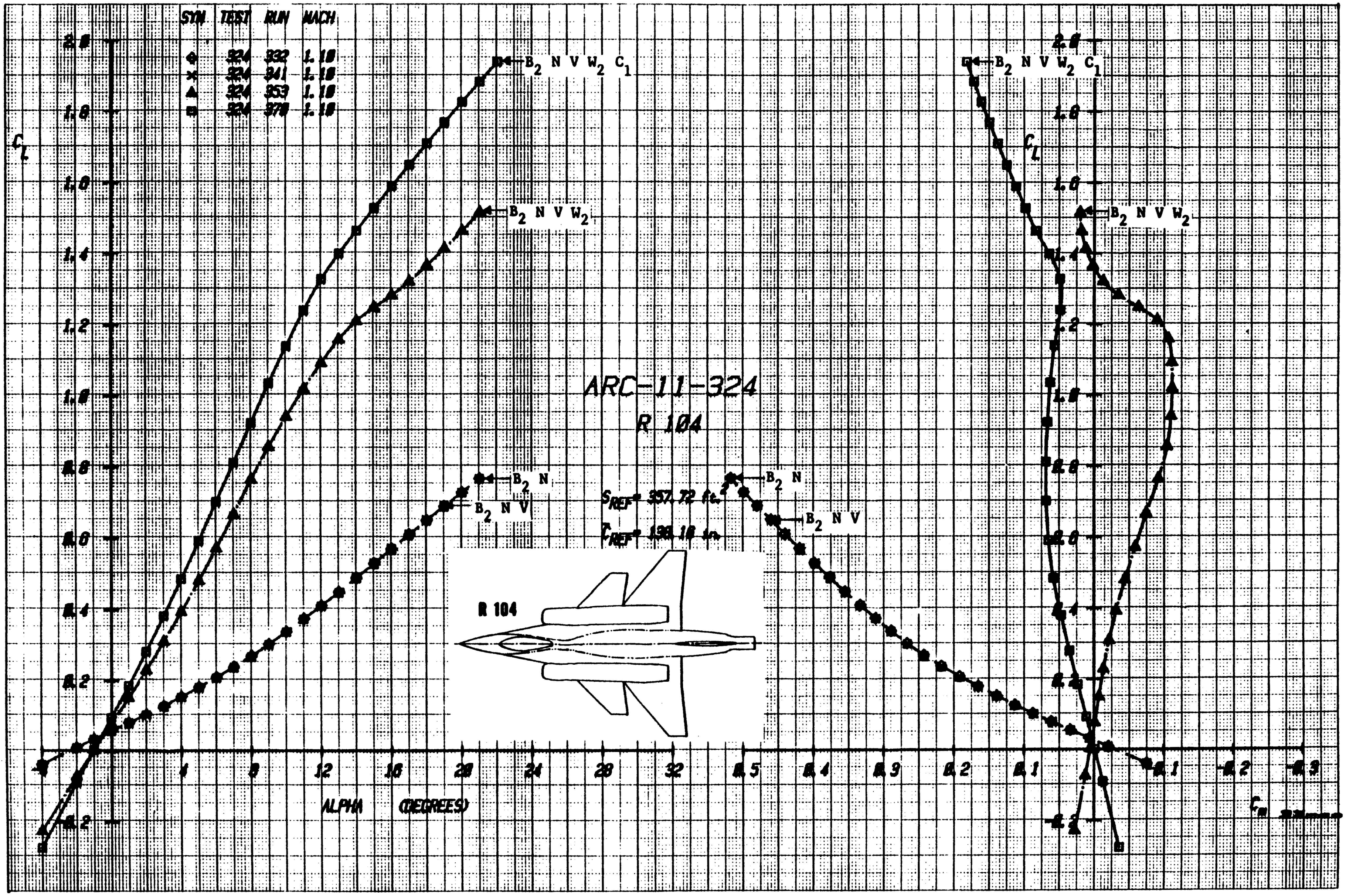

Figure 1-9a Effect of Component Buildup on Lift and Moment, Mach = 1.10

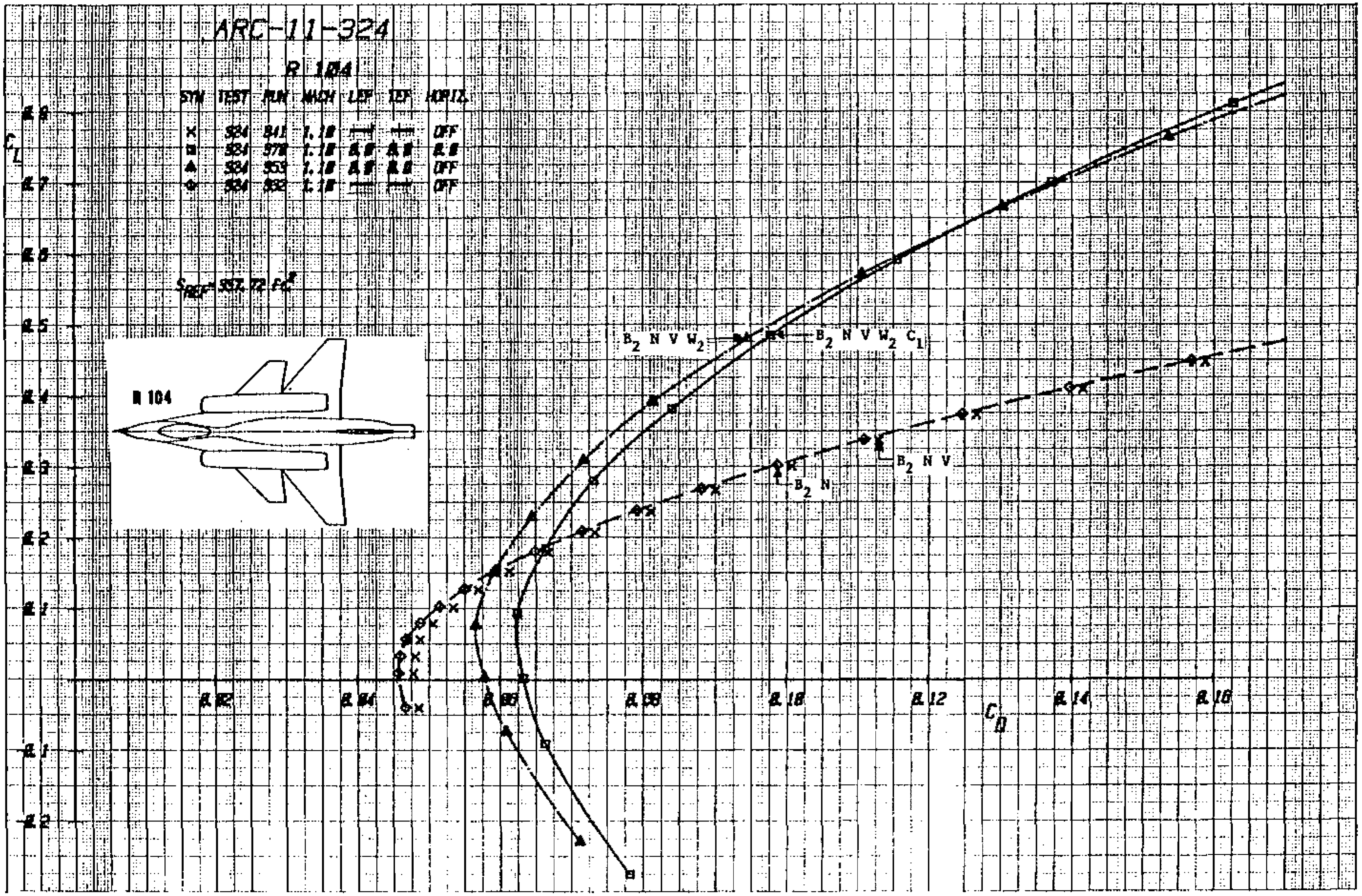

Figure 1-9b Effect of Component Buildup on Drag, Mach = 1.10

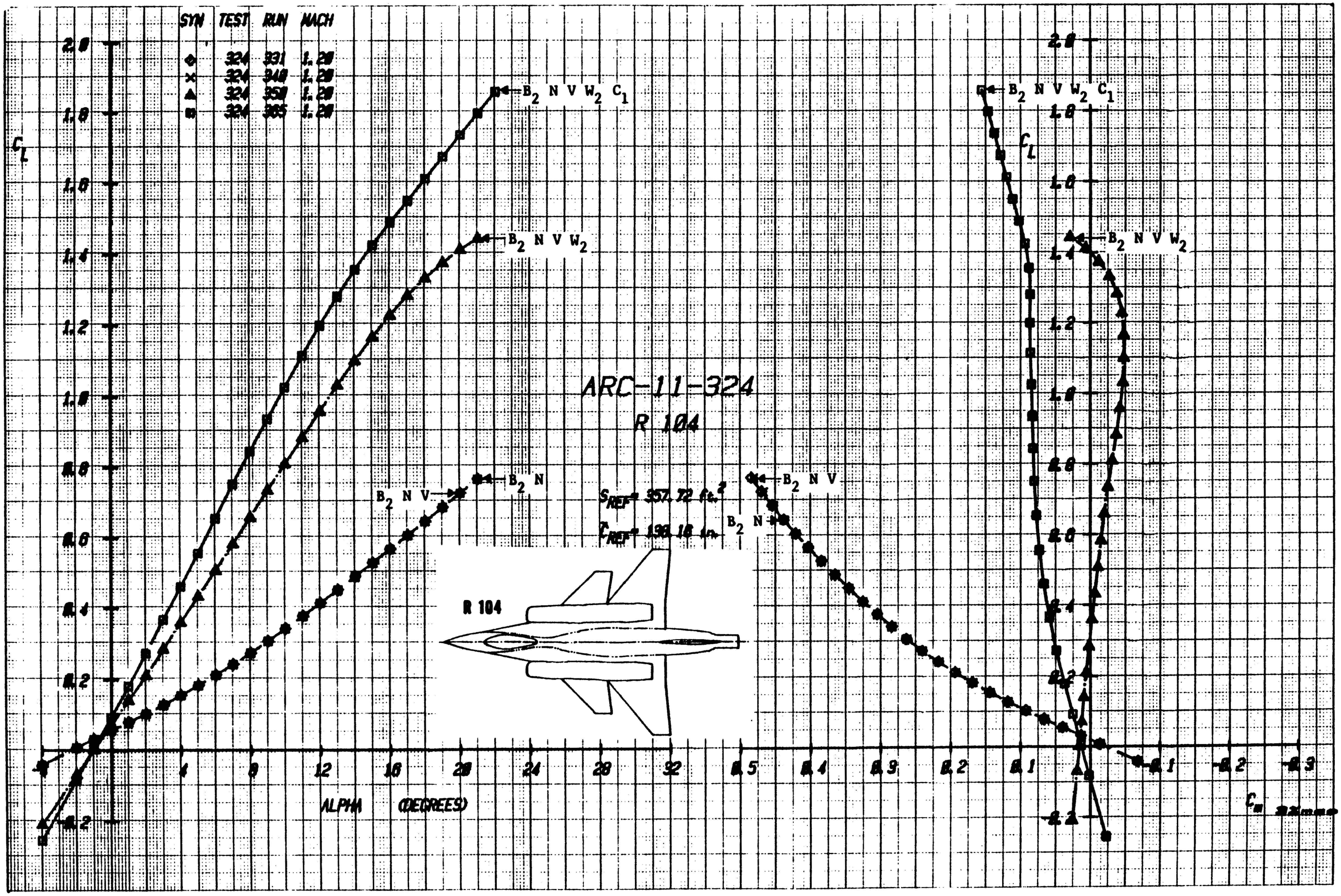

Figurel-10aEffect of Component Buildup on Lift and Moment, Mach = 1.20

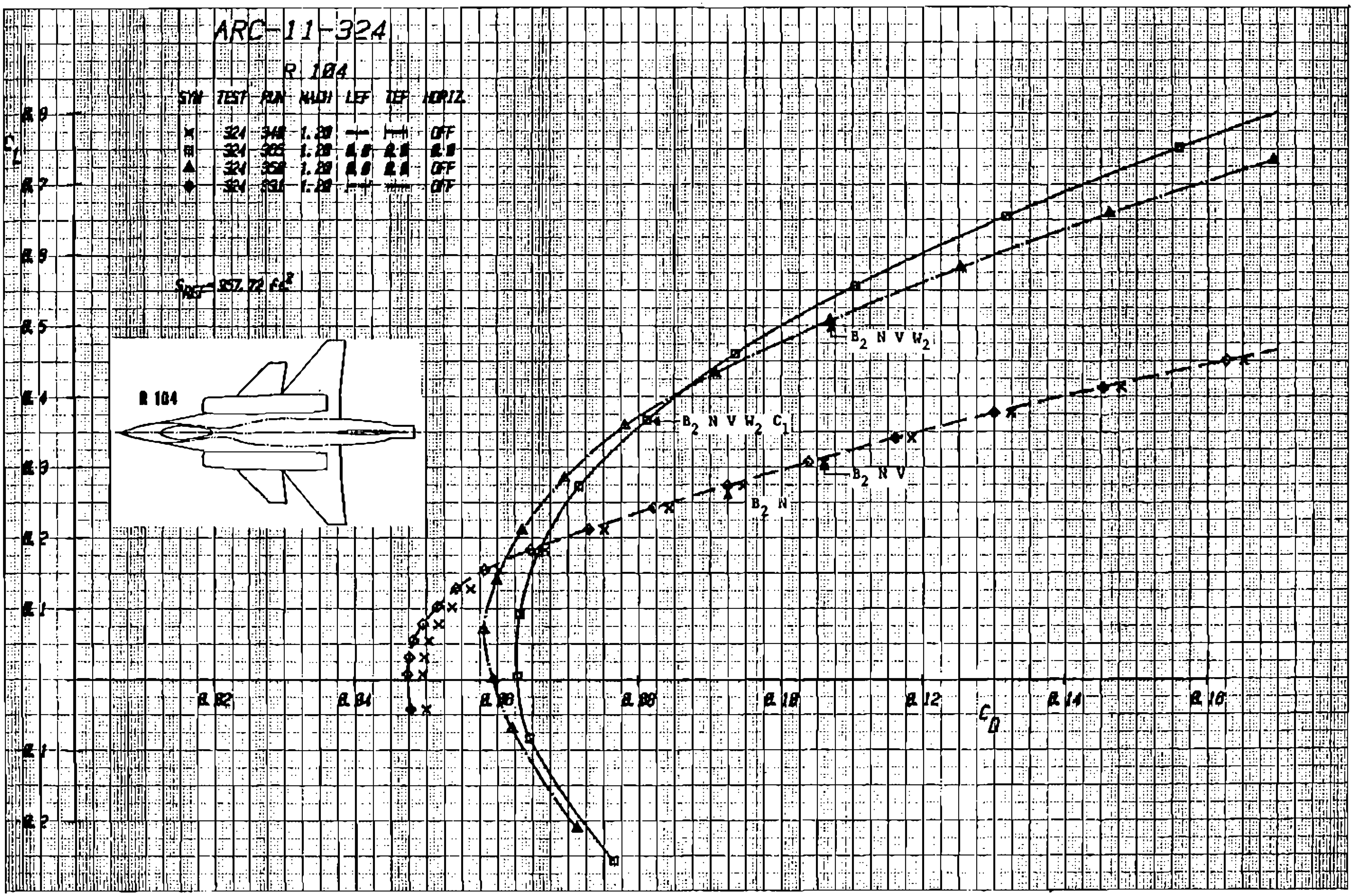

Figure1-10b Effect of Component Buildup on Drag, Mach = 1.20

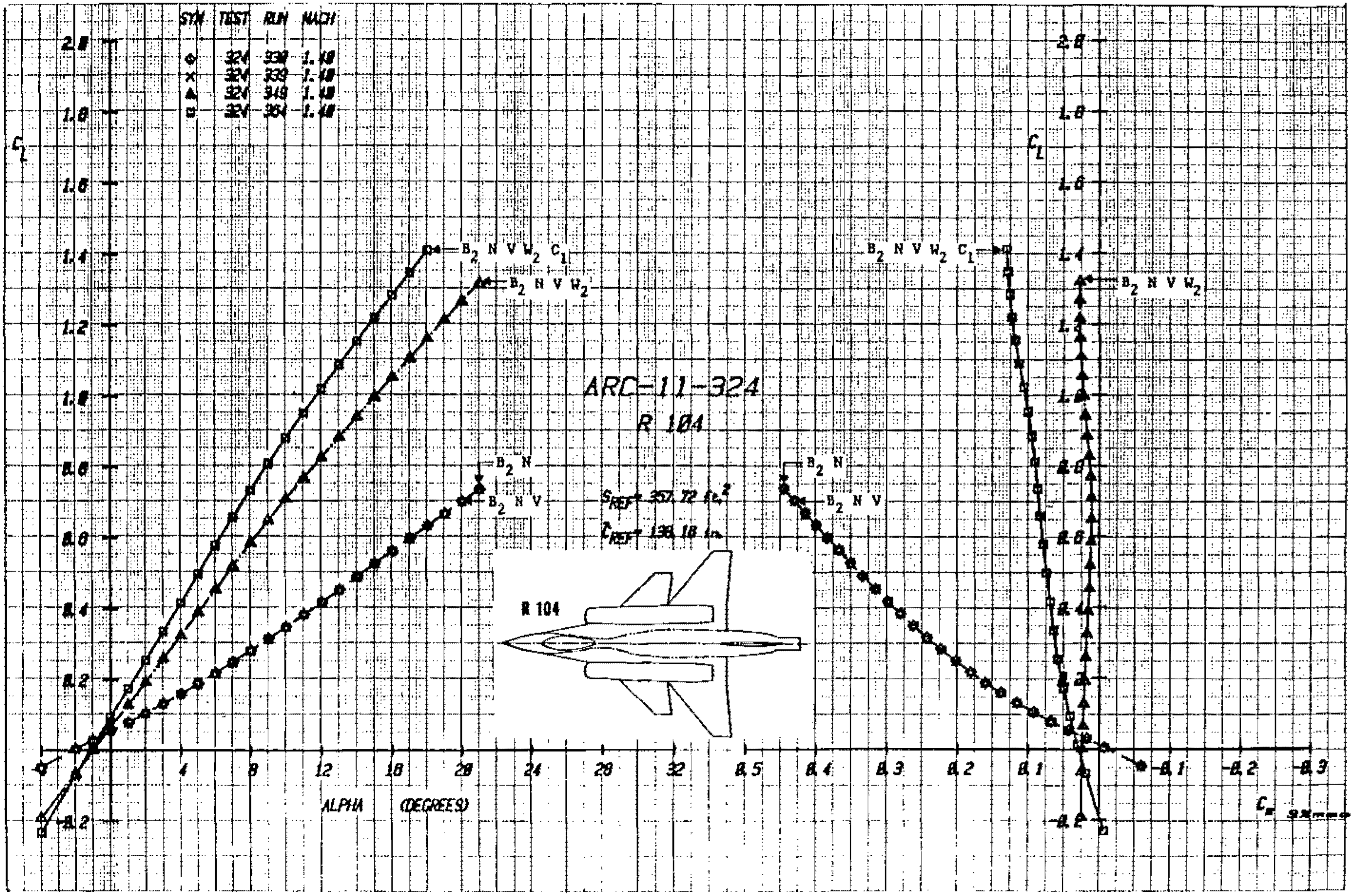

Figure1-11aEffect of Component Buildup on Lift and Moment, Mach = 1.4

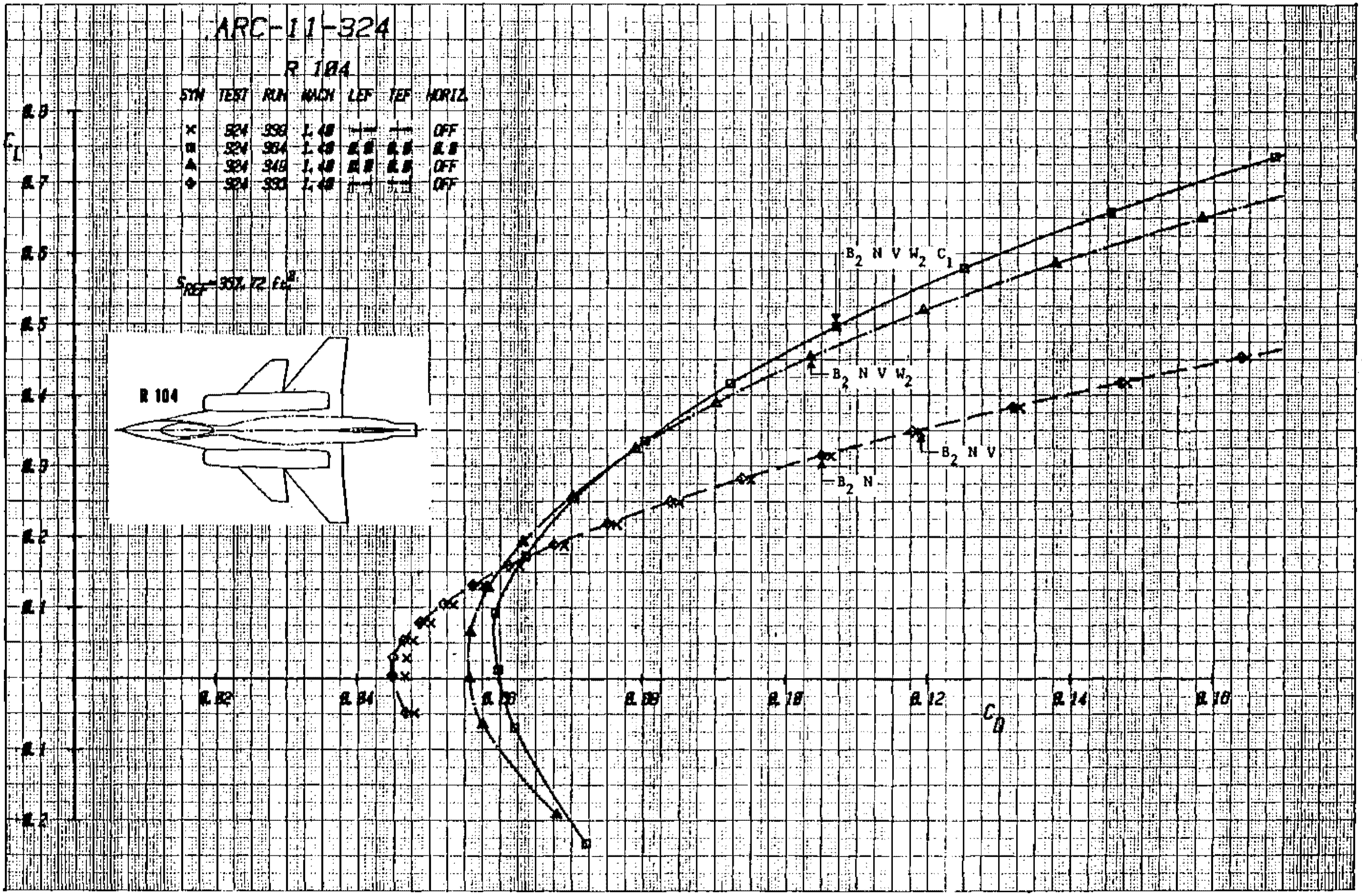

Figure1-11bEffect of Component Buildup on Drag, Mach = 1.4

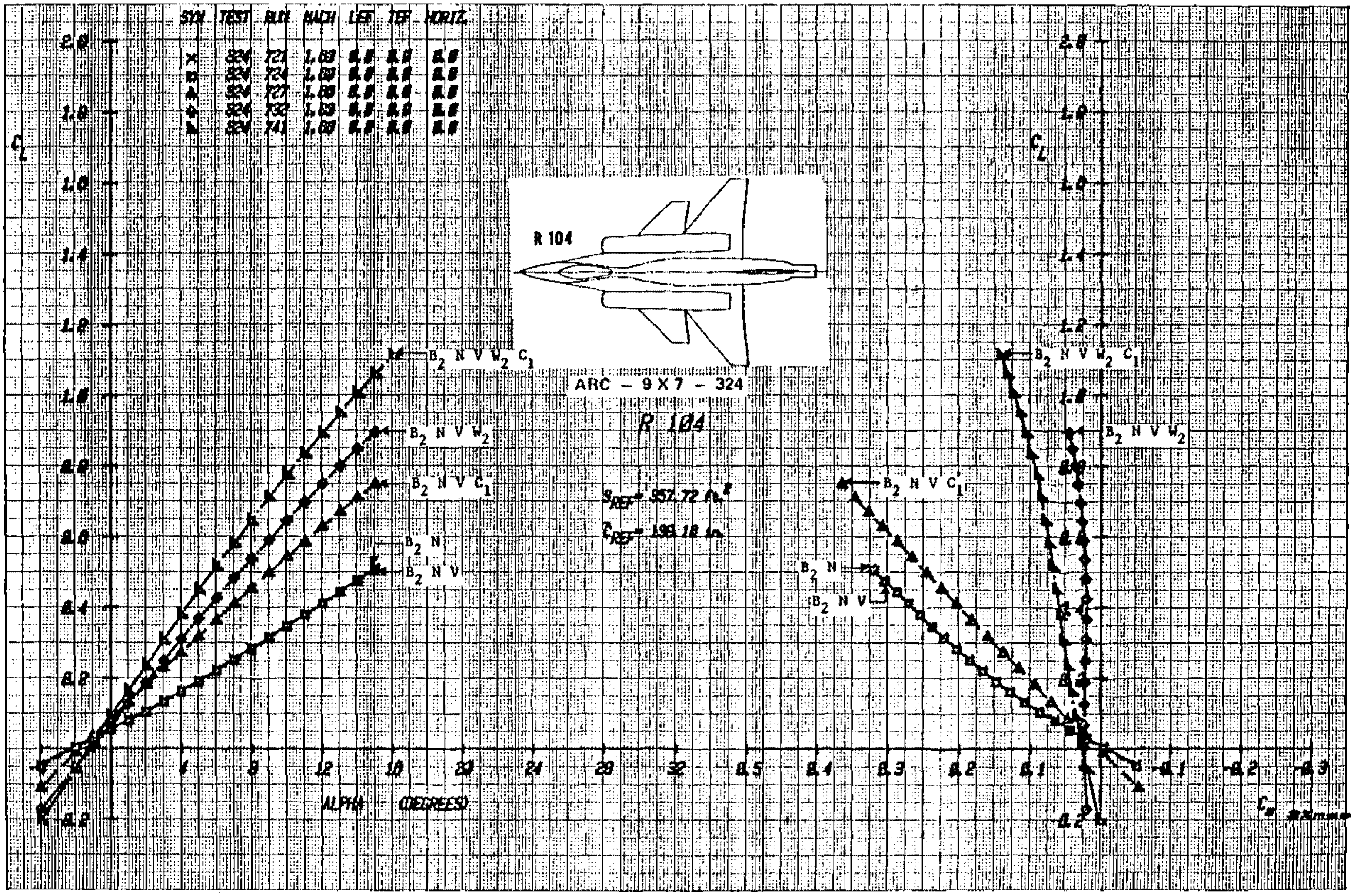

Figure1-12aEffect of Component Buildup on Lift and Moment, Mach = 1.6

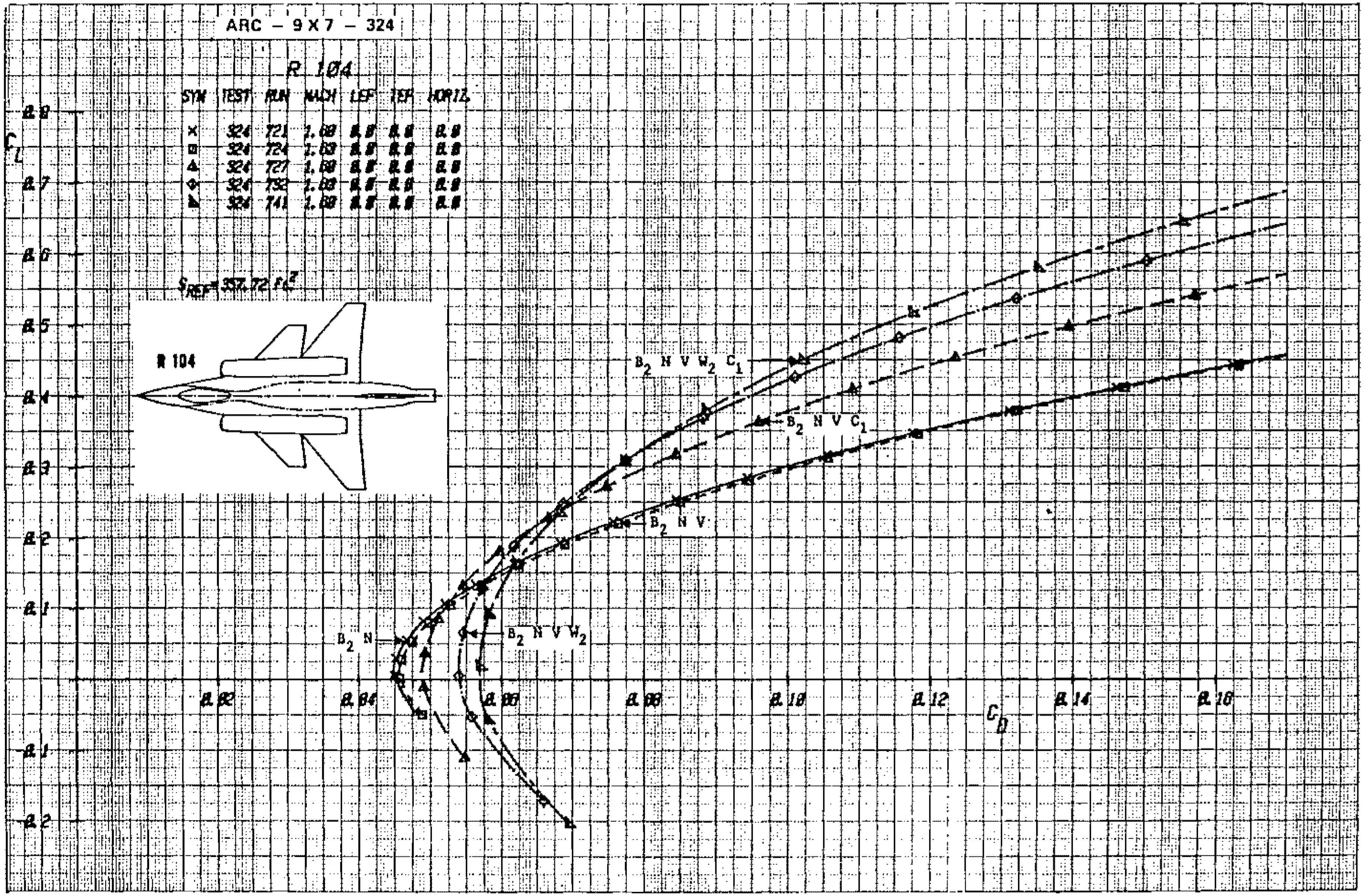

Figure1-12bEffect of Component Buildup on Drag (Expanded Drag Scale), Mach = 1.6

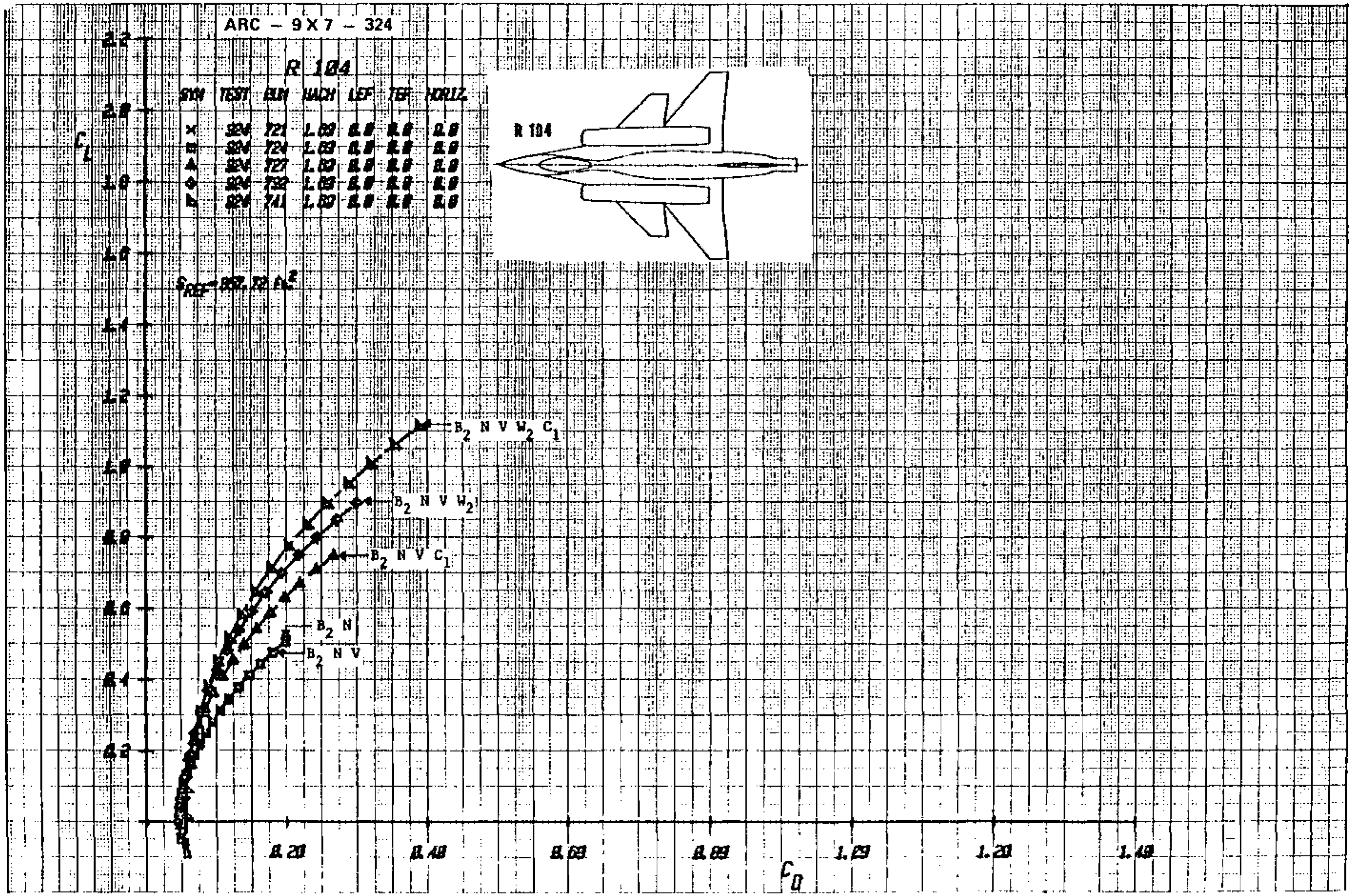

Figurel-12cEffect of Component Buildup on Drag, Mach = 1.6

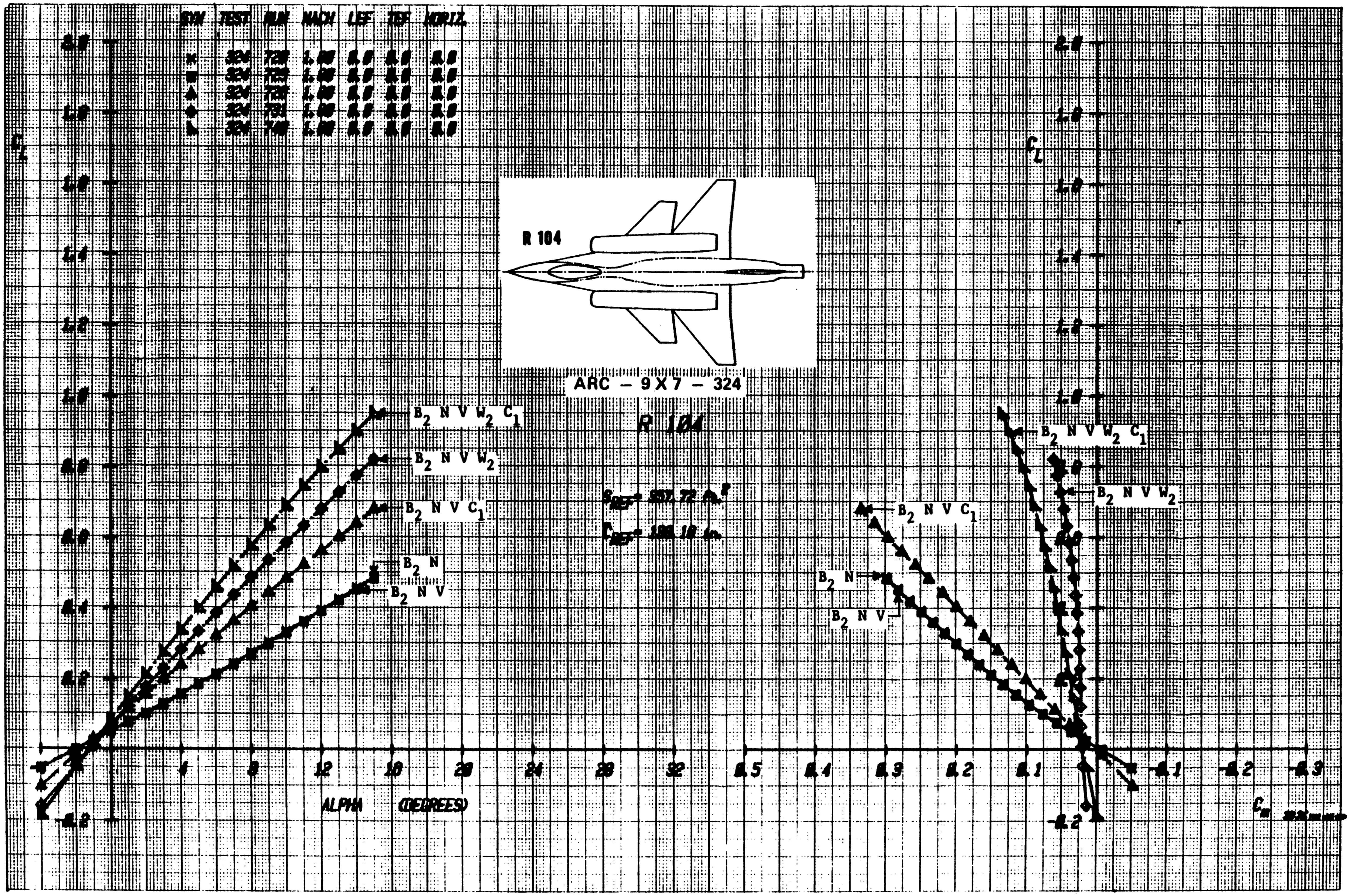

Figure1-13aEffect of Component Buildup on Lift and Moment, Mach = 1.8

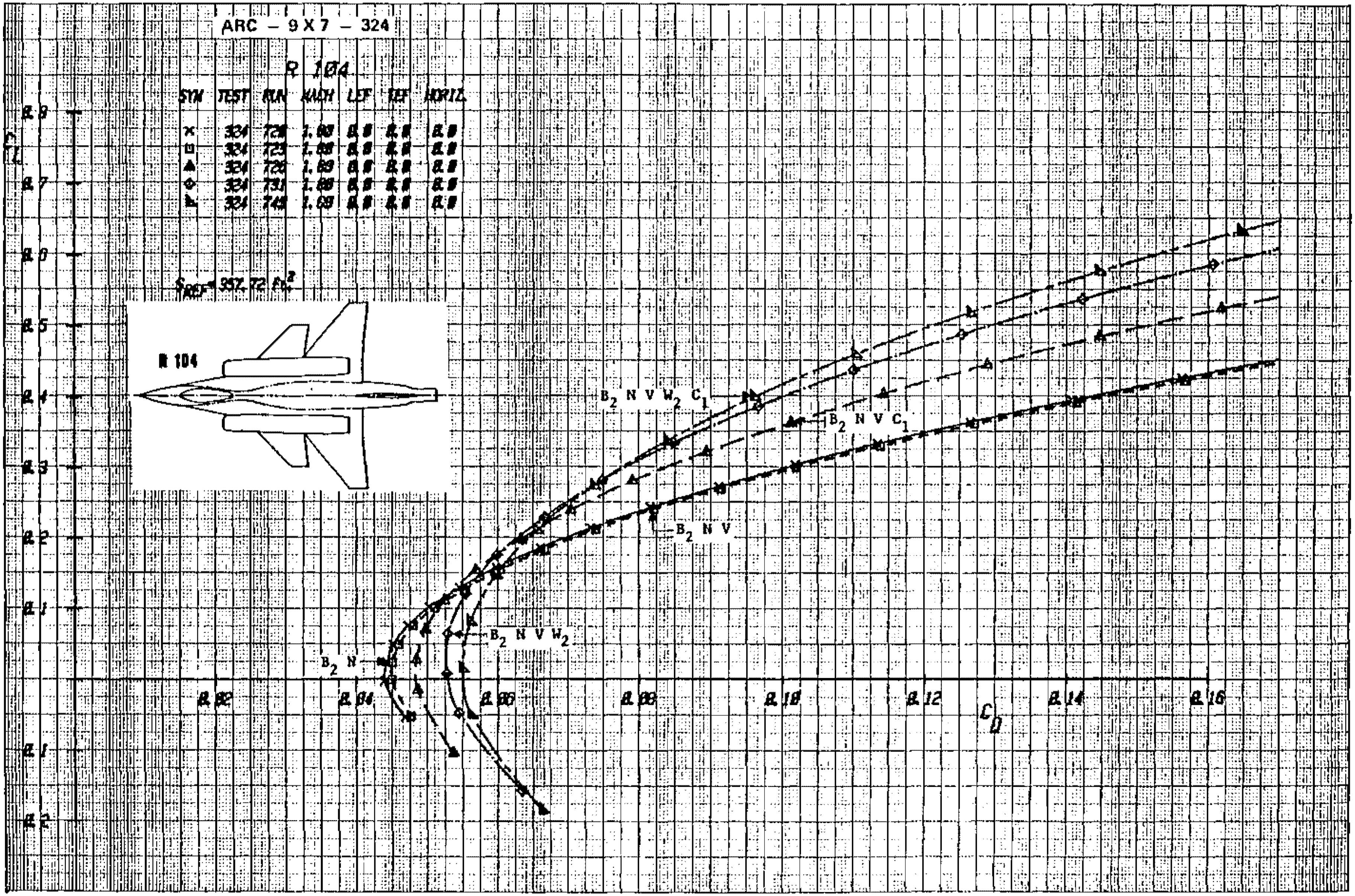

Figurel-13bEffect of Component Buildup on Drag, (Expanded Drag Scale), Mach = 1.8

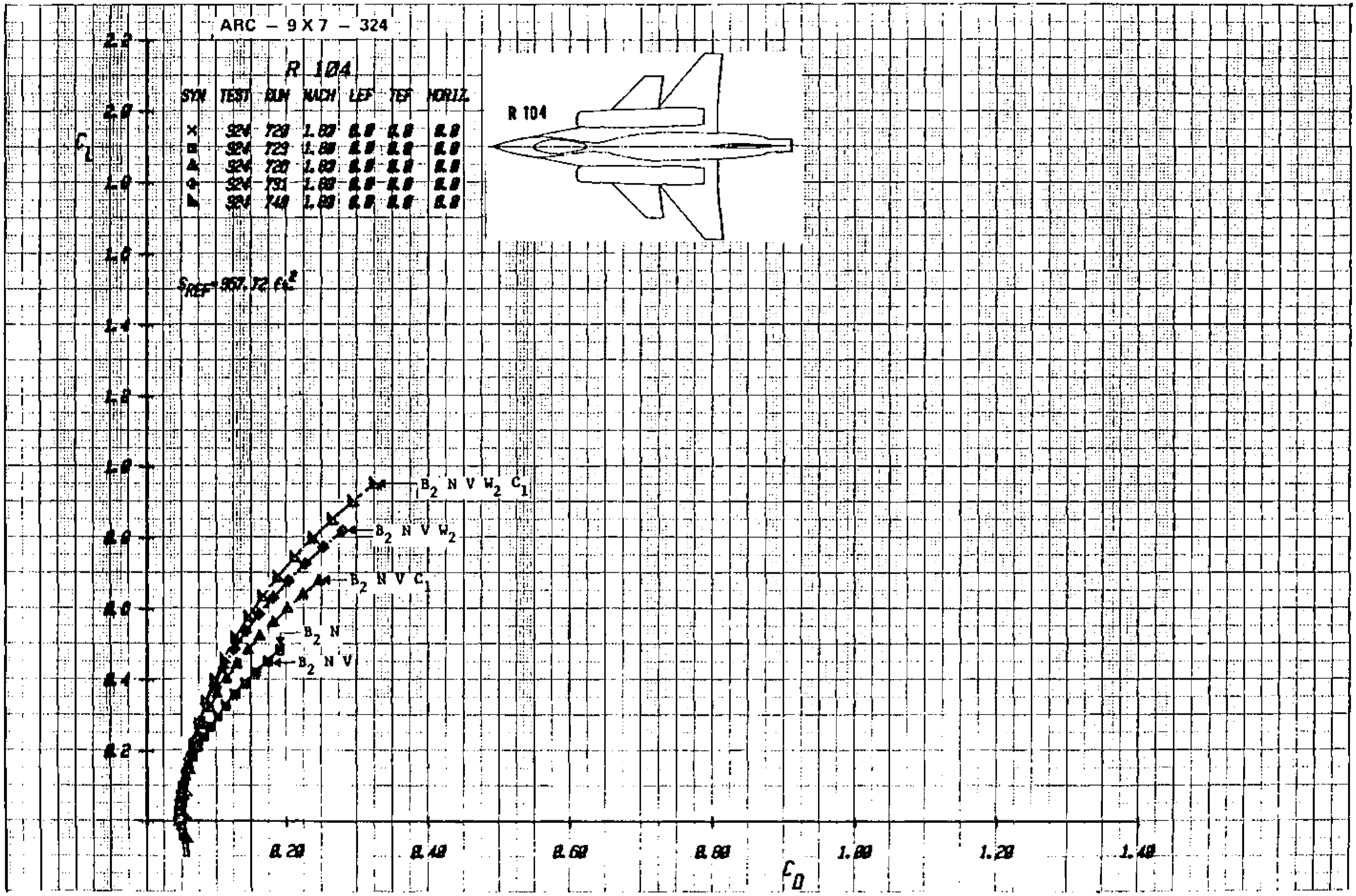

Figure1-13cEffect of Component Buildup on Drag, Mach = 1.8

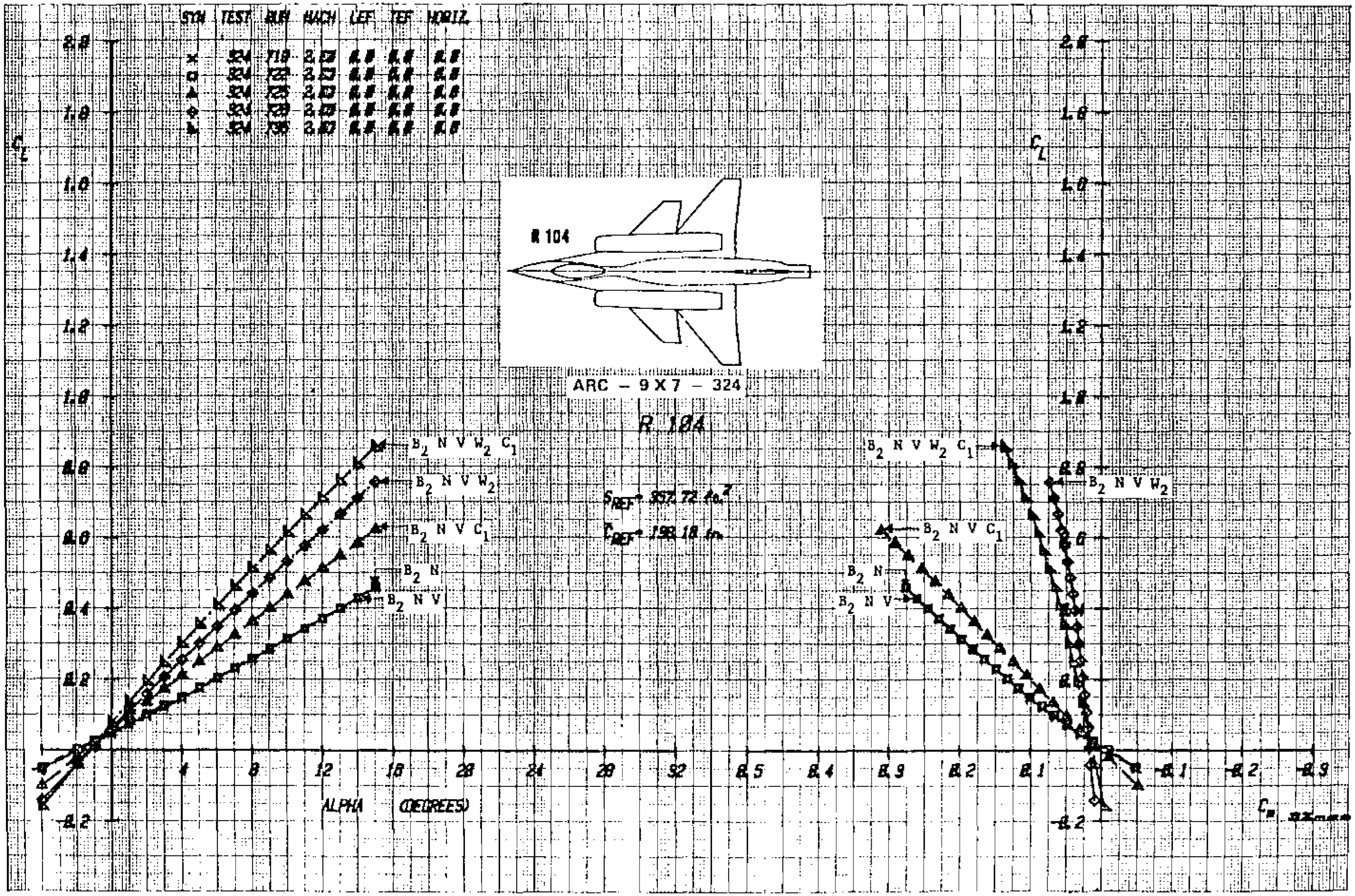

Figure1-14aEffect of Component Buildup on Lift and Moment, Mach = 2.0

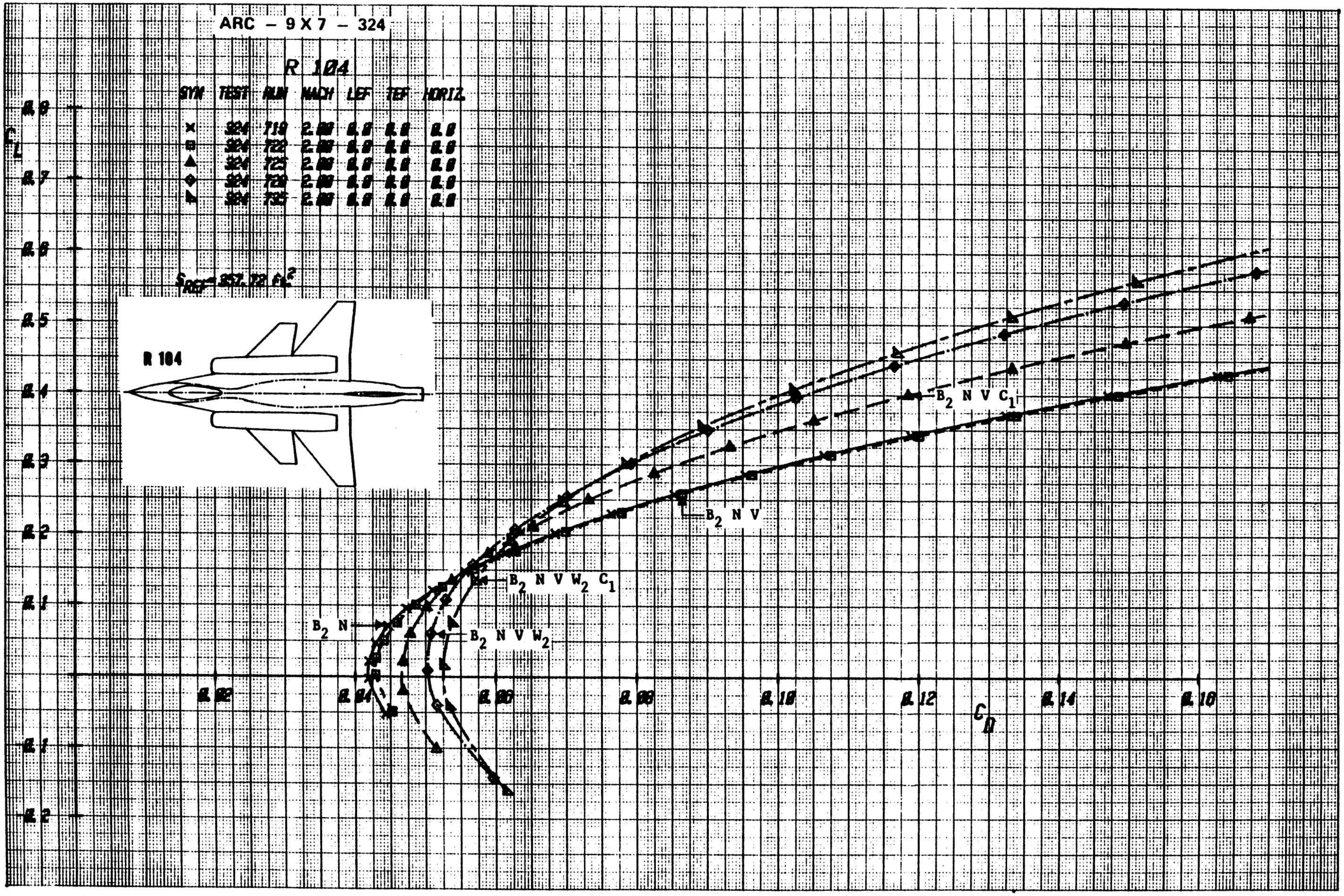

Figure1-14bEffect of Component Buildup on Drag, (Expanded Drag Scale), Mach = 2.0

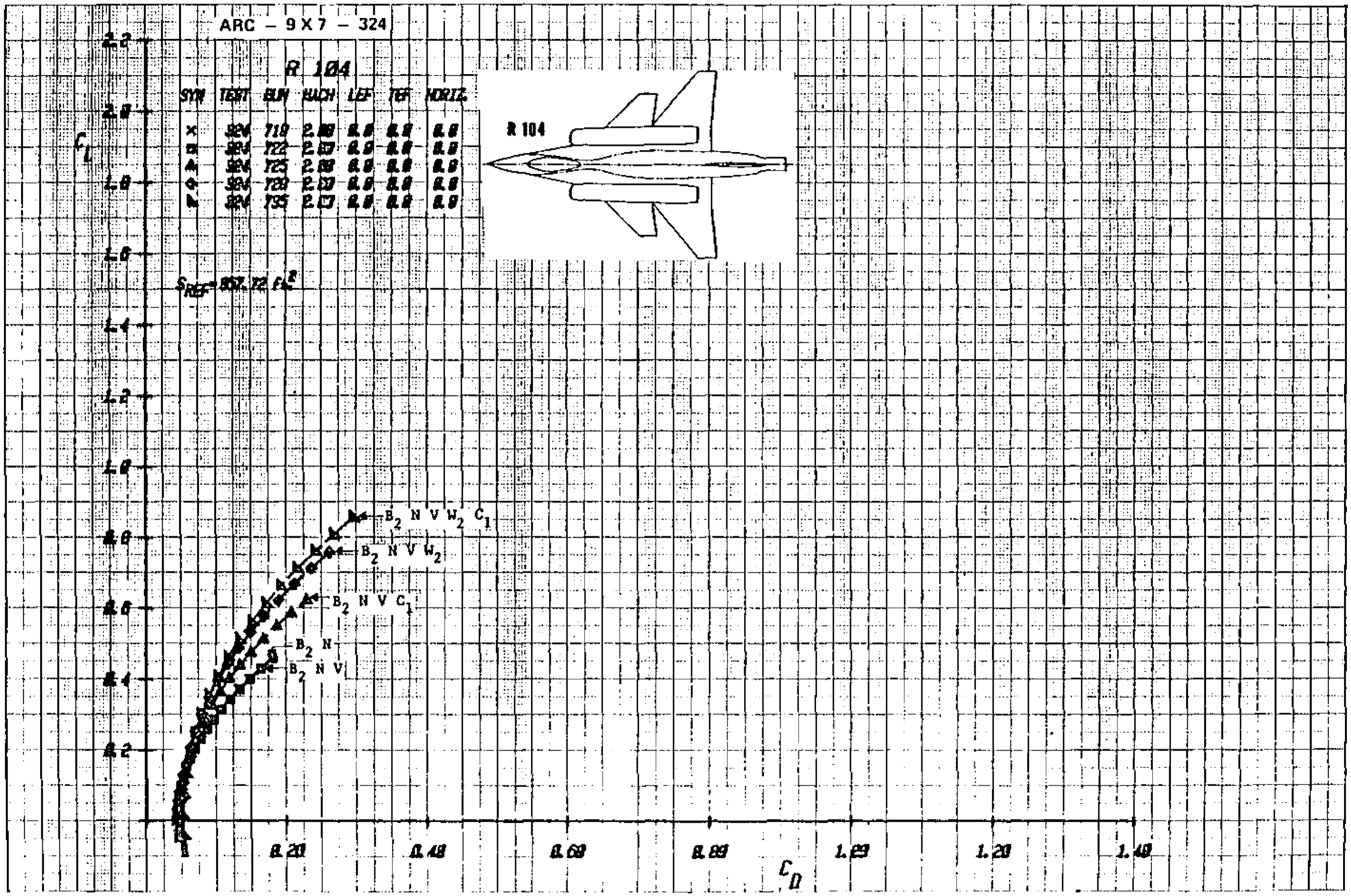

Figure1-14cEffect of Component Buildup on Drag, Mach = 2.0

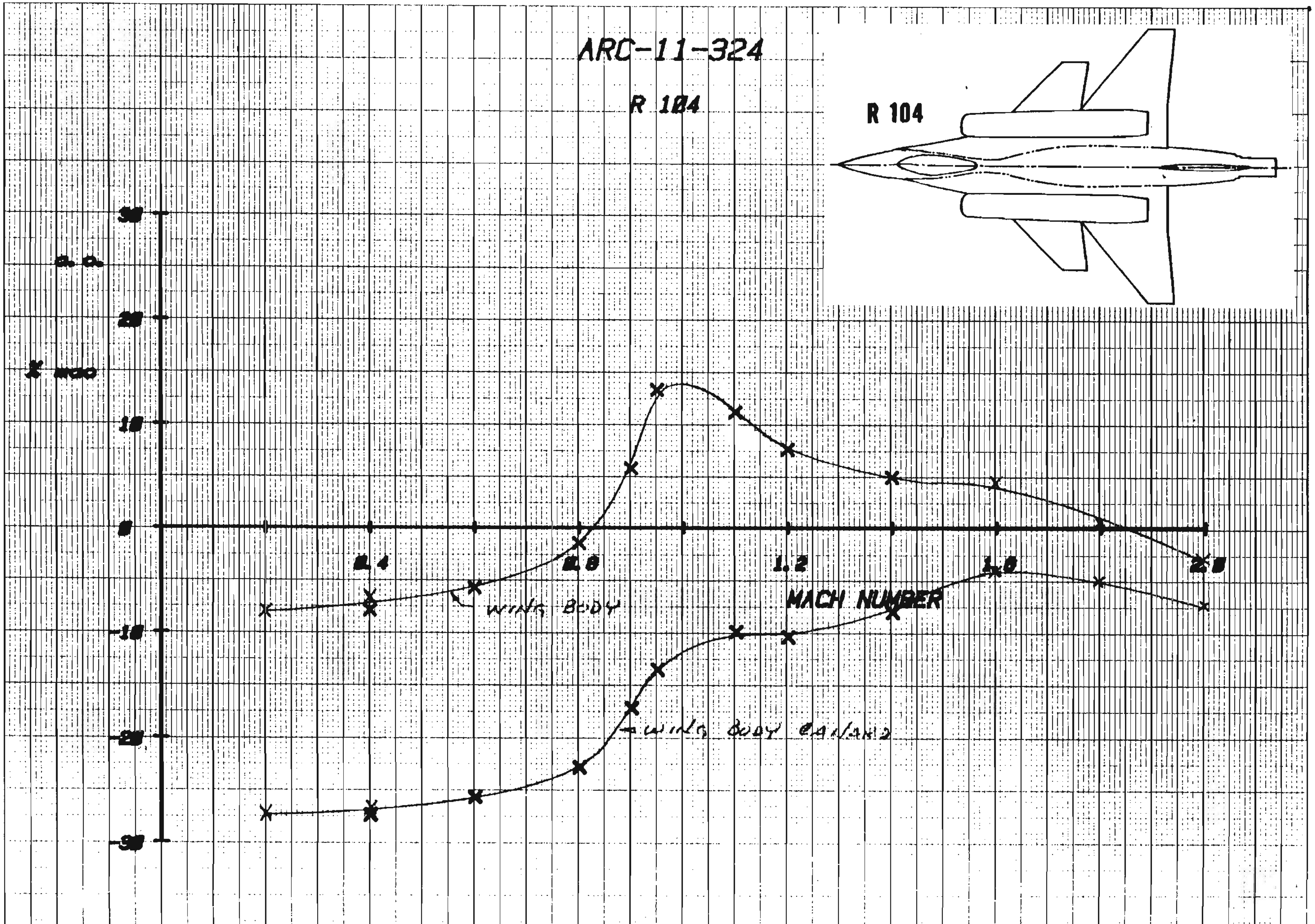

Figure 1-15 R104 Aerodynamic Center Variation with Mach Number

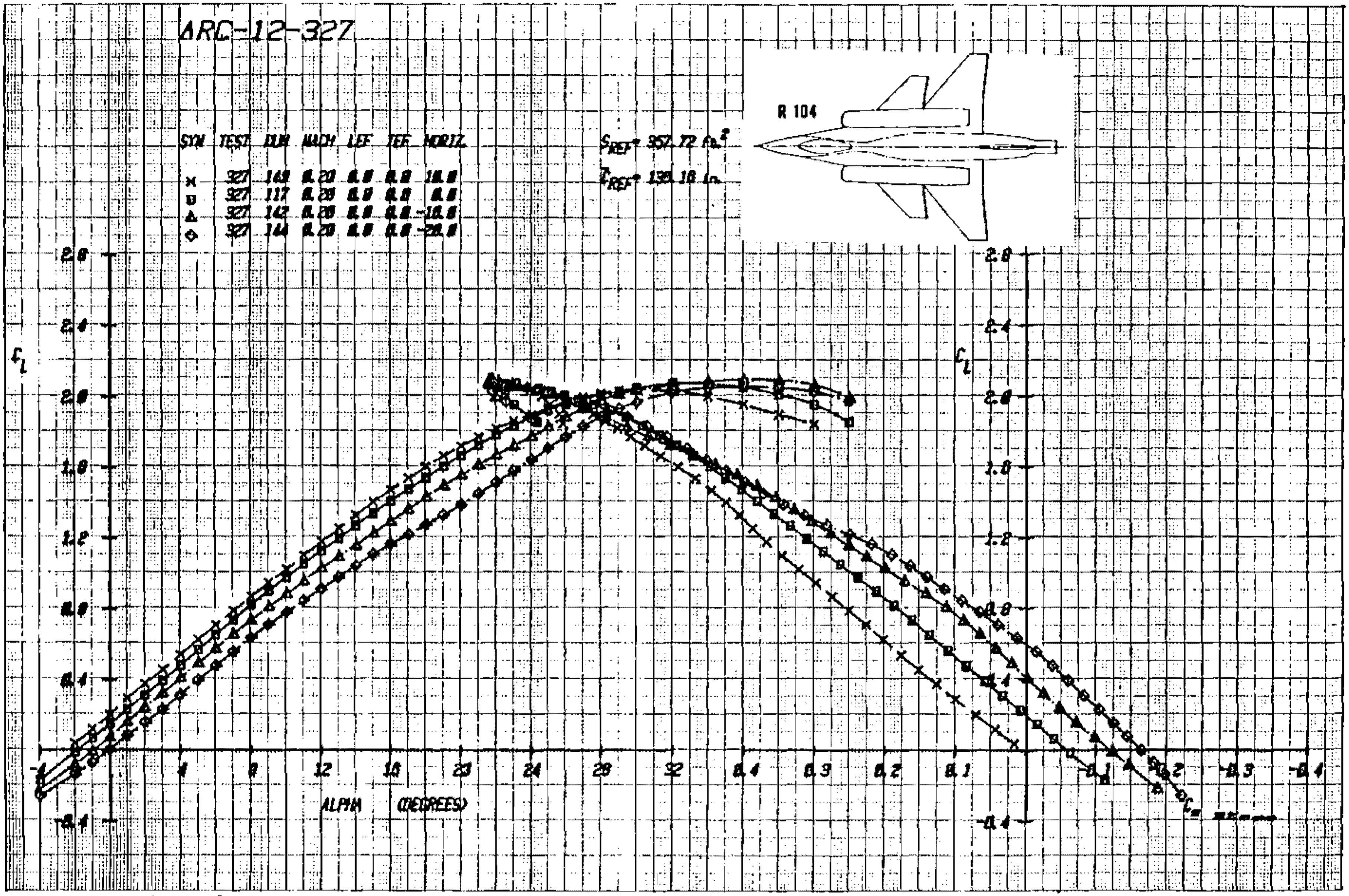

Figurel-16aEffect of Canard Deflection on Lift and Moment with Wing Trailing-Edge
Flap Undeflected, Mach = .2

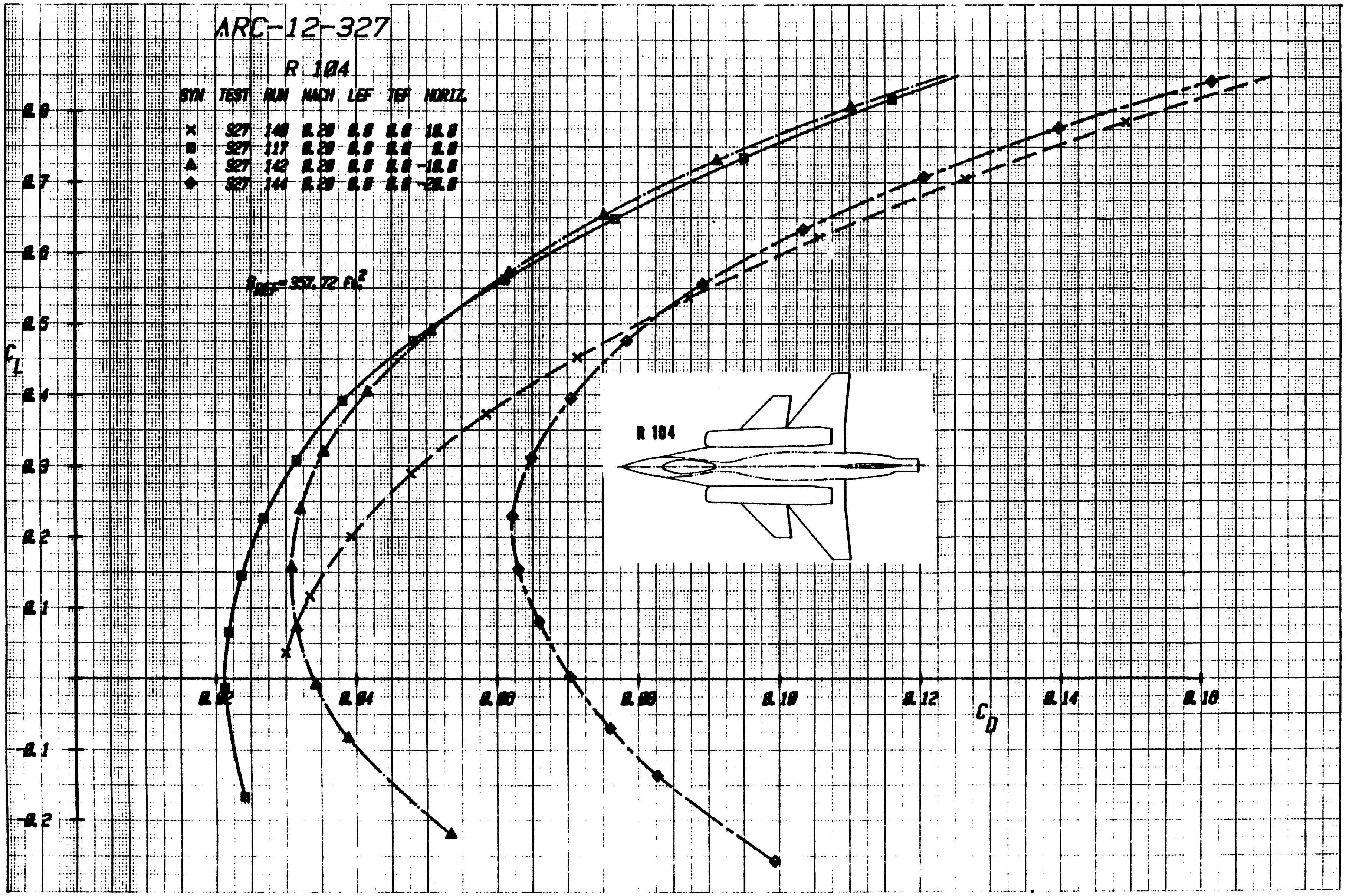

Figure1-16b Effect of Canard Deflection on Drag with Wing Trailing-Edge Flap Undeflected, (Expanded Drag Scale), Mach = .2

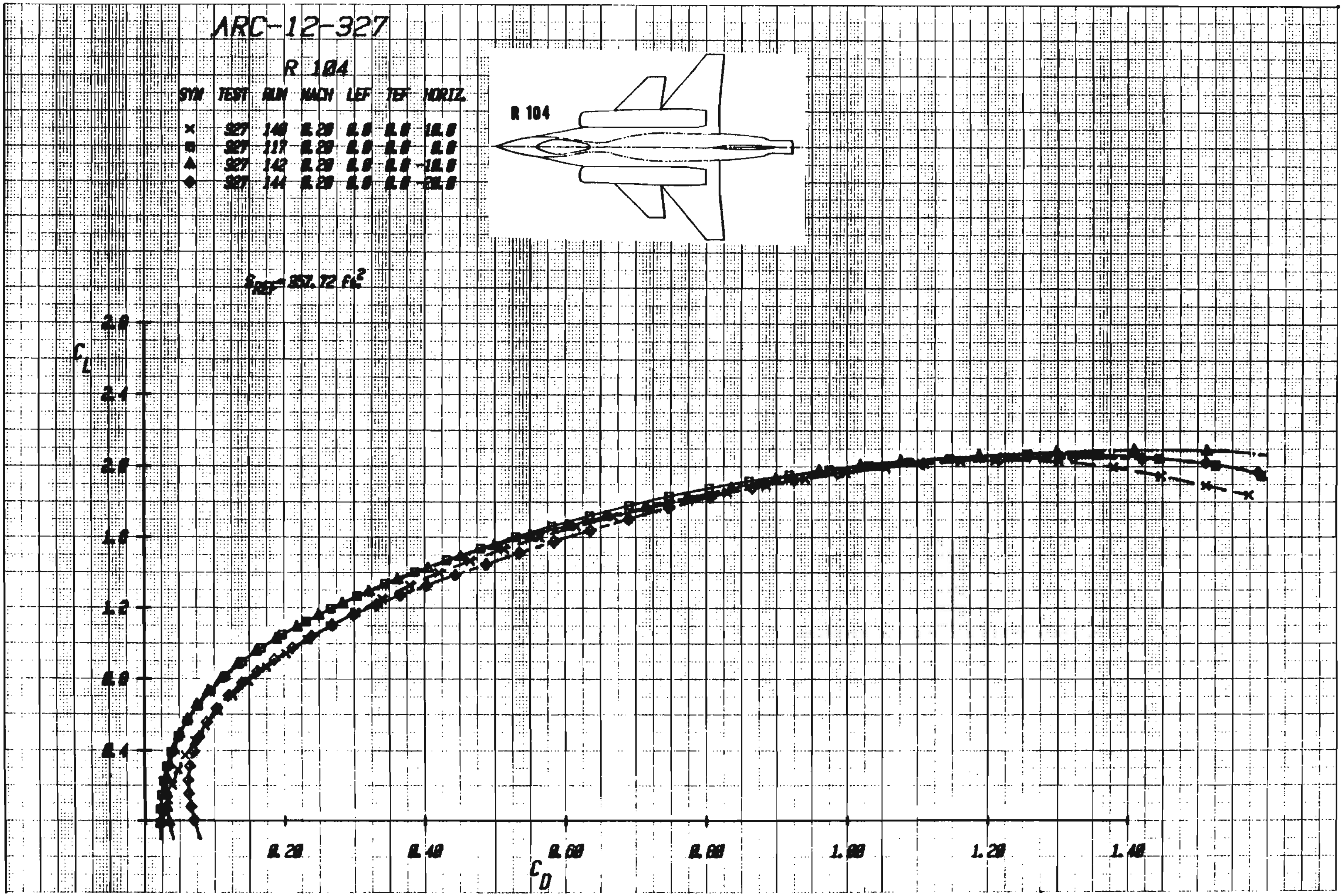

Figurel-16cEffect of Canard Deflection on Drag with Wing Trailing-Edge Flap
Undeflected, Mach = .2

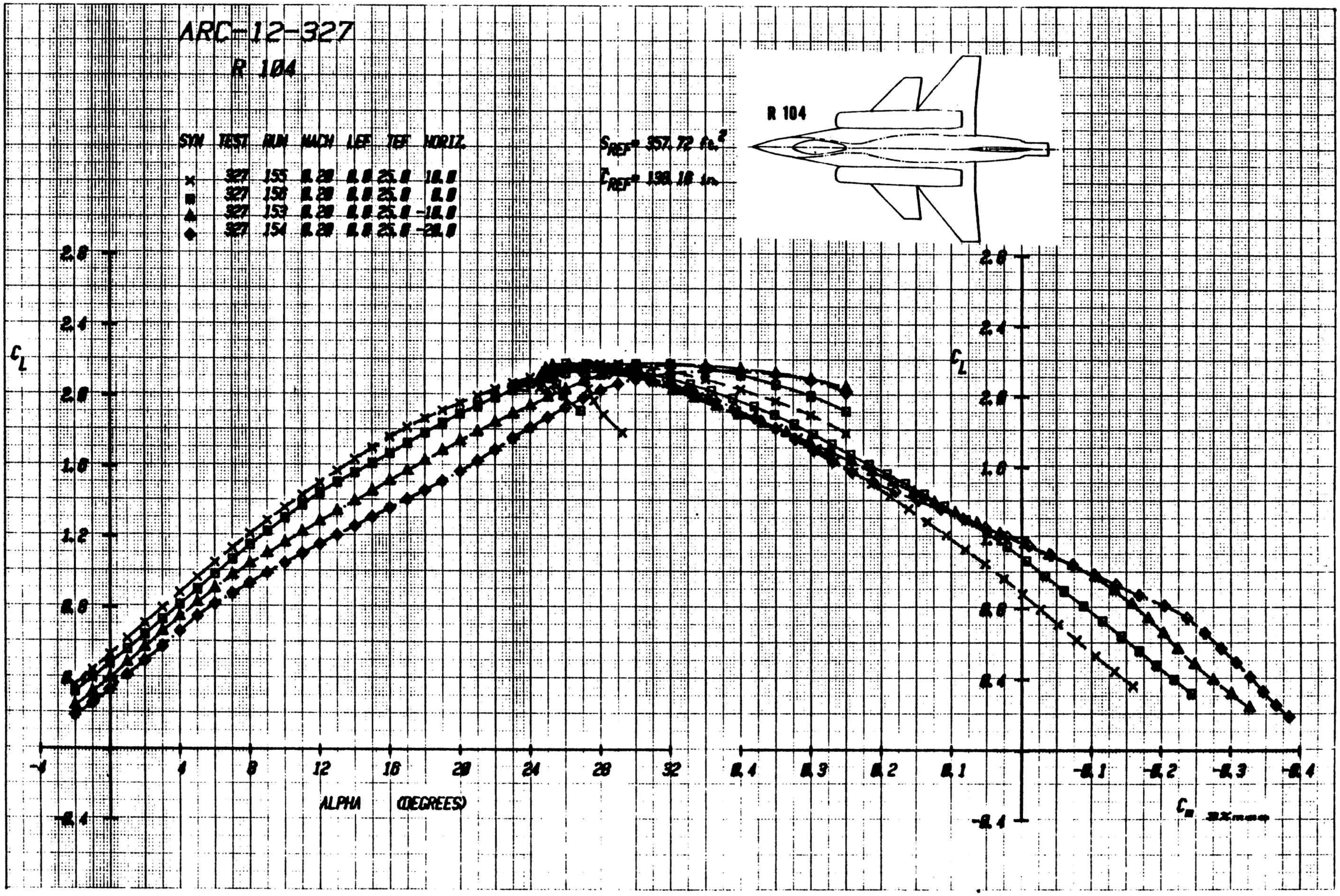

Figure1-17aEffect of Canard Deflection on Lift and Moment with Wing Trailing-Edge Flap Deflected +25°, Mach = .2

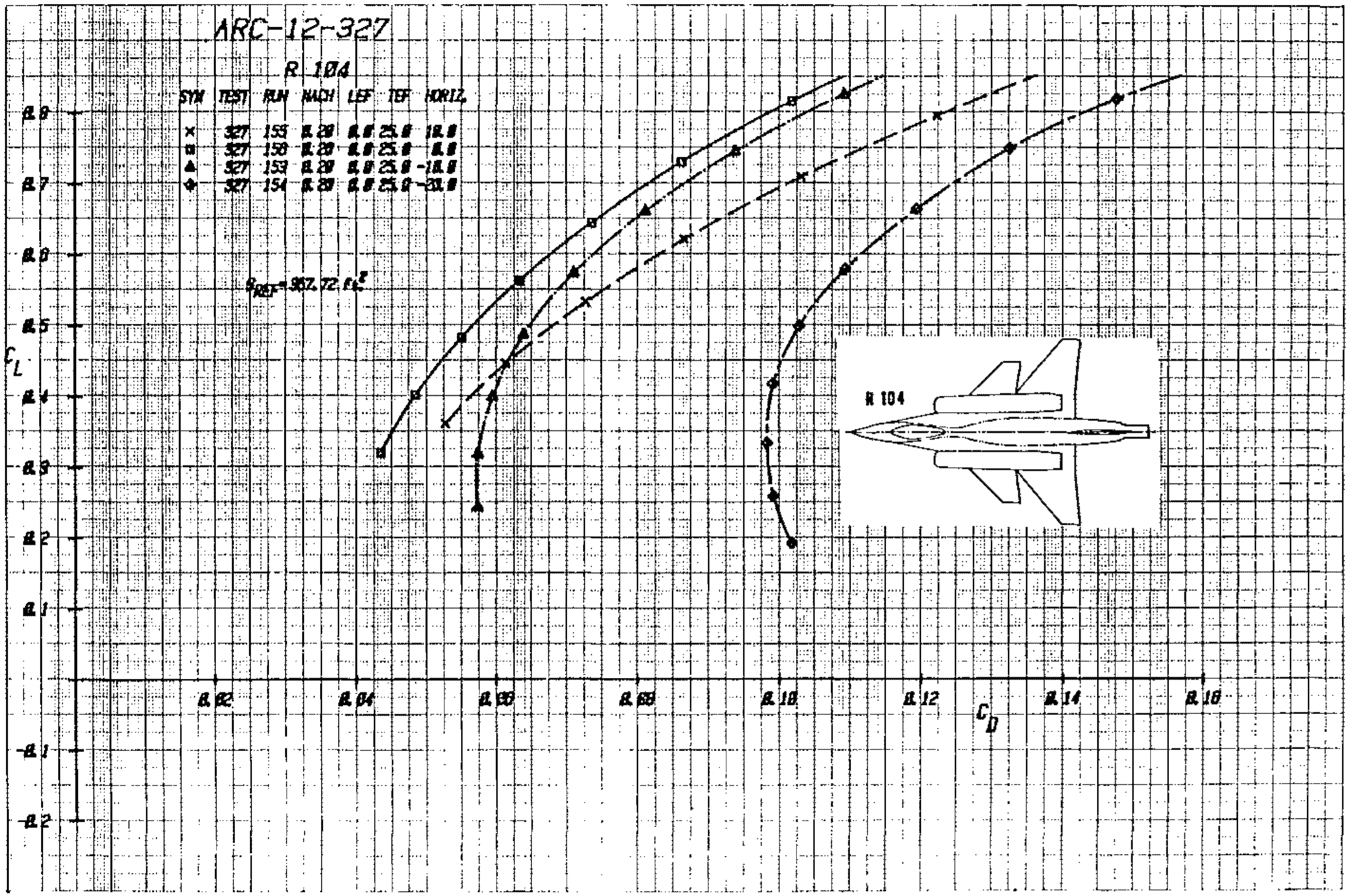

Figure1-17bEffect of Canard Deflection on Drag with Wing Trailing-Edge Flap Deflected +25° (Expanded Drag Scale), Mach = .2

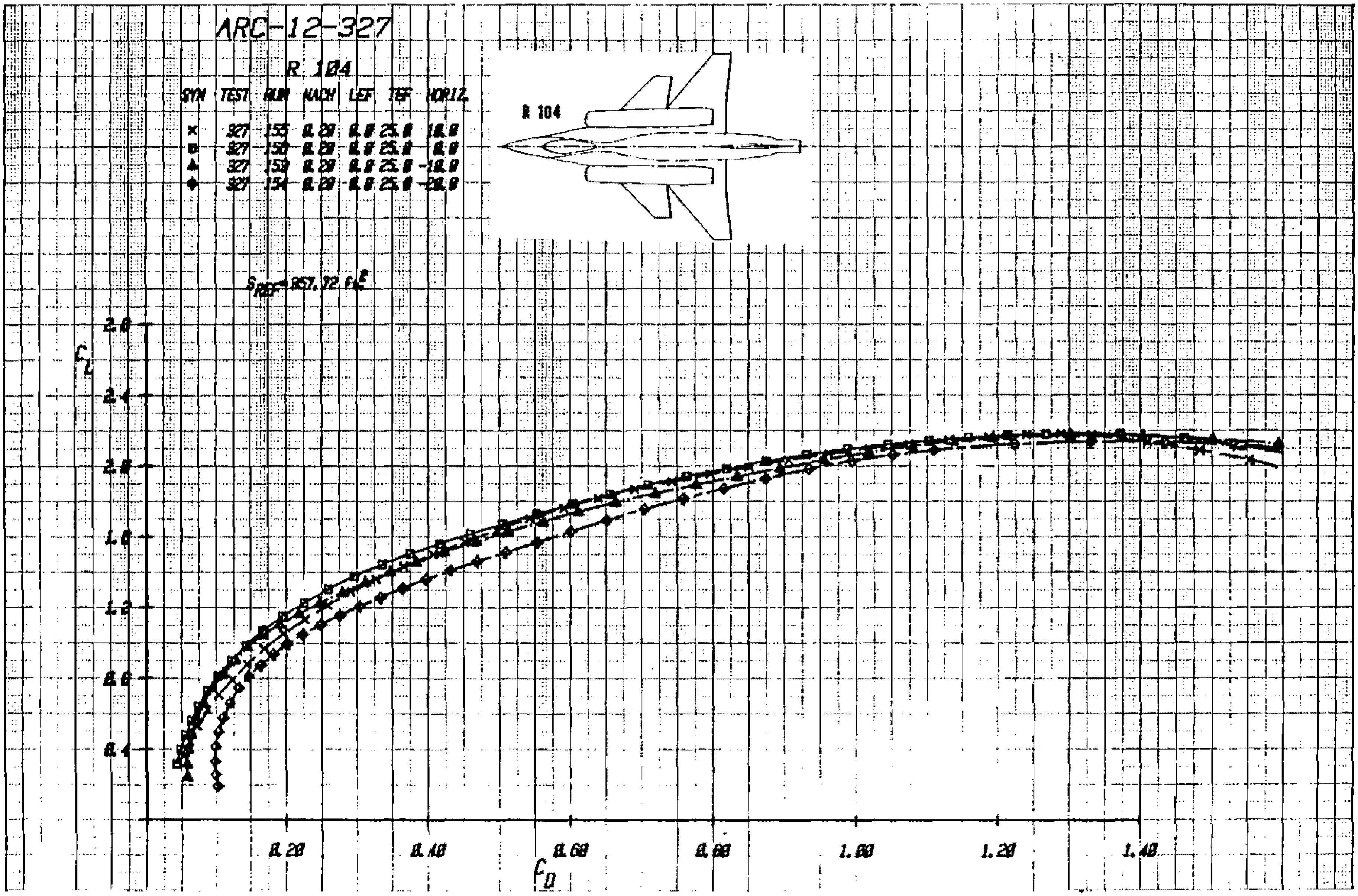

Figure1-17cEffect of Canard Deflection on Drag with Wing Trailing-Edge Flap
Deflected +25°, Mach = .2

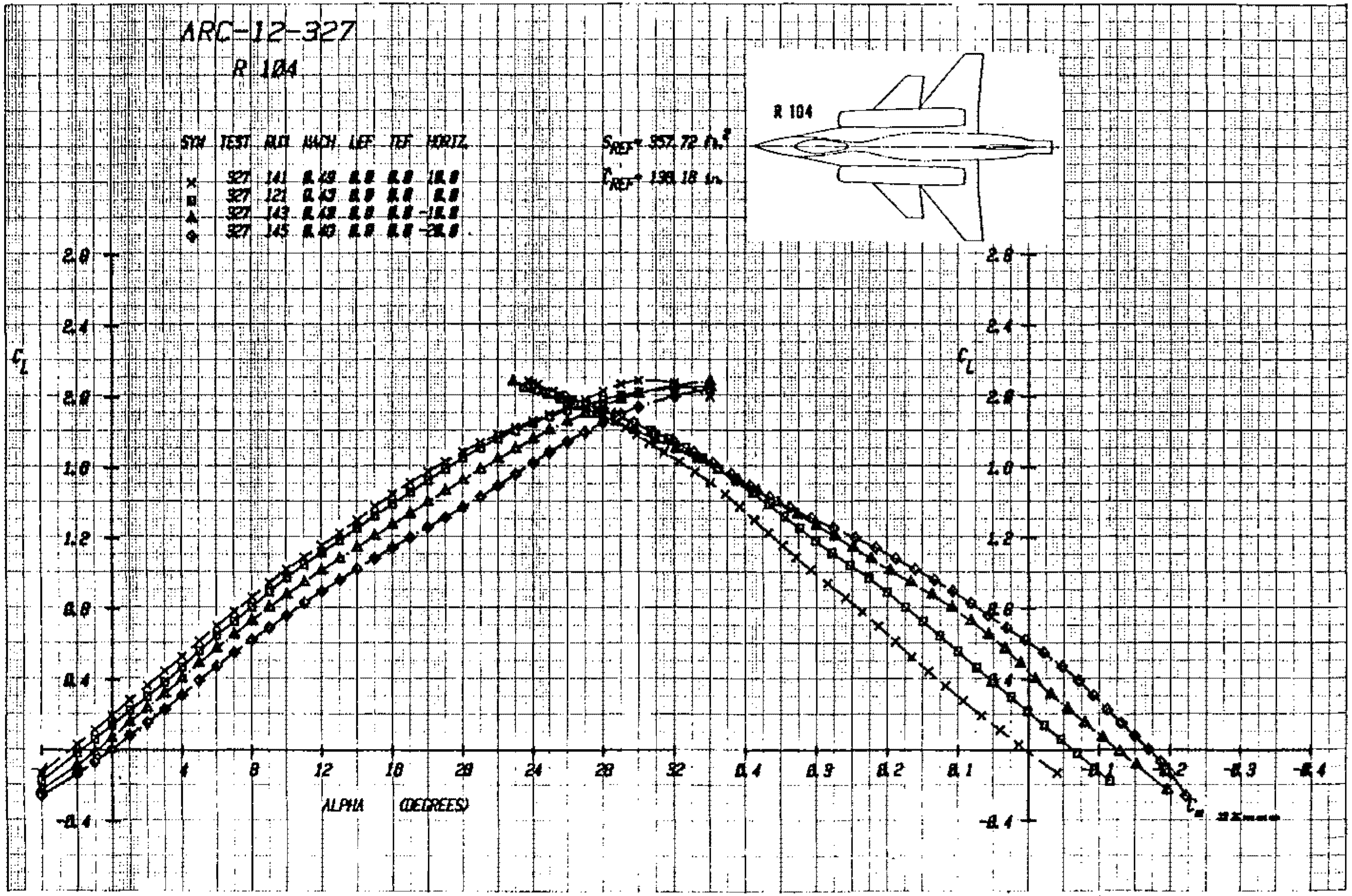

Figure1-18aEffect of Canard Deflection on Lift and Moment with Wing Trailing-Edge Flap Undeflected, Mach = .4

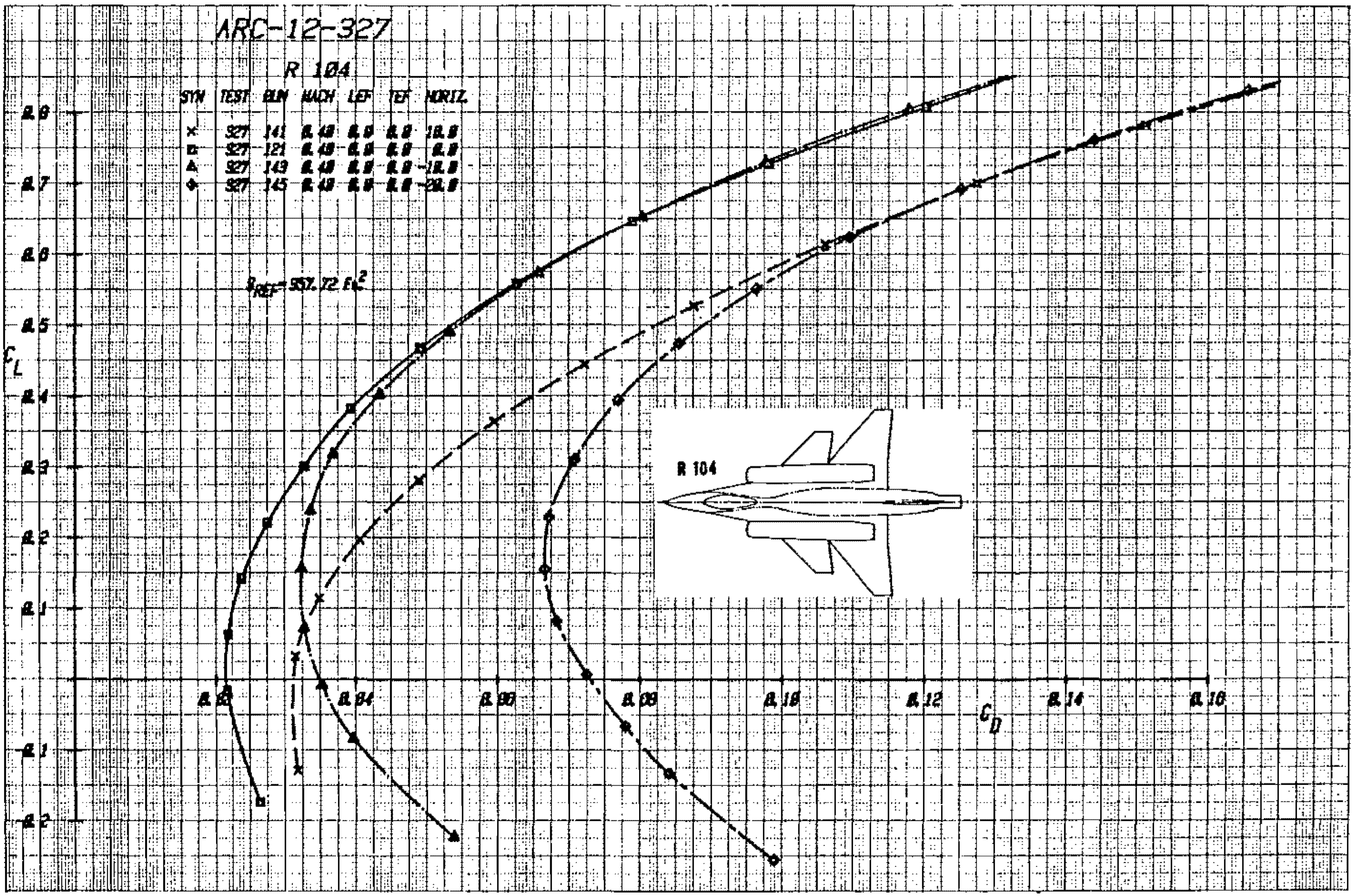

Figure1-18bEffect of Canard Deflection on Drag with Wing Trailing-Edge Flap Undeflected, (Expanded Drag Scale), Mach = .4

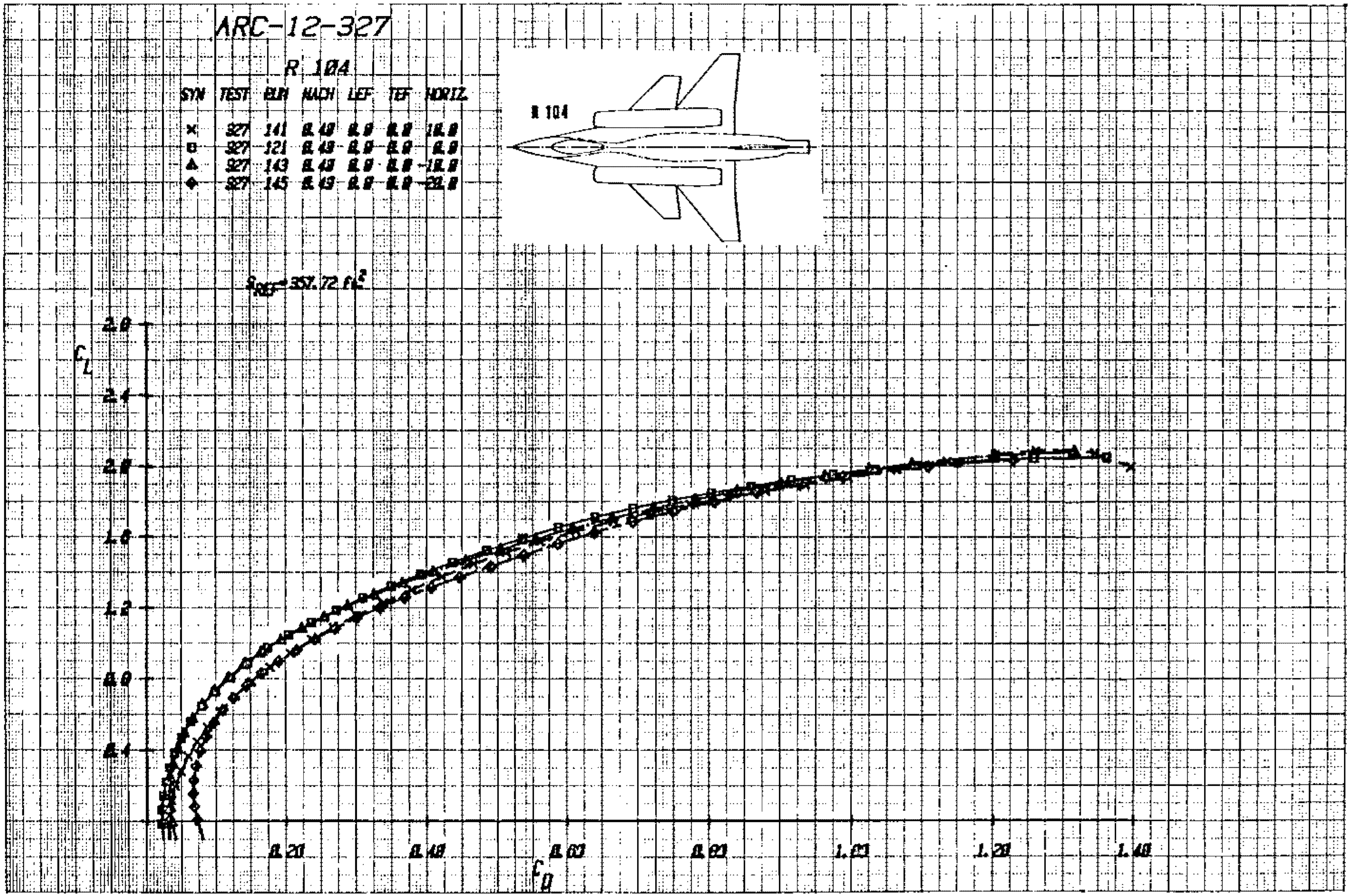

Figure1-18cEffect of Canard Deflection on Drag with Wing Trailing-Edge Flap Undeflected, Mach = .4

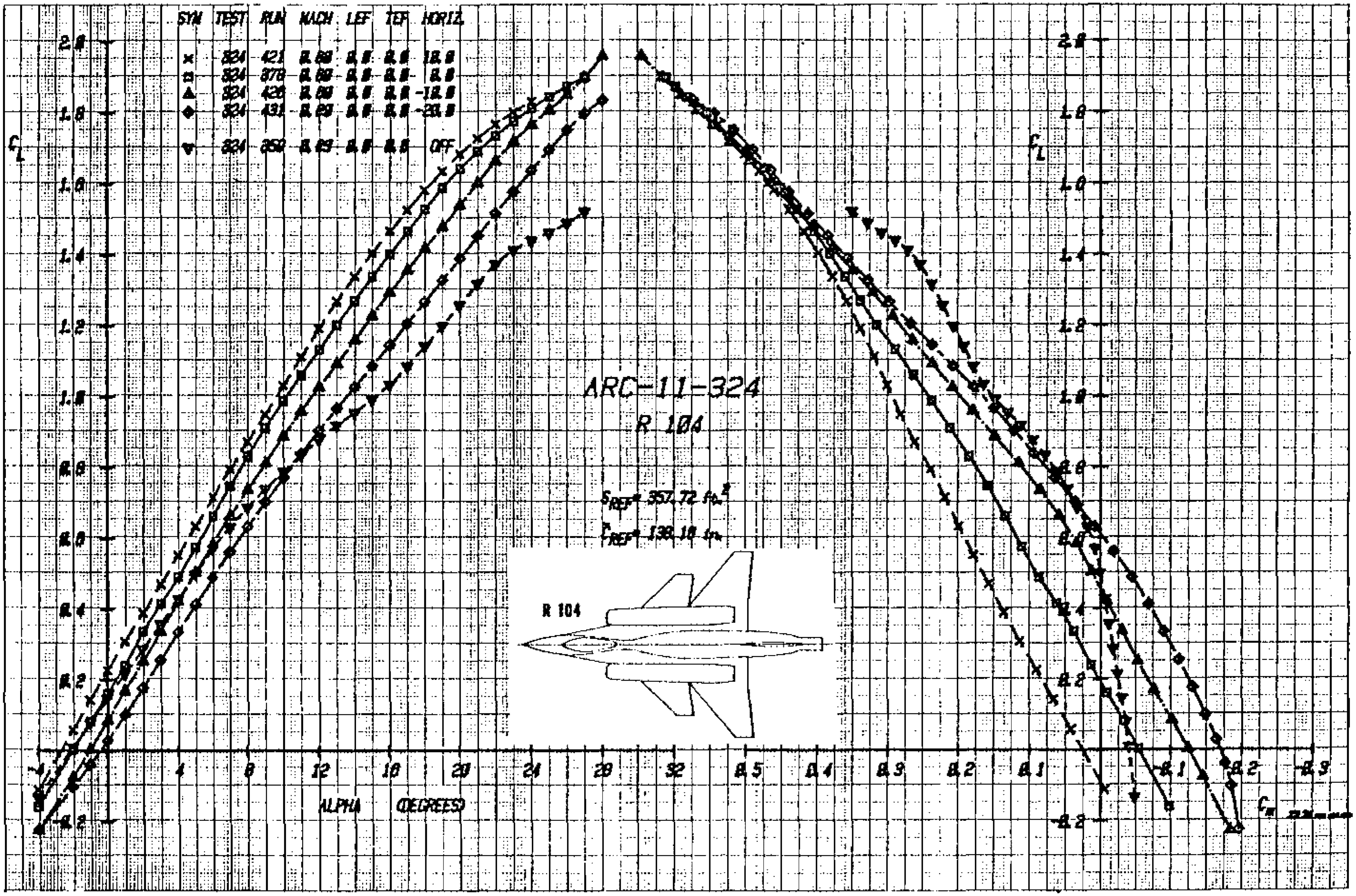

Figure1-19aEffect of Canard Deflection on Lift and Moment with Wing Trailing-Edge Flap Undeflected, Mach = .6

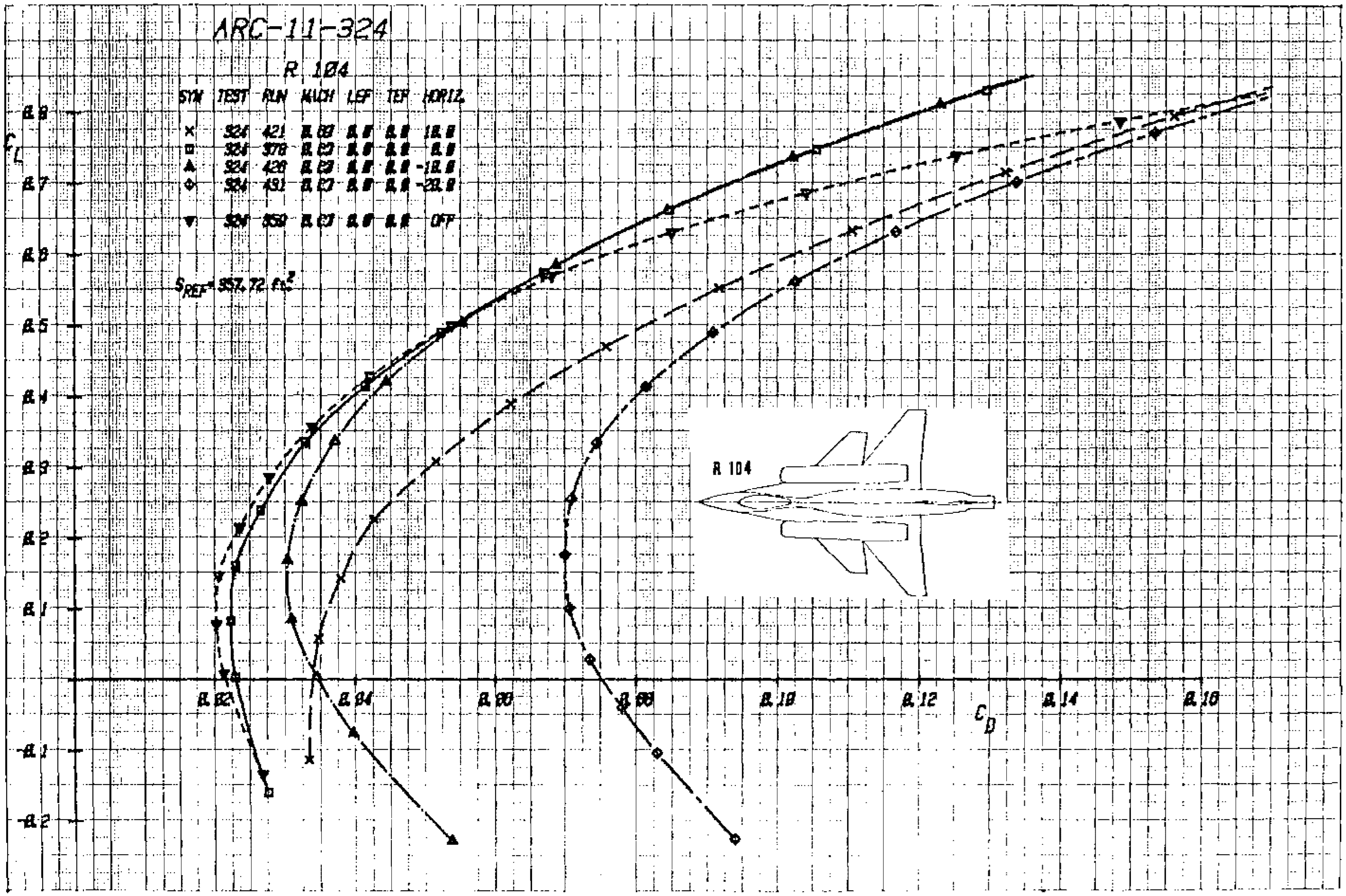

Figure1-19bEffect of Canard Deflection on Drag with Wing Trailing-Edge Flap
Undeflected, Mach = .6

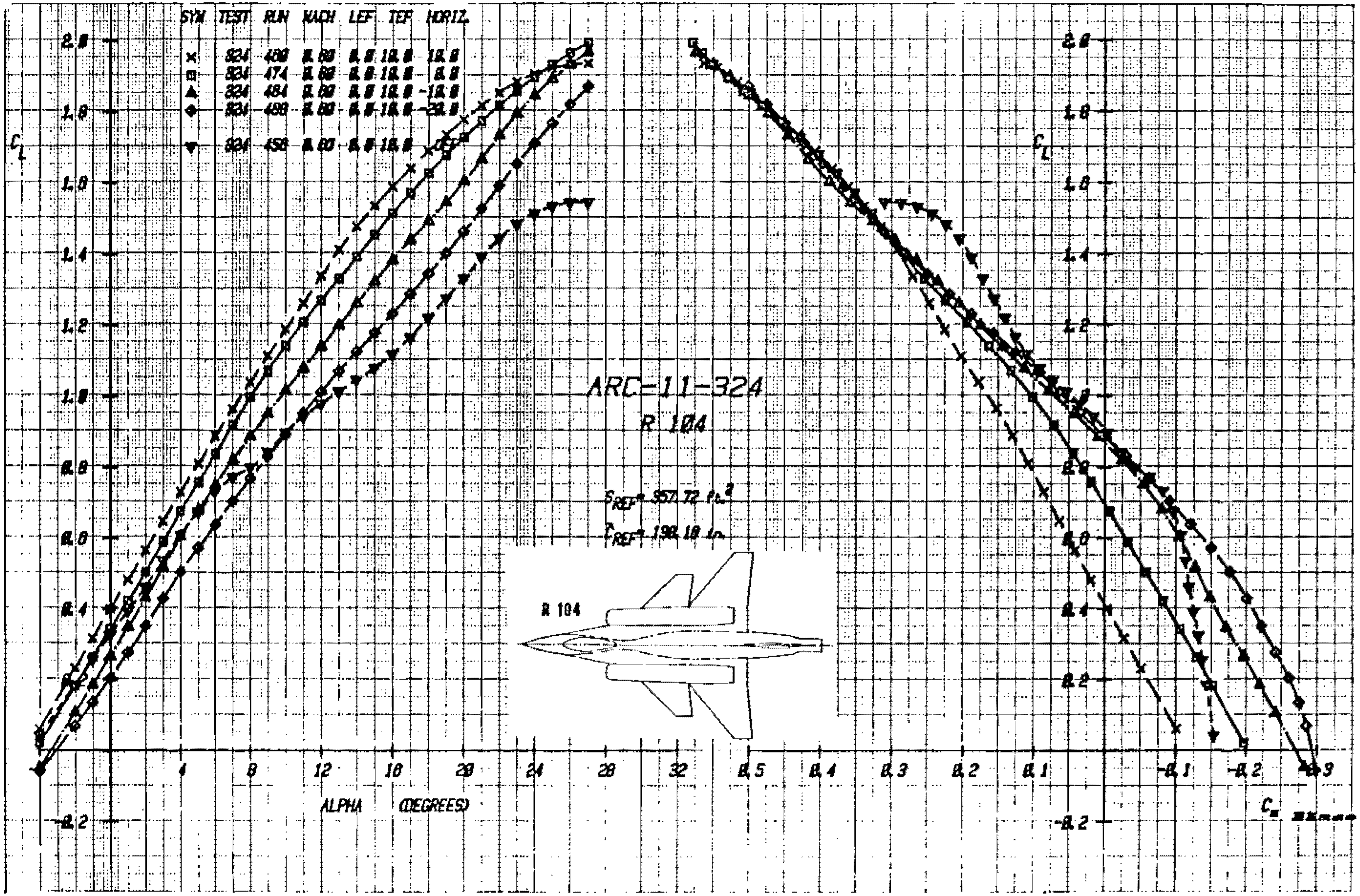

Figure1-20aEffect of Canard Deflection on Lift and Moment with Wing Trailing-Edge Flap Deflected +10°, Mach = .6

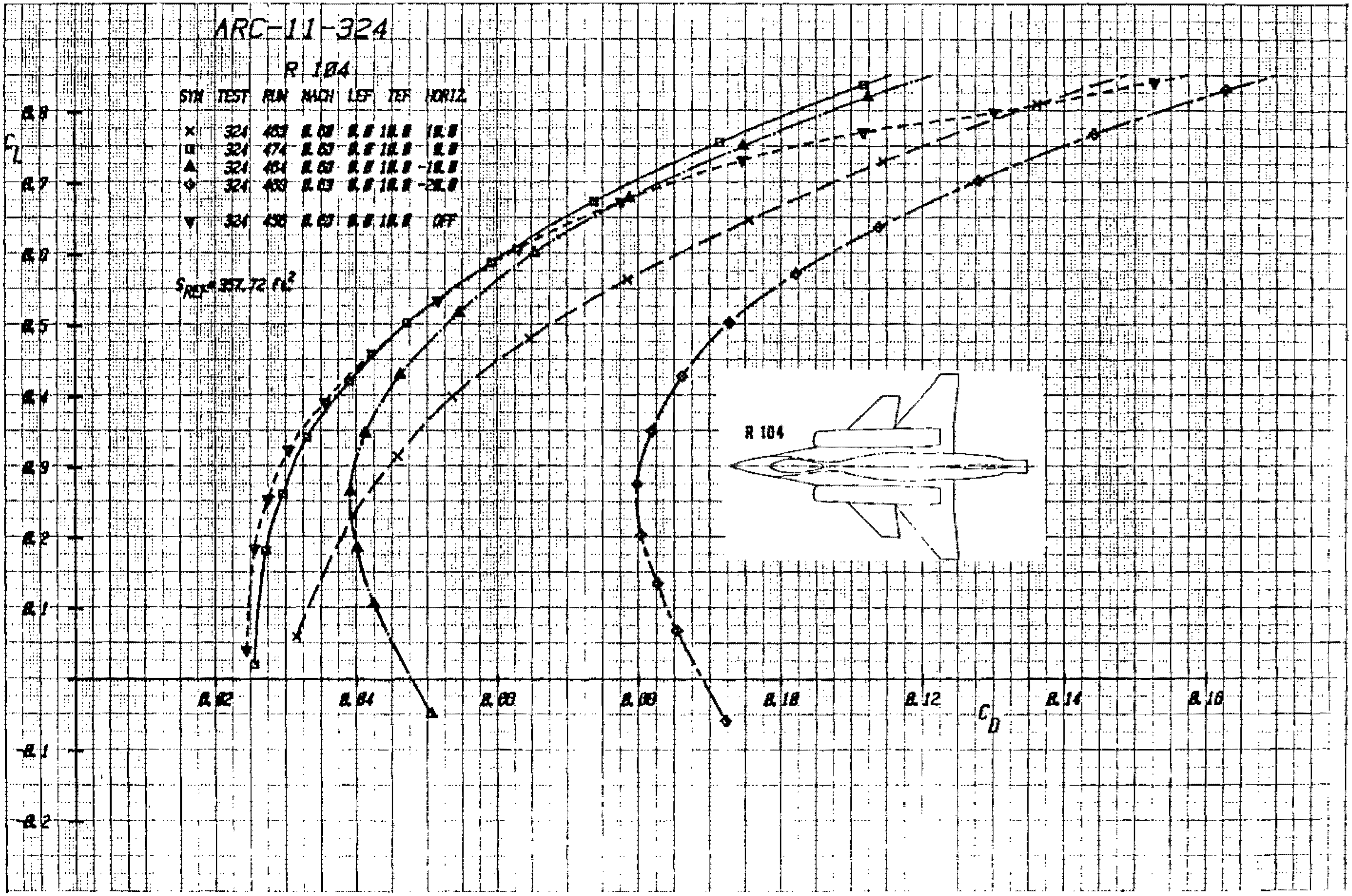

Figure1-20bEffect of Canard Deflection on Drag with Wing Trailing-Edge Flap Deflected +10°, Mach = .6

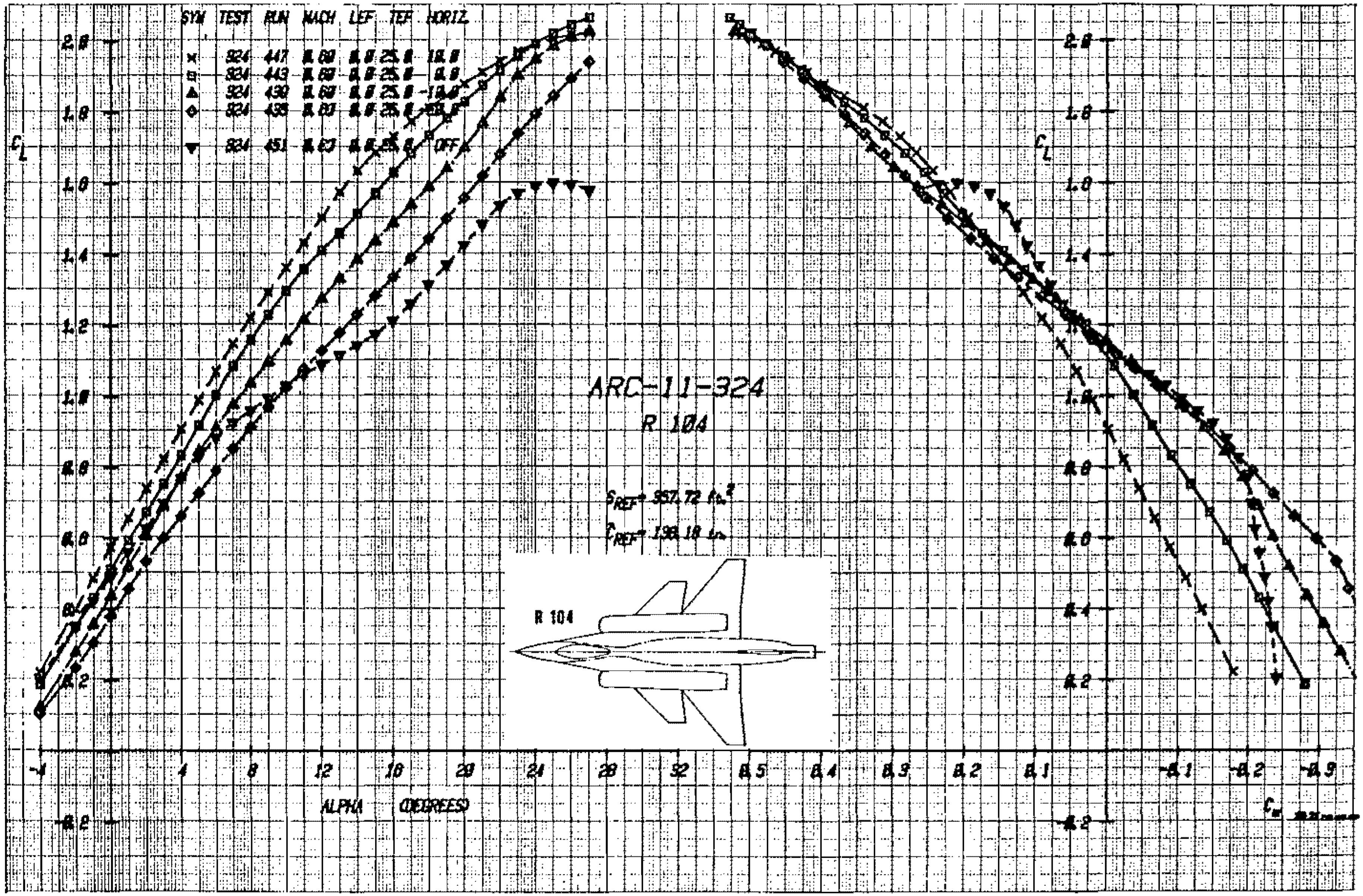

Figure1-21aEffect of Canard Deflection on Lift and Moment with Wing Trailing-Edge Flap Deflected +25°, Mach = .6

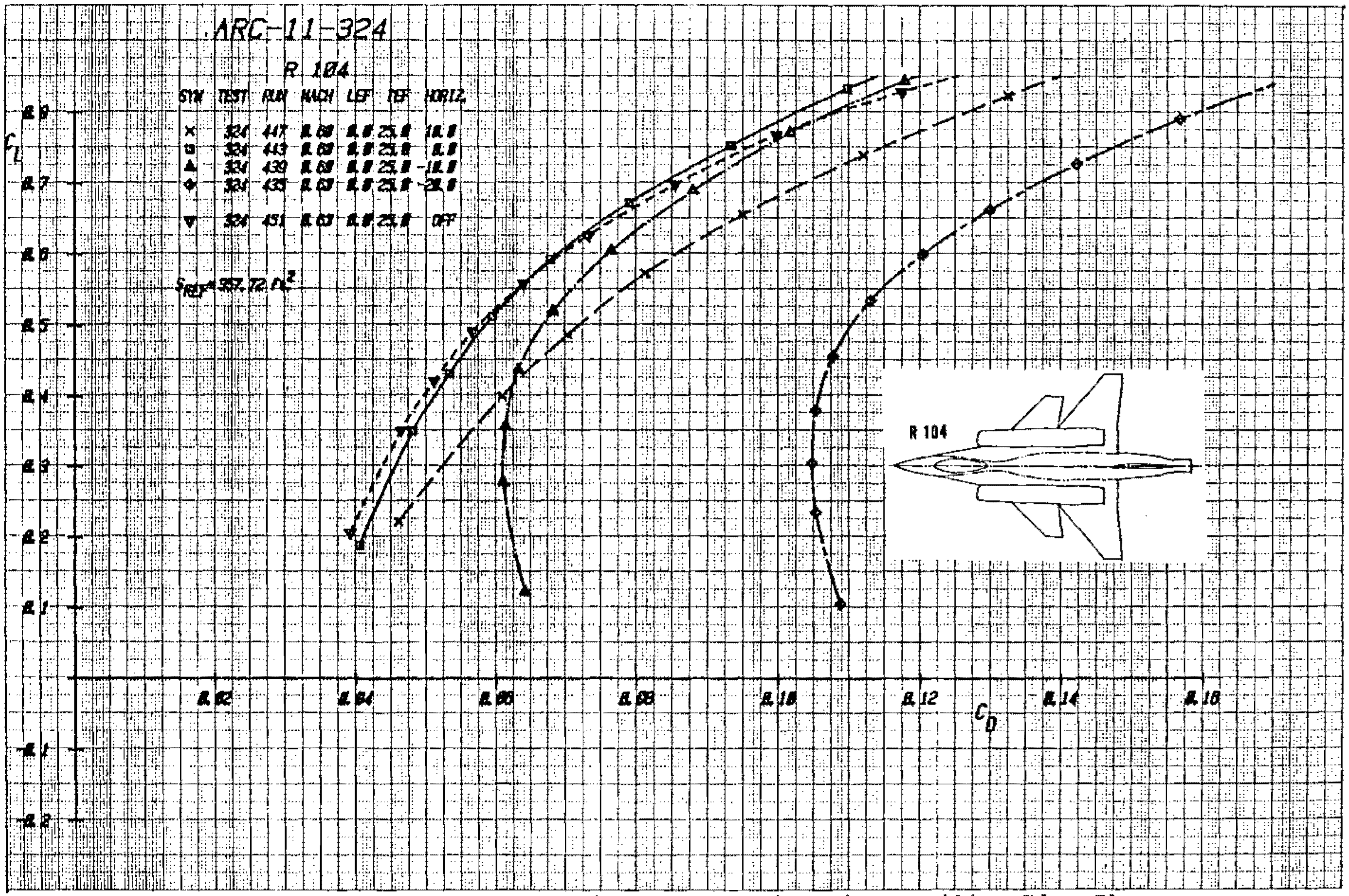

Figure1-21bEffect of Canard Deflection on Drag with Wing Trailing-Edge Flap Deflected +25°, Mach = .6

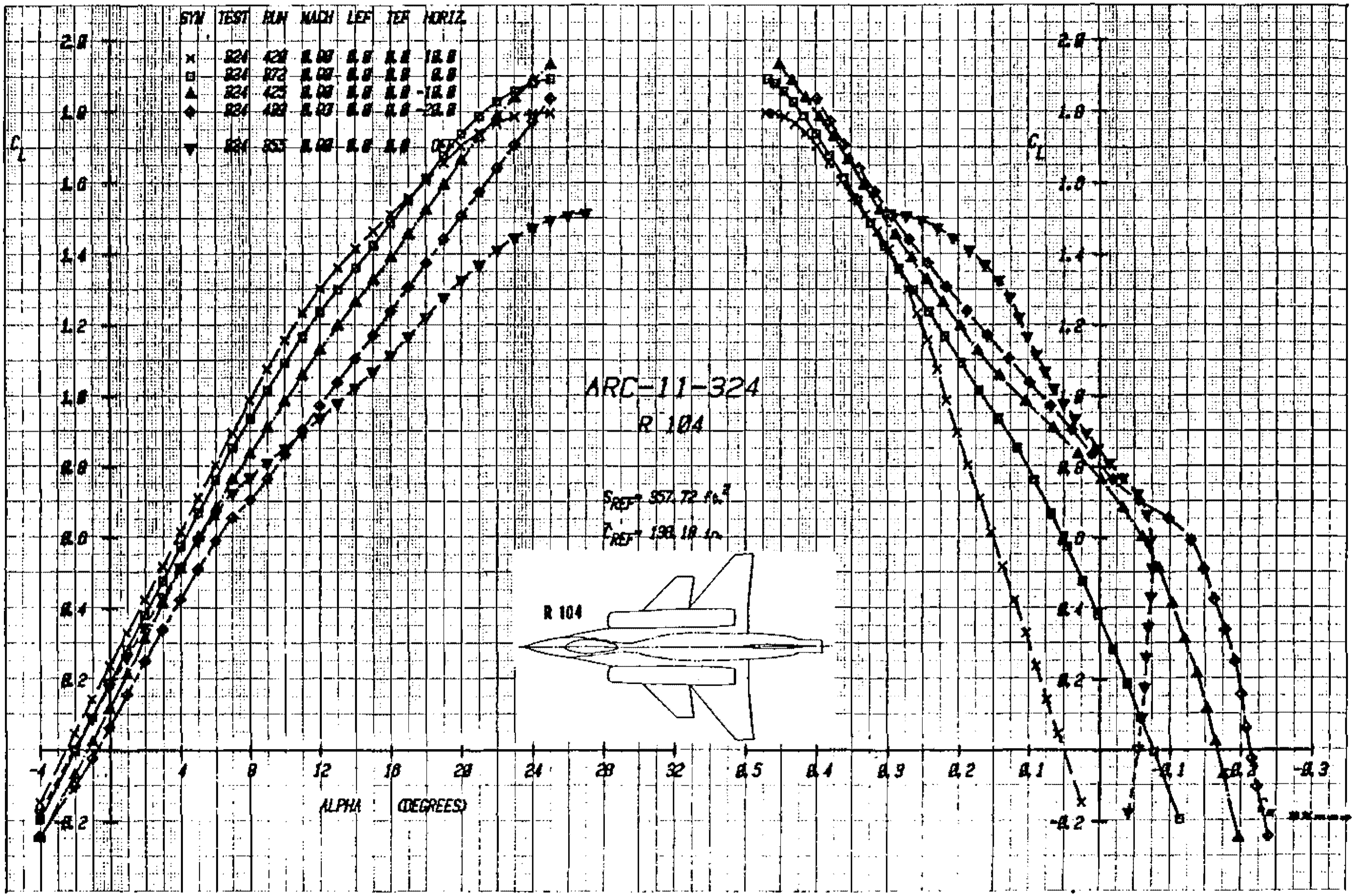

Figurel-22aEffect of Canard Deflection on Lift and Moment with Wing Trailing-Edge Flap Undeflected, Mach = .9

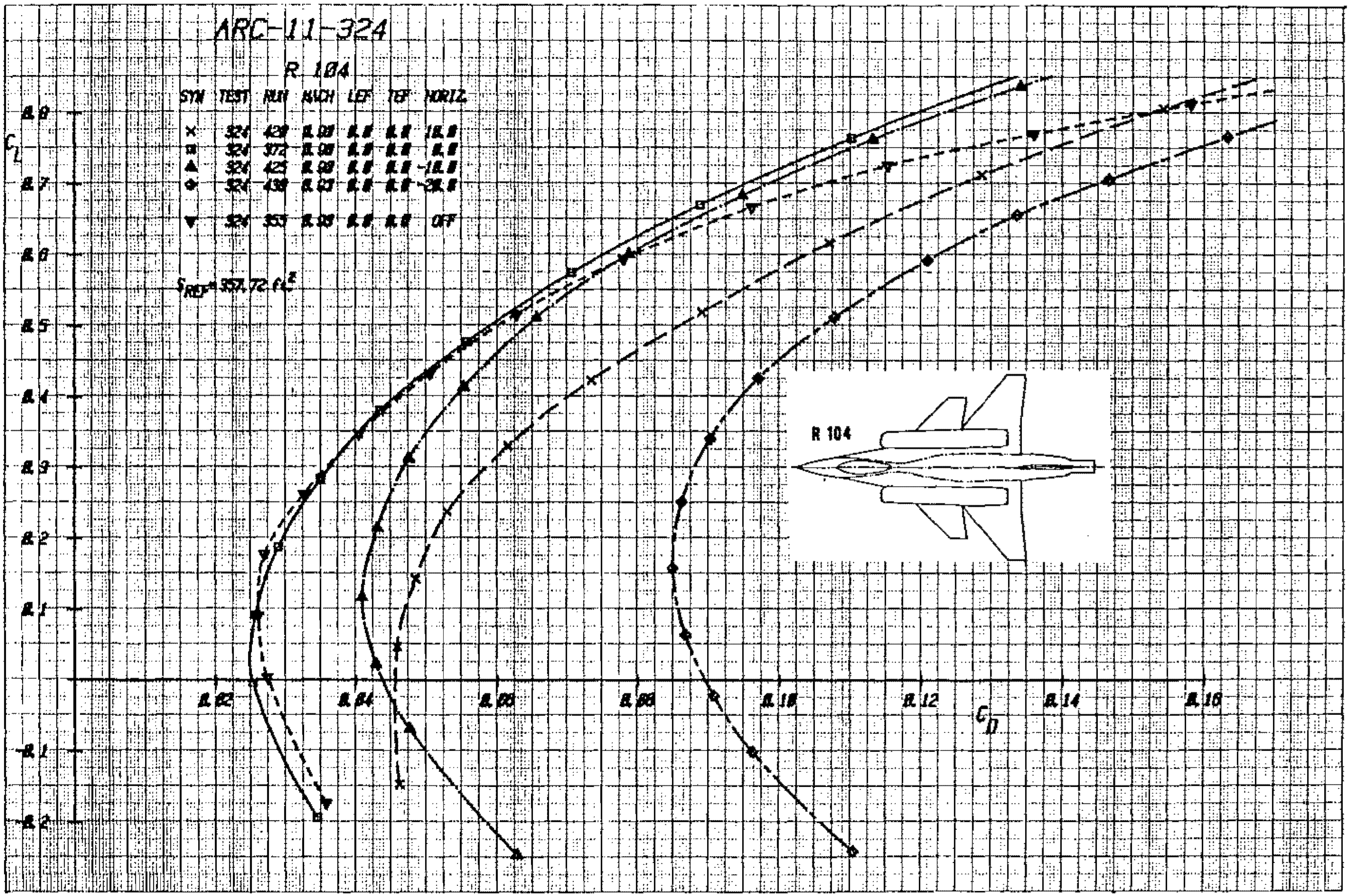

Figure1-22bEffect of Canard Deflection on Drag with Wing Trailing-Edge Flap Undeflected, Mach = .9

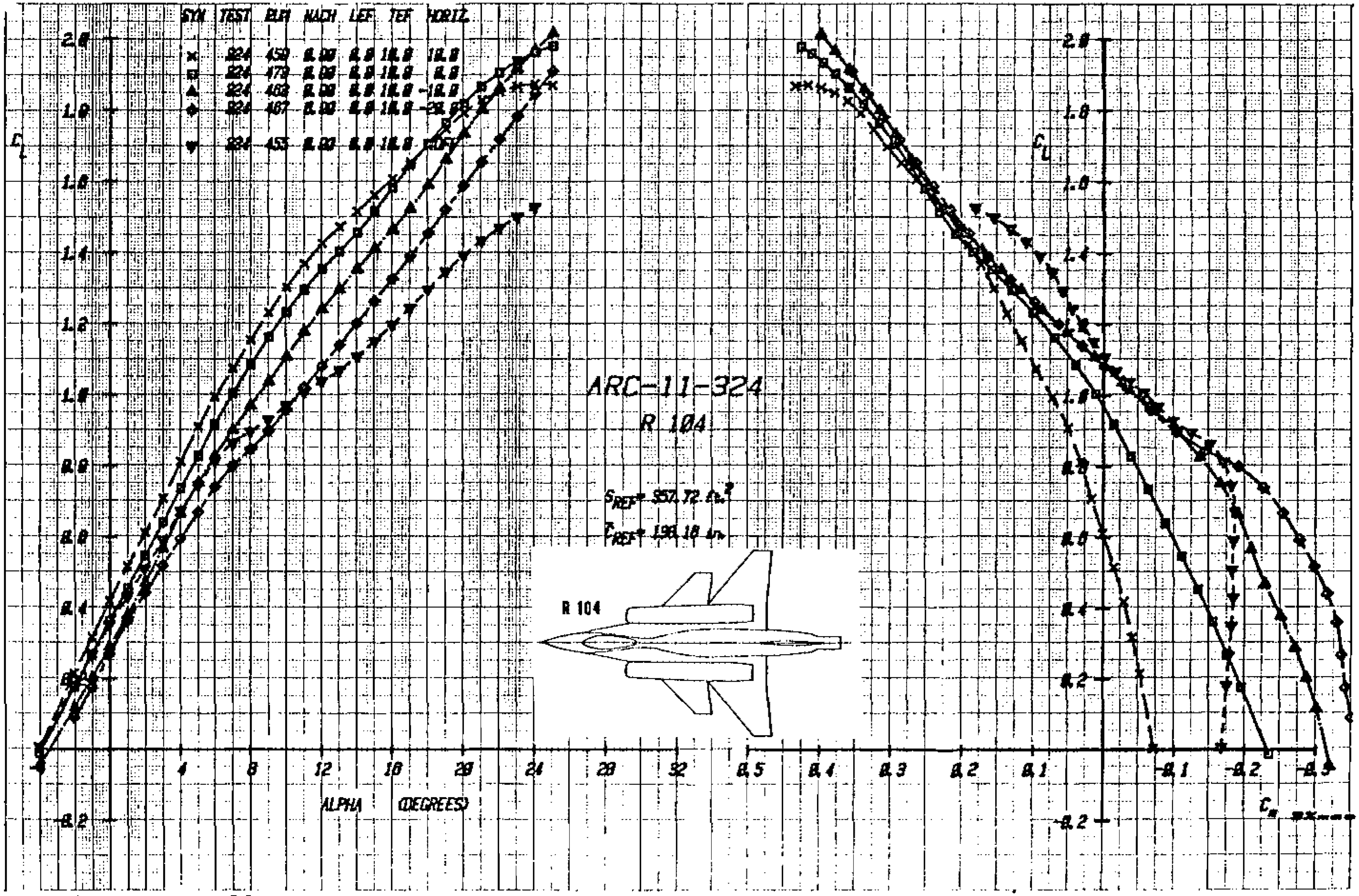

Figure1-23aEffect of Canard Deflection on Lift and Moment with Wing Trailing-Edge Flap Deflected +10°, Mach = .9

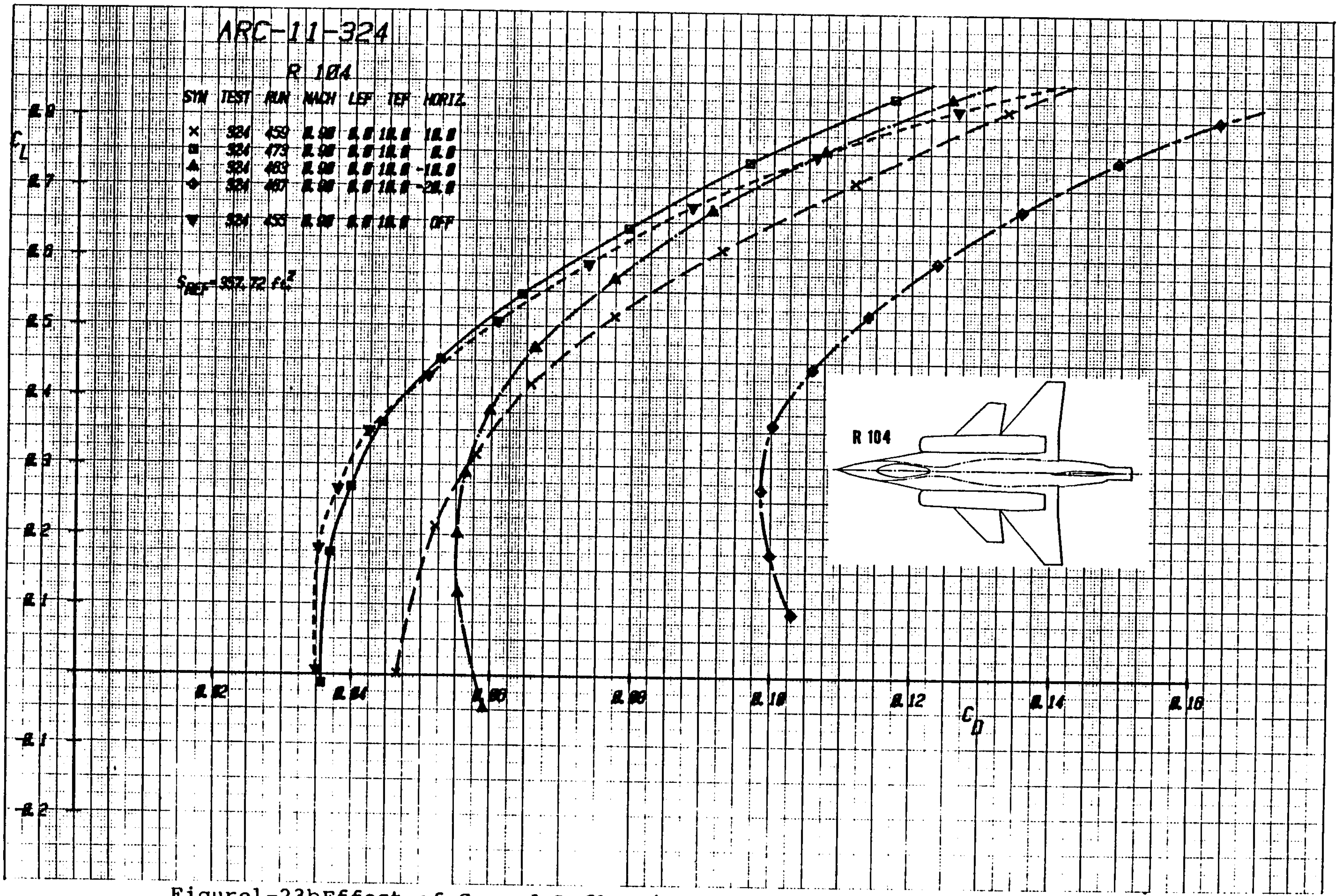

Figurel-23bEffect of Canard Deflection on Drag with Wing Trailing-Edge Flap Deflected +10°, Mach = .9

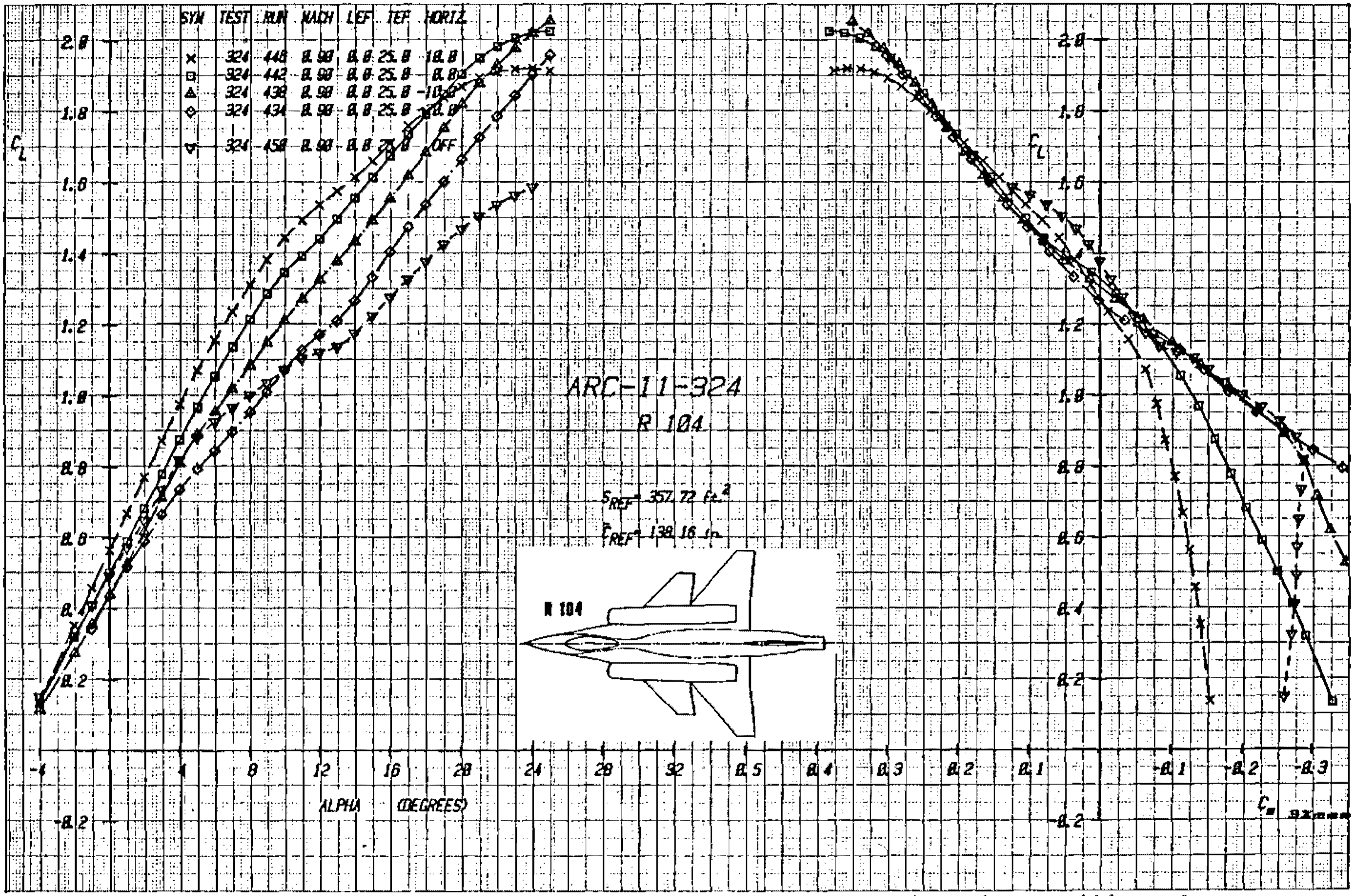

Figure1-24aEffect of Canard Deflection on Lift and Moment with Wing Trailing-Edge Flap Deflected +25°, Mach = .9

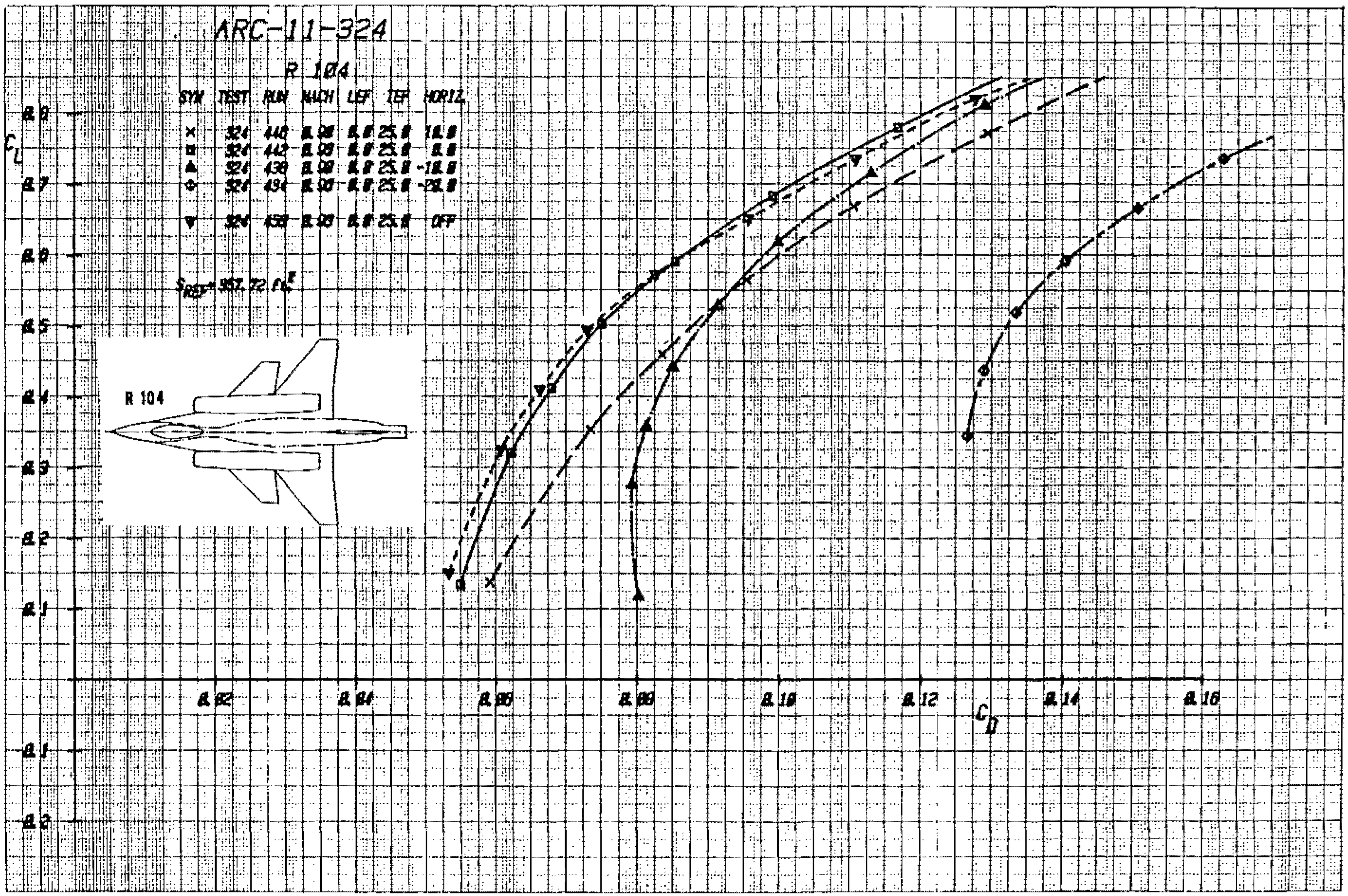

Figure1-24bEffect of Canard Deflection on Drag with Wing Trailing-Edge Flap Deflected +25°, Mach = .9

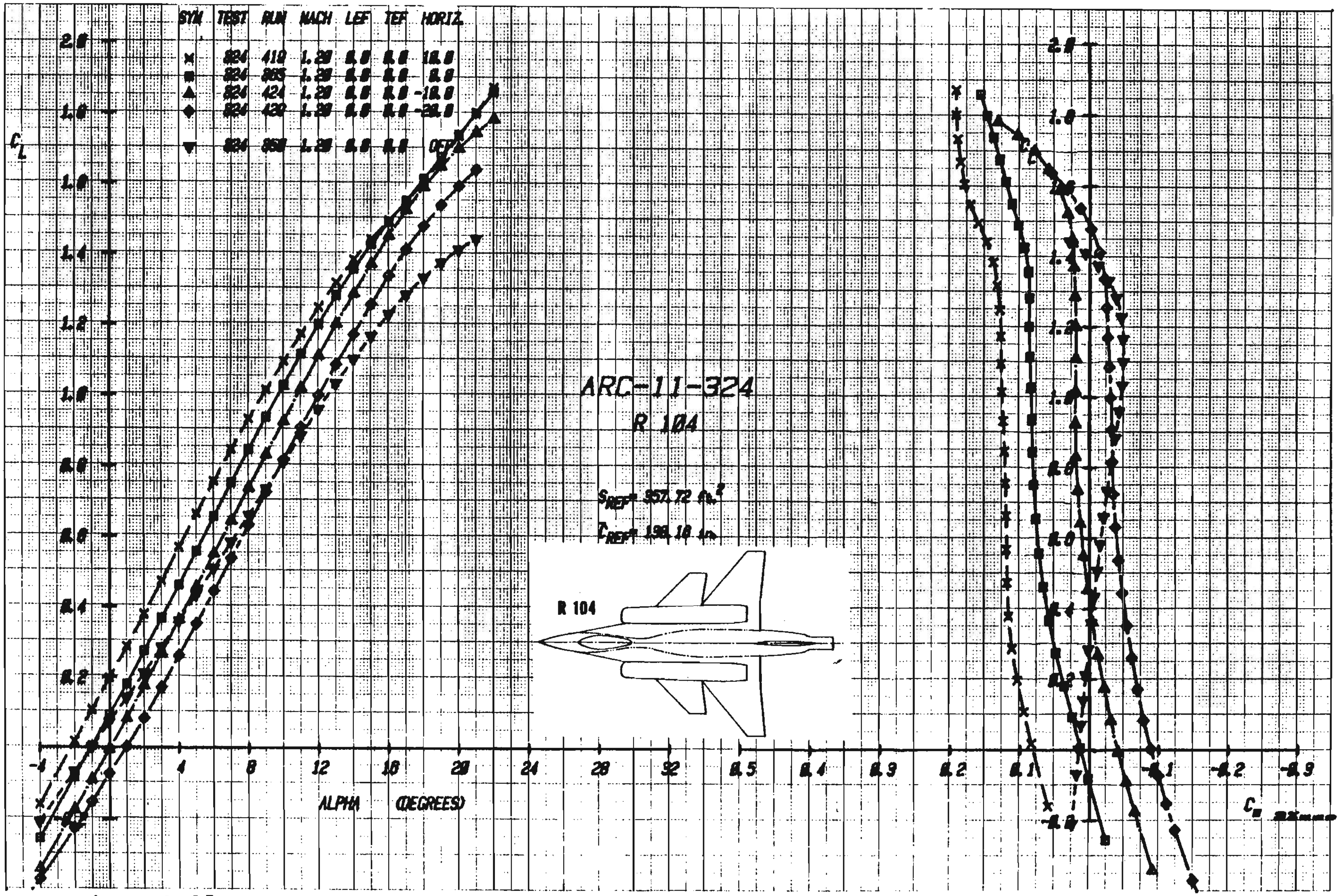

Figure1-25aEffect of Canard Deflection on Lift and Moment with Wing Trailing-Edge Flap Undeflected, Mach = 1.2

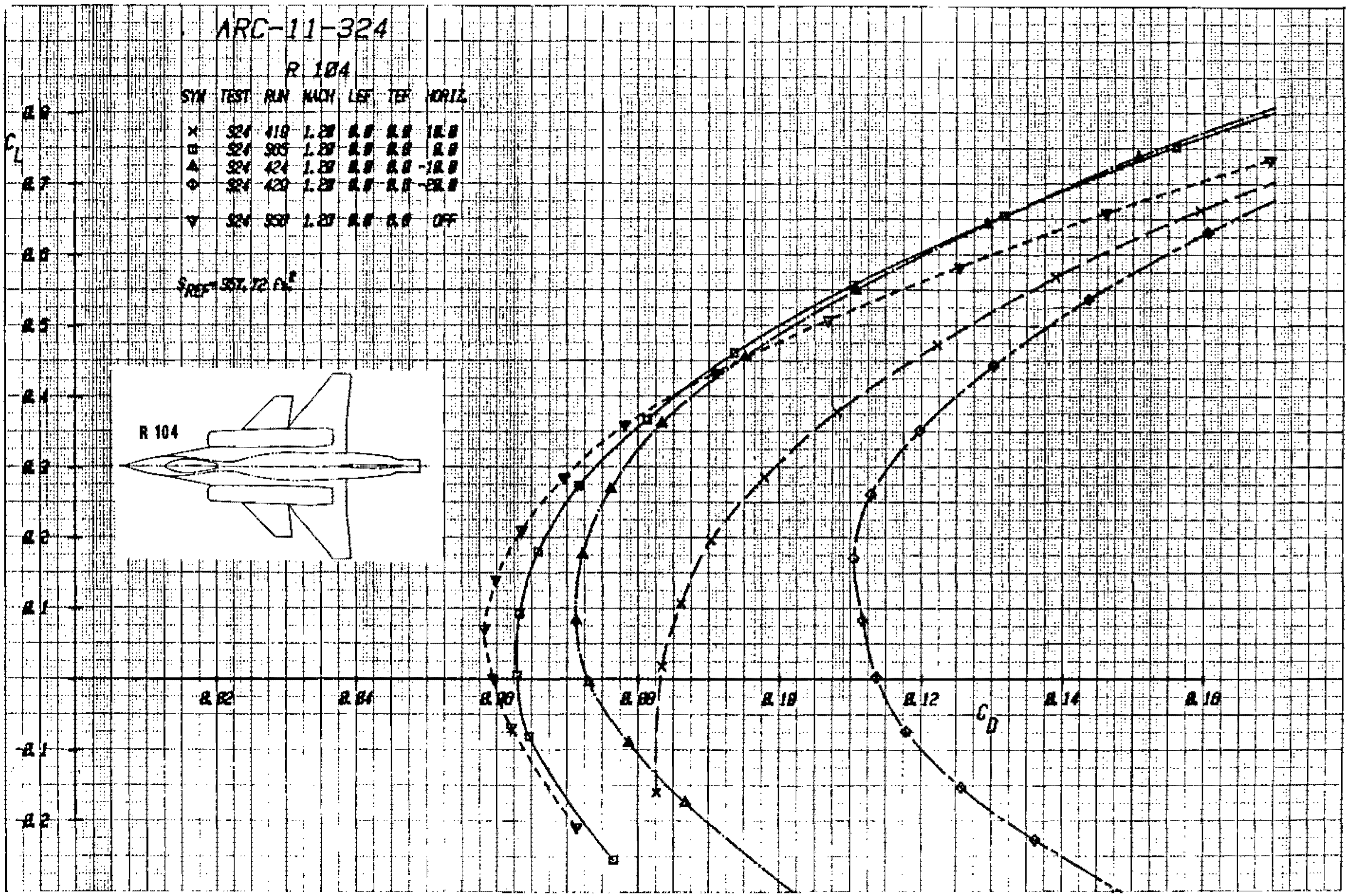

Figure1-25bEffect of Canard Deflection on Drag with Wing Trailing-Edge Flap Undeflected, Mach = 1.2

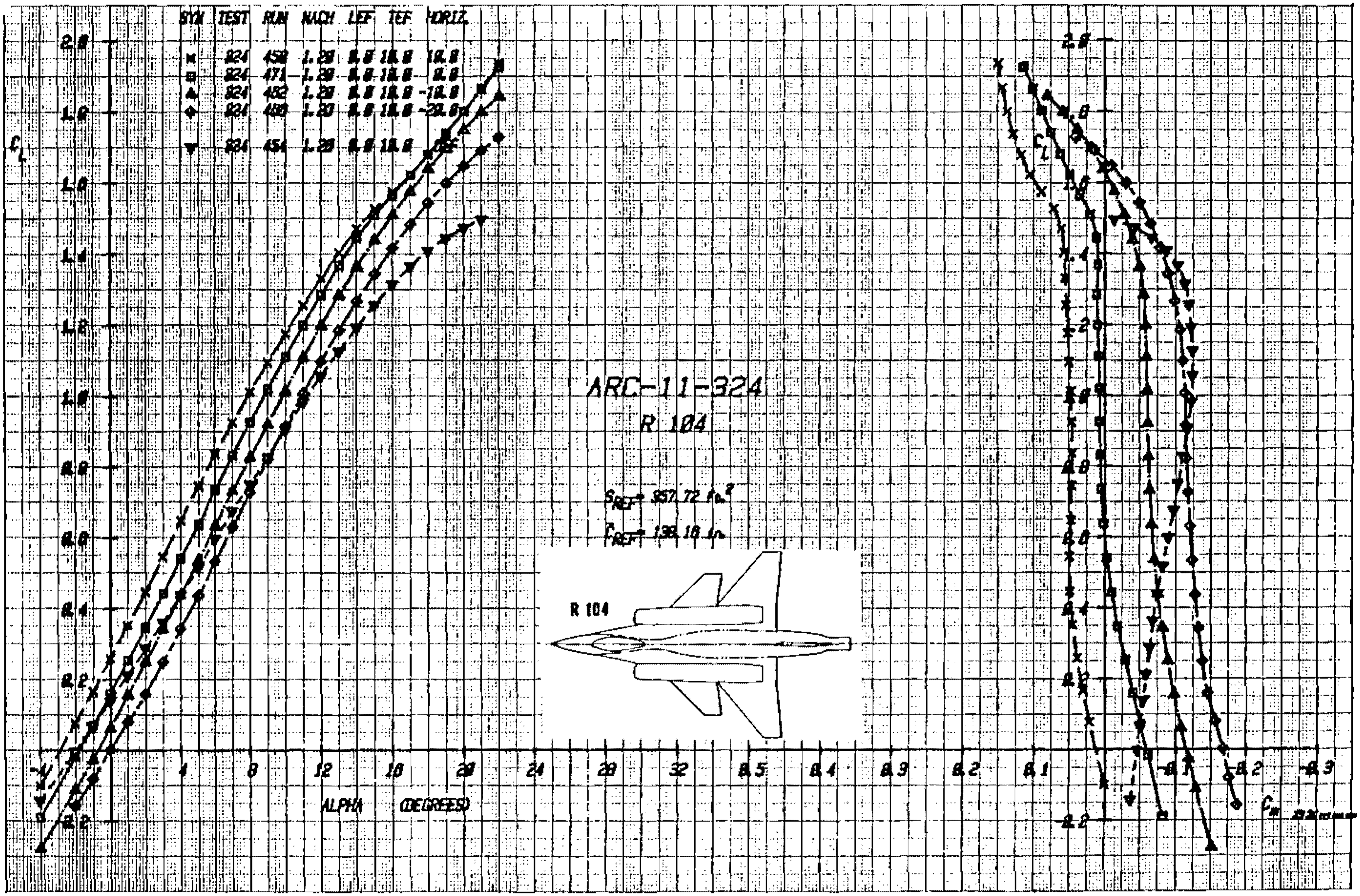

Figure1-26aEffect of Canard Deflection on Lift and Moment with Wing Trailing-Edge Flap Deflected +10°, Mach = 1.2

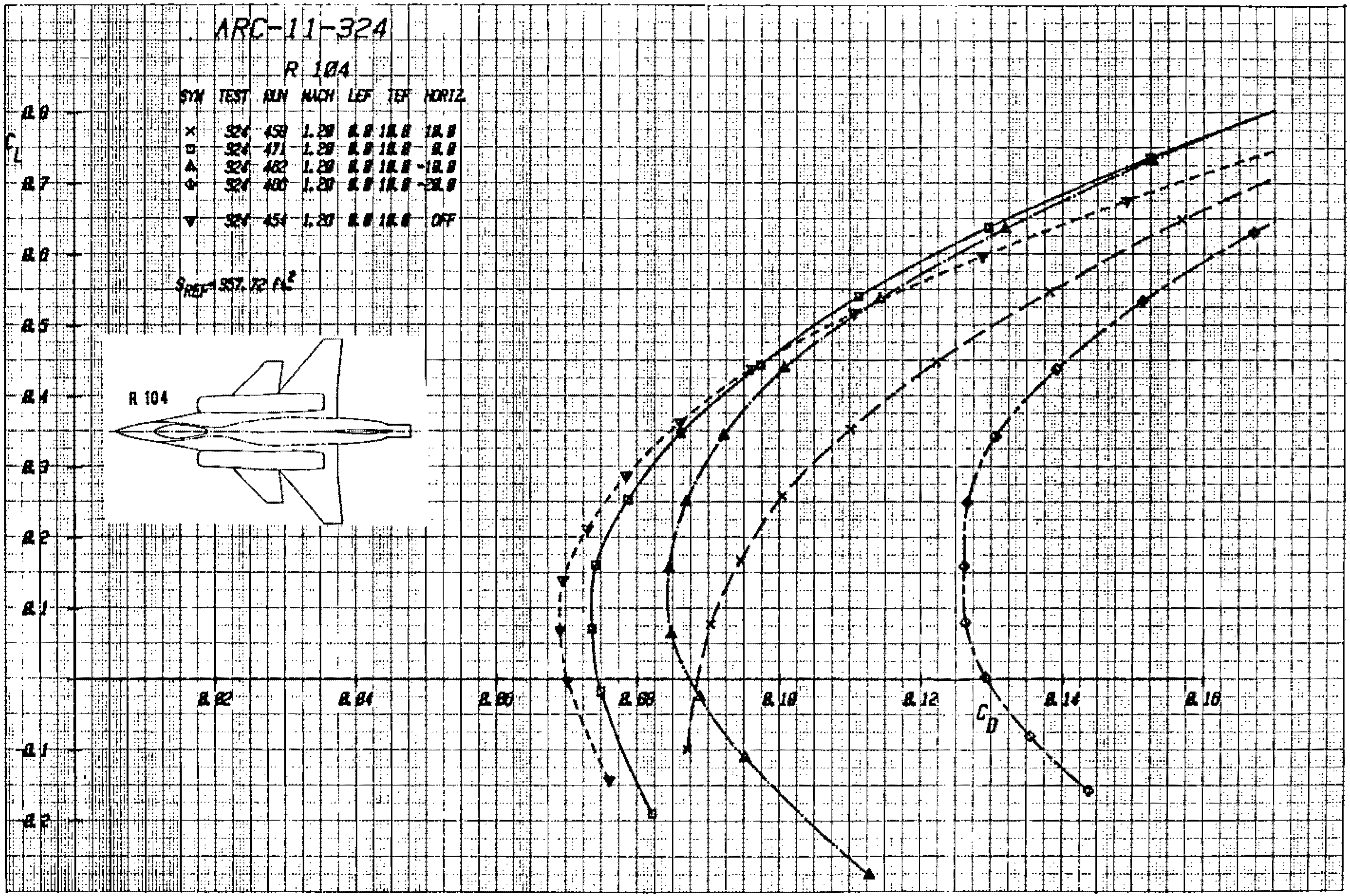

Figure1-26bEffect of Canard Deflection on Drag with Wing Trailing-Edge Flap Deflected +10°, Mach = 1.2

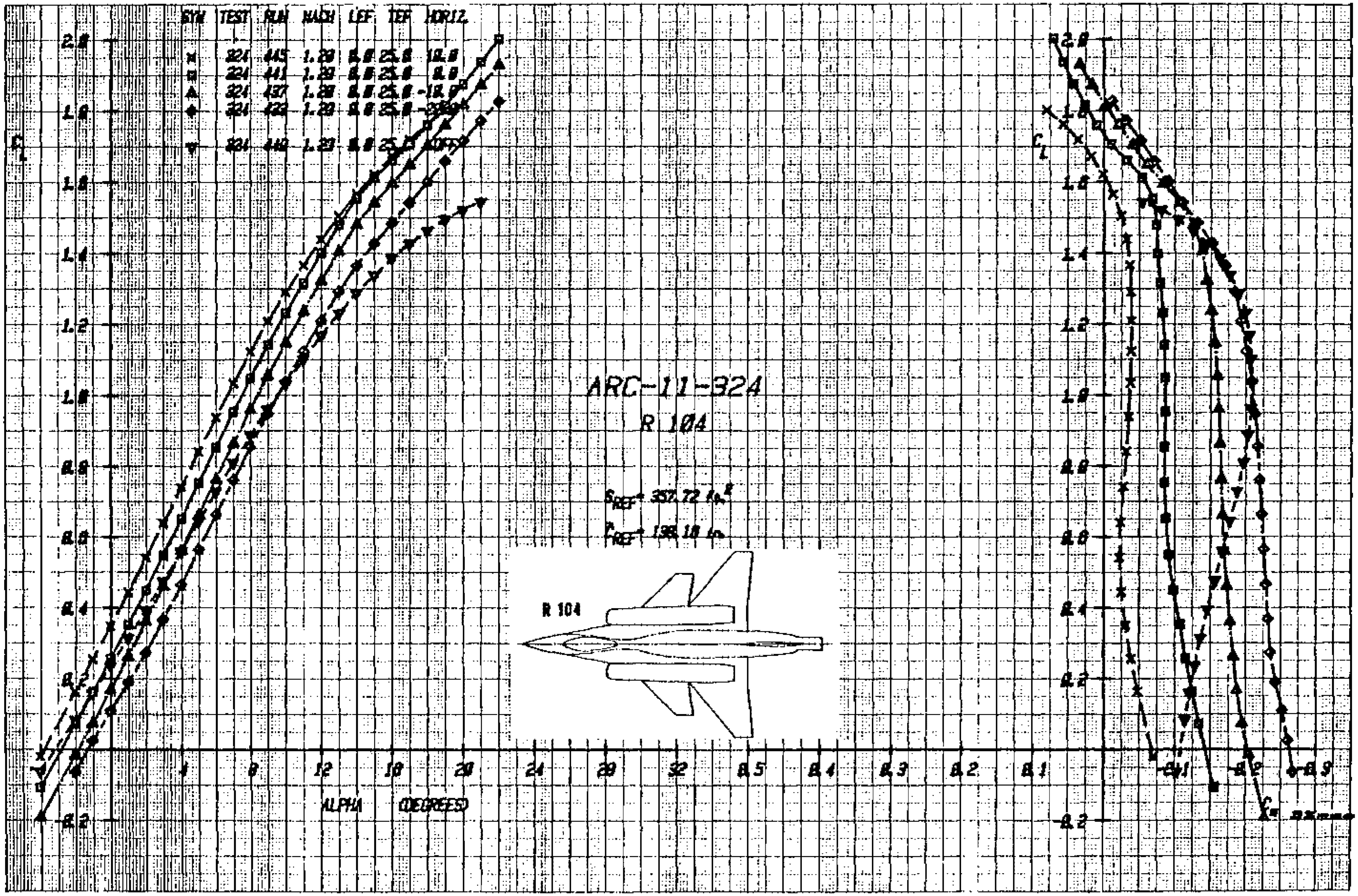

Figure1-27aEffect of Canard Deflection on Lift and Moment with Wing Trailing-Edge Flap Deflected +25°, Mach = 1.2

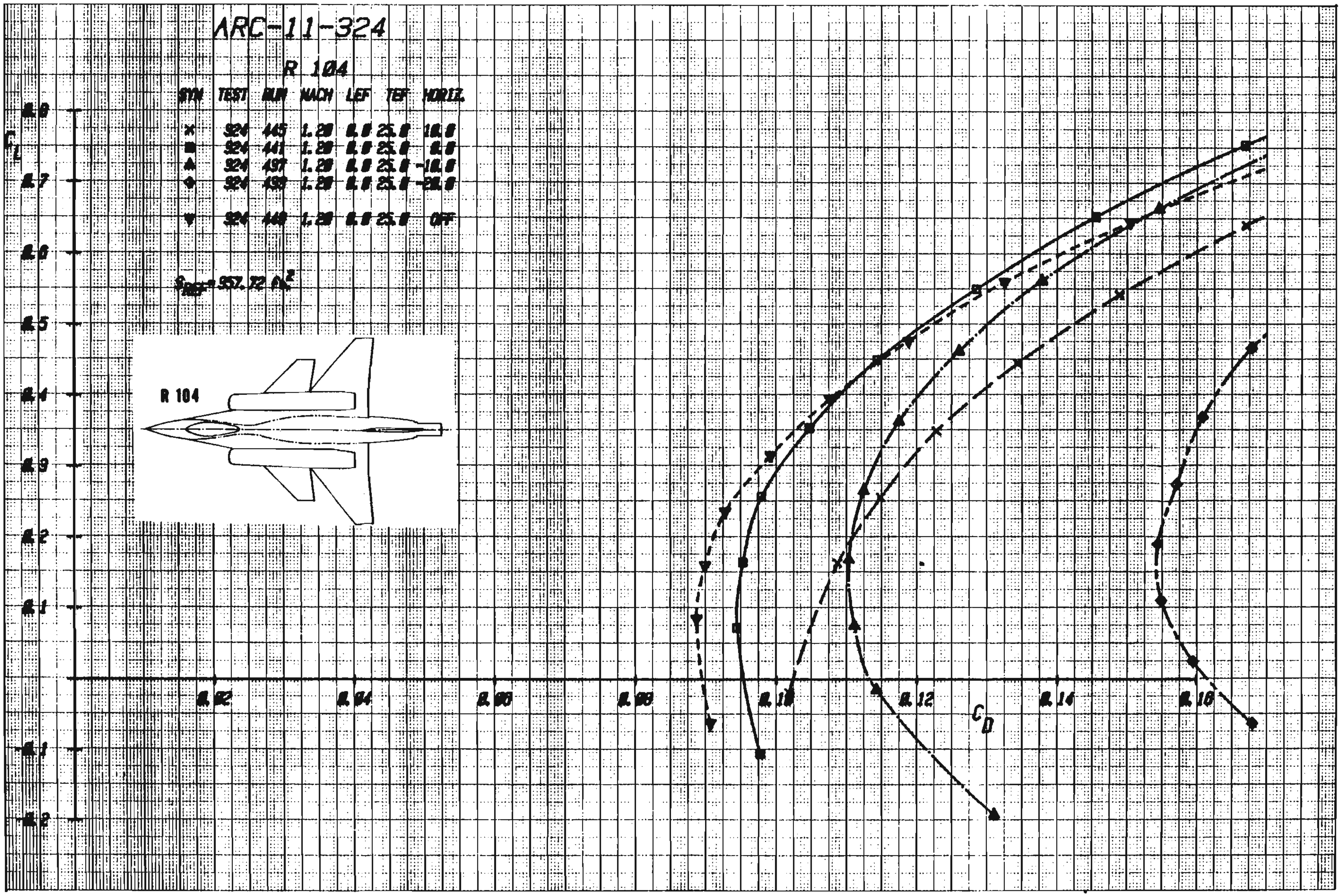

Figure1-27bEffect of Canard Deflection on Drag with Wing Trailing-Edge Flap Deflected +25°, Mach = 1.2

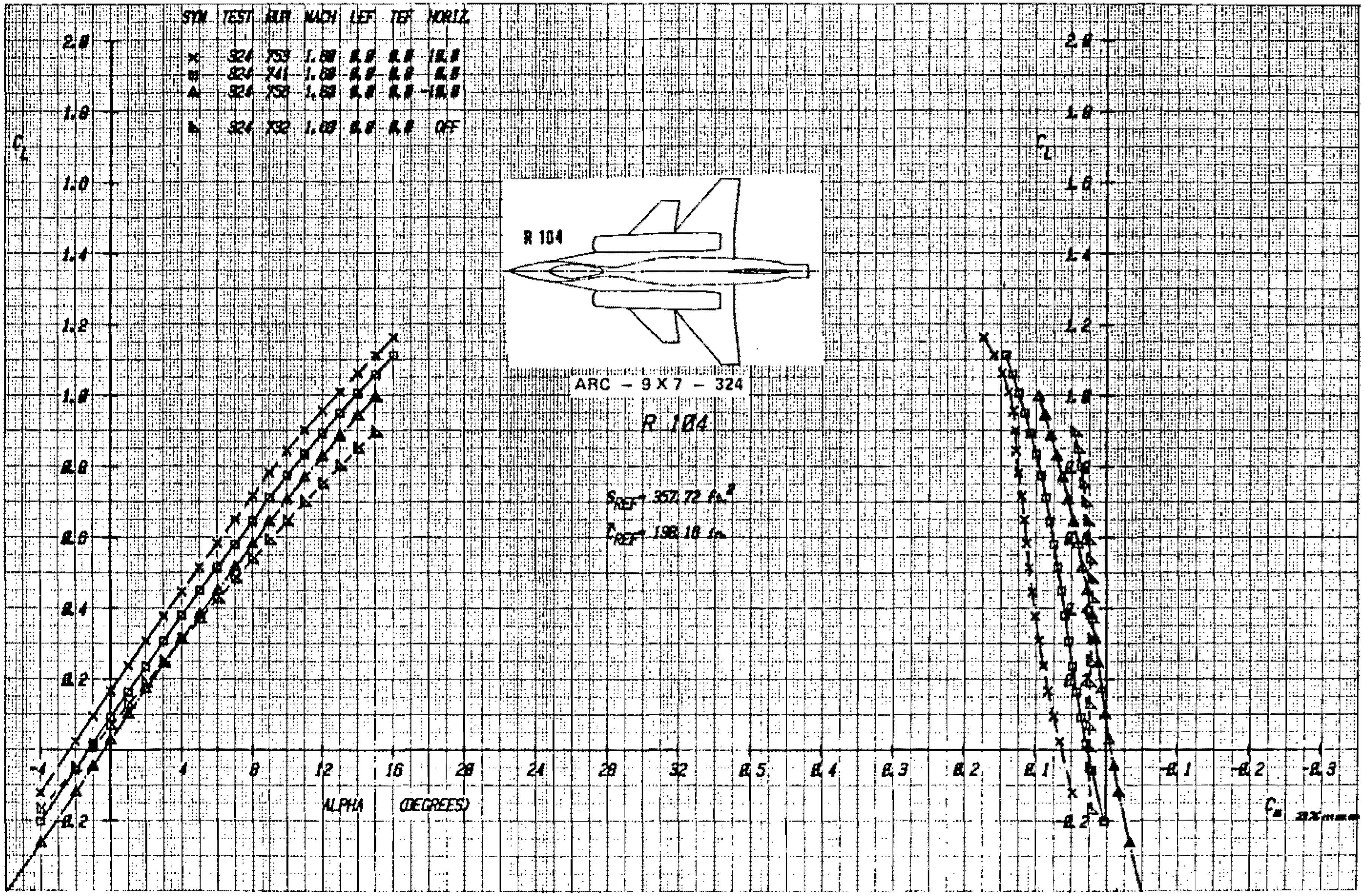

Figure1-28aEffect of Canard Deflection on Lift and Moment with Wing Trailing-Edge Flap Undeflected, Mach = 1.6

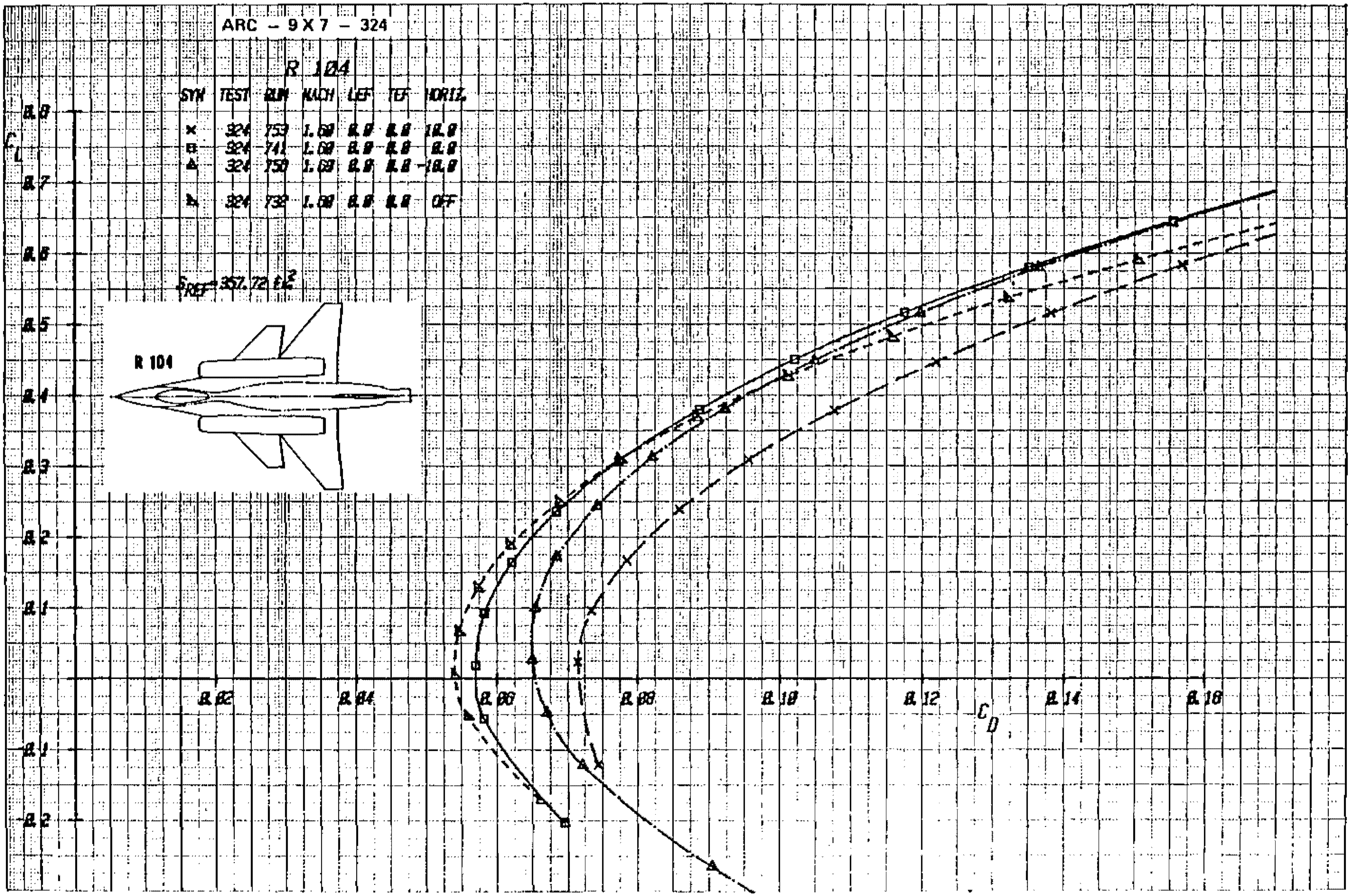

Figure1-28bEffect of Canard Deflection on Drag wth Wing Trailing-Edge Undeflected, (Expanded Drag Scale), Mach = 1.6

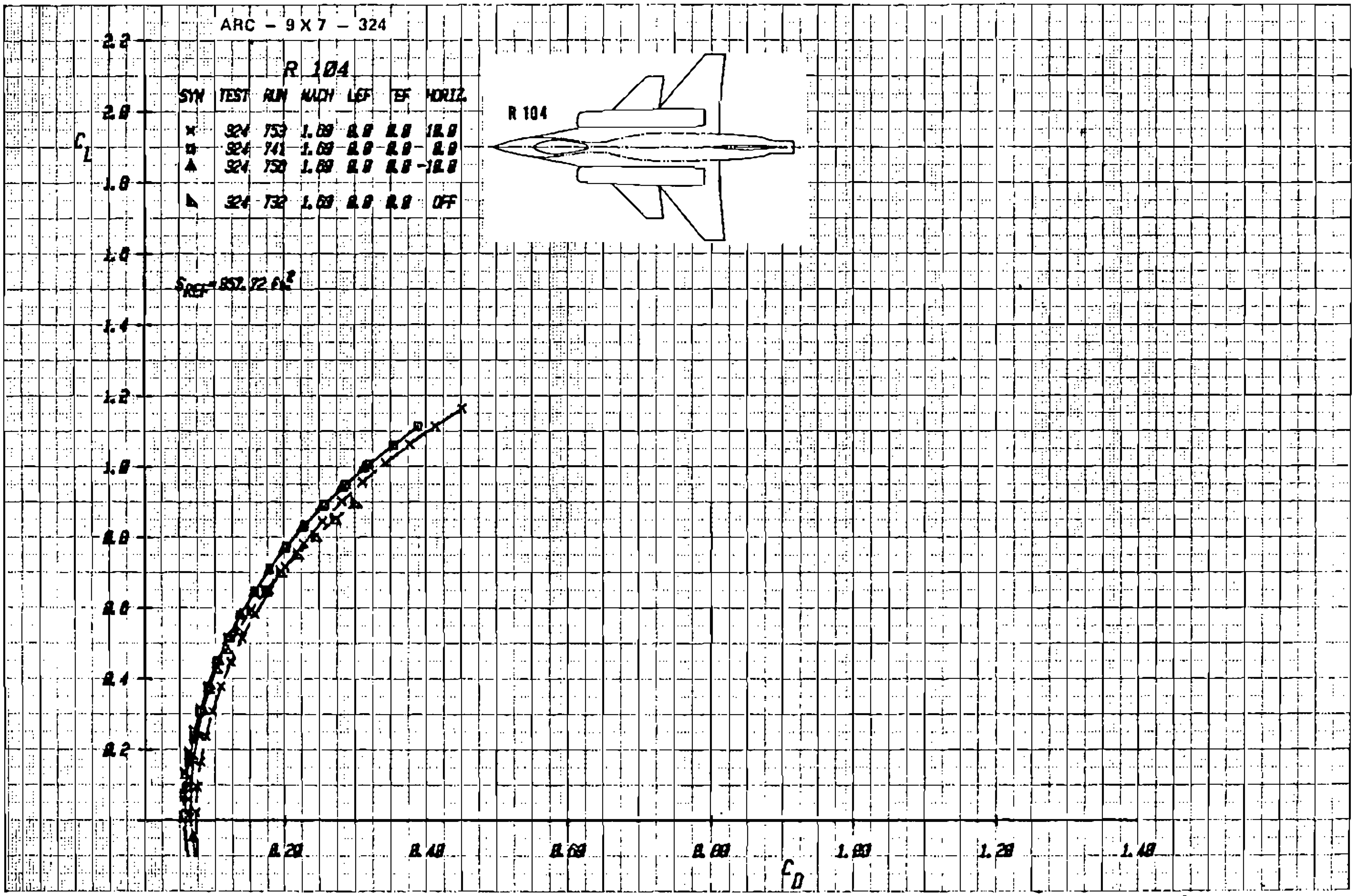

Figure1-28cEffect of Canard Deflection on Drag with Wing Trailing-Edge Flap Undeflected, Mach = 1.6

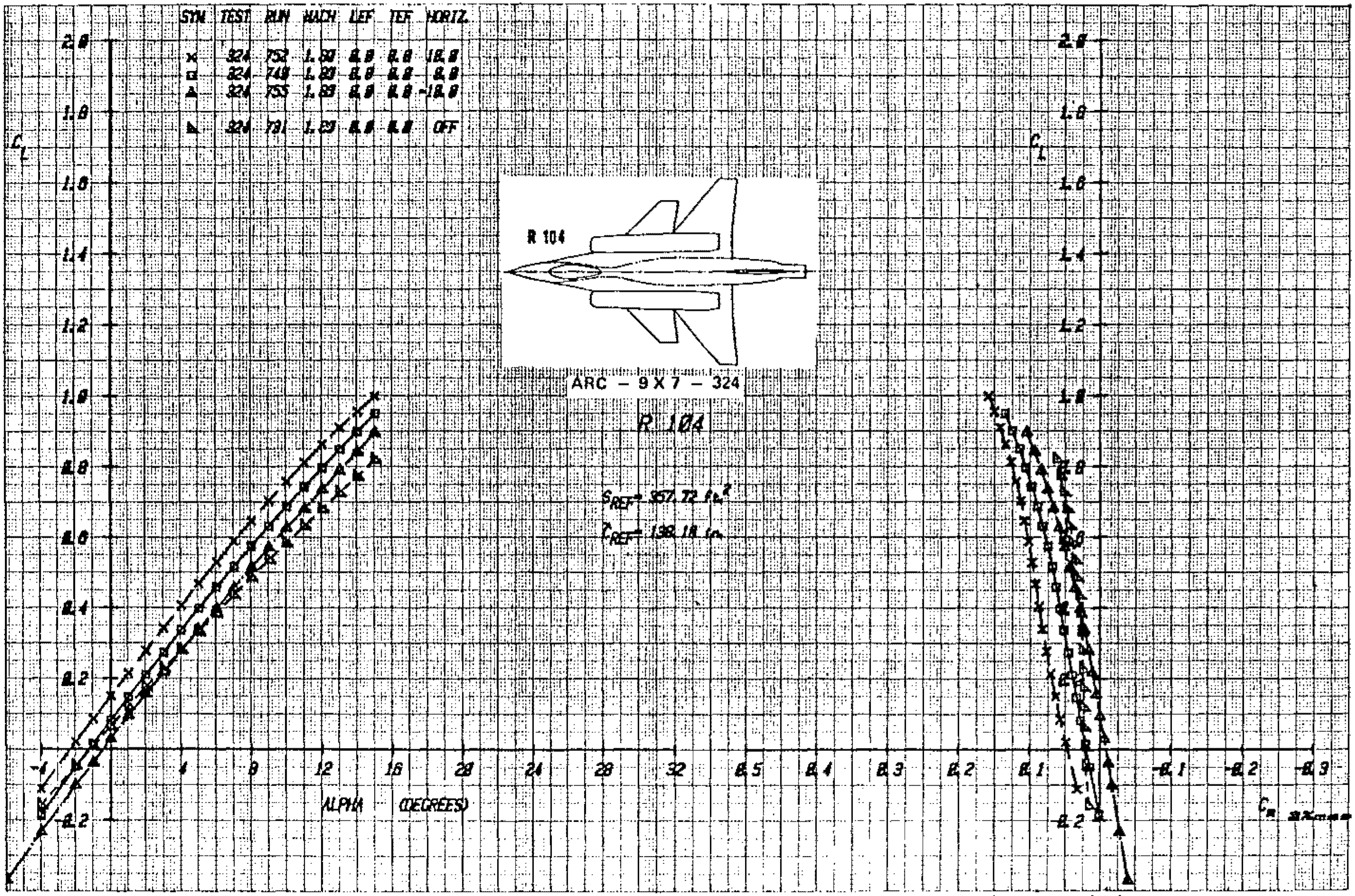

Figure1-29a Effect of Canard Deflection on Lift and Moment with Wing Trailing-Edge Flap Undeflected, Mach = 1.8

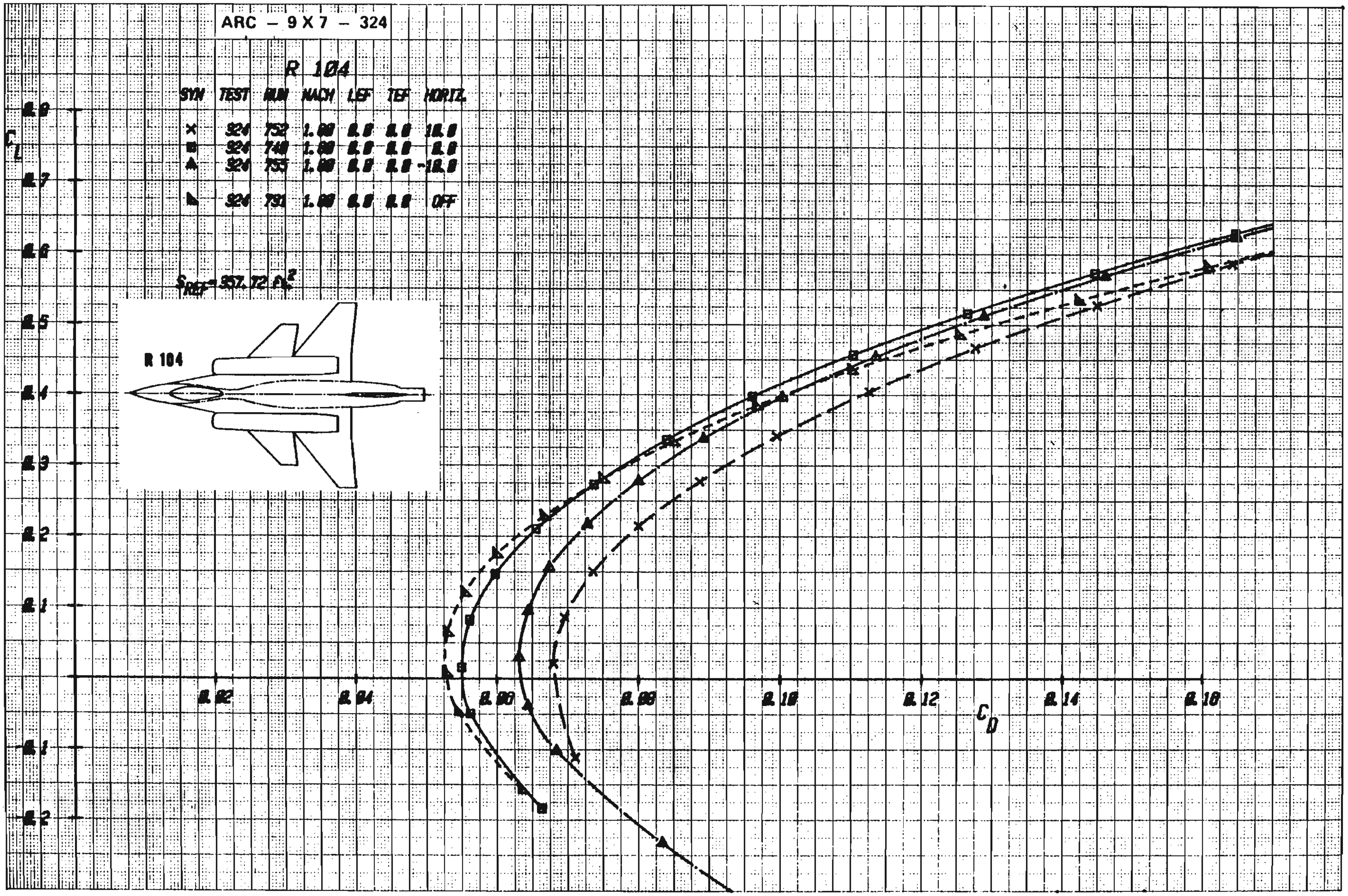

Figure1-29bEffect of Canard Deflection on Drag with Wing Trailing-Edge Flap Undeflected, (Expanded Drag Scale), Mach = 1.8

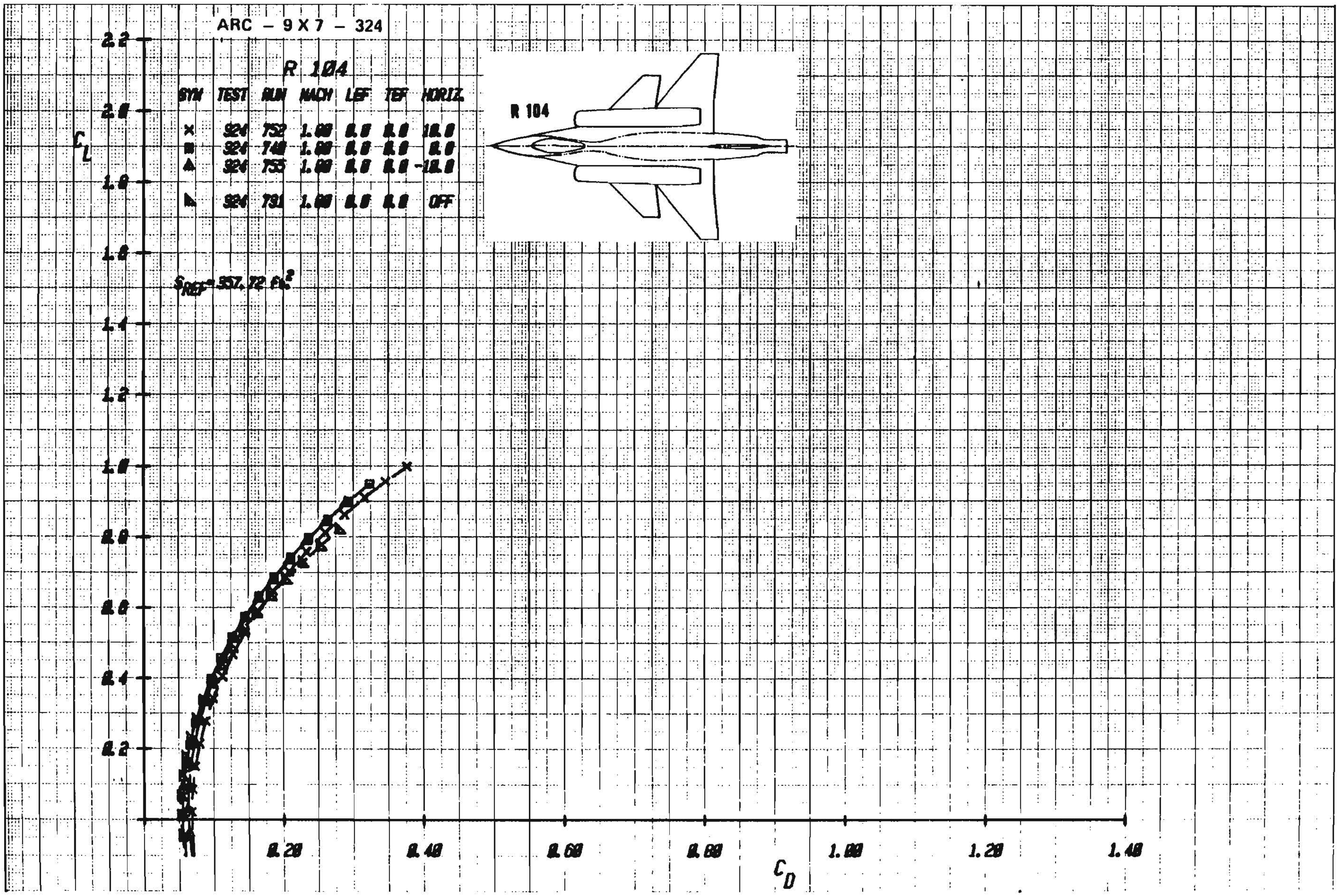

Figure1-29cEffect of Canard Deflection on Drag with Wing Trailing-Edge Flap Undeflected, Mach = 1.8

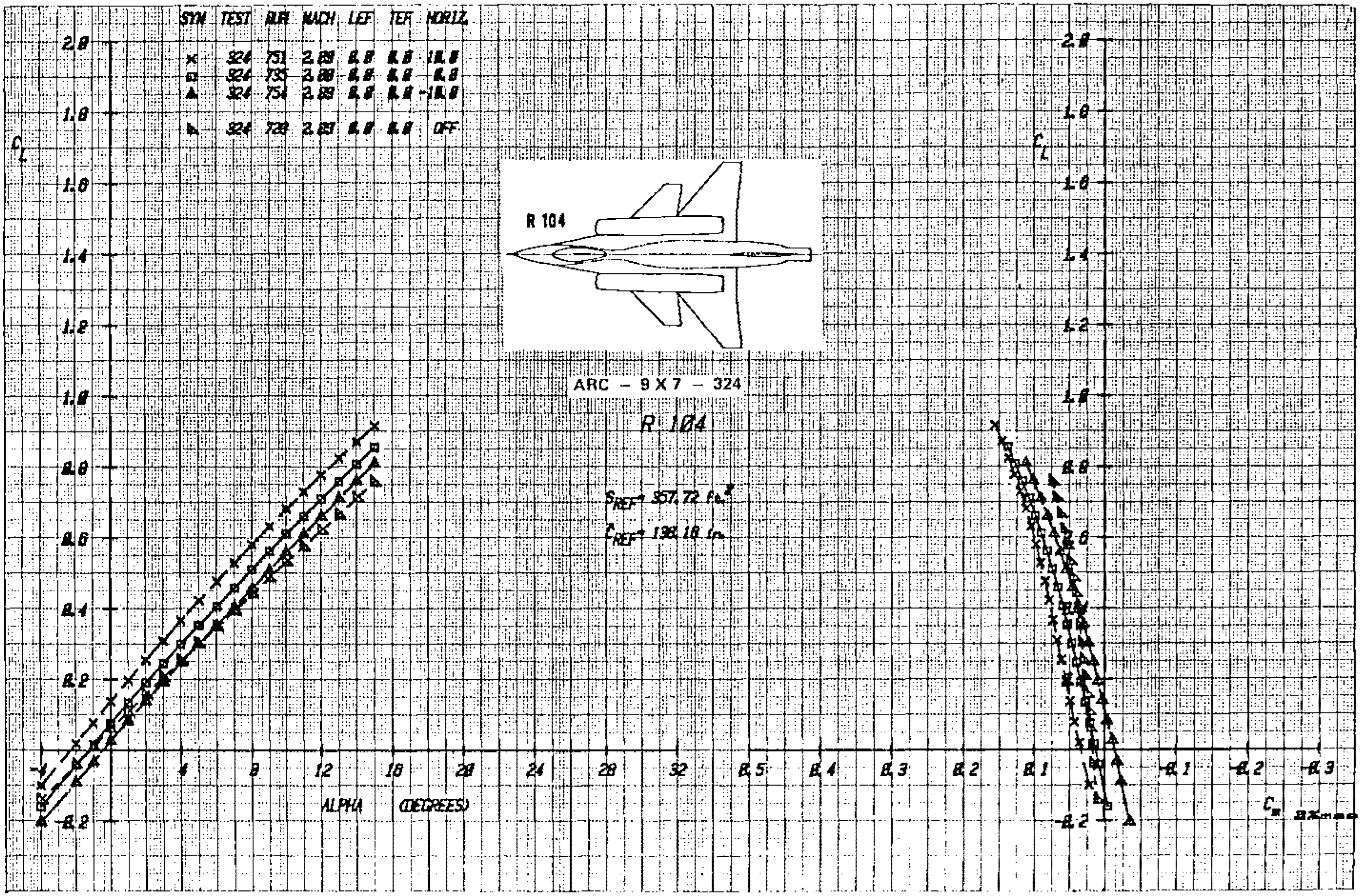

Figure1-30aEffect of Canard Deflection on Lift and Moment with Wing Trailing-Edge Flap Undeflected, Mach = 2.0

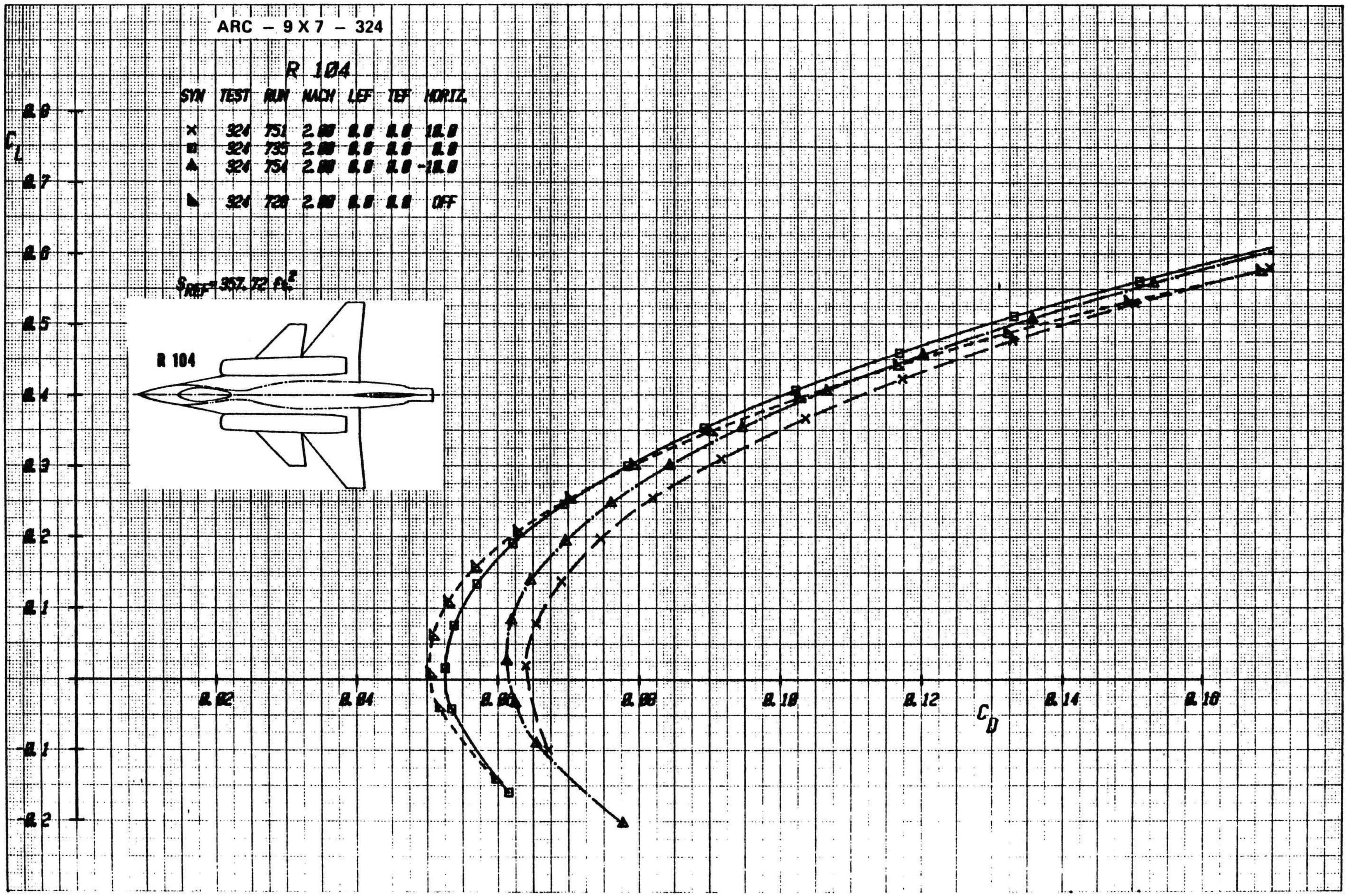

Figure1-30b Effect of Canard Deflection on Drag with Wing Trailing-Edge Flap Undeflected, (Expanded Drag Scale), Mach = 2.0

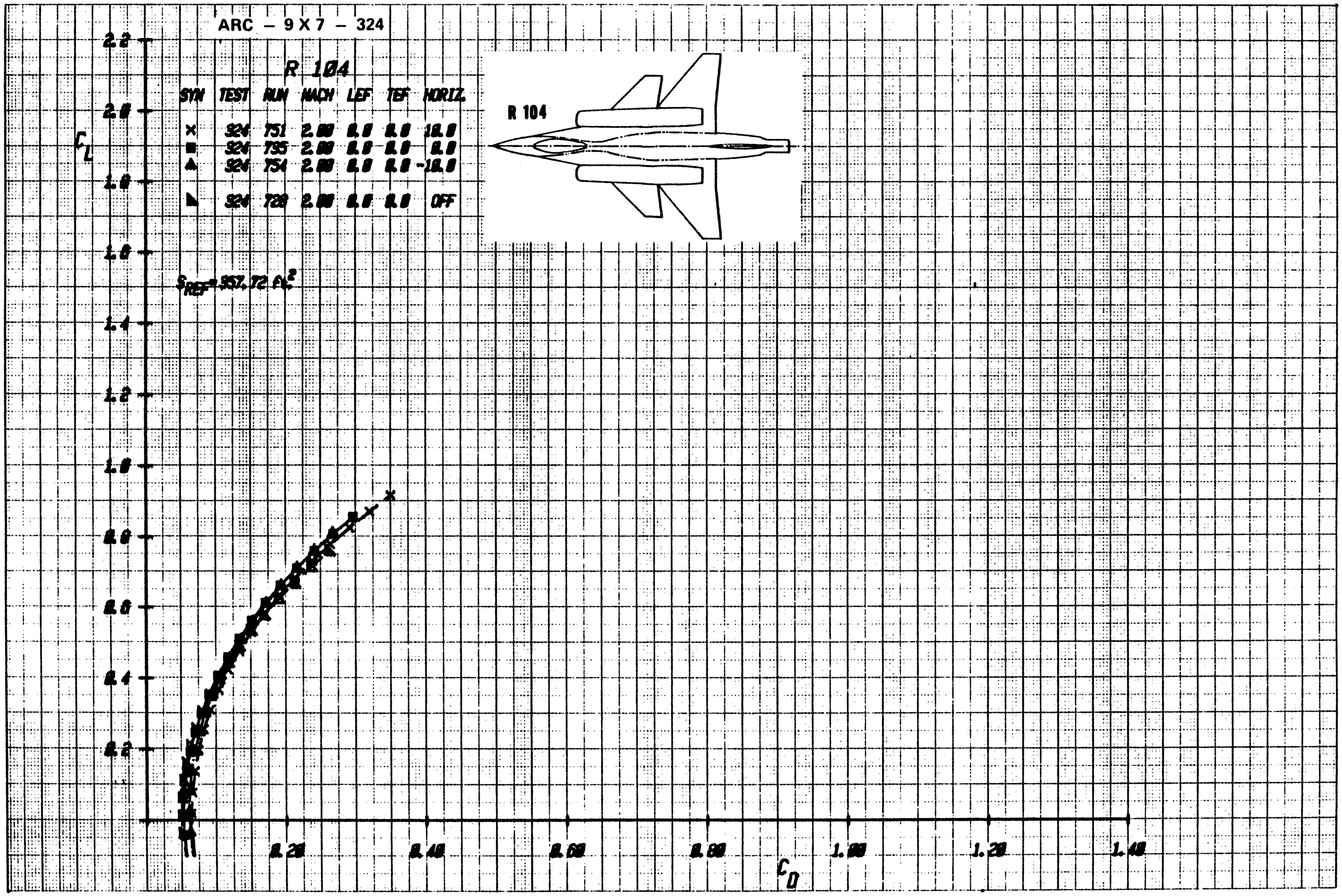

Figure1-30c Effect of Canard Deflection on Drag with Wing Trailing-Edge Flap Undeflected, Mach = 2.0

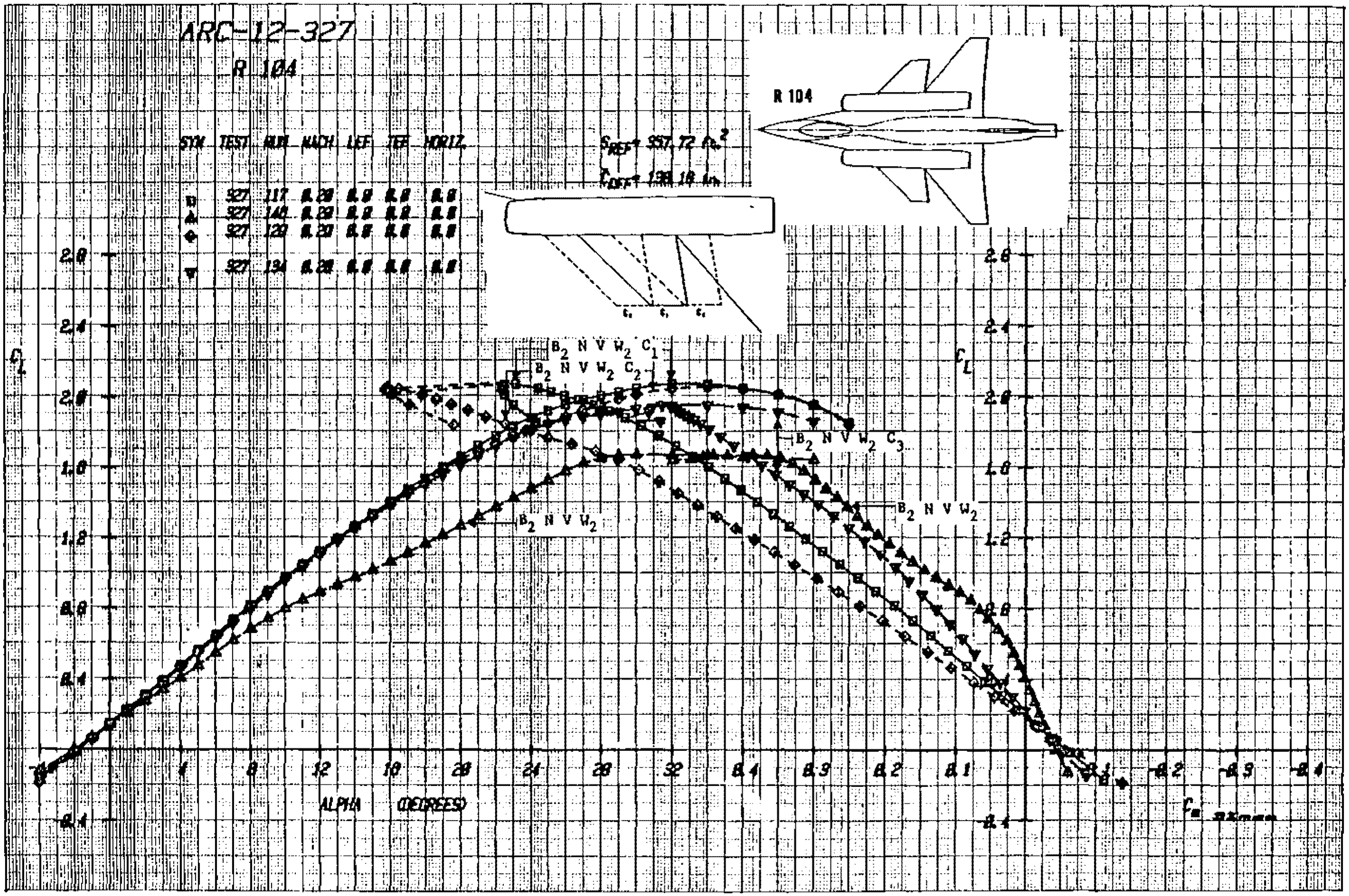

Figure1-31aEffect of Canard Longitudinal Location on Lift and Moment, Mach = .2

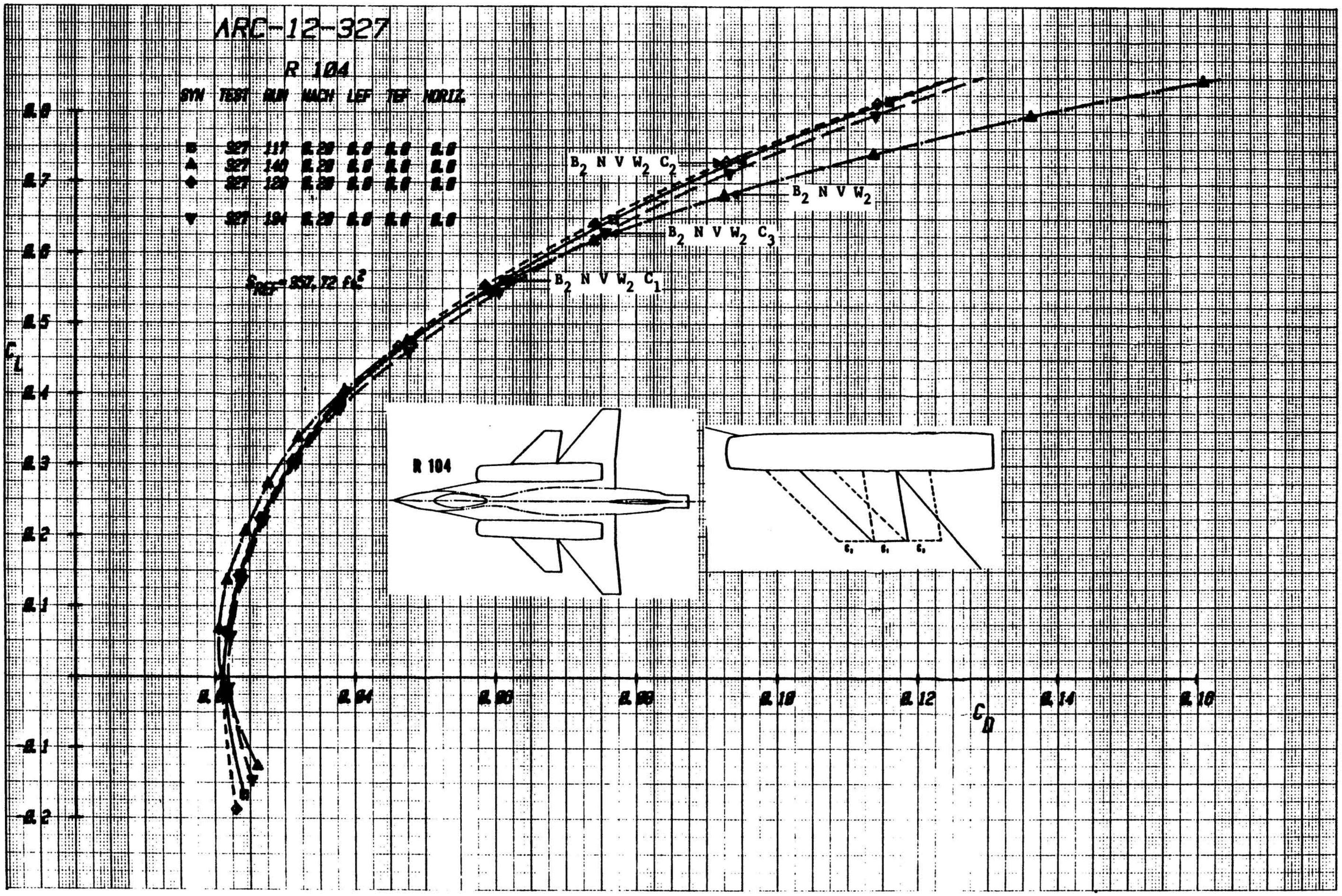

Figurel-31bEffect of Canard Longitudinal Location on Drag, (Expanded Drag Scale), Mach = .2

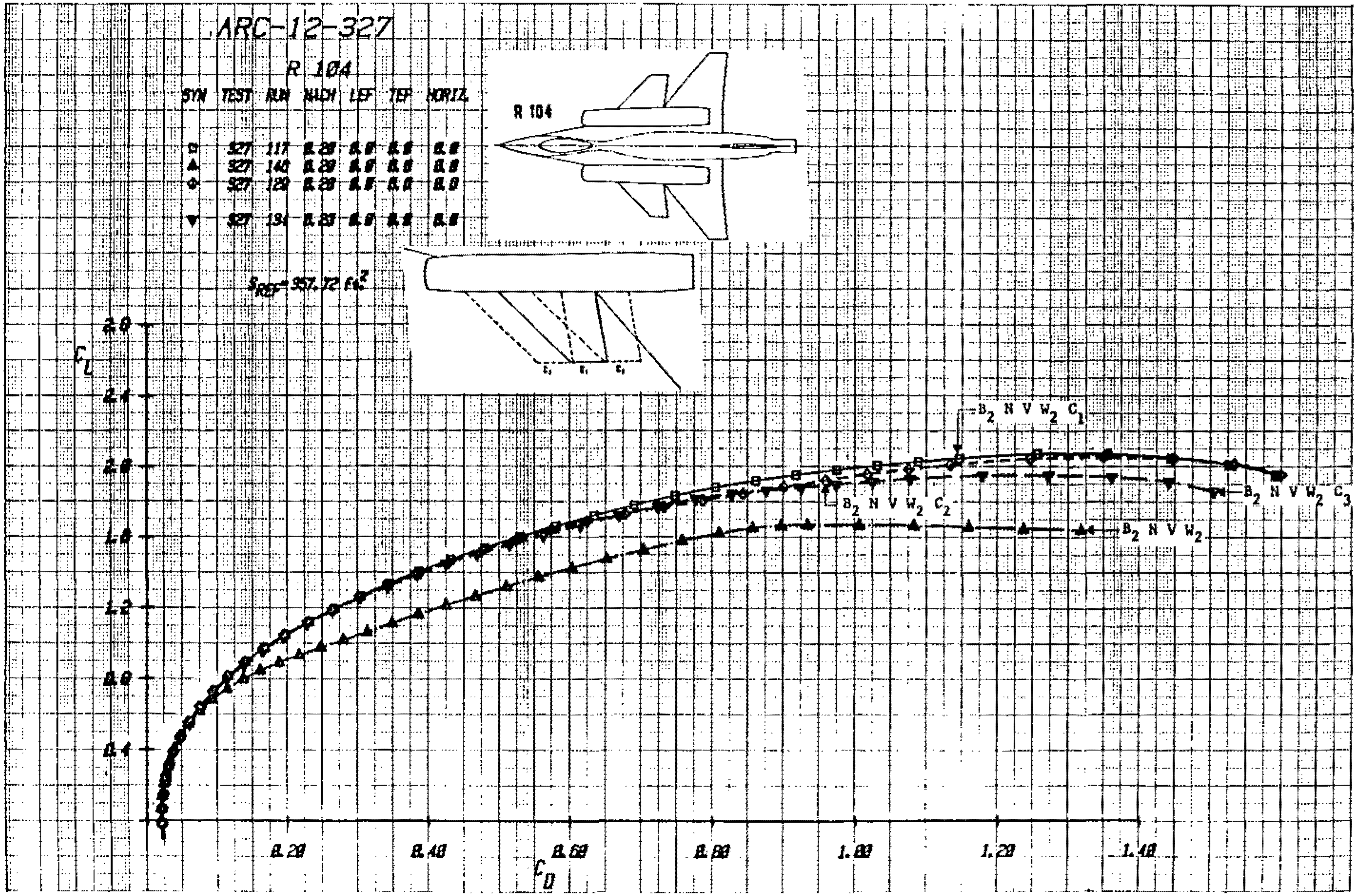

Figure1-31cEffect of Canard Longitudinal Location on Drag, Mach = .2

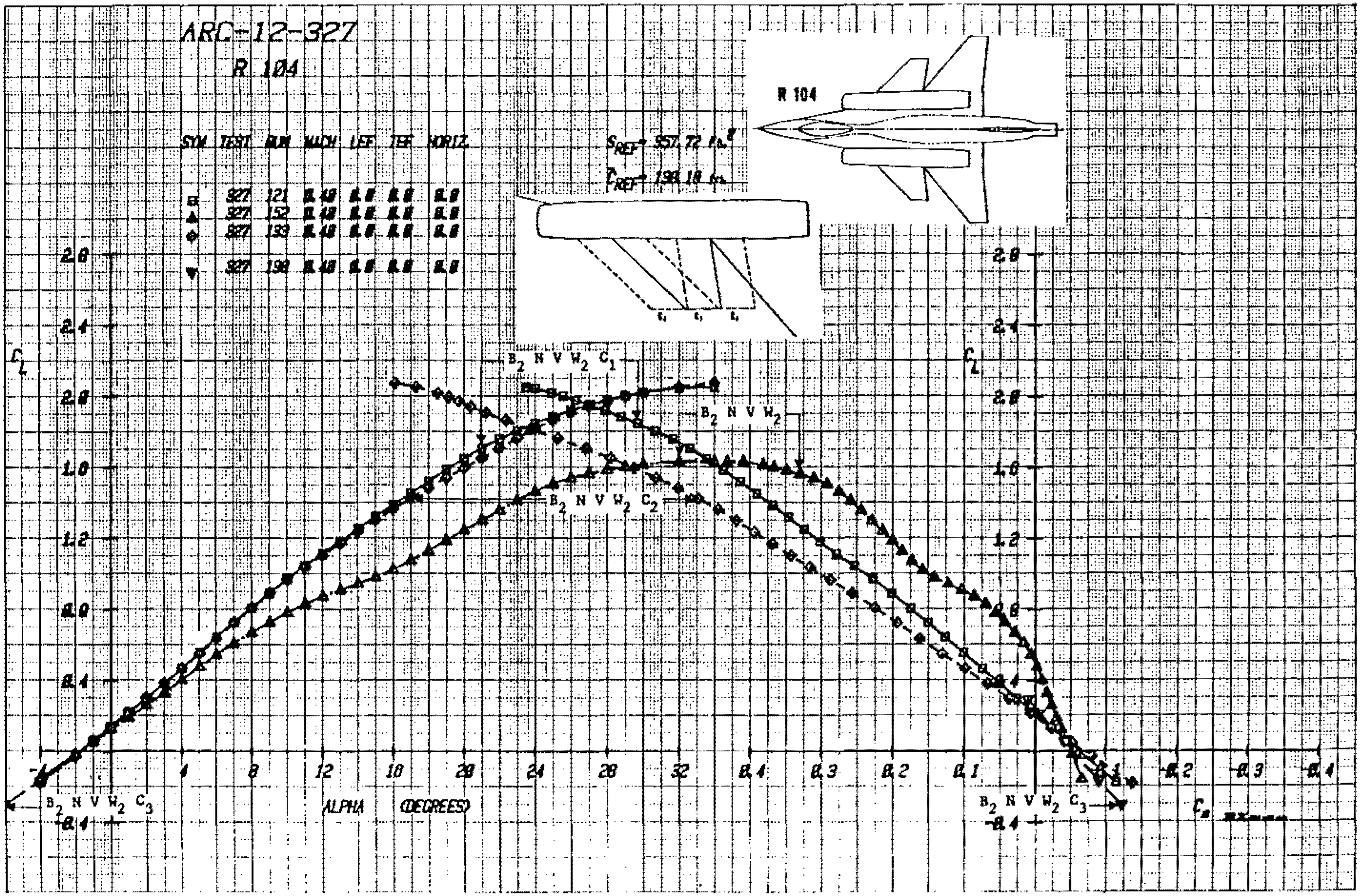

Figure1-32aEffect of Canard Longitudinal Location on Lift and Moment, Mach = .4

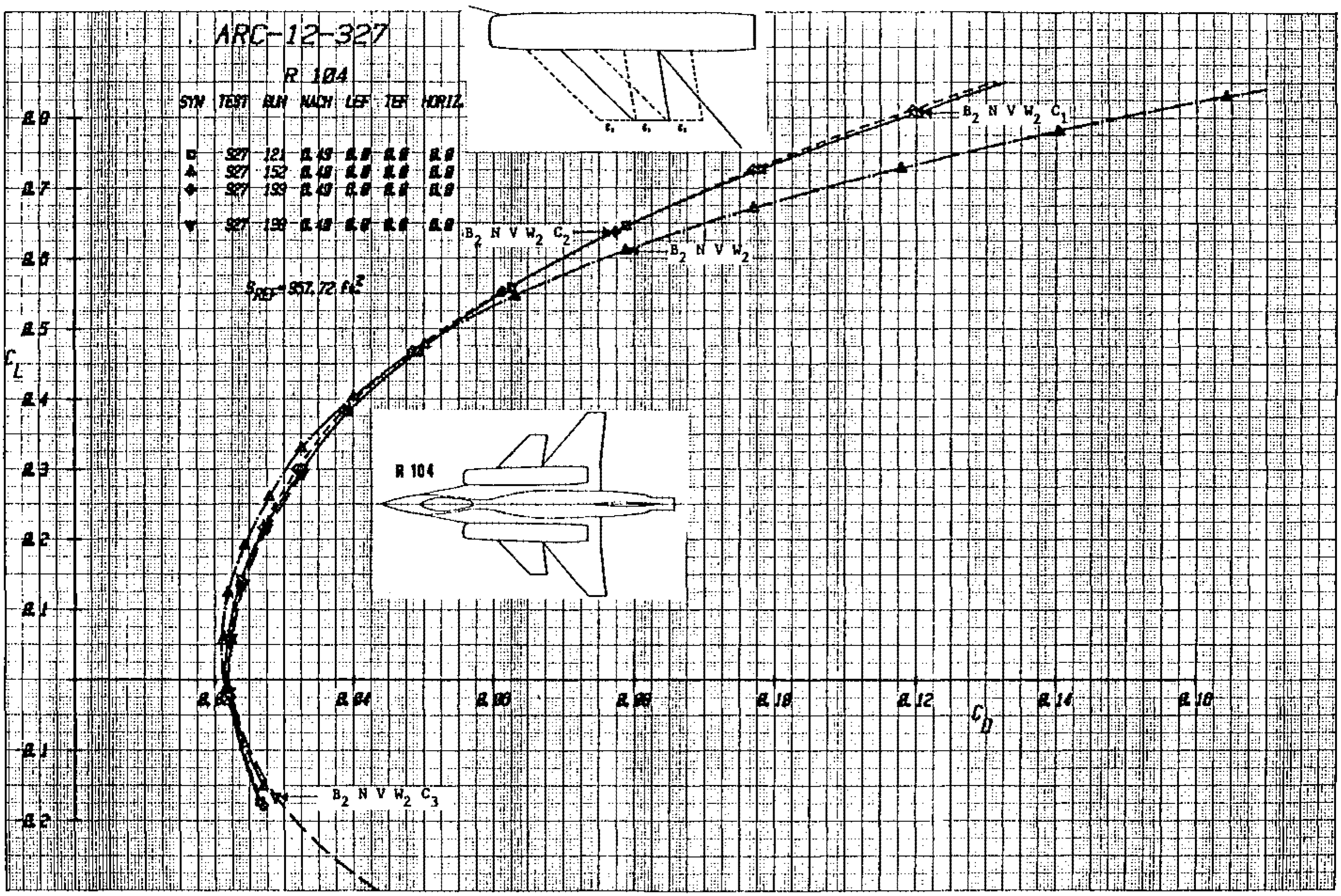

Figure1-32bEffect of Canard Longitudinal Location on Drag, (Expanded Drag Scale), Mach = .4

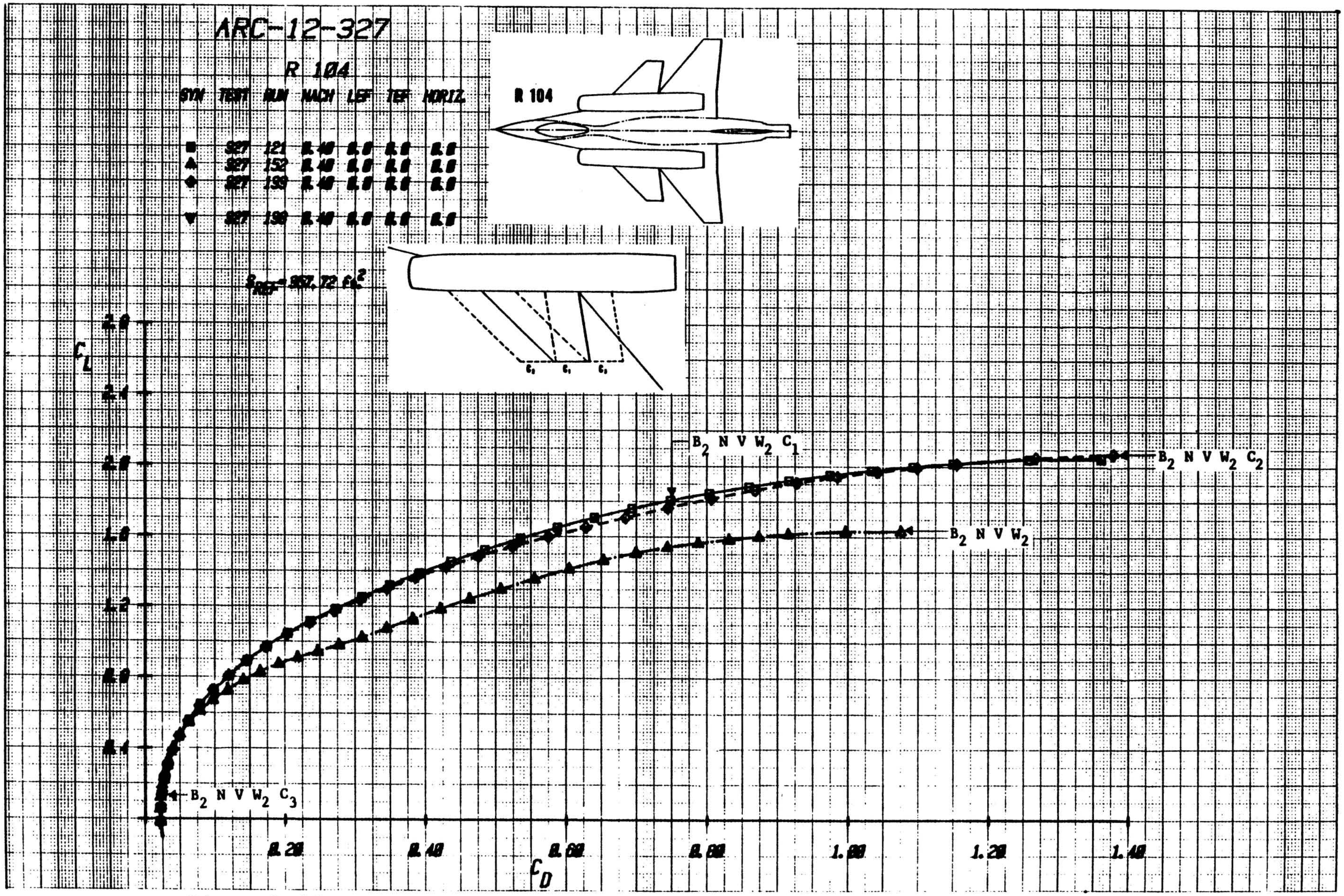

Figure1-32cEffect of Canard Longitudinal Location on Drag, Mach = .4

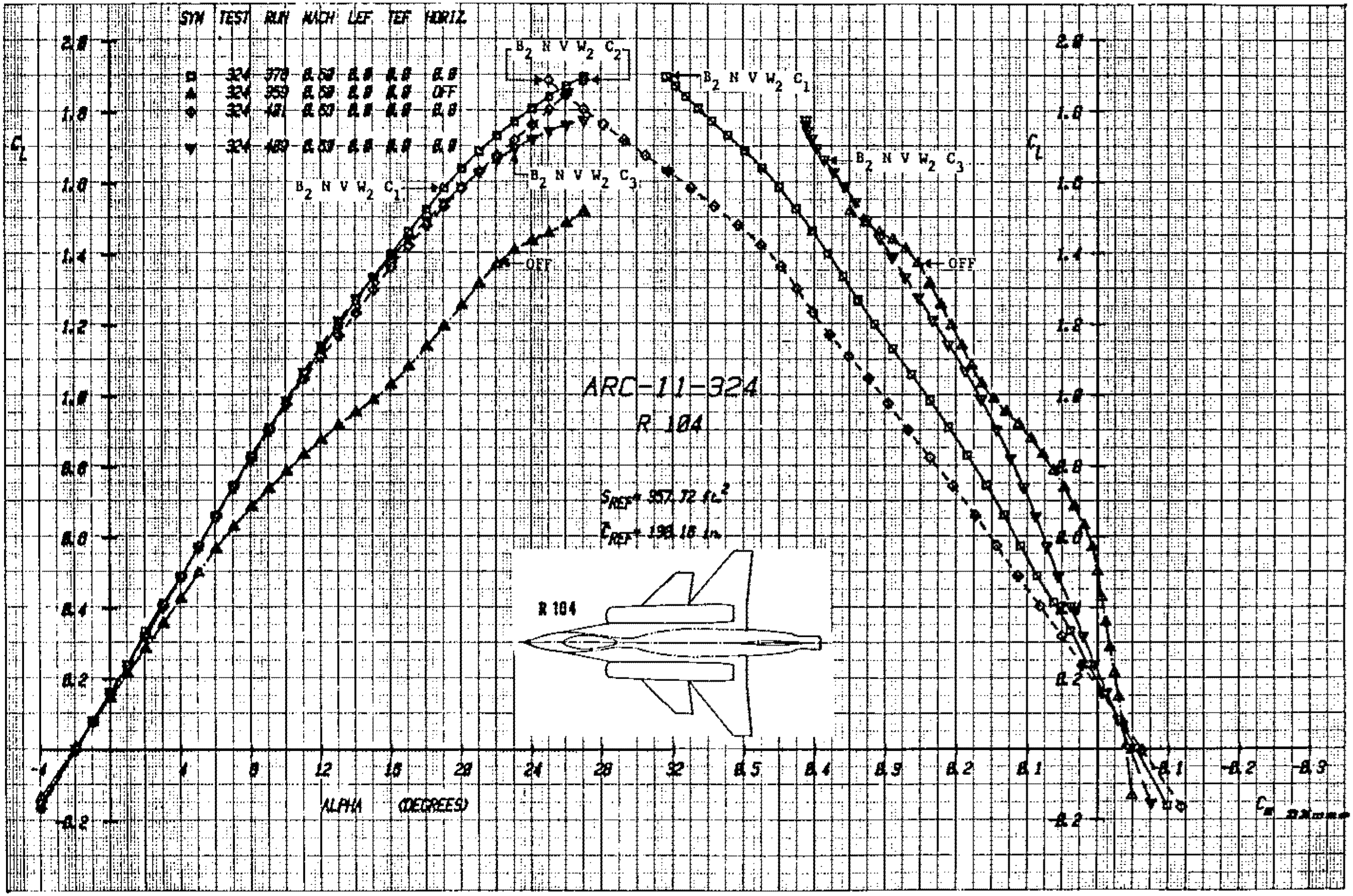

Figure1-33aEffect of Canard Longitudinal Location on Lift and Moment, Mach = .6

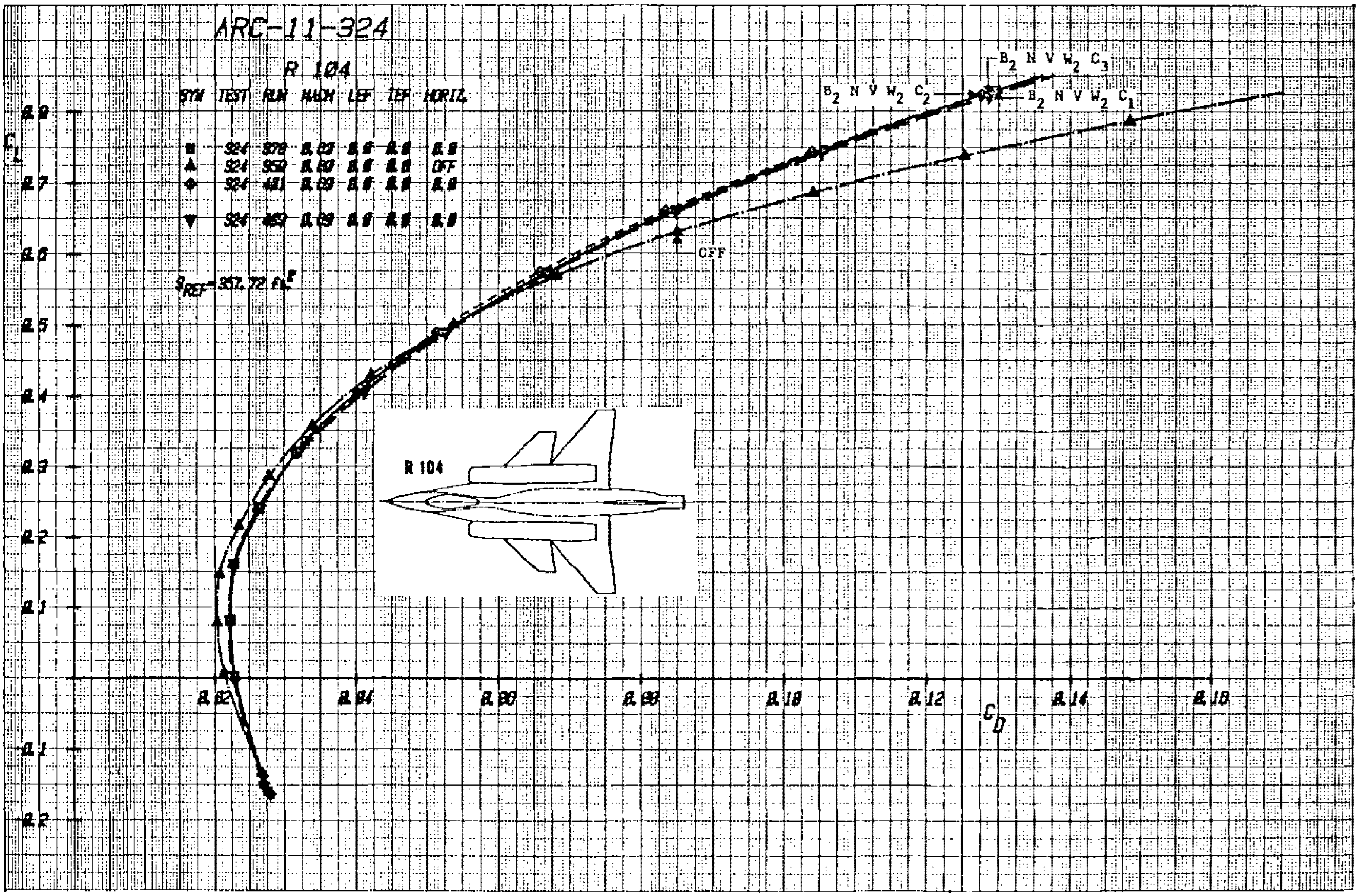

Figure1-33bEffect of Canard Longitudinal Location on Drag, Mach = .6

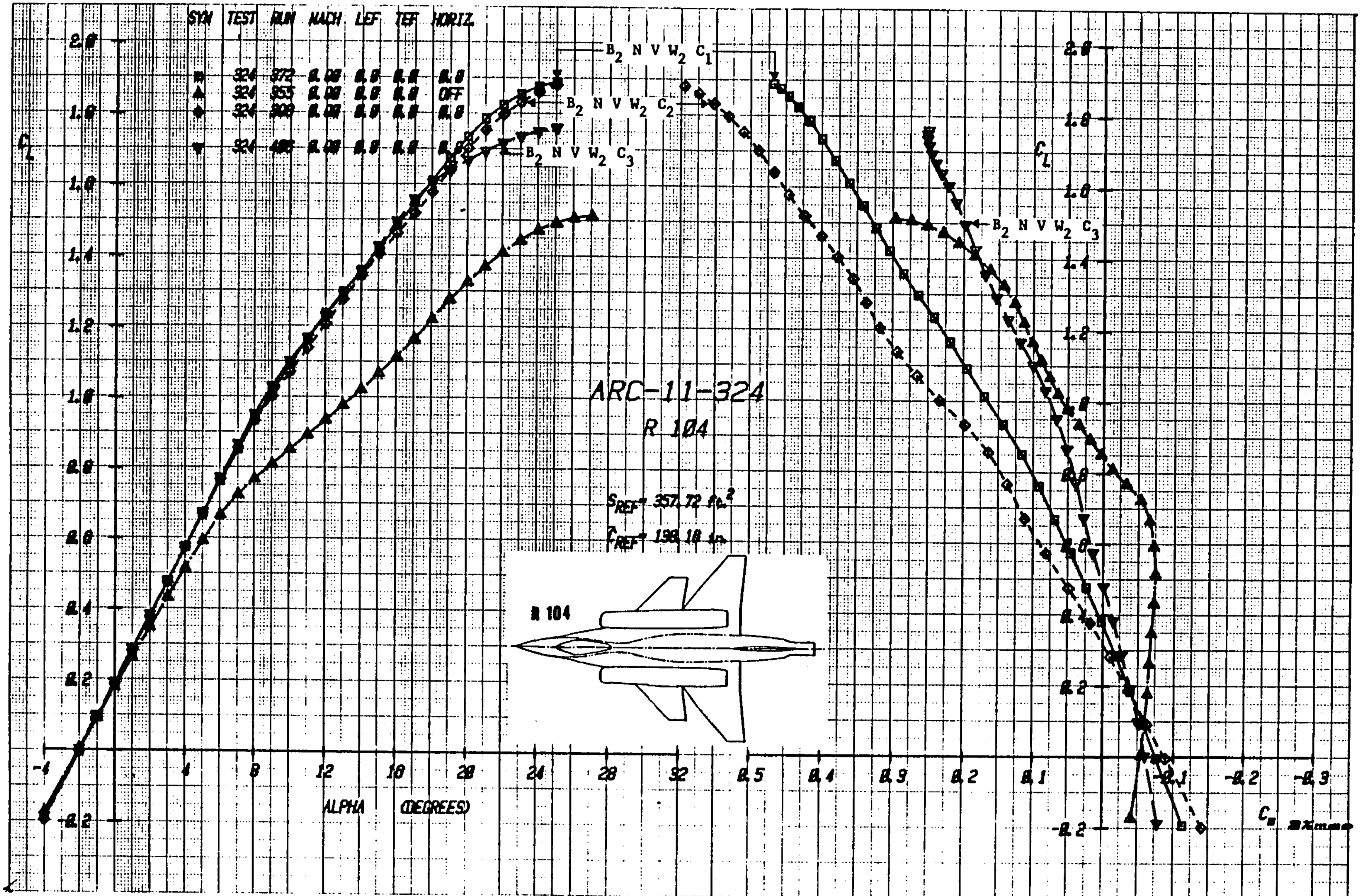

Figure1-34a Effect of Canard Longitudinal Location on Lift and Moment, Mach = .9

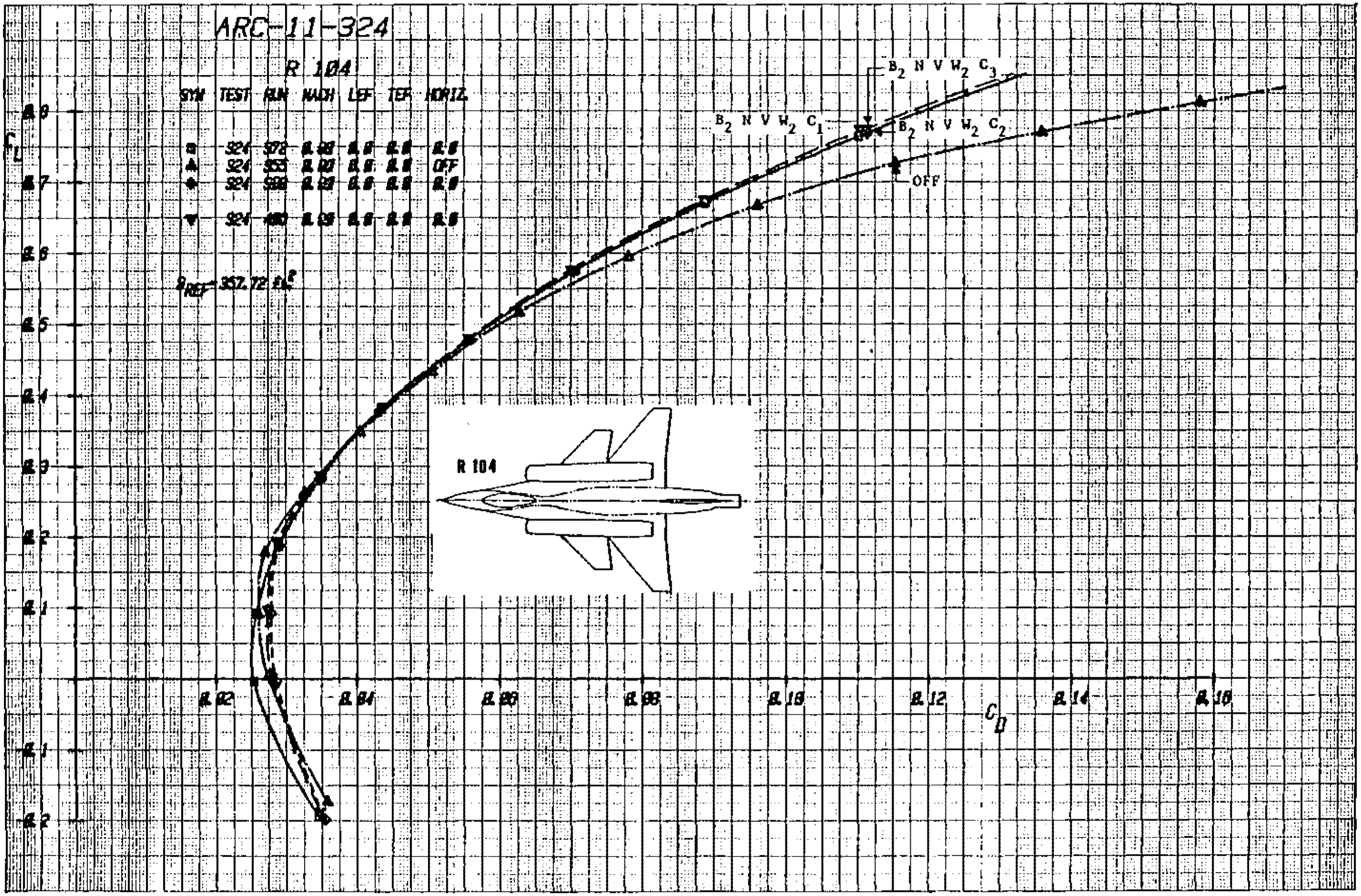

Figurel-34bEffect of Canard Longitudinal Location on Drag, Mach = .9

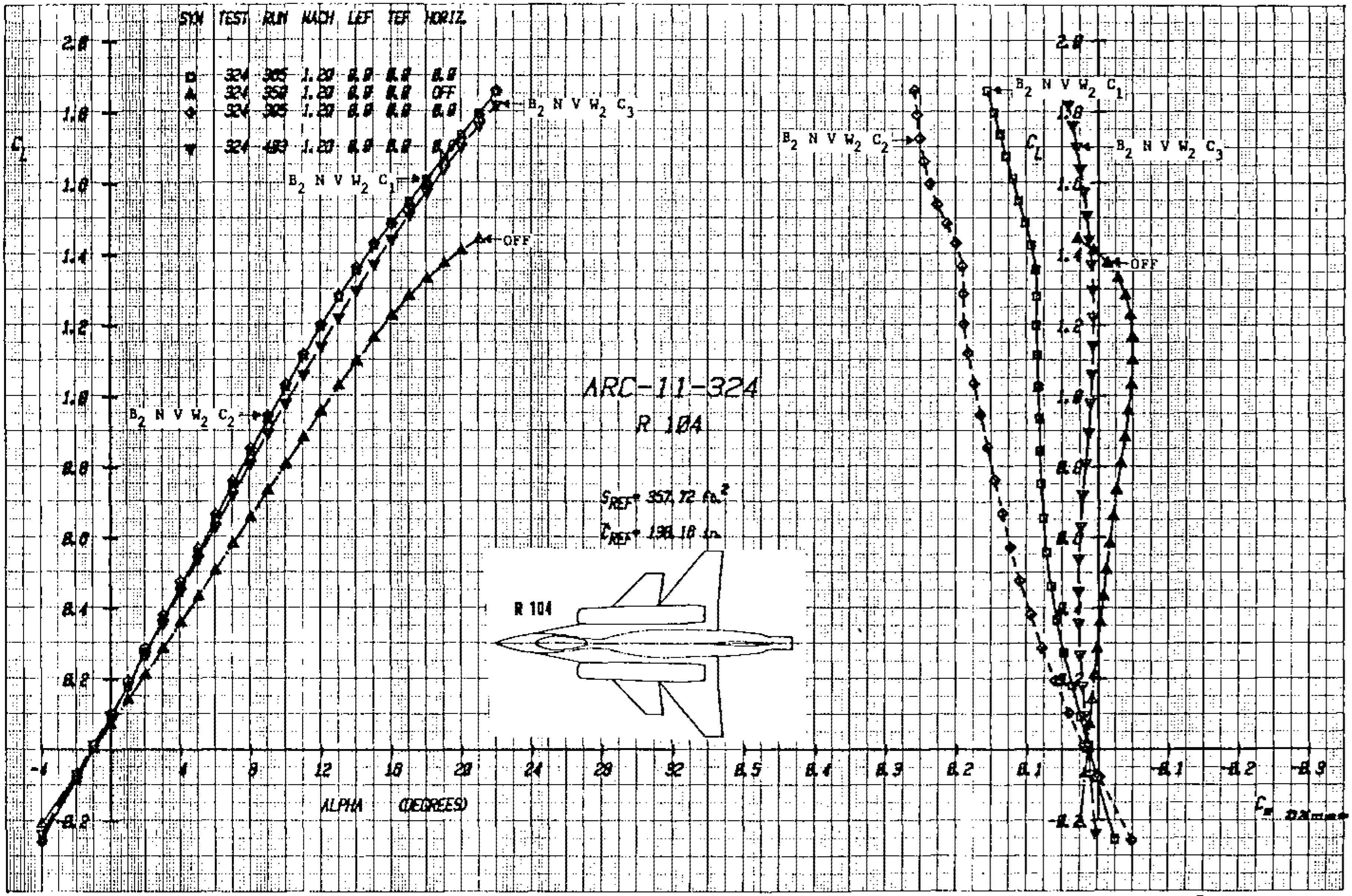

Figure1-35a Effect of Canard Longitudinal Location on Lift and Moment, Mach = 1.2

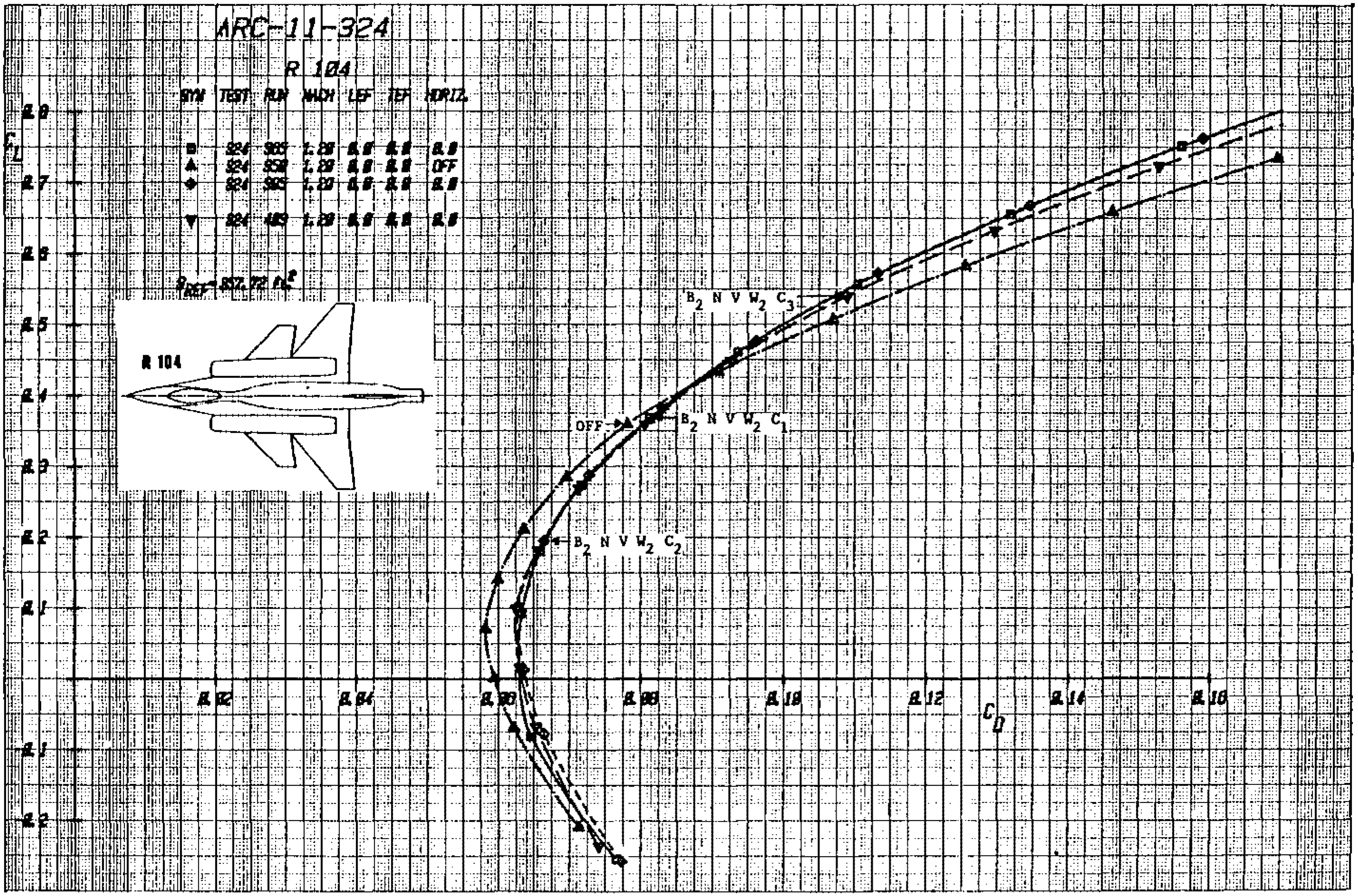

Figure1-35bEffect of Canard Longitudinal Location on Drag, Mach = 1.2

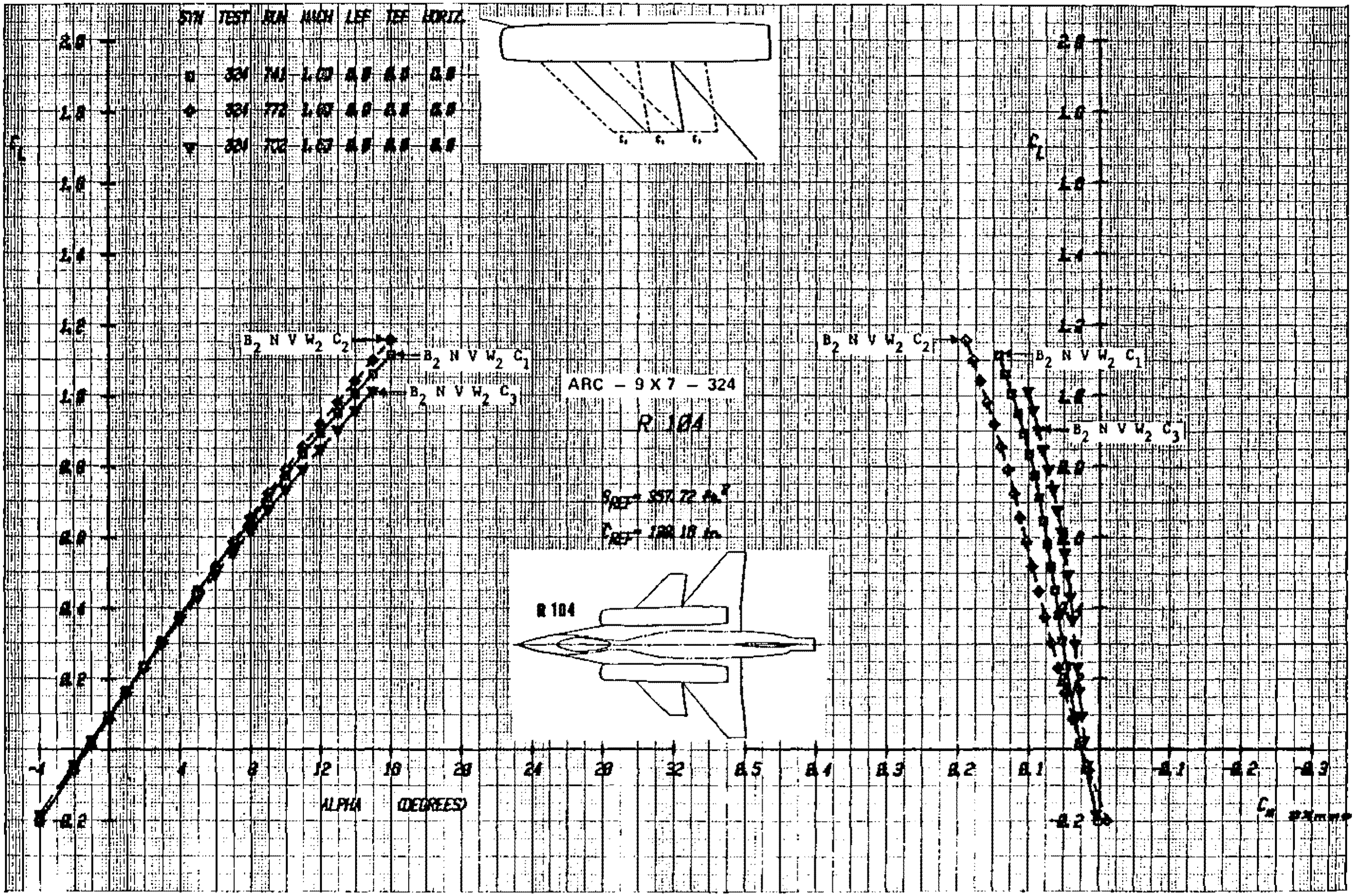

Figure1-36aEffect of Canard Longitudinal Location on Lift and Moment, Mach = 1.6

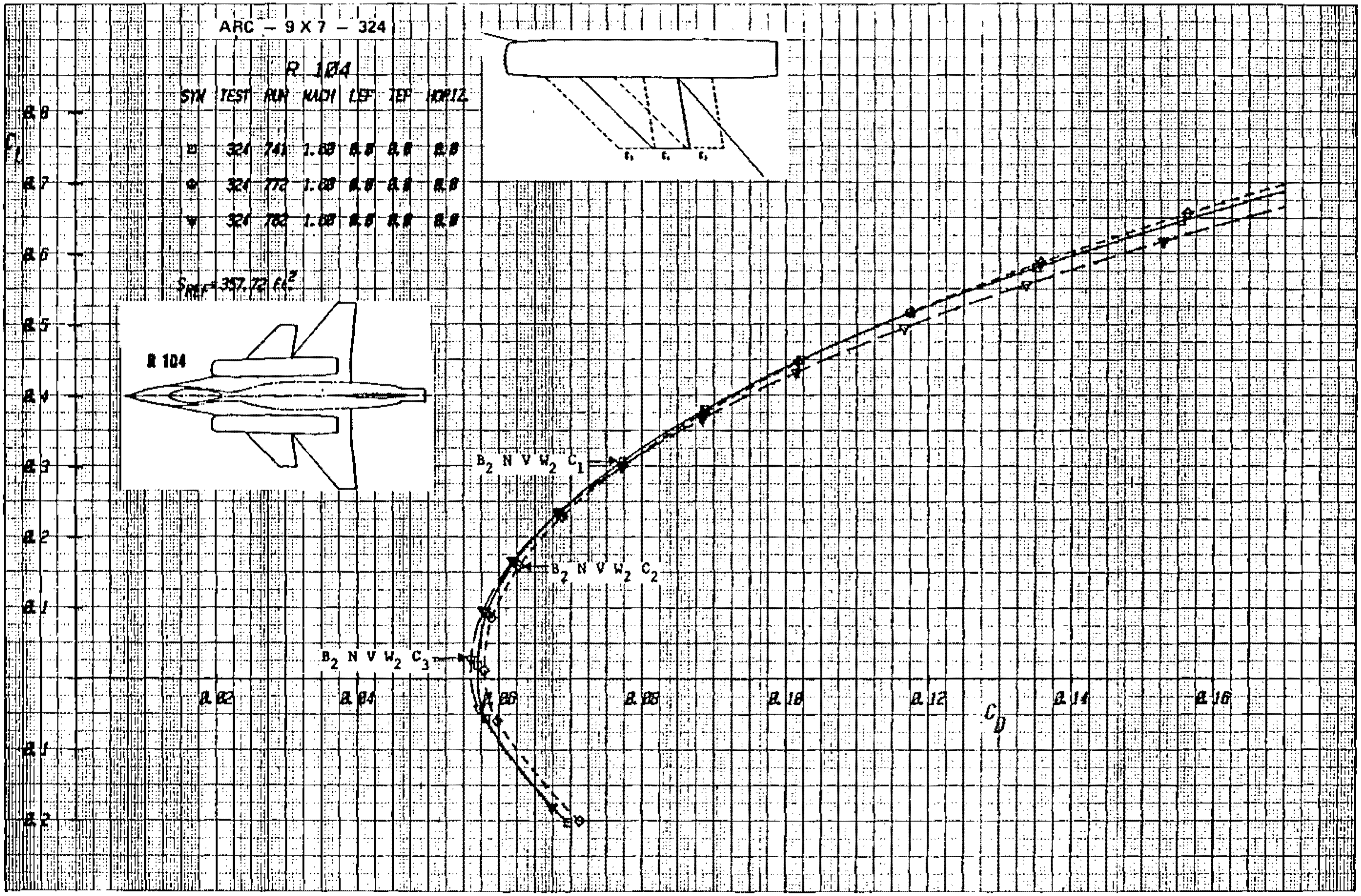

Figure1-36b Effect of Canard Longitudinal Location on Drag, (Expanded Drag Scale), Mach = 1.6

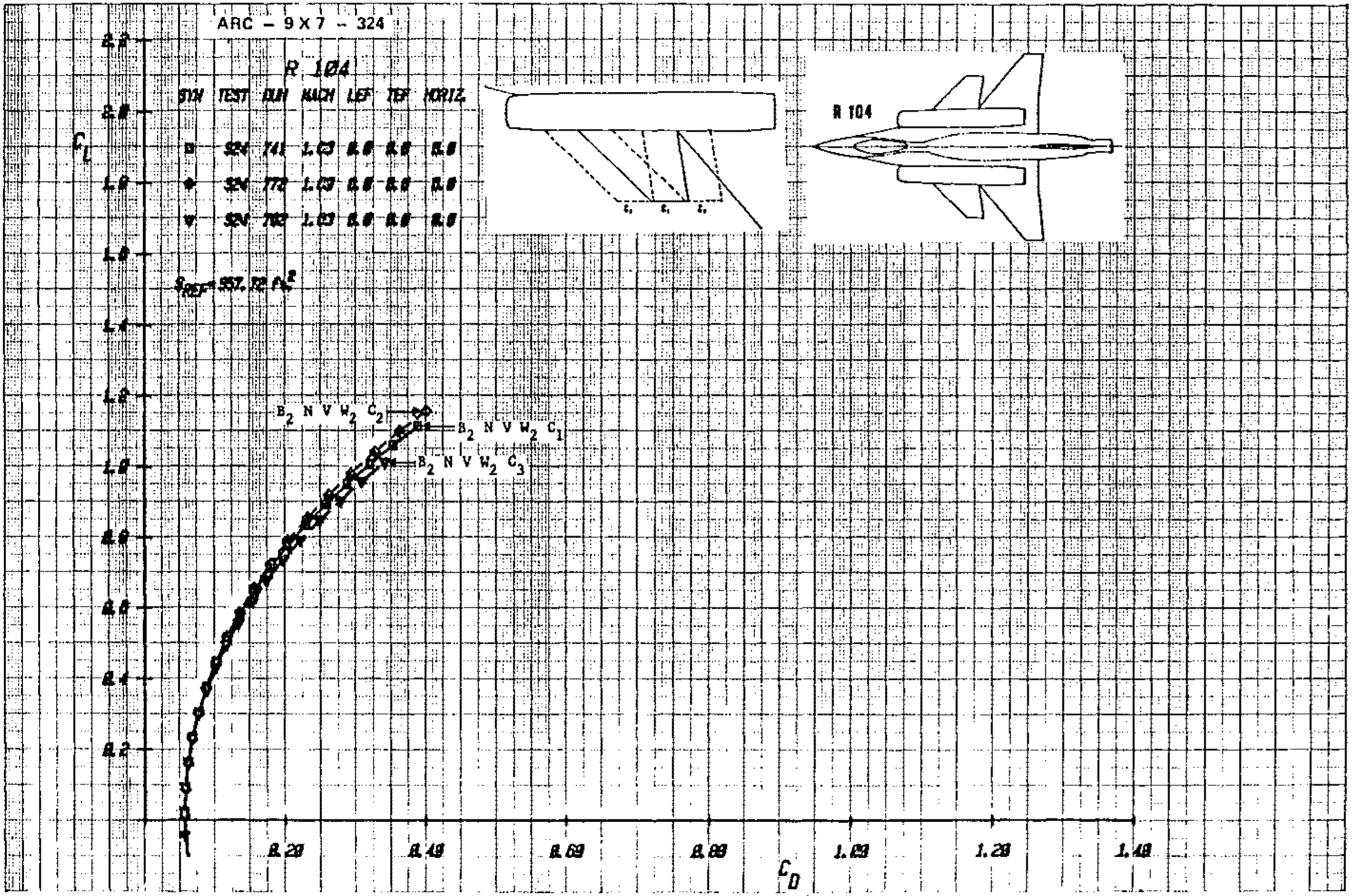

Figure1-36cEffect of Canard Longitudinal Location on Drag, Mach = 1.6

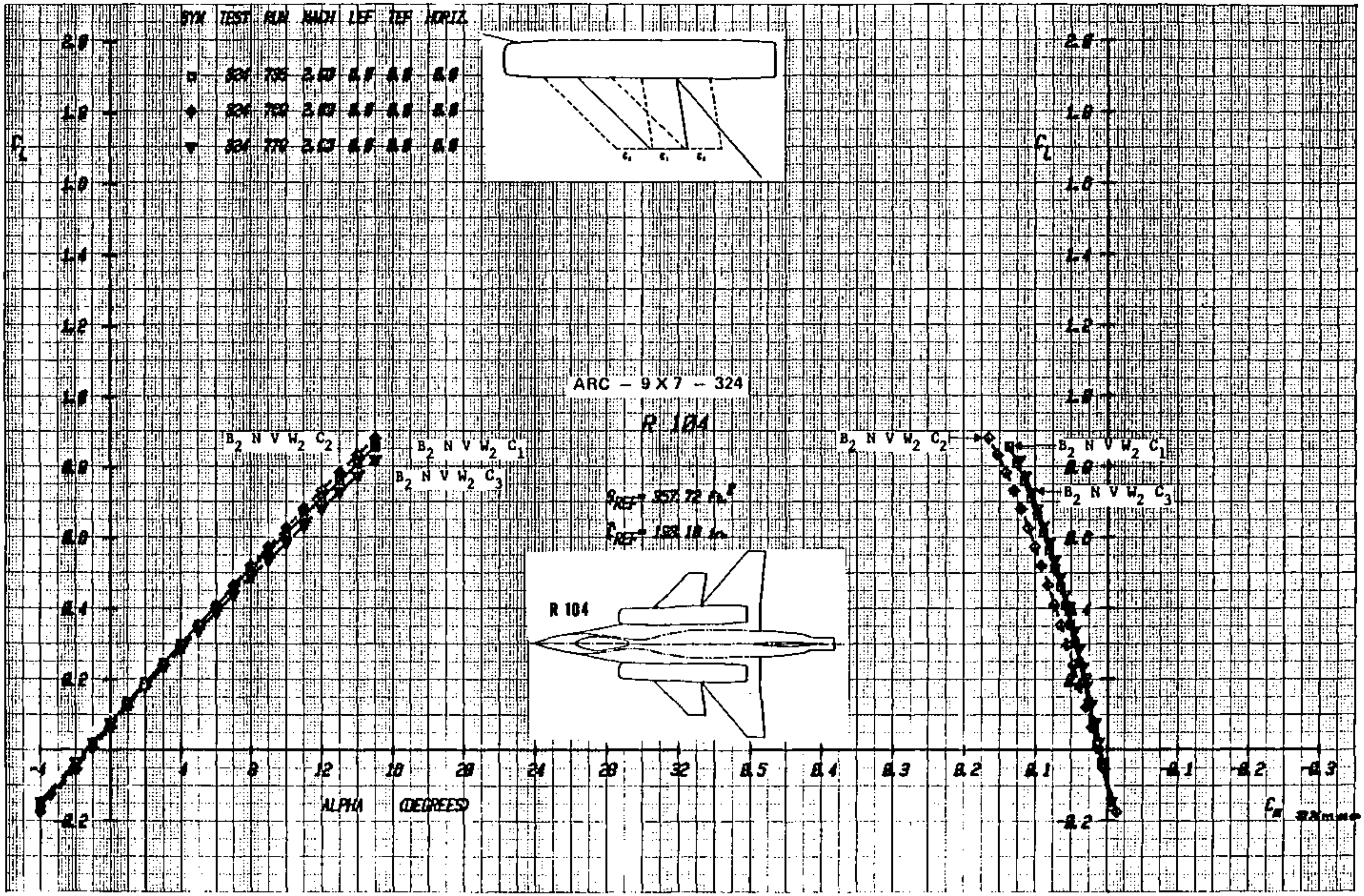

Figure1-37aEffect of Canard Longitudinal Location on Lift and Moment, Mach = 2.0

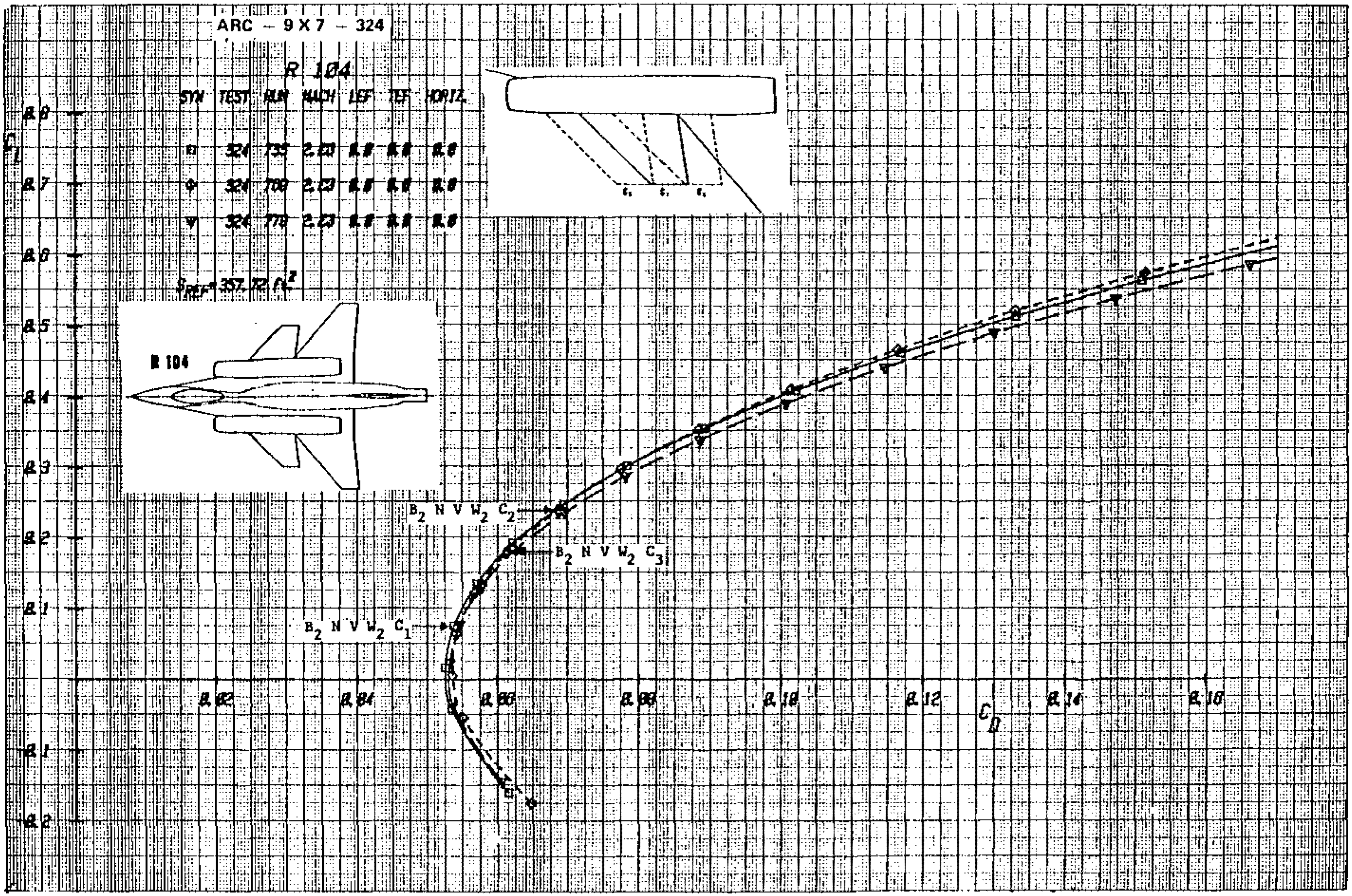

Figure1-37bEffect of Canard Longitudinal Location on Drag (Expanded Drag Scale), Mach = 2.0

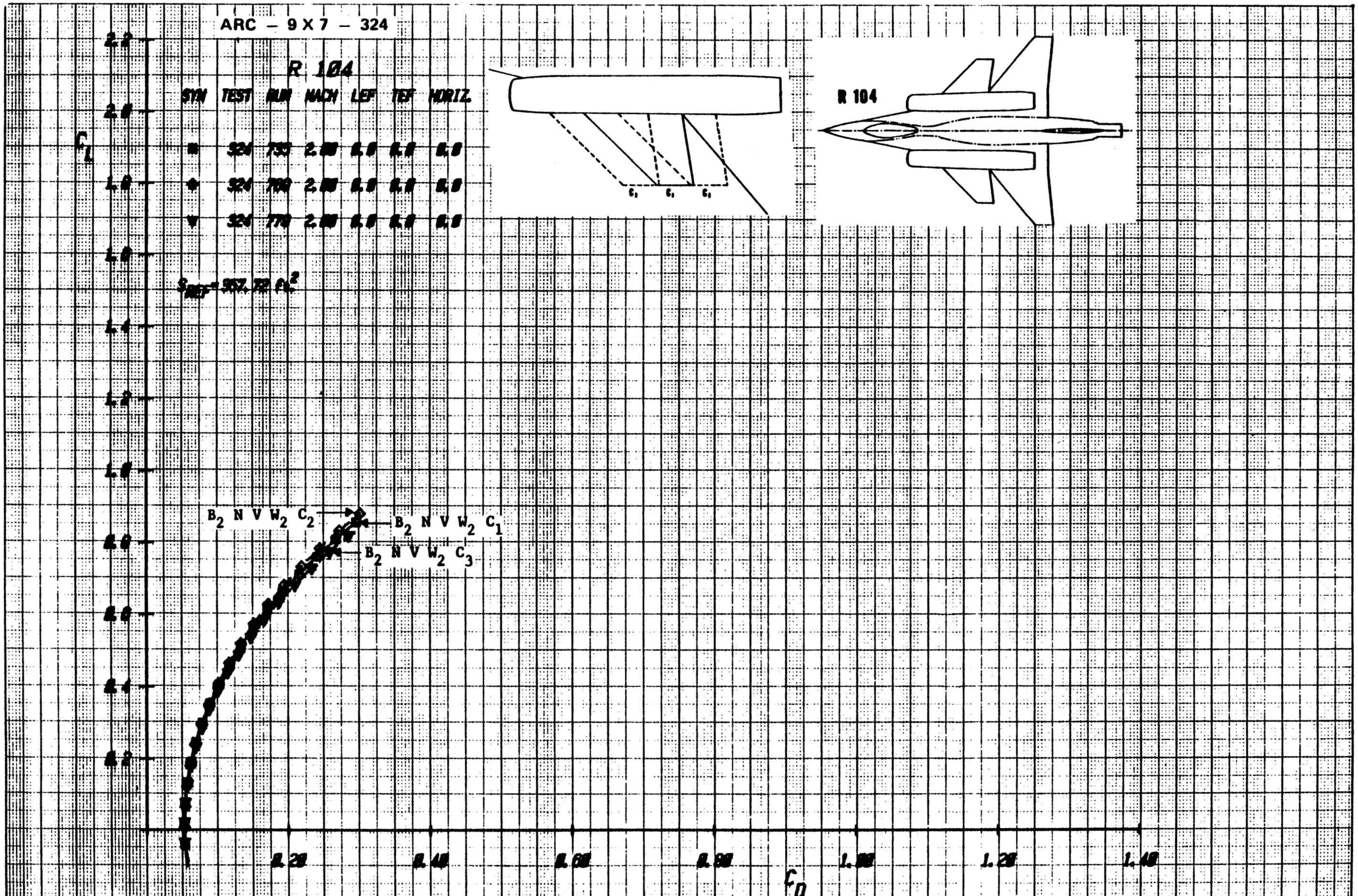

Figure 1-37c Effect of Canard Longitudinal Location on Drag, Mach = 2.0

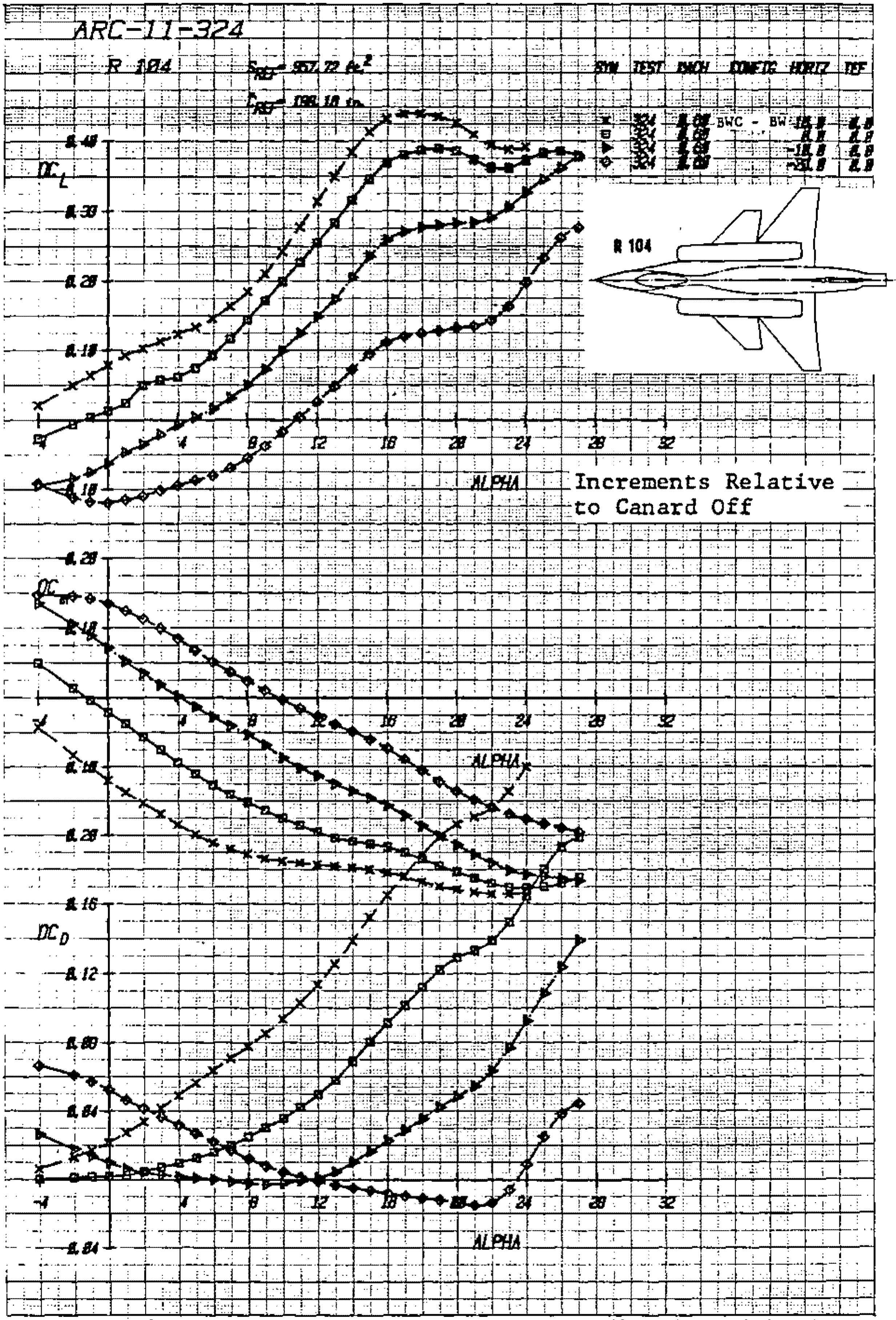

Figure 1-38 Incremental Effects of Canard Deflection with Wing Trailing-Edge Flap Undeflected, Mach = .6

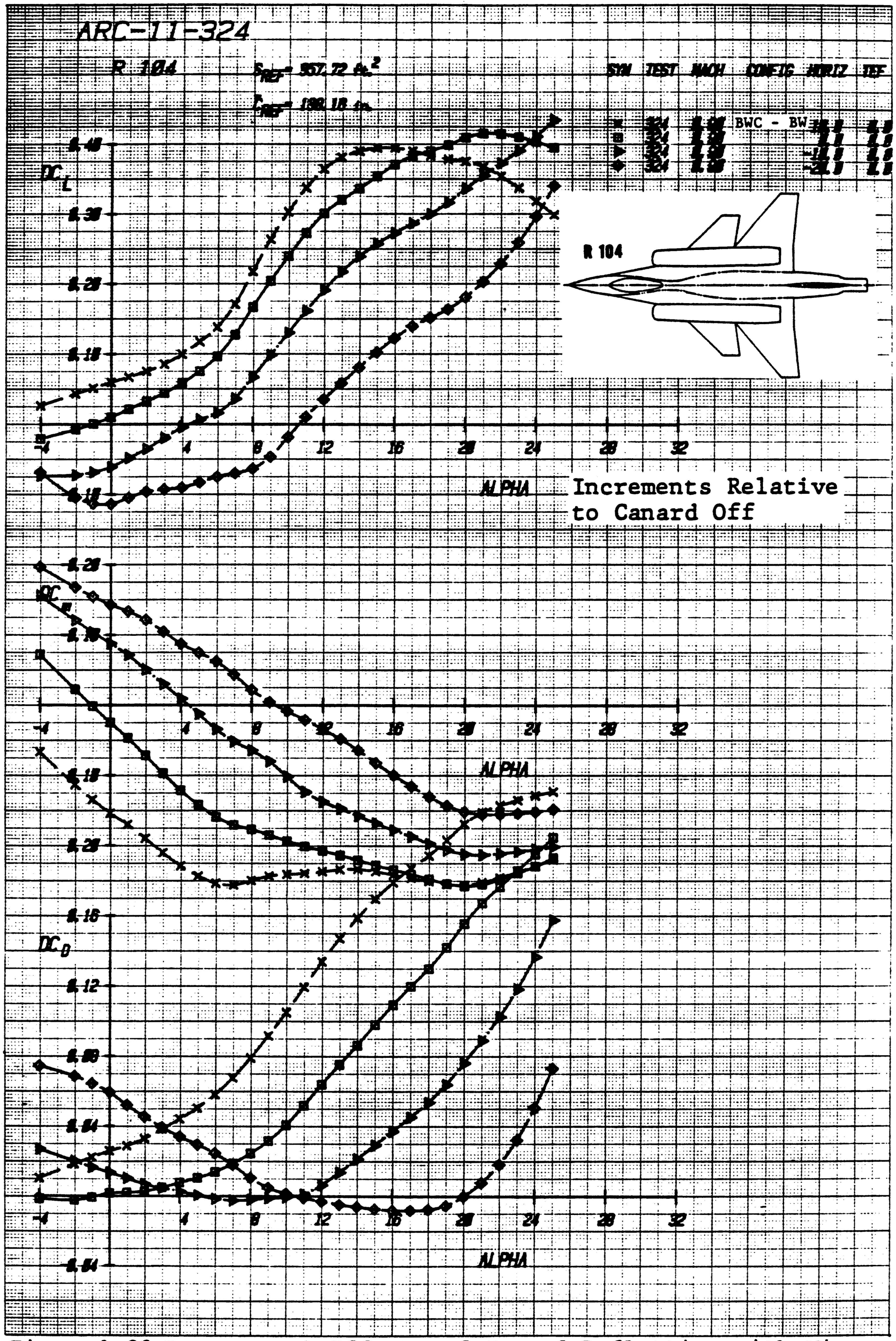

Figure 1-39 Incremental Effects of Canard Deflection with Wing Trailing-Edge Flap Undeflected, Mach = .9

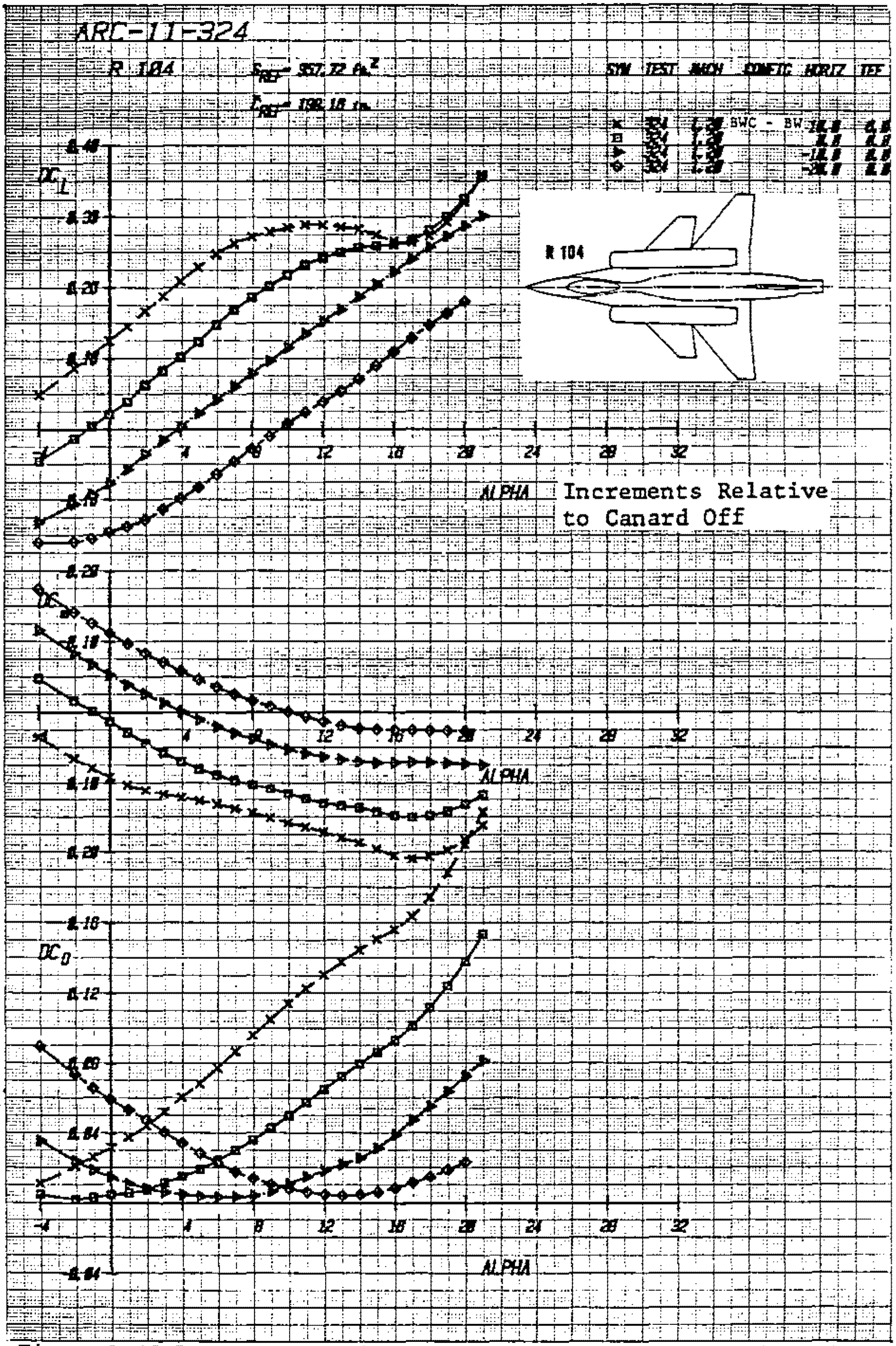

Figure 1-40 Incremental Effects of Canard Deflection with Wing Trailing-Edge Flap Undeflected, Mach = 1.2

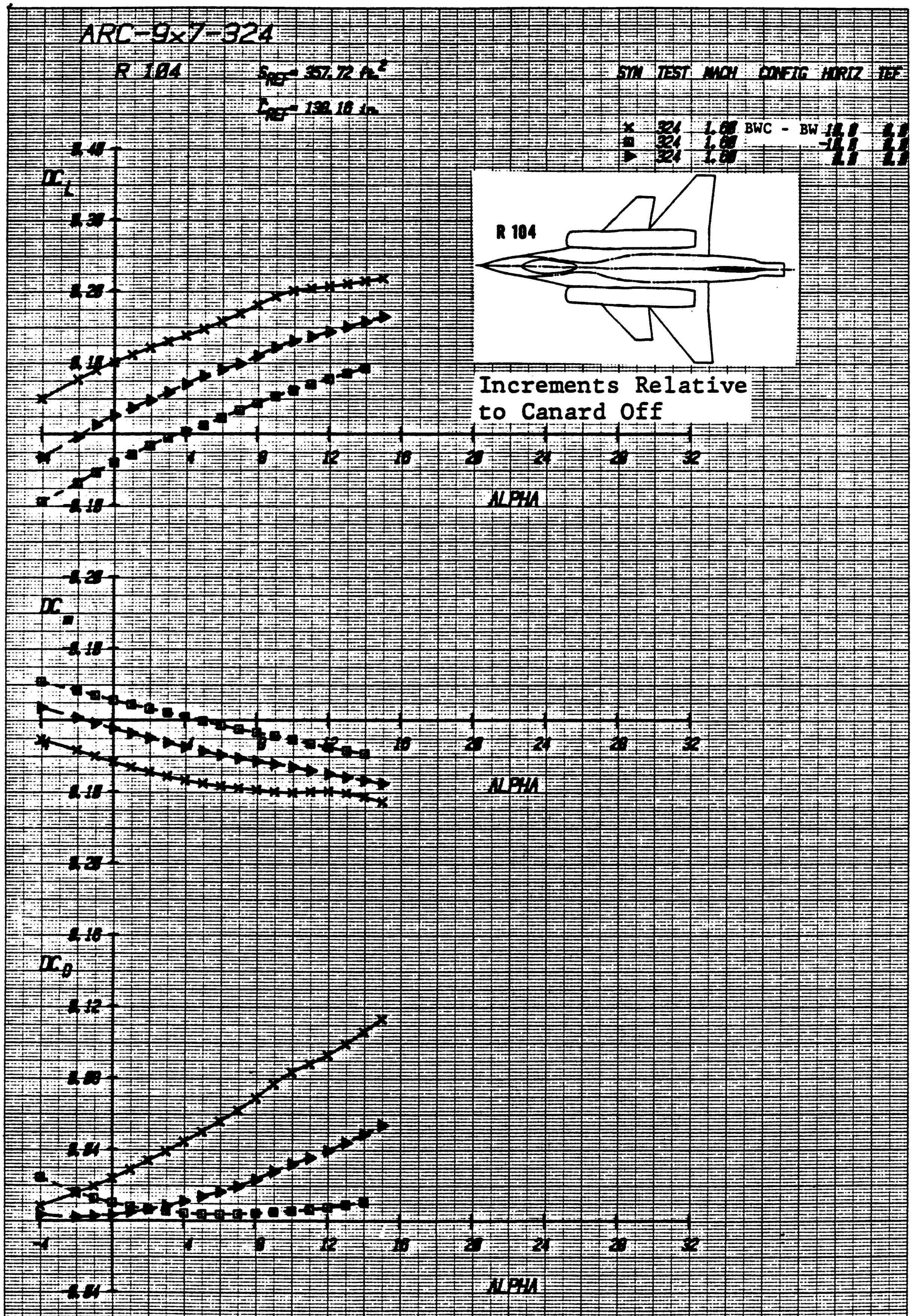

Figure 1-41 Incremental Effects of Various Canard Deflections, Mach = 1.60

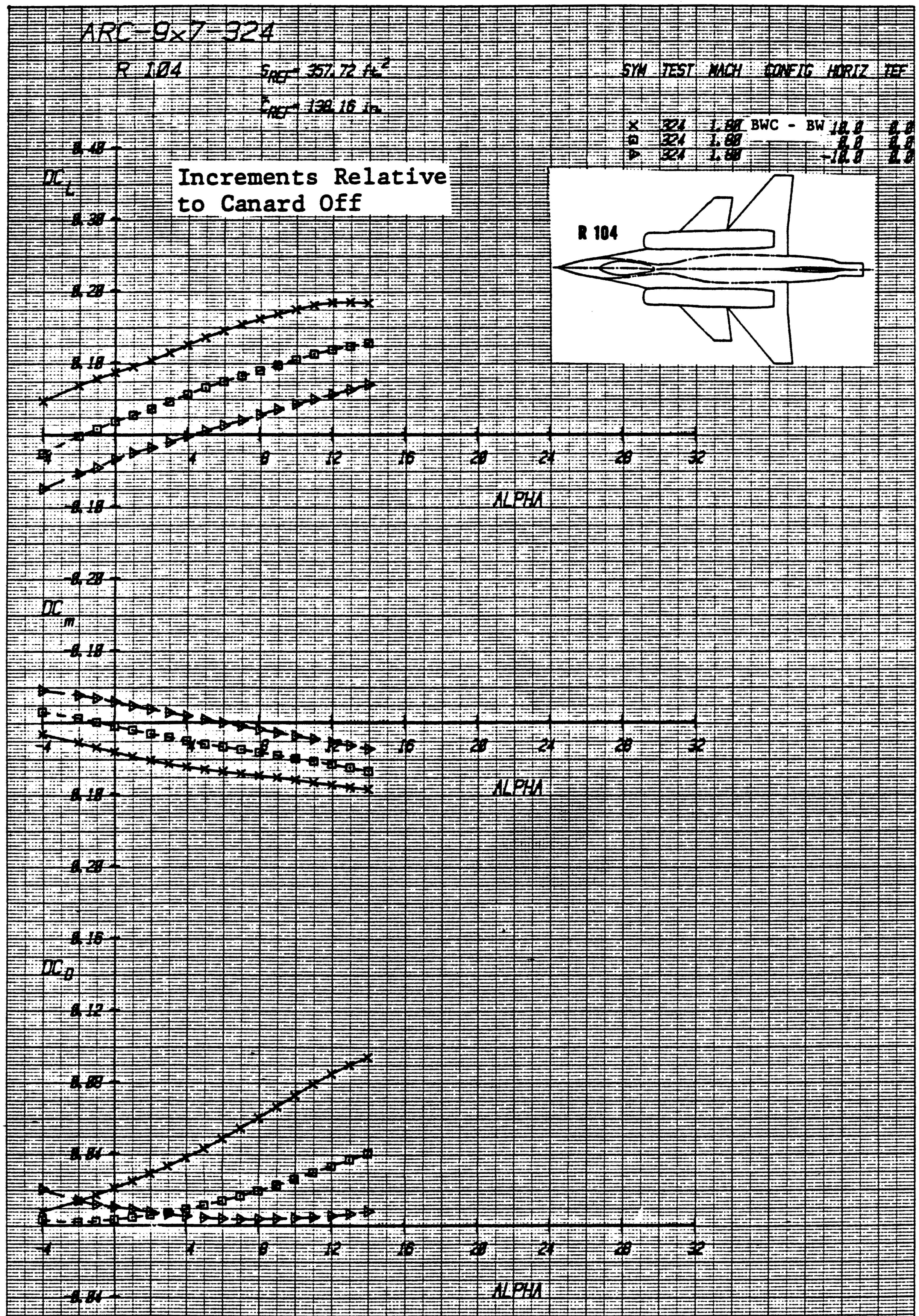

Figure 1-42 Incremental Effects of Various Canard Deflections, Mach = 1.80

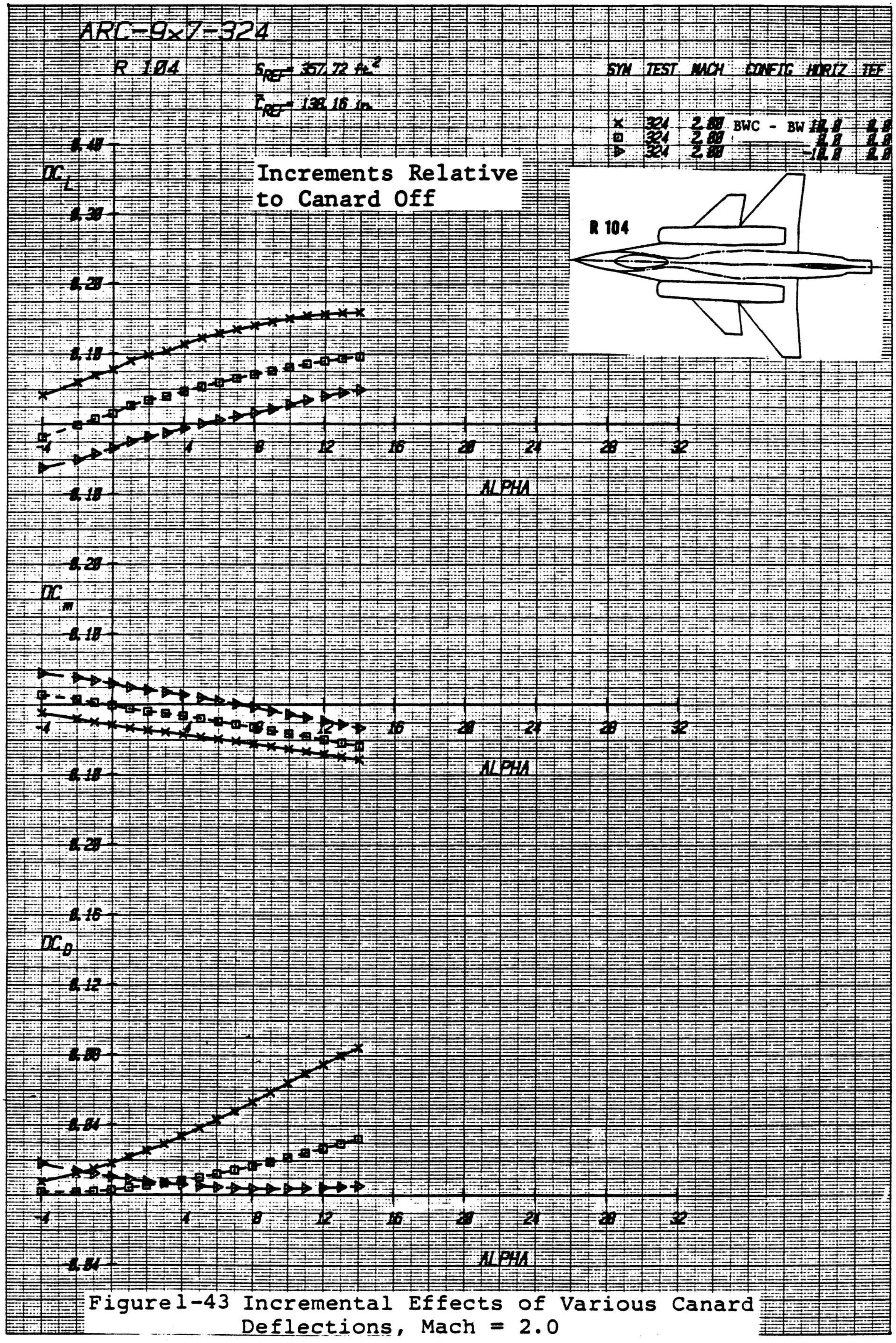

Figure 1-43 Incremental Effects of Various Canard Deflections, Mach = 2.0

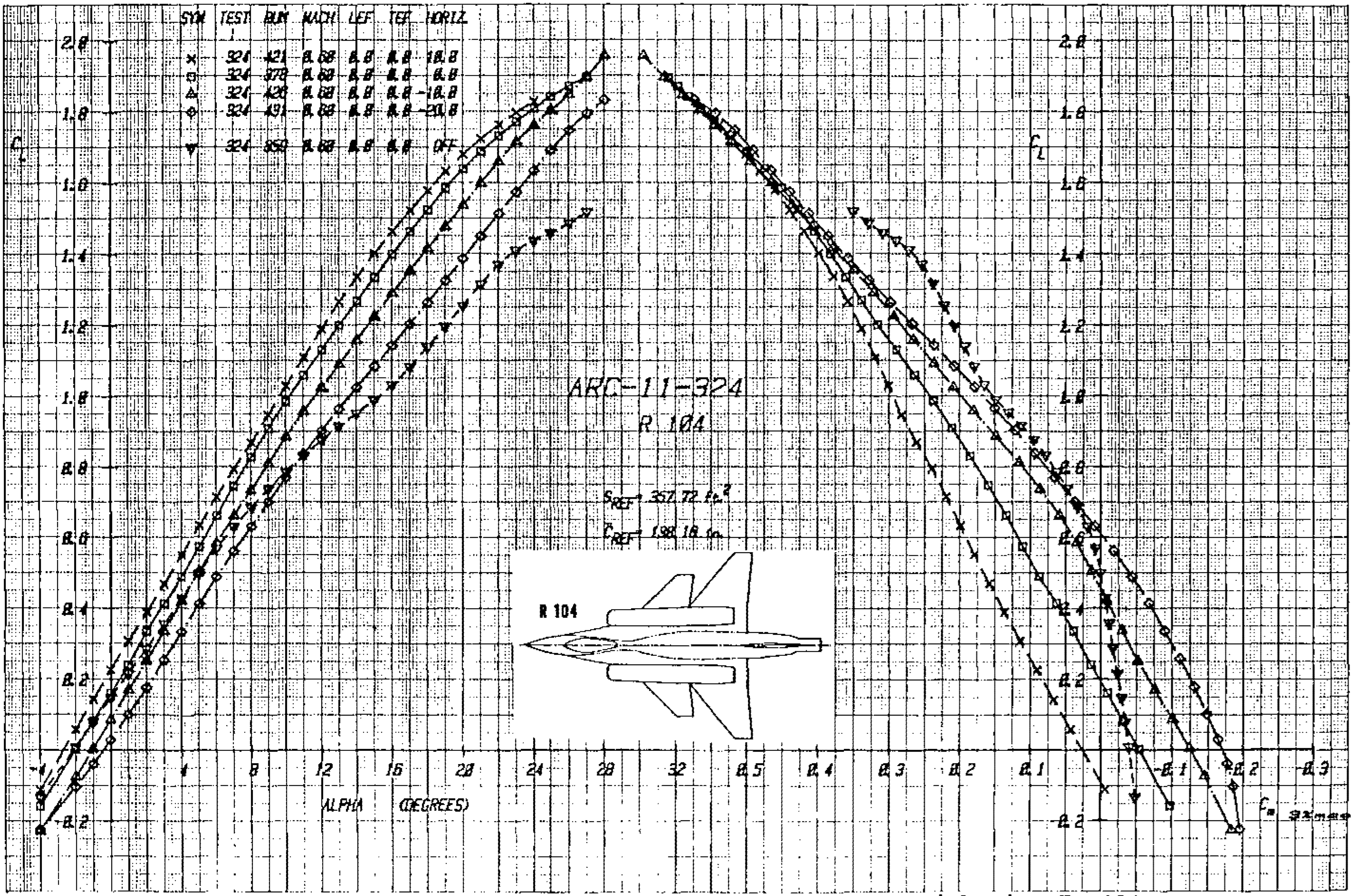

Figure1-44aEffect of Canard Deflection on Lift and Moment with Wing Trailing-Edge Flap Undeflected, Mach = .6

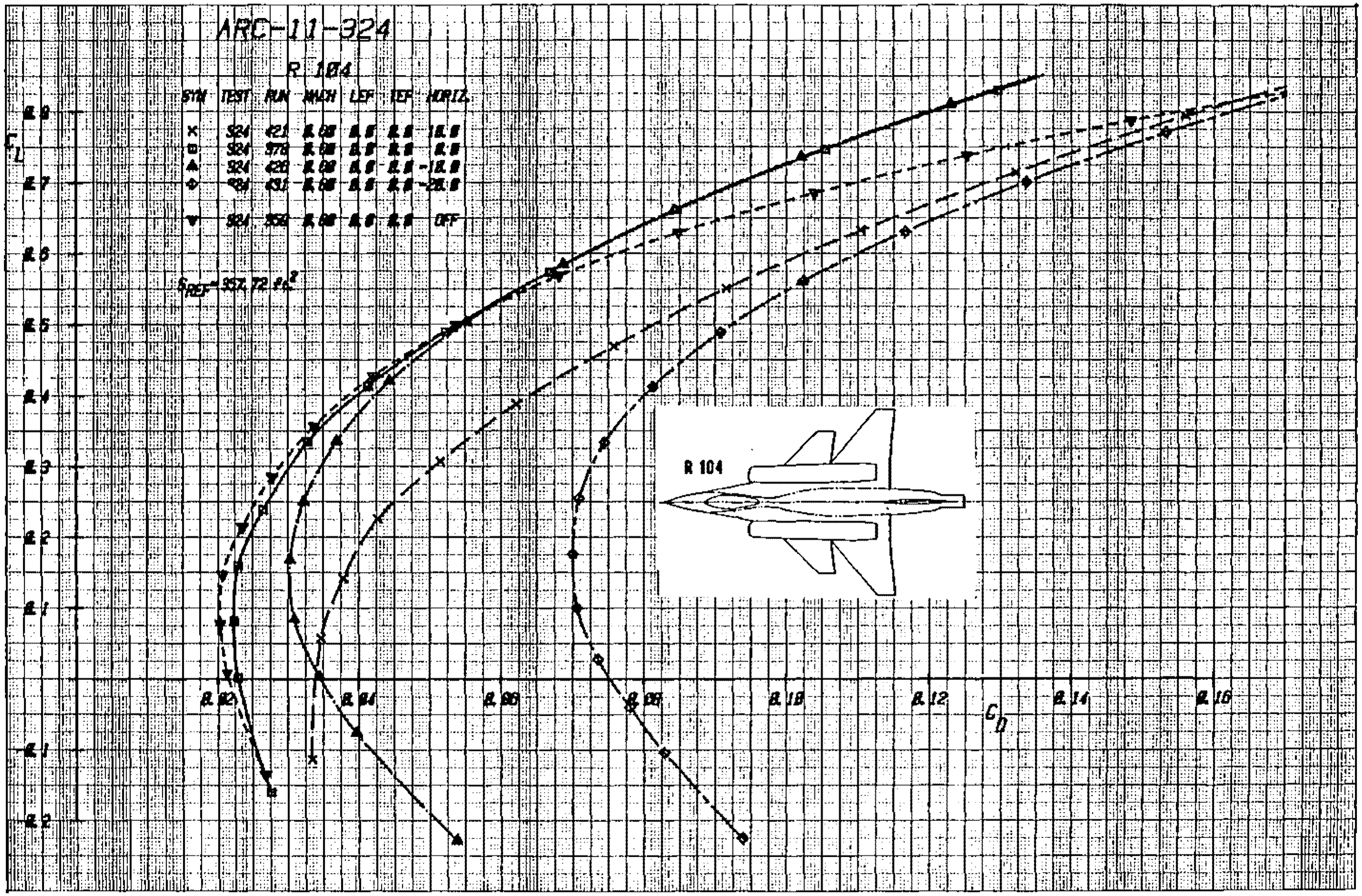

Figure1-44bEffect of Canard Deflection on Drag with Wing Trailing-Edge Flap Undeflected, Mach = .6

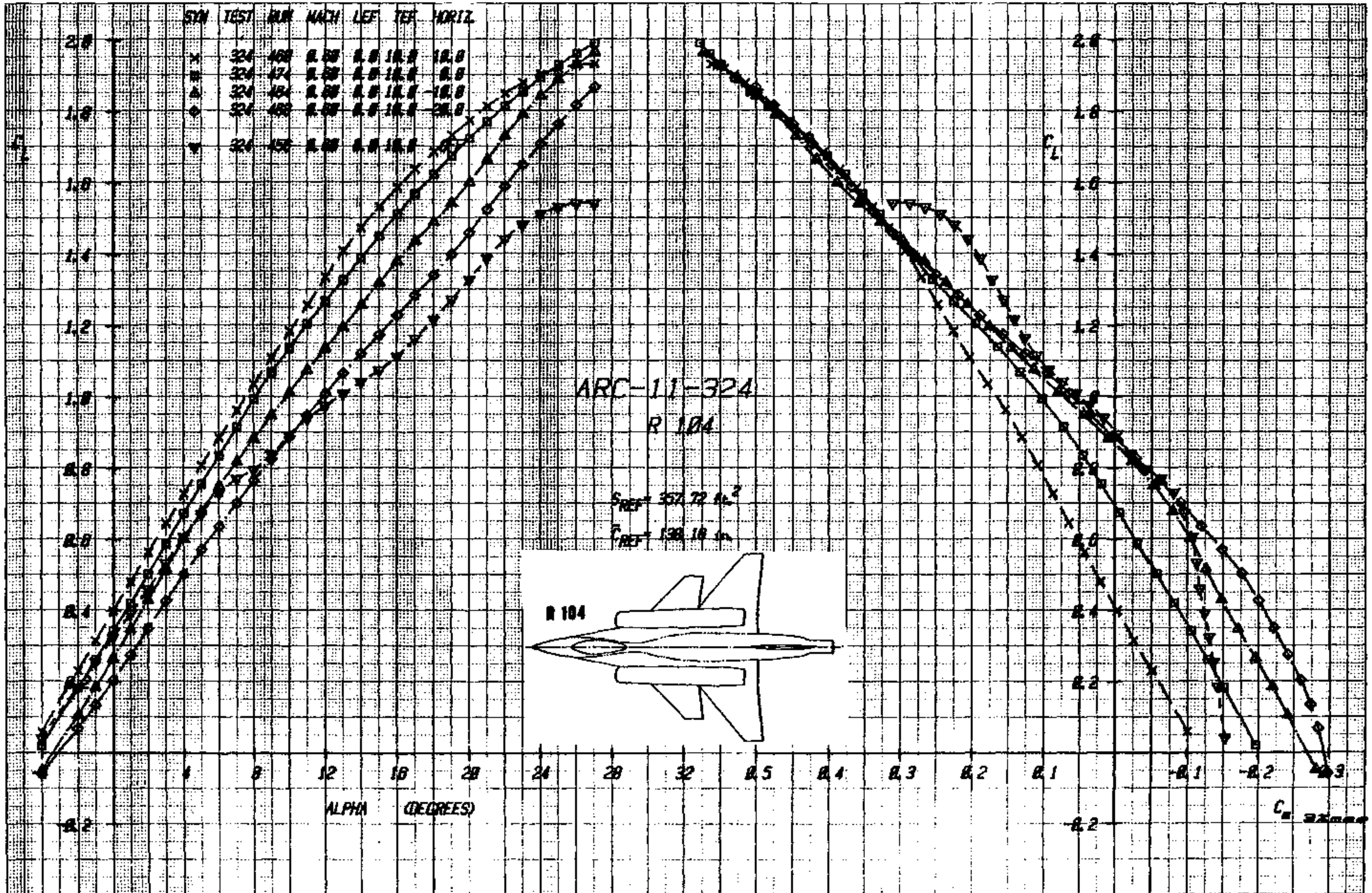

Figure1-45aEffect of Canard Deflection on Lift and Moment with Wing Trailing-Edge Flap Deflected +10°, Mach = .6

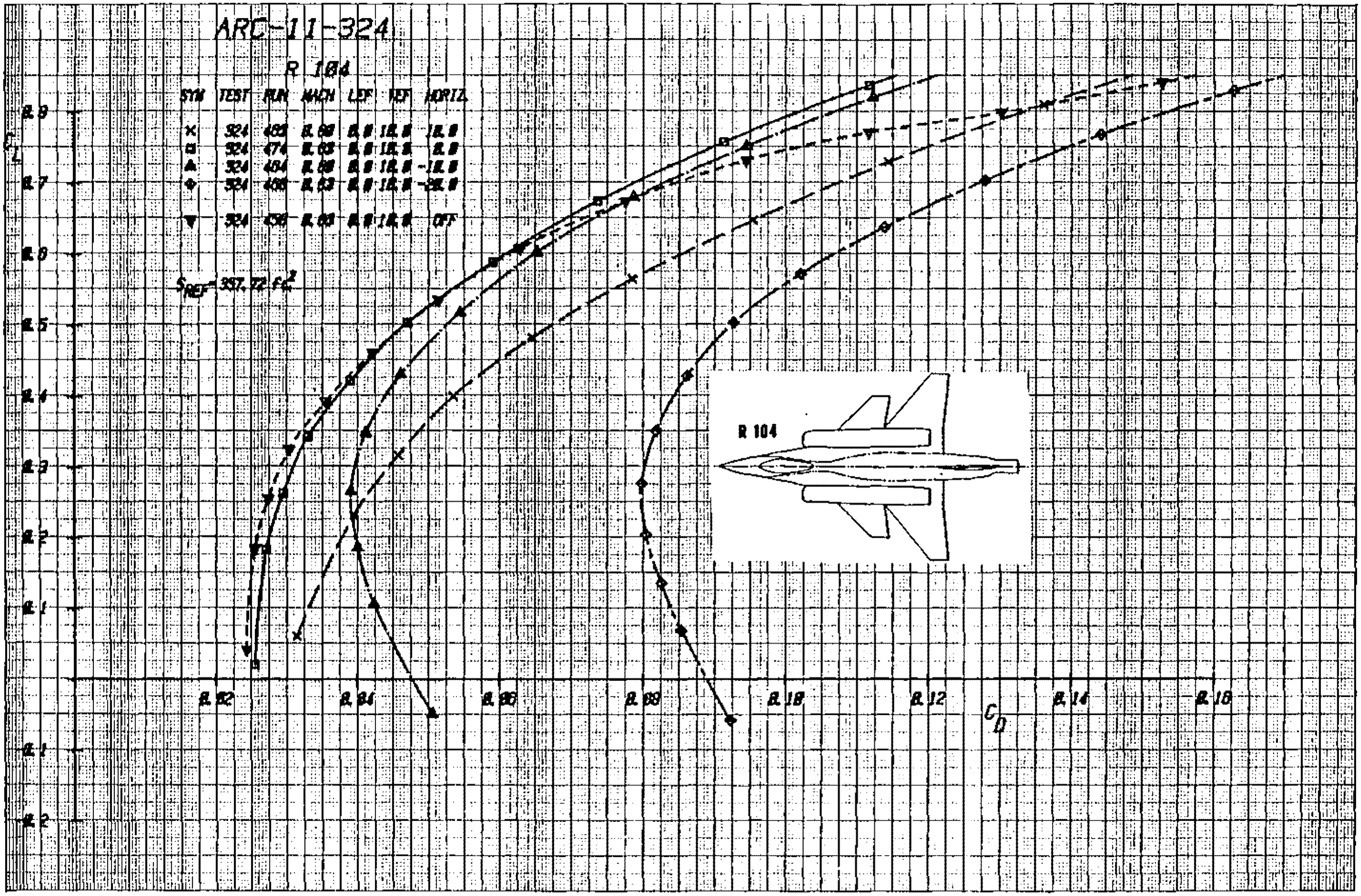

Figure1-45bEffect of Canard Deflection on Drag with Wing Trailing-Edge Flap
Deflected +10°, Mach = .6

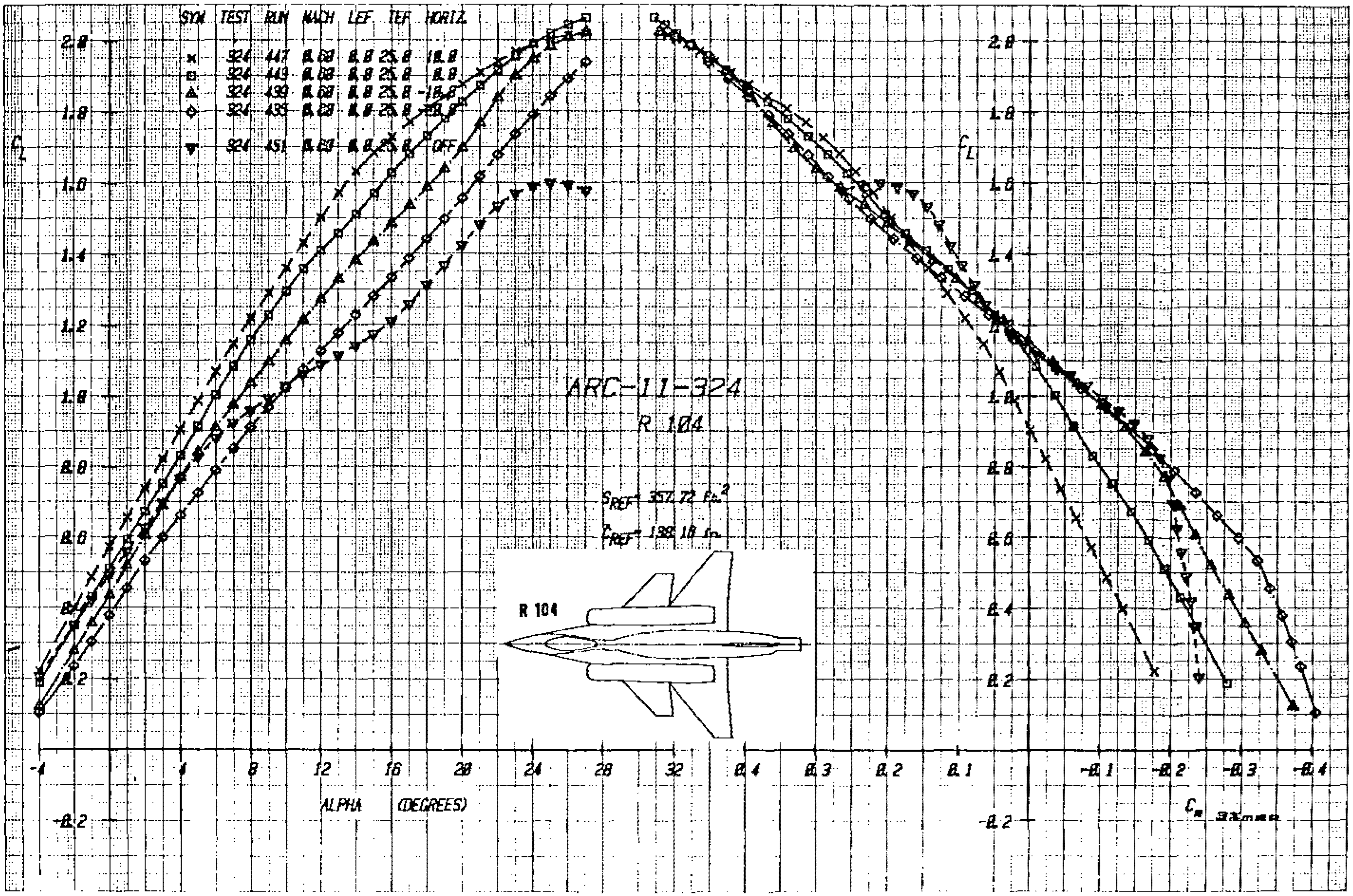

Figure1-46aEffect of Canard Deflection on Lift and Moment with Wing Trailing-Edge Flap Deflected +25°, Mach = .6

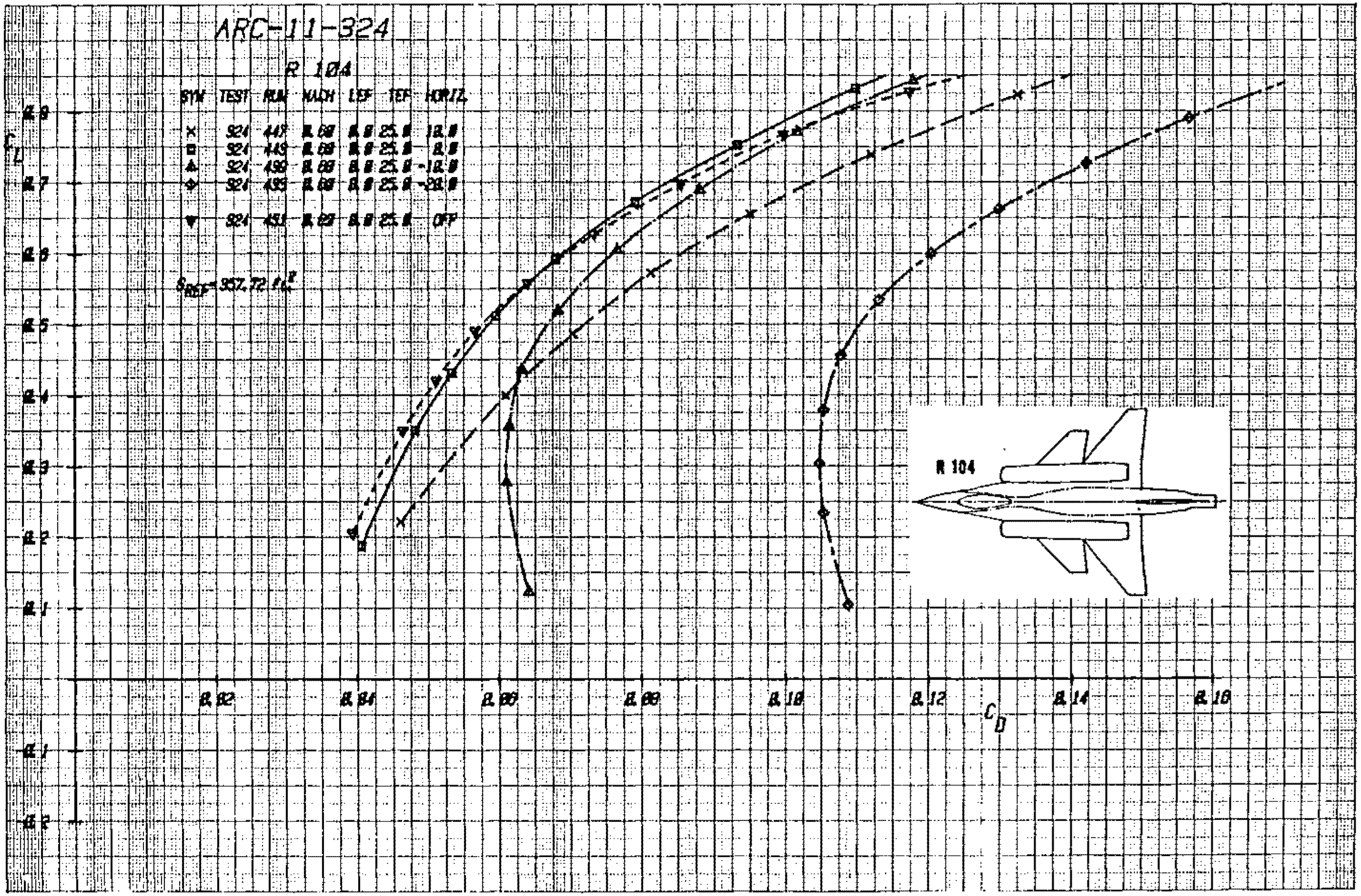

Figure1-46bEffect of Canard Deflection on Drag with Wing Trailing-Edge Flap
Deflected +25°, Mach = .6

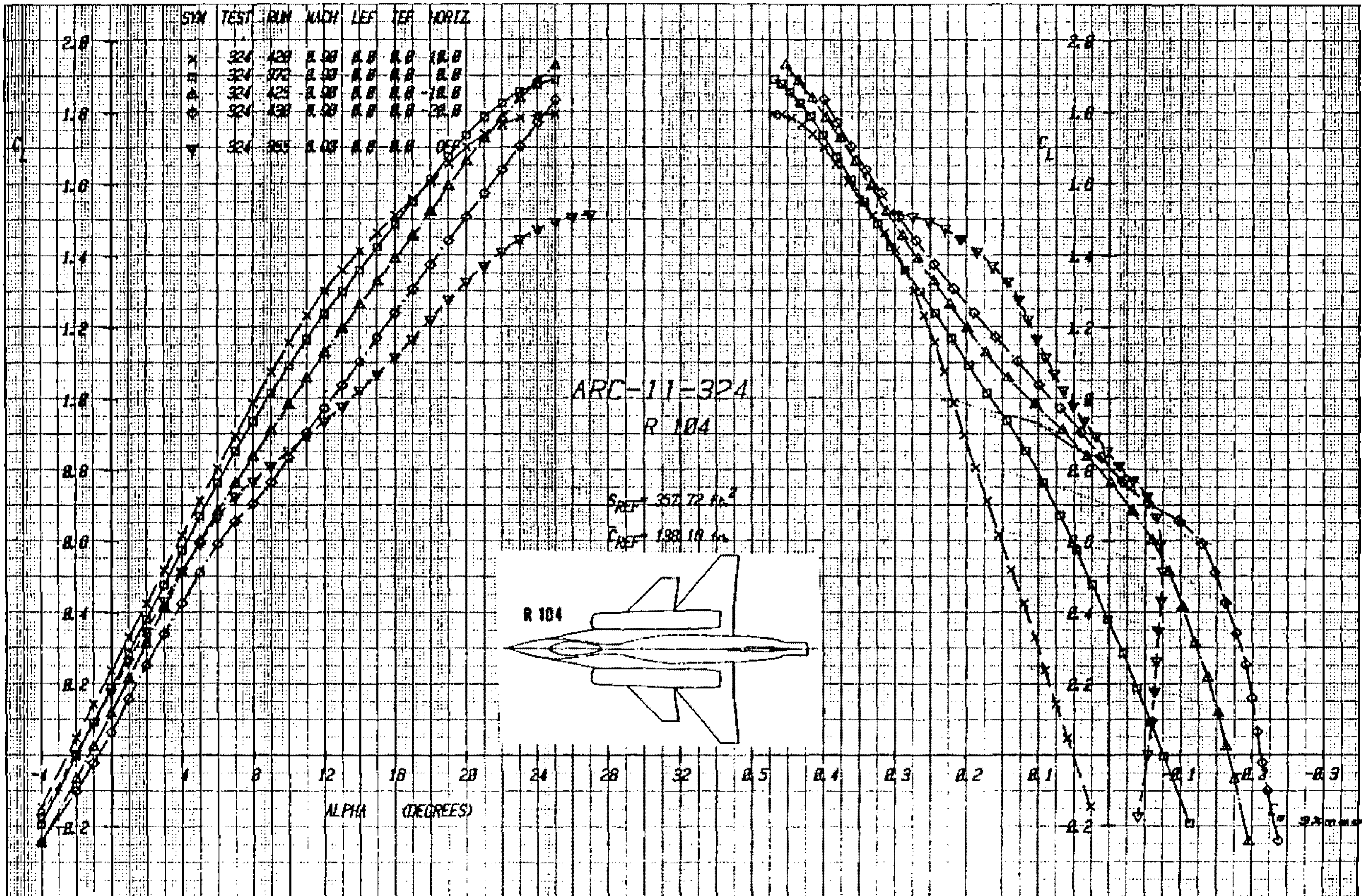

Figurel-47aEffect of Canard Deflection on Lift and Moment with Wing Trailing-Edge Flap Undeflected, Mach = .9

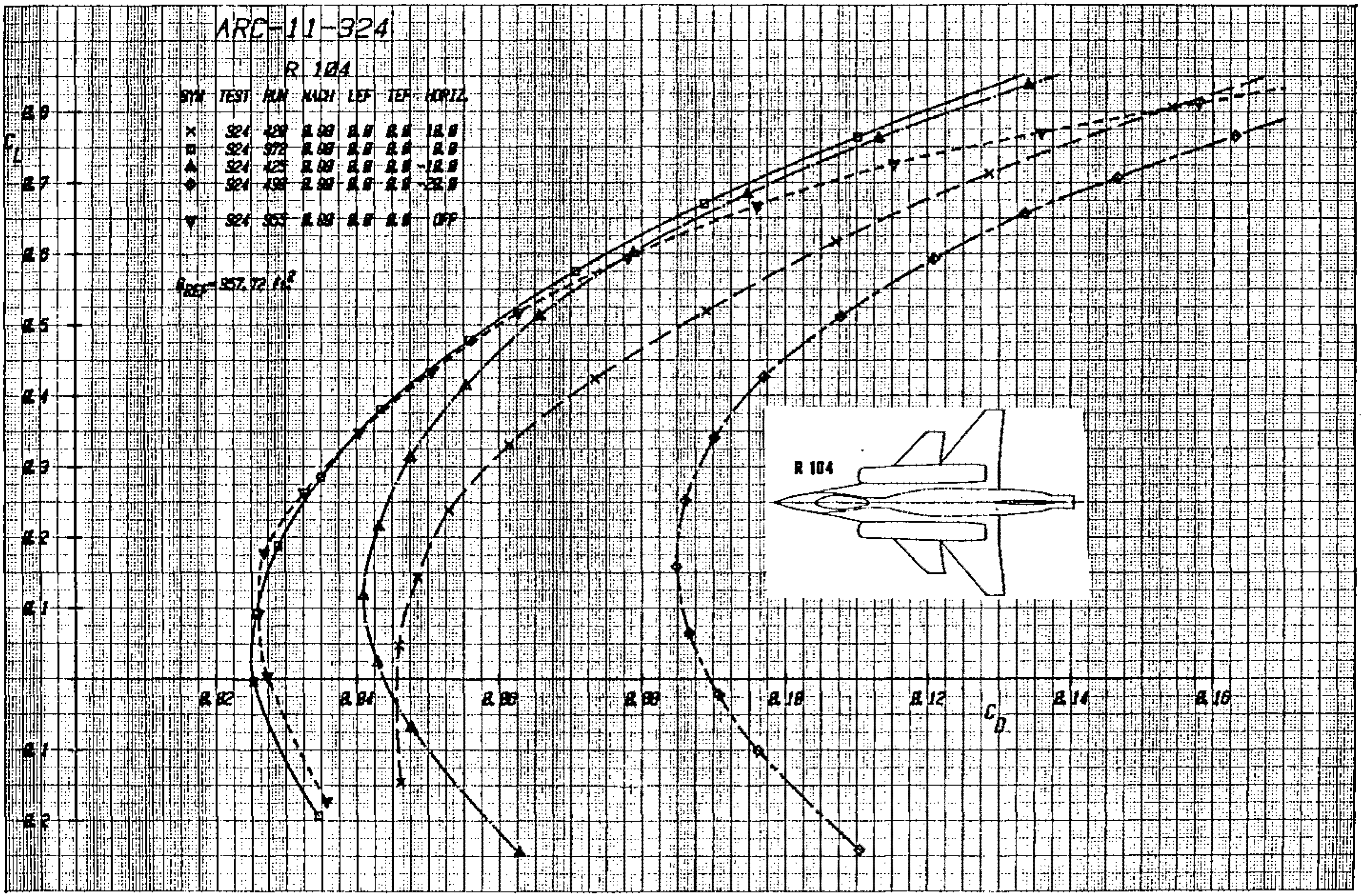

Figure1-47bEffect of Canard Deflection on Drag with Wing Trailing-Edge Flap Undeflected, Mach = .9

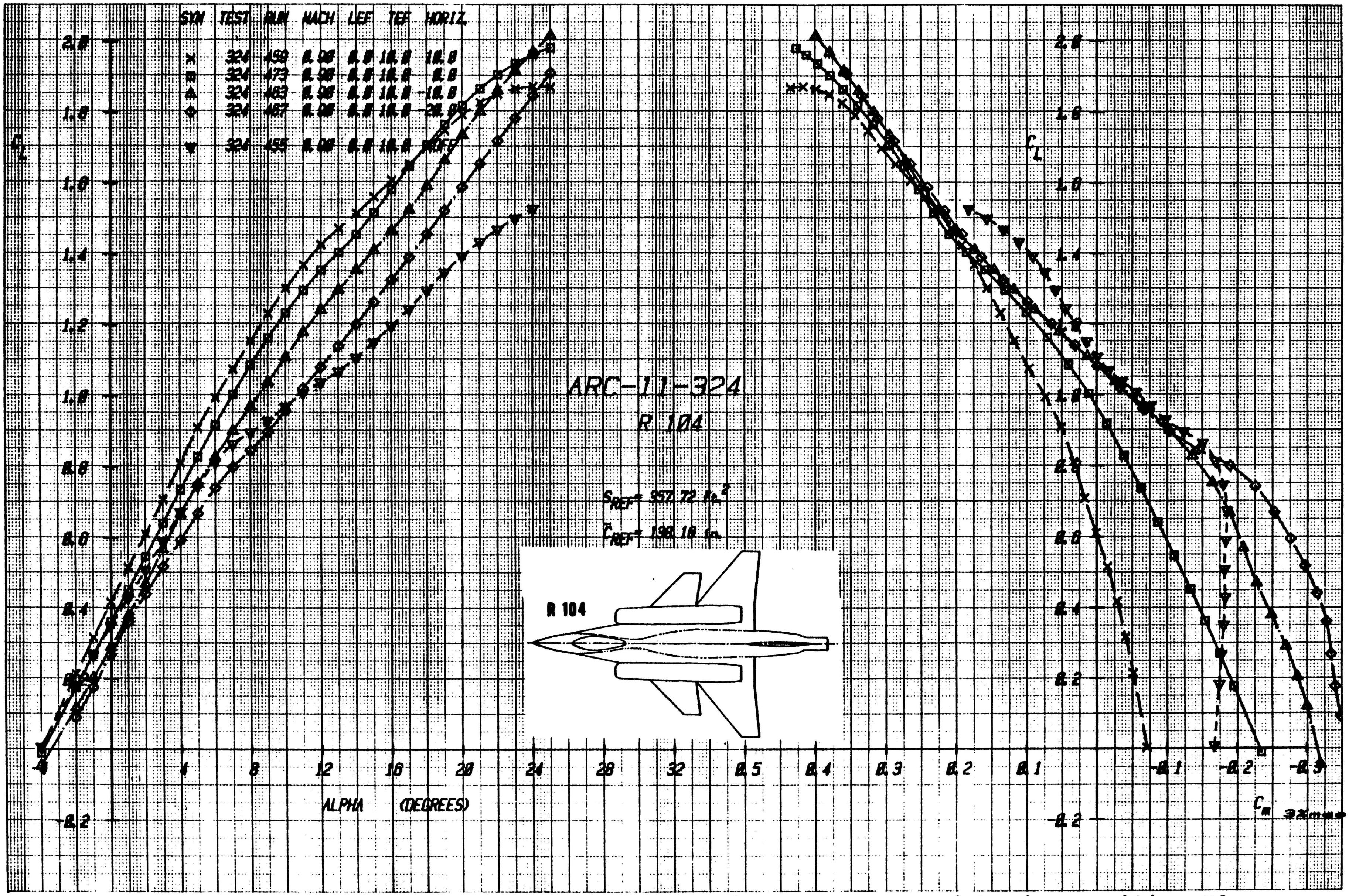

Figure1-48aEffect of Canard Deflection on Lift and Moment with Wing Trailing-Edge Flap Deflected +10°, Mach = .9

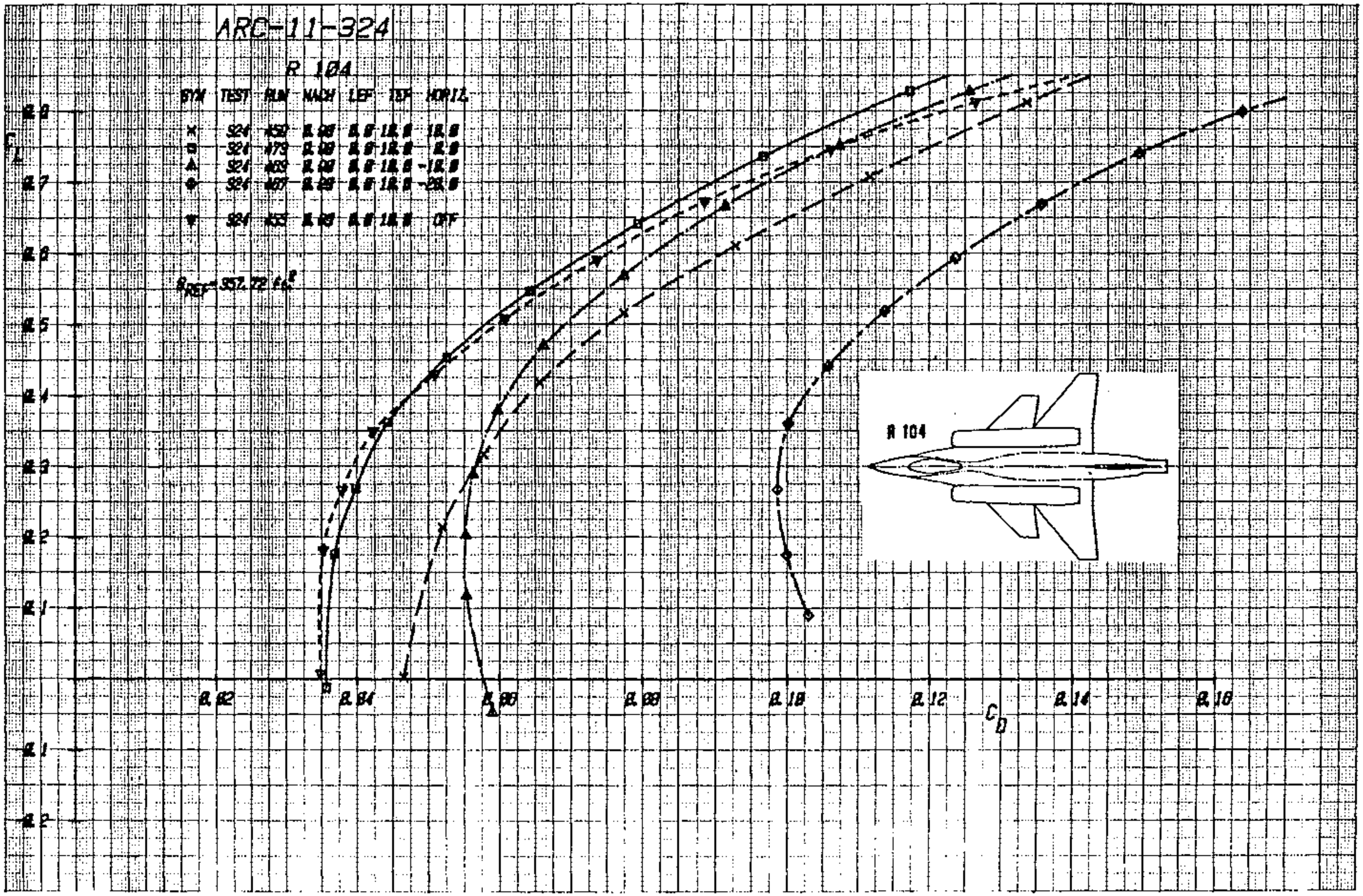

Figure1-48bEffect of Canard Deflection on Drag with Wing Trailing-Edge Flap Deflected +10°, Mach = .9

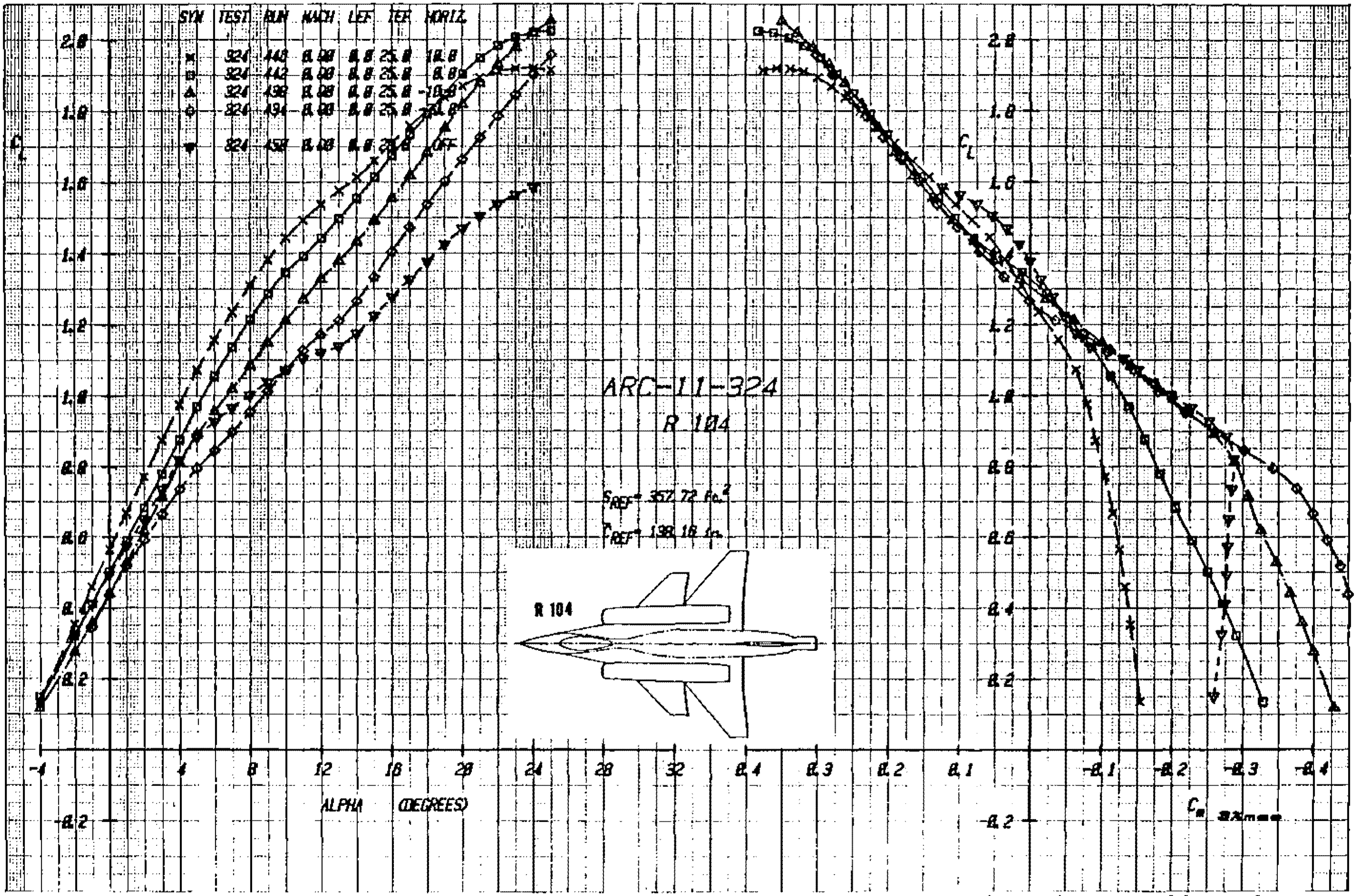

Figure1-49aEffect of Canard Deflection on Lift and Moment with Wing Trailing-Edge Flap Deflected +25°, Mach = .9

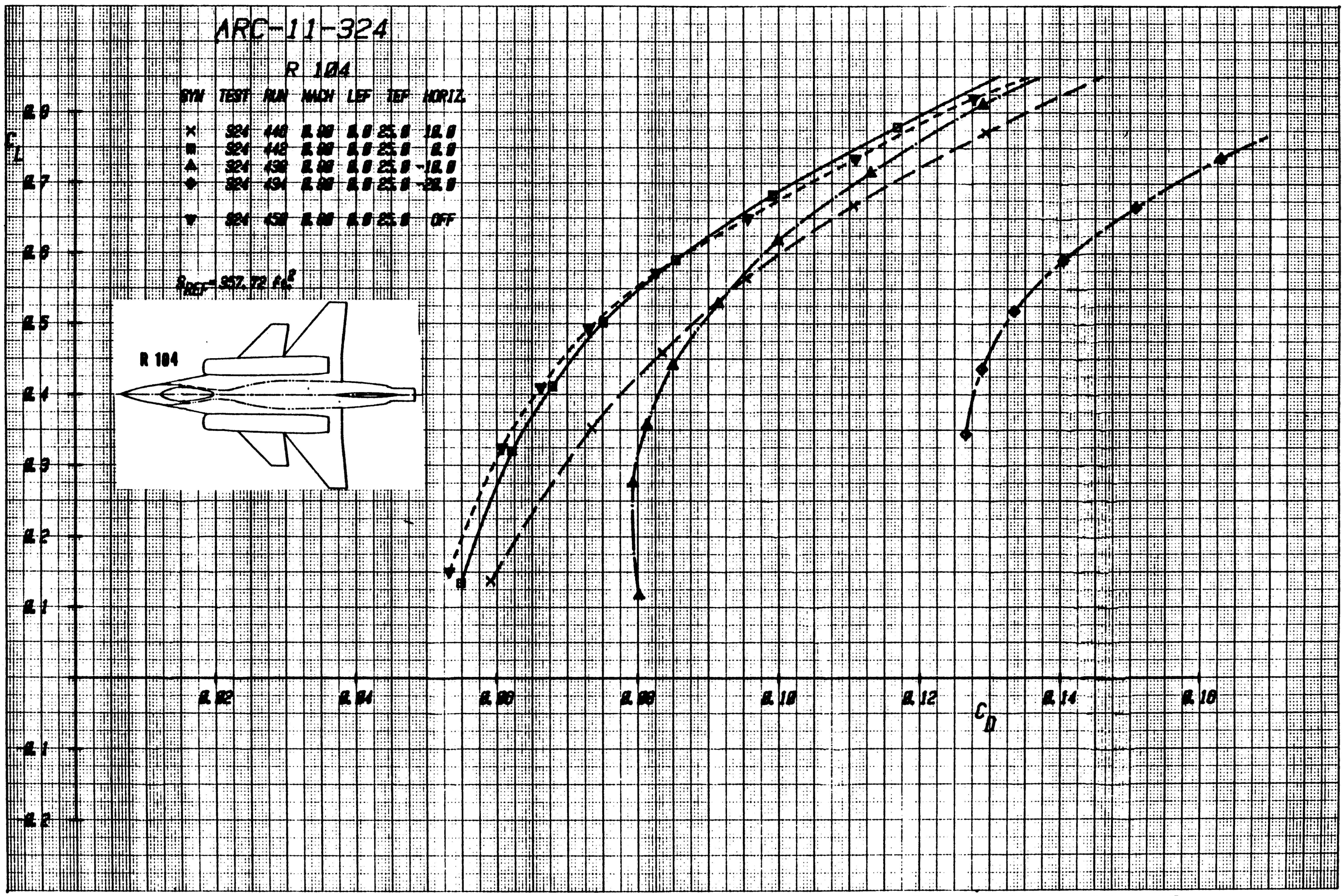

Figure1-49bEffect of Canard Deflection on Drag with Wing Trailing-Edge Flap Deflected +25°, Mach = .9

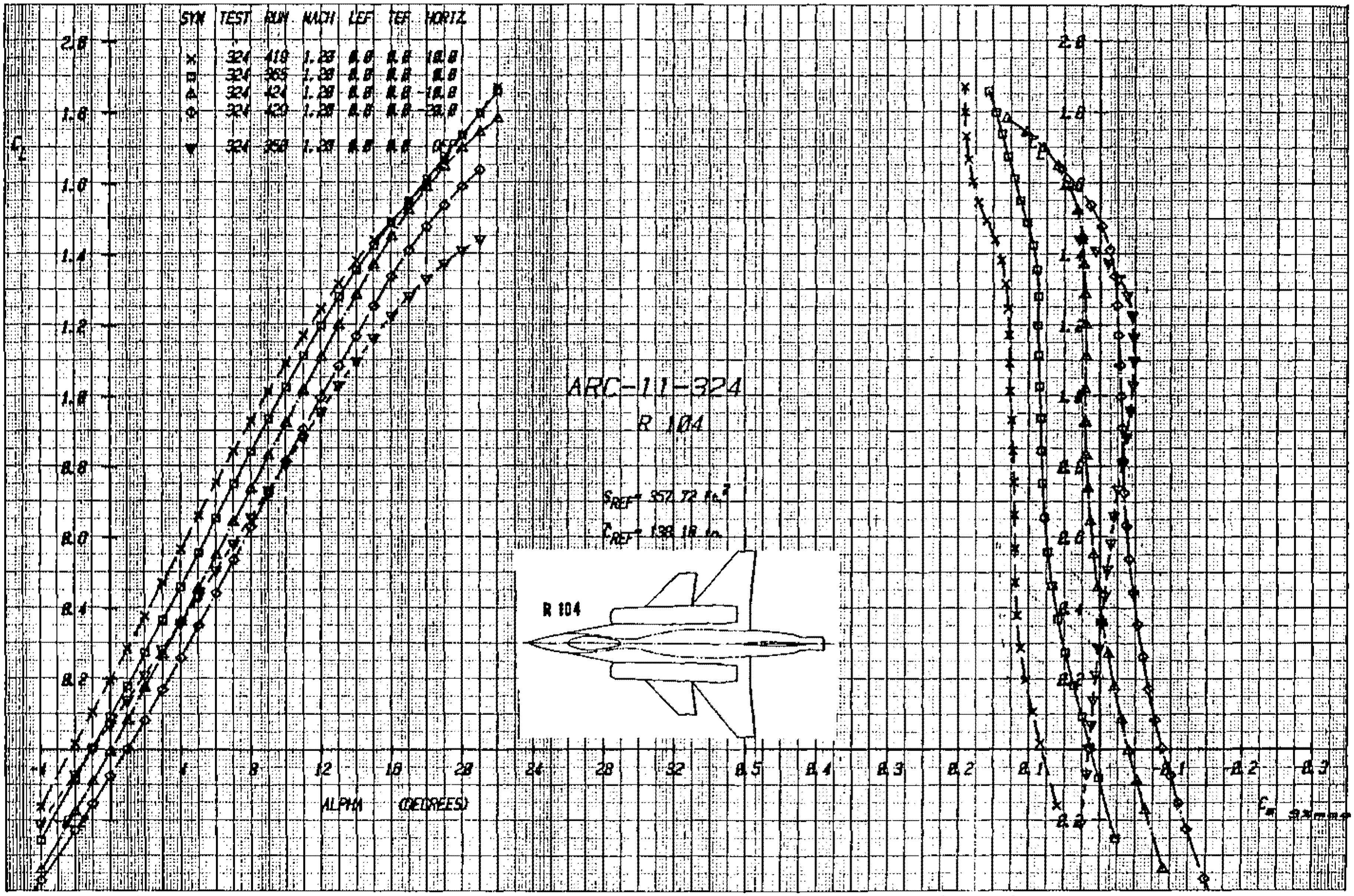

Figure1-50aEffect of Canard Deflection on Lift and Moment with Wing Trailing-Edge Flap Undeflected, Mach = 1.2

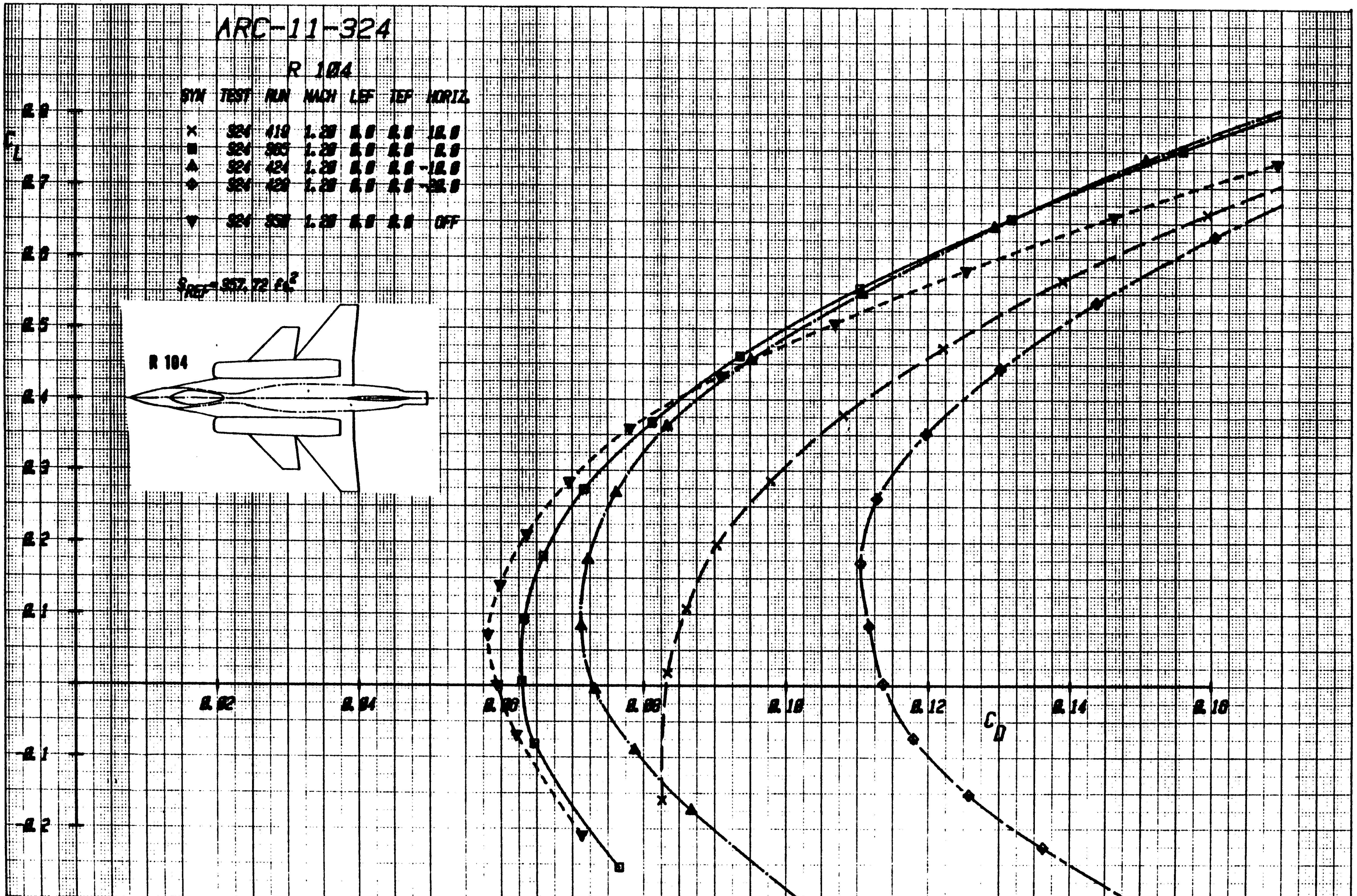

Figure1-50bEffect of Canard Deflection on Drag with Wing Trailing-Edge Flap Undeflected, Mach = 1.2

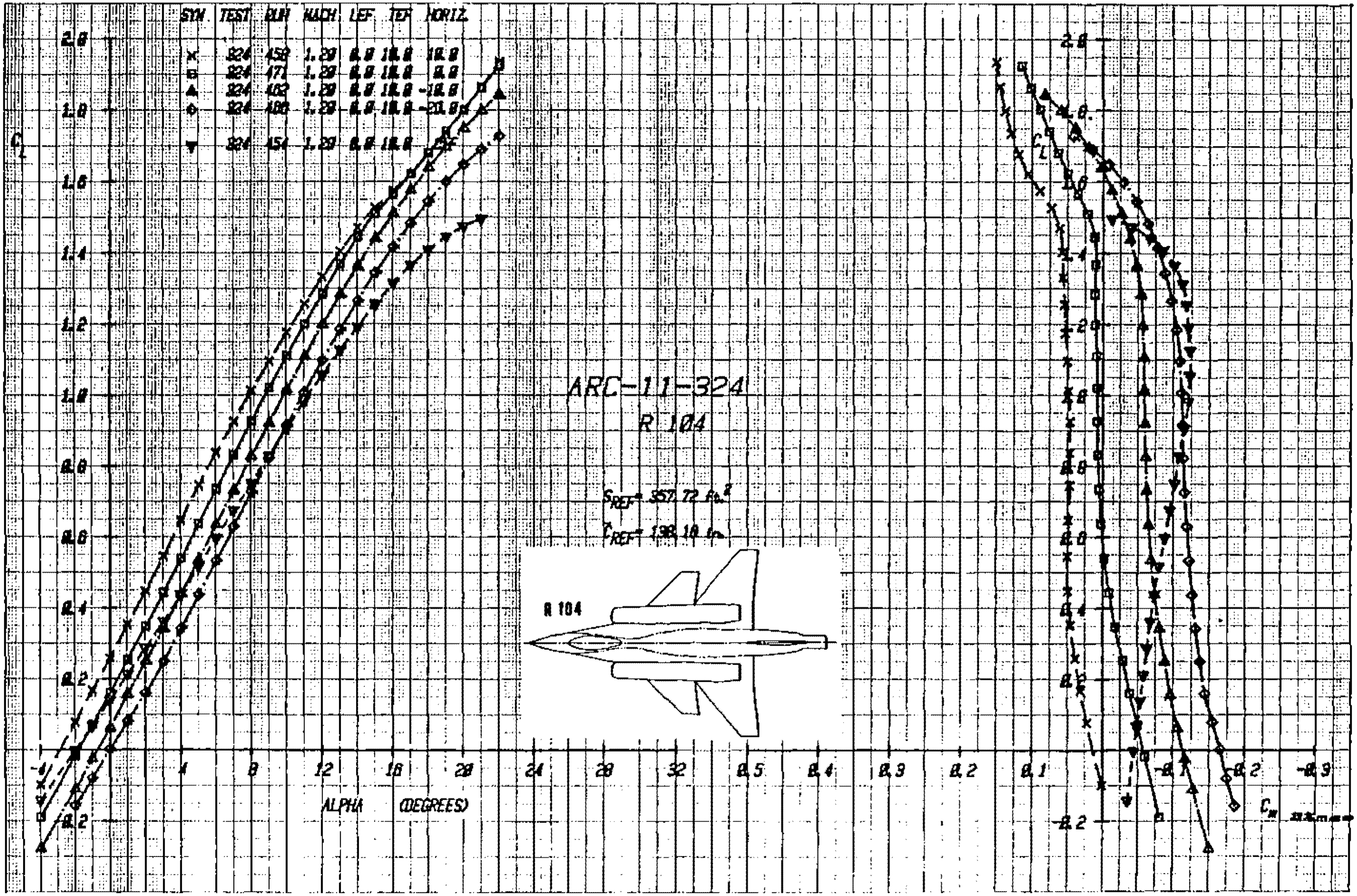

Figure1-51aEffect of Canard Deflection on Lift and Moment with Wing Trailing-Edge Flap Deflected +10°, Mach = 1.2

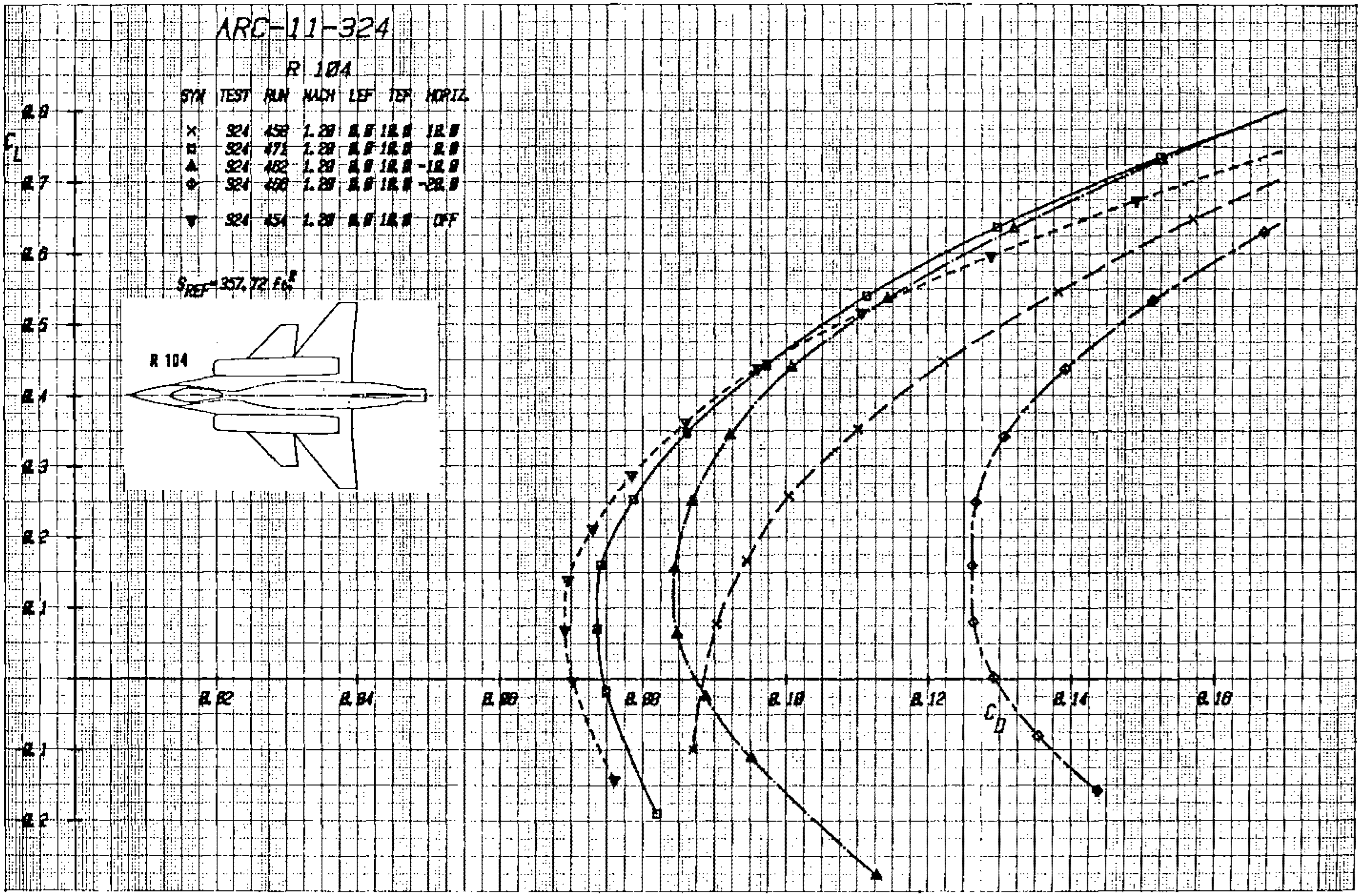

Figure1-51bEffect of Canard Deflection on Drag with Wing Trailing-Edge Flap Deflected +10°, Mach = 1.2

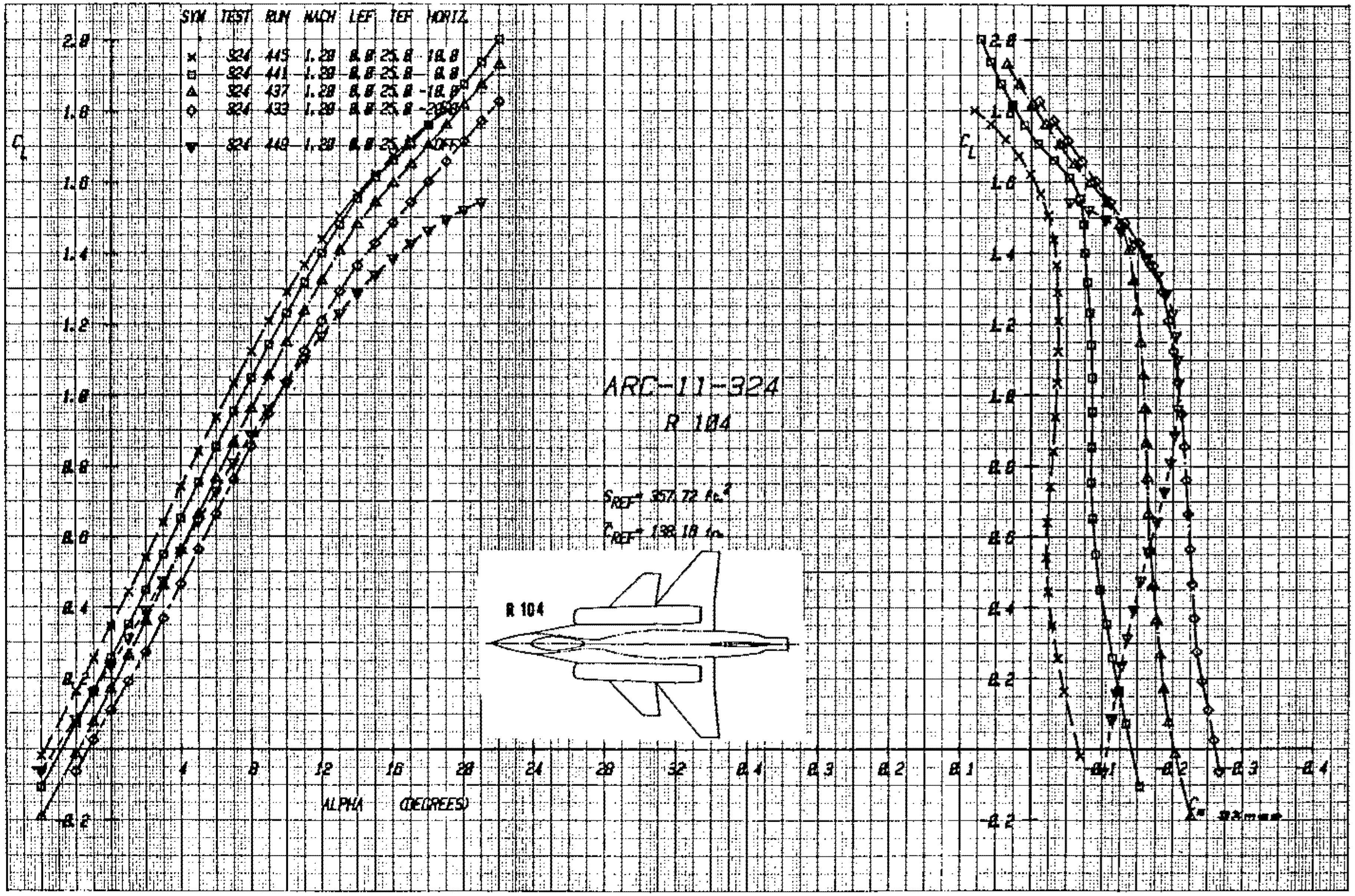

Figure1-52aEffect of Canard Deflection on Lift and Moment with Wing Trailing-Edge Flap Deflected +25°, Mach = 1.2

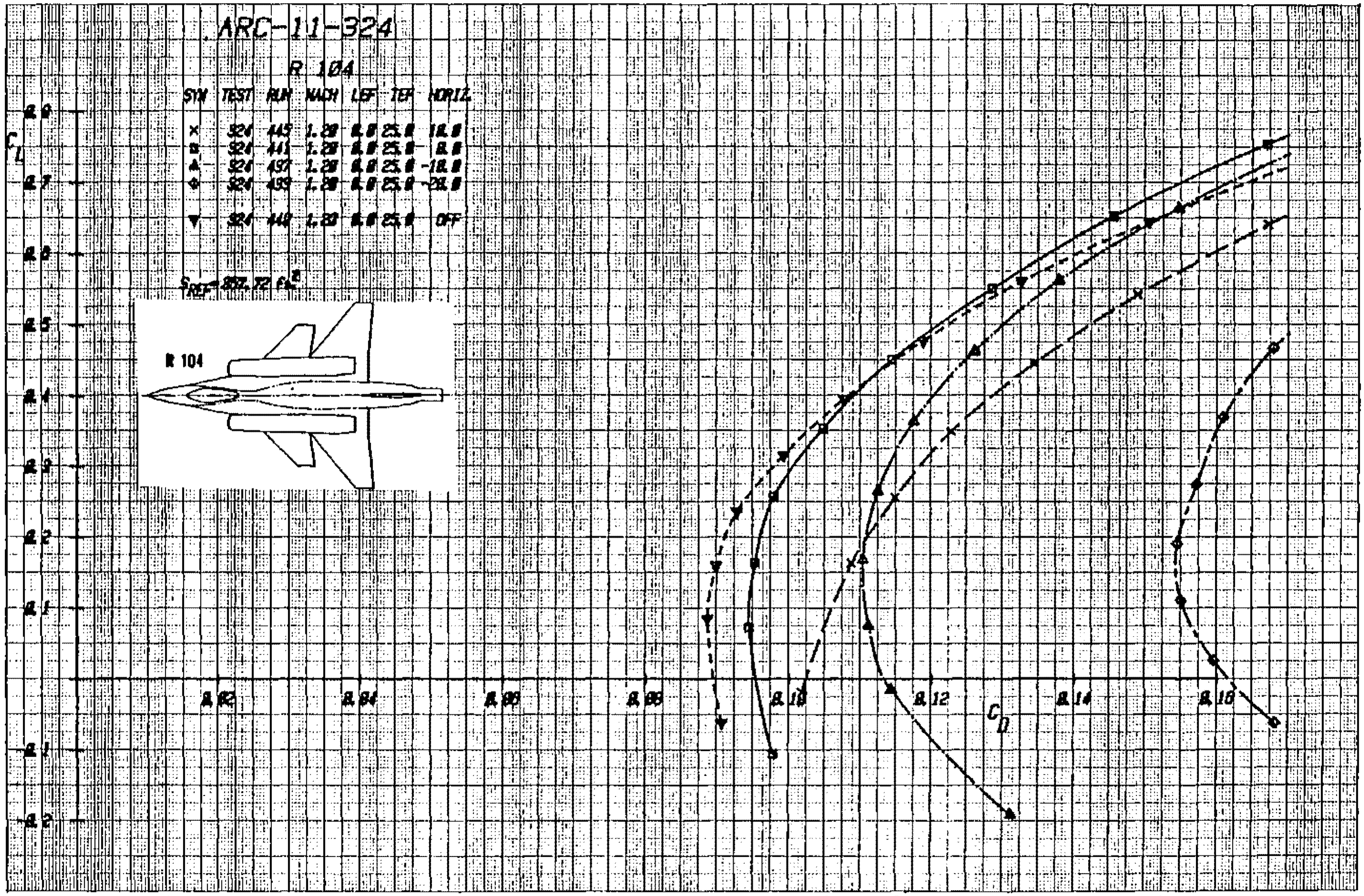

Figure1-52bEffect of Canard Deflection on Drag with Wing Trailing-Edge Flap
Deflected +25°, Mach = 1.2

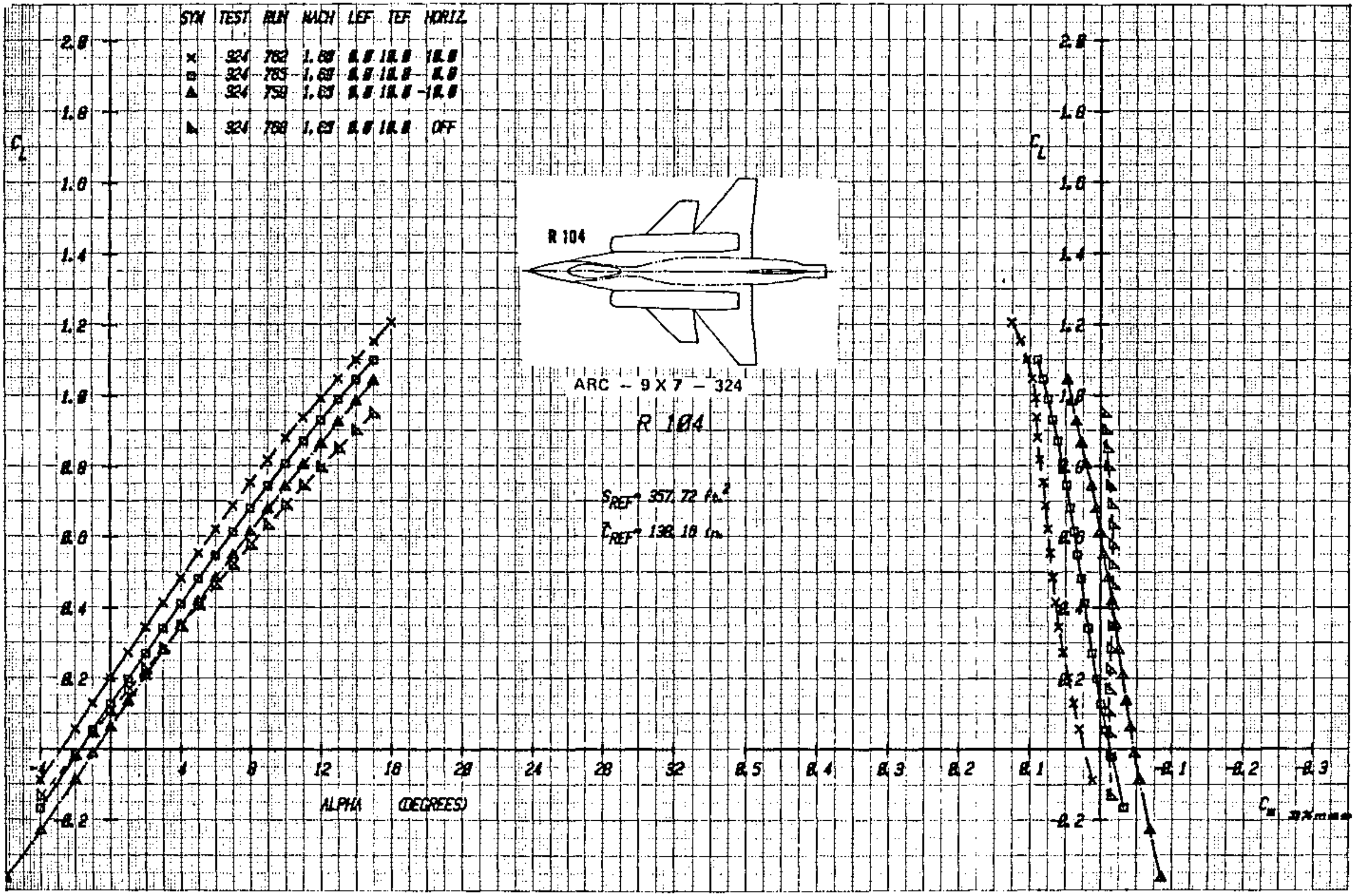

Figurel-53aEffect of Canard Deflection on Lift and Moment with Wing Trailing-Edge Flap Deflected +10°, Mach = 1.6

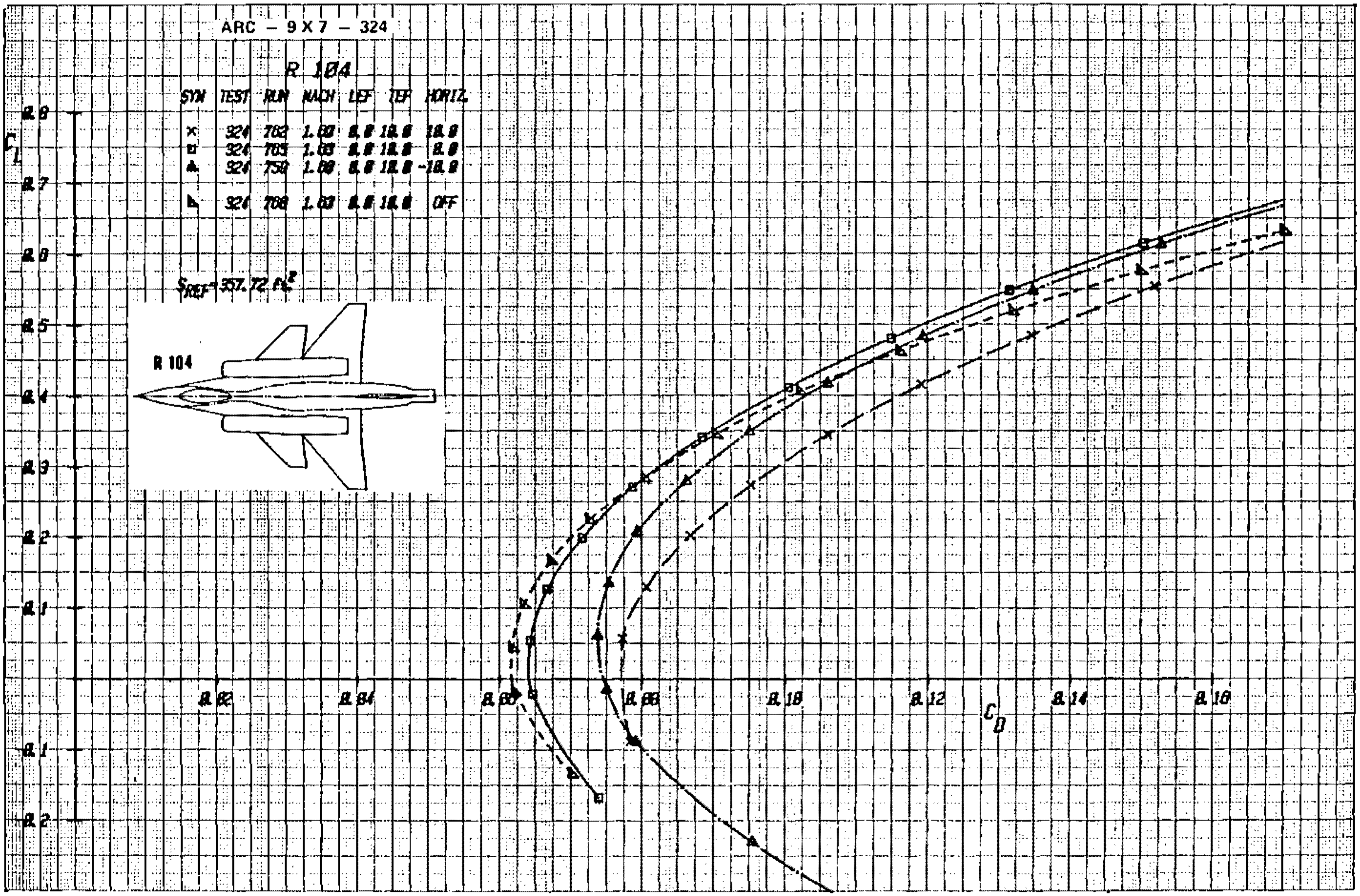

Figure1-53bEffect of Canard Deflection on Drag with Wing Trailing-Edge Flap Deflected +10°, (Expanded Drag Scale), Mach = 1.6

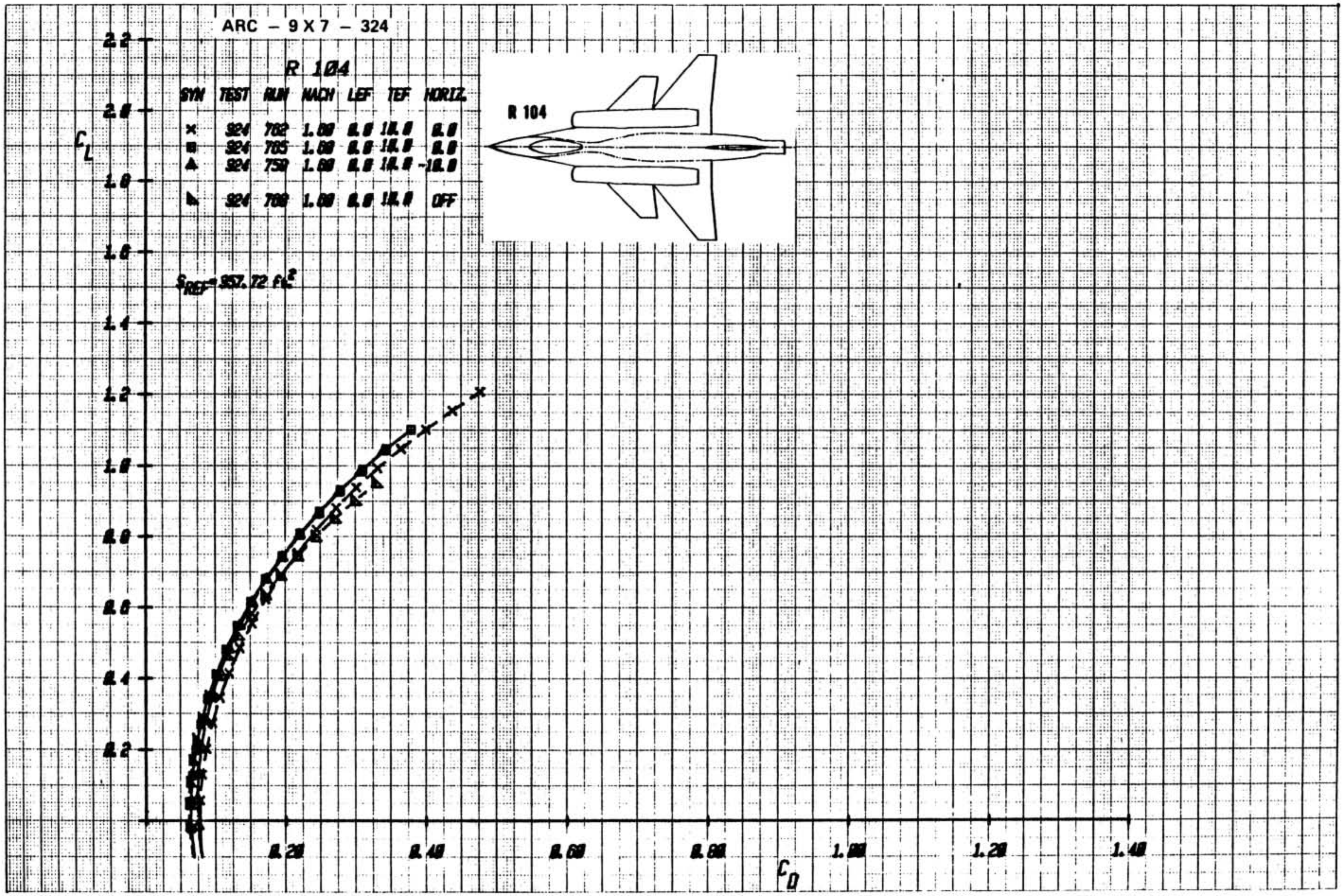

Figure1-53cEffect of Canard Deflection on Drag with Wing Trailing-Edge Flap
Deflected +10°, Mach = 1.6

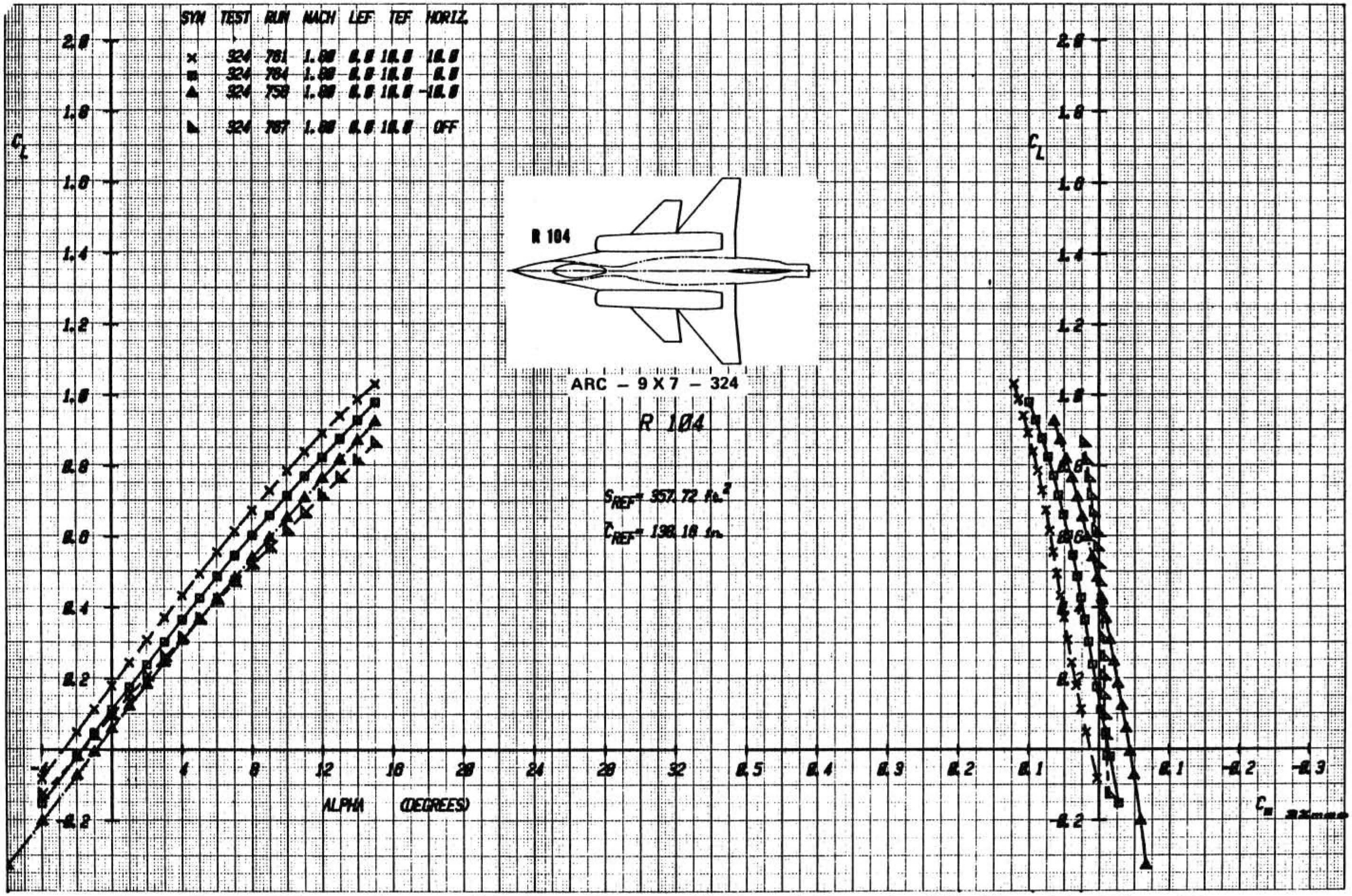

Figurel-54aEffect of Canard Deflection on Lift and Moment with Wing Trailing-Edge Flap Deflected +10°, Mach = 1.8

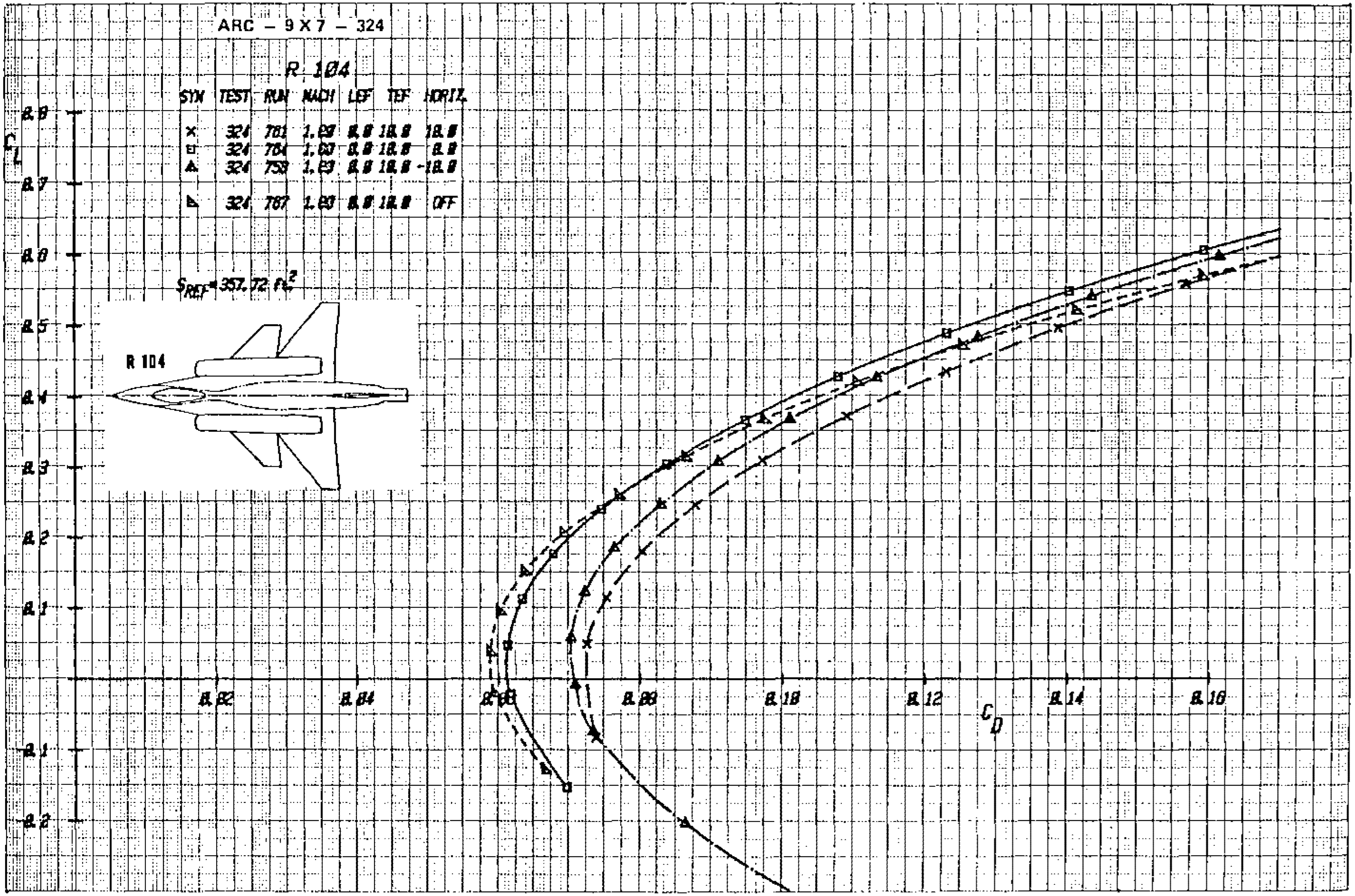

Figure1-54bEffect of Canard Deflection on Drag with Wing Trailing-Edge Flap Deflected +10°, (Expanded Drag Scale), Mach = 1.8

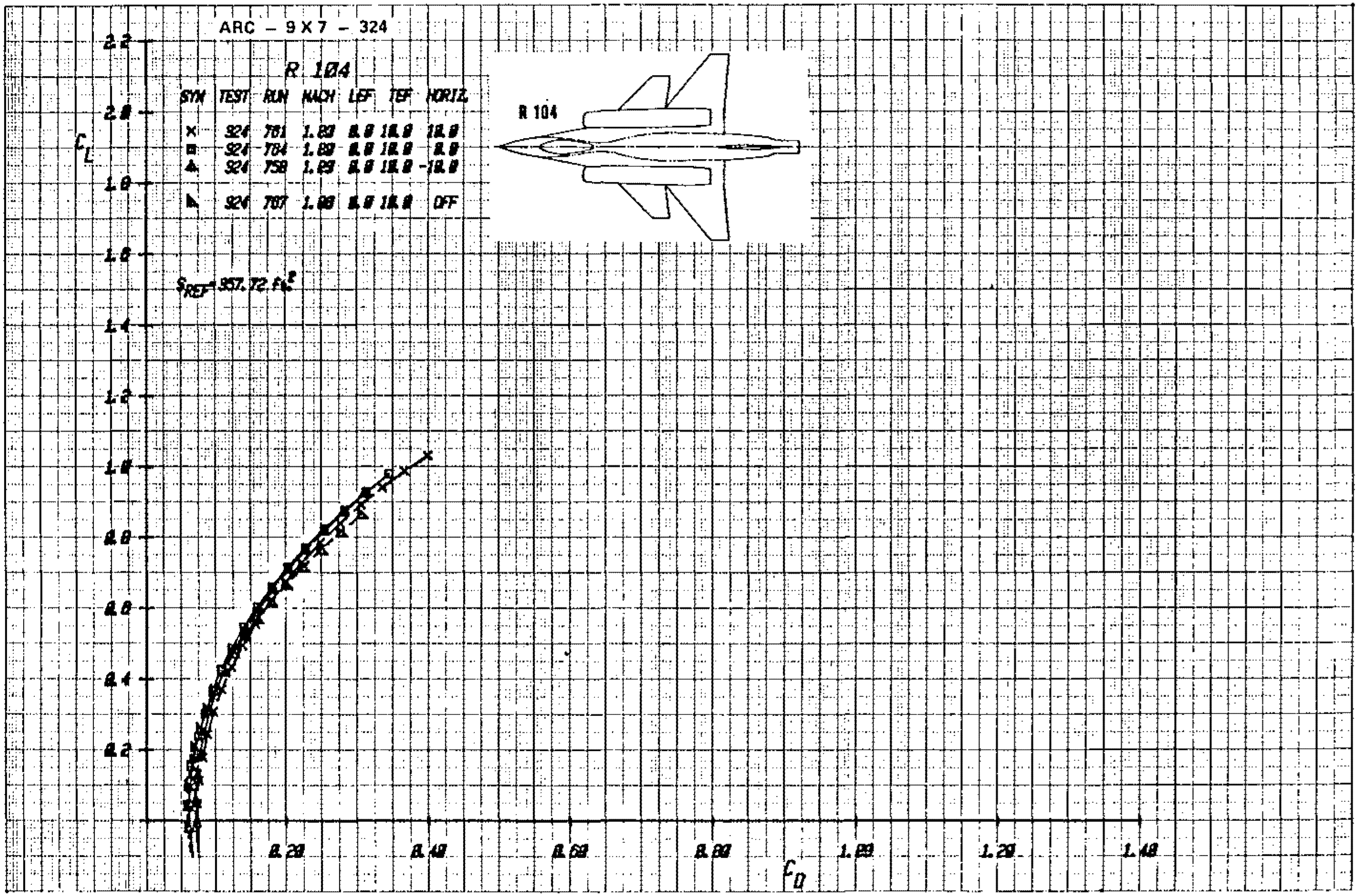

Figure1-54cEffect of Canard Deflection on Drag with Wing Trailing-Edge Flap
Deflected +10°, Mach = 1.8

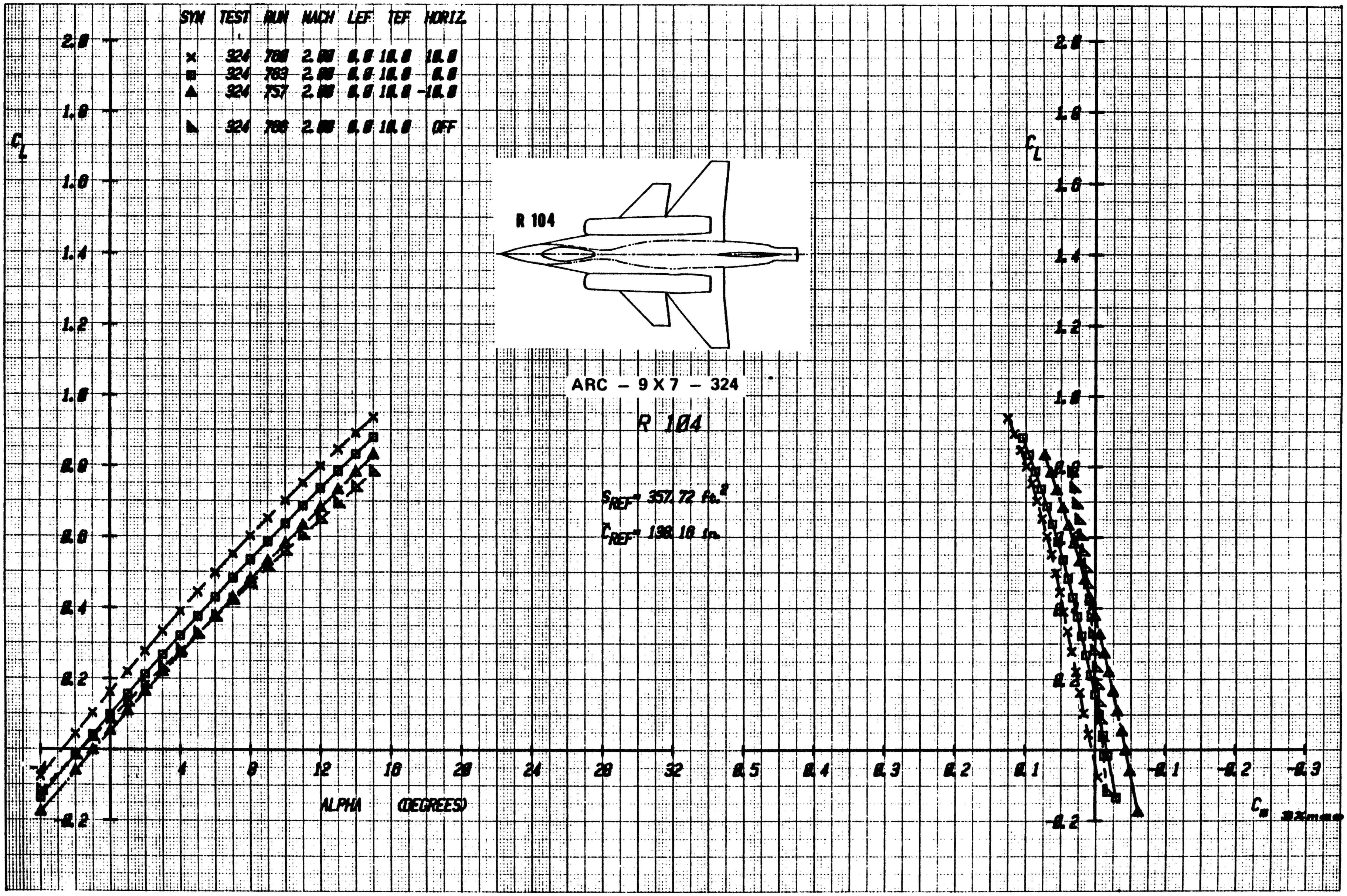

Figure1-55aEffect of Canard Deflection on Lift and Moment with Wing Trailing-Edge Flap Deflected +10°, Mach = 2.0

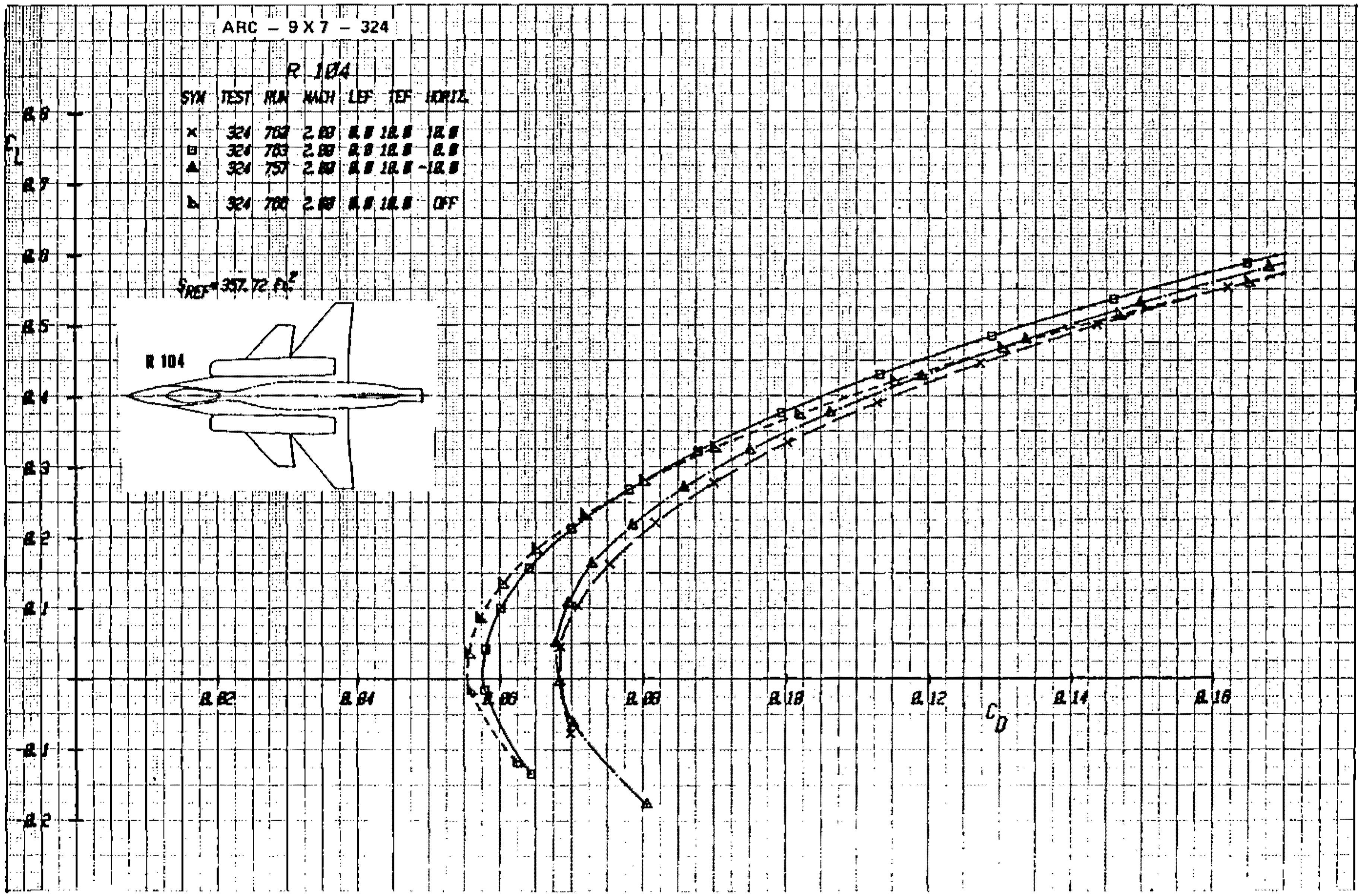

Figure1-55bEffect of Canard Deflection on Drag with Wing Trailing-Edge Flap Deflected +10°, (Expanded Drag Scale), Mach = 2.0

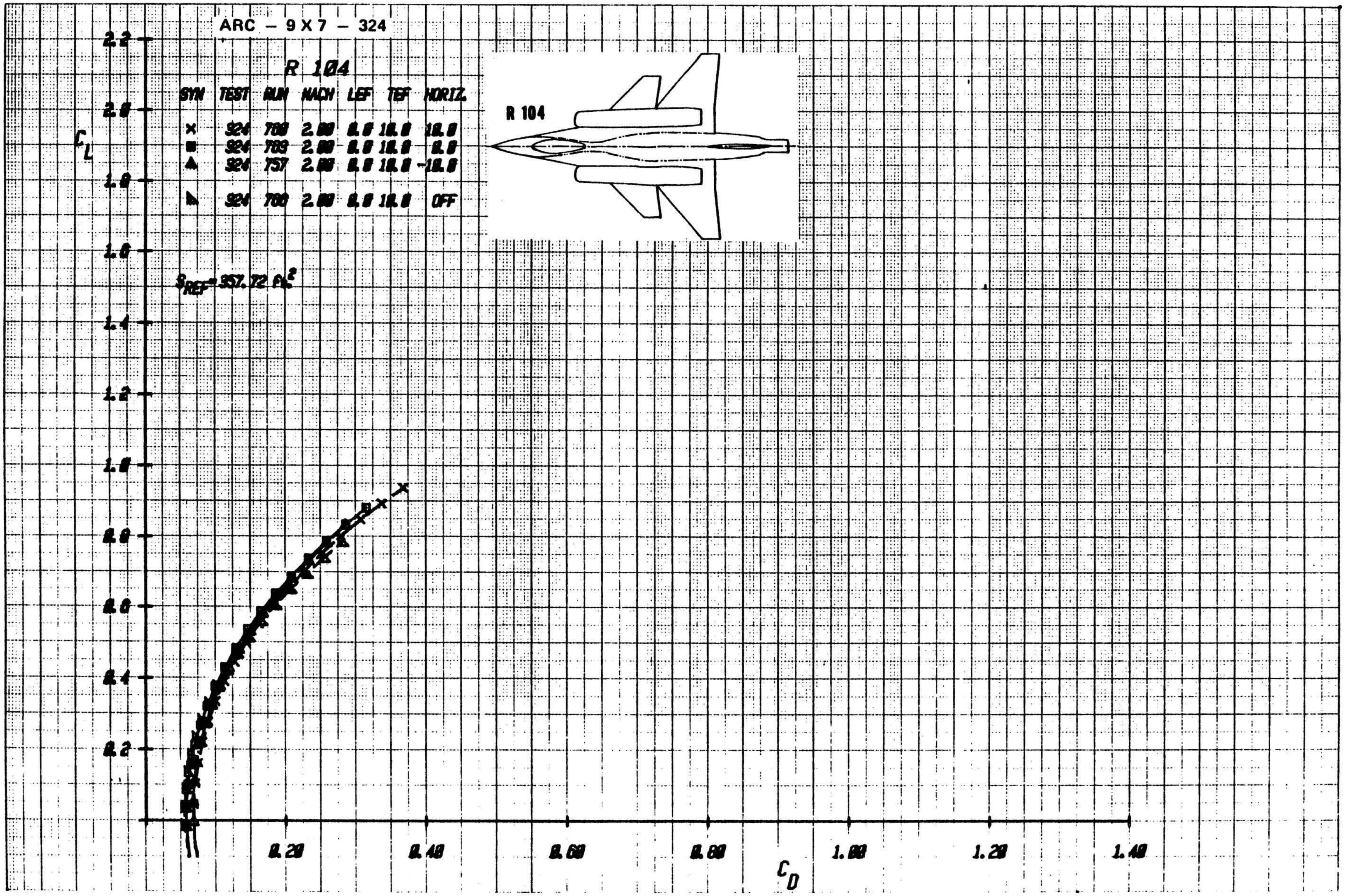

Figure1-55cEffect of Canard Deflection on Drag with Wing Trailing-Edge Flap Deflected +10°, Mach = 2.0

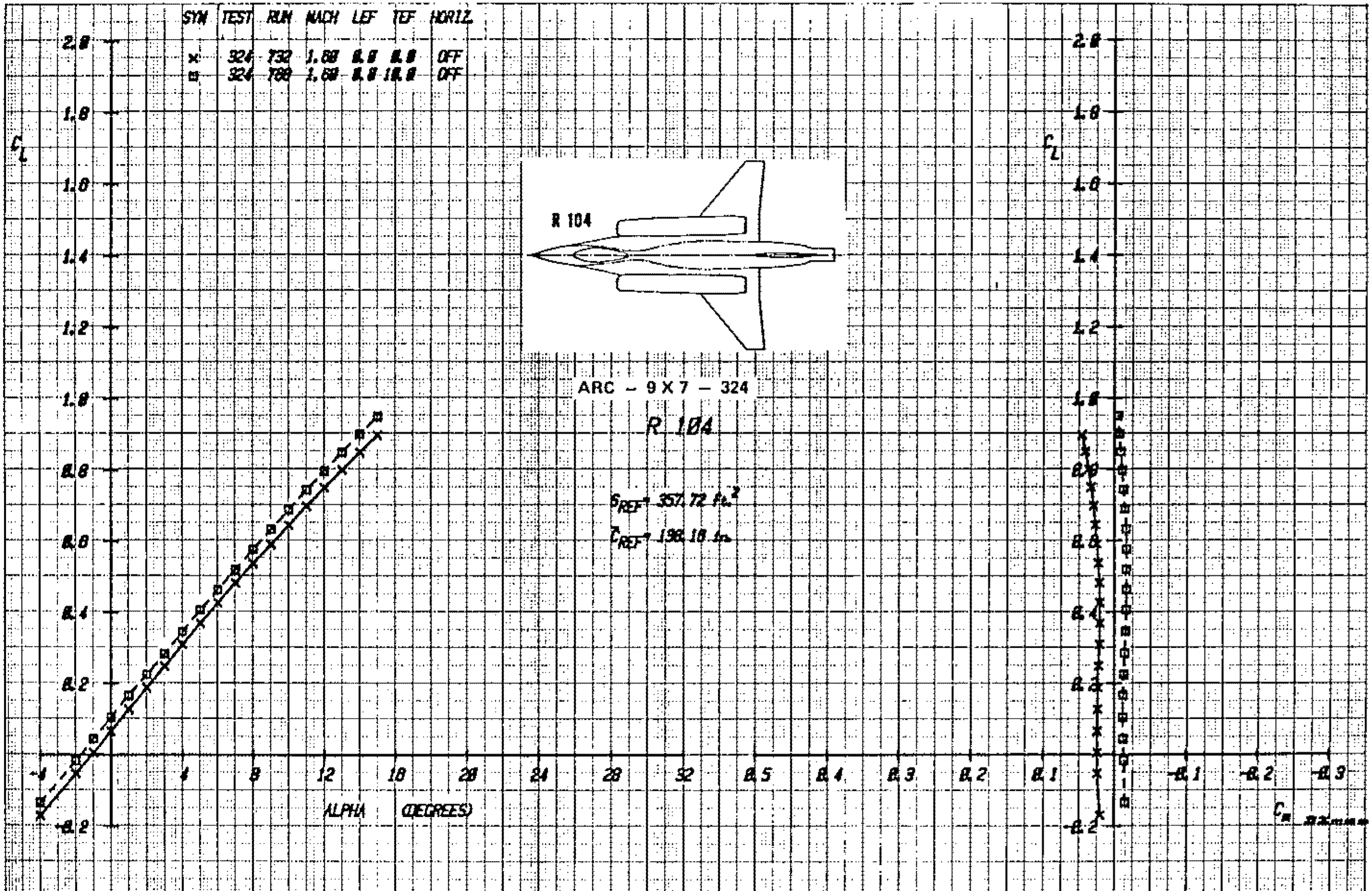

Figure1-56aEffect of Wing Trailing-Edge Flap Deflection on Lift and Moment with Canard Off, Mach = 1.6

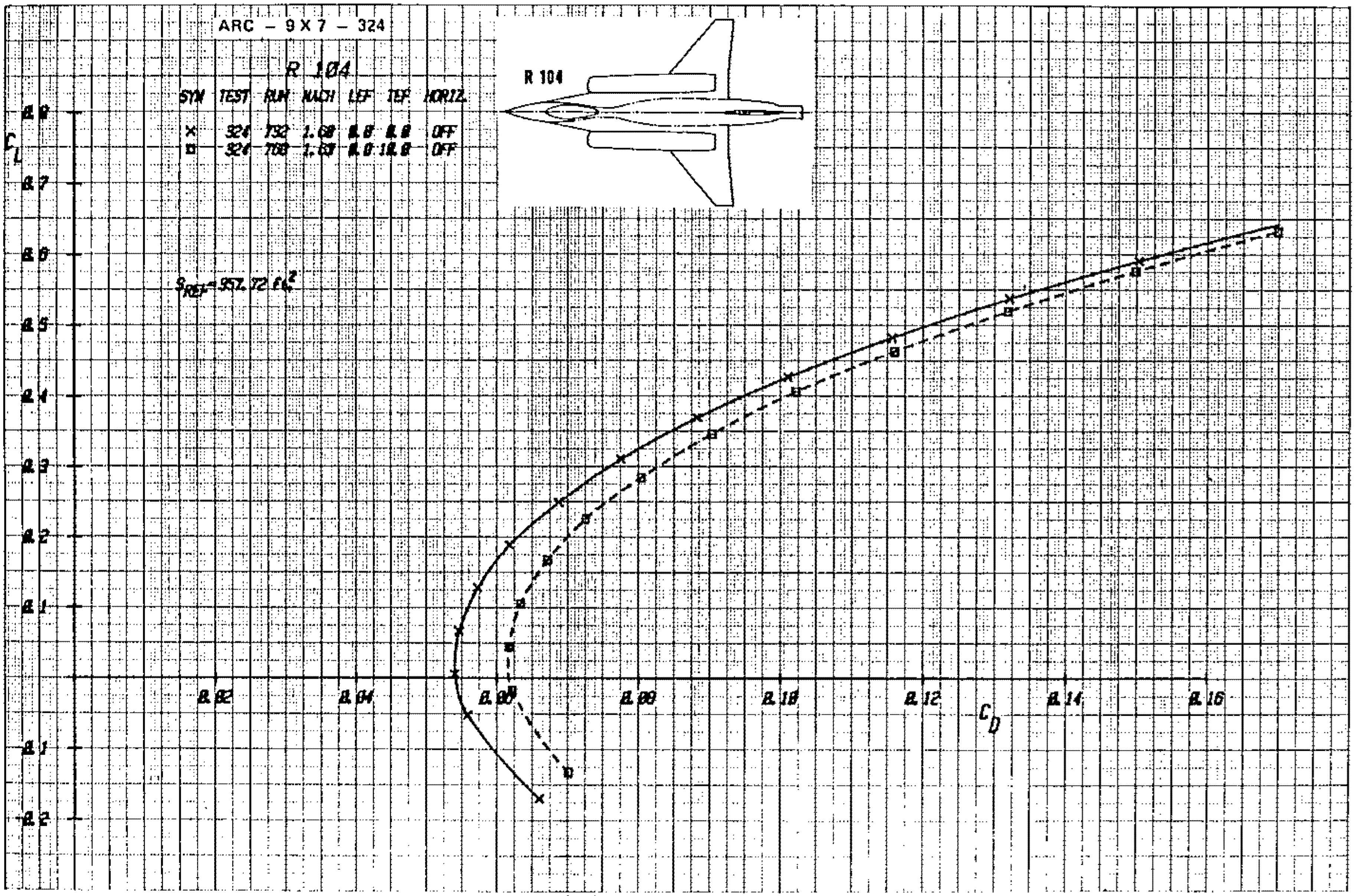

Figure1-56bEffect of Wing Trailing-Edge Flap Deflection on Drag with Canard Off, (Expanded Drag Scale), Mach = 1.6

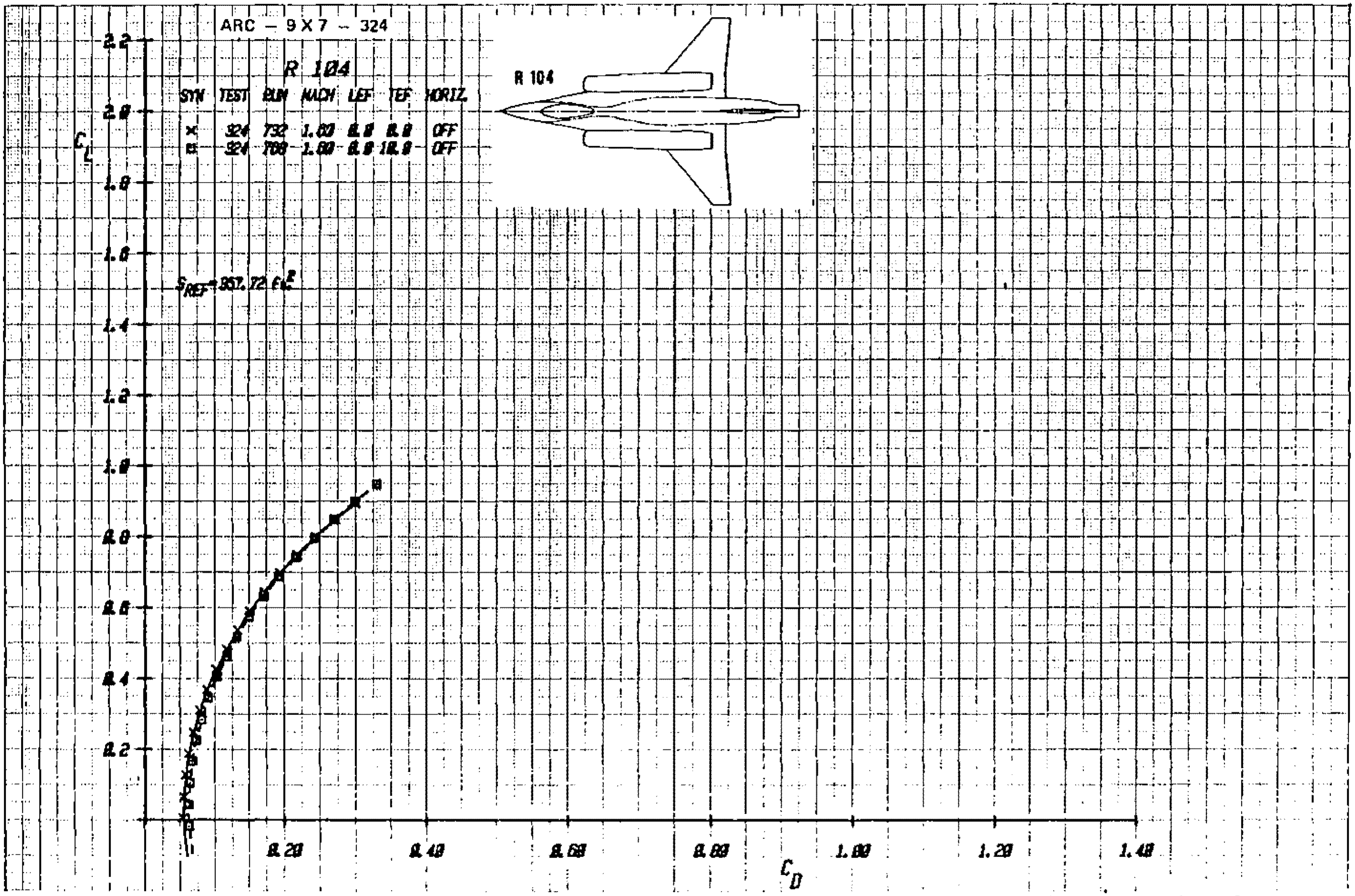

Figure1-56cEffect of Wing Trailing-Edge Flap Deflection on Drag with Canard Off, Mach = 1.6

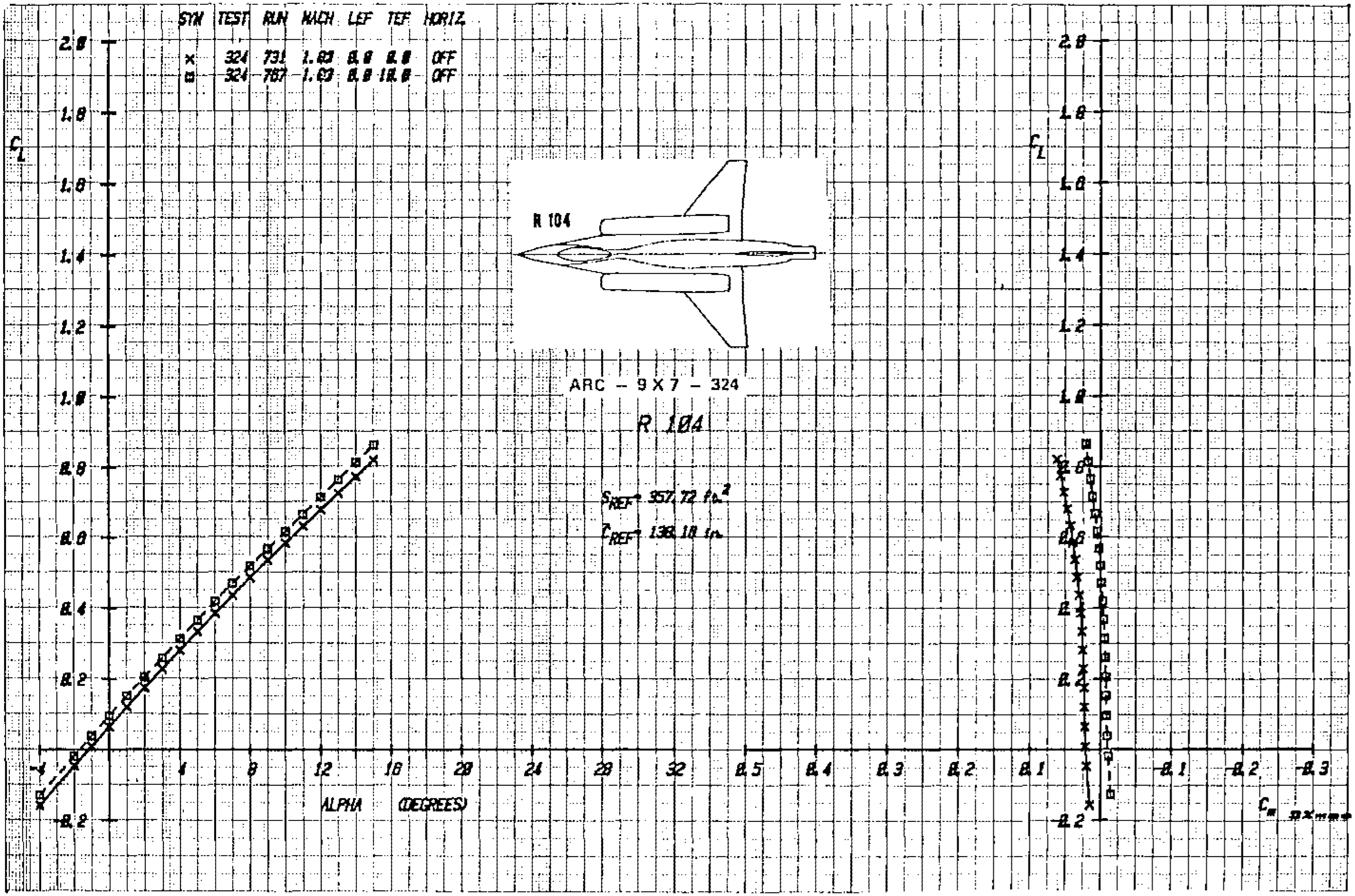

Figure1-57aEffect of Wing Trailing-Edge Flap Deflection on Lift and Moment with Canard Off, Mach = 1.8

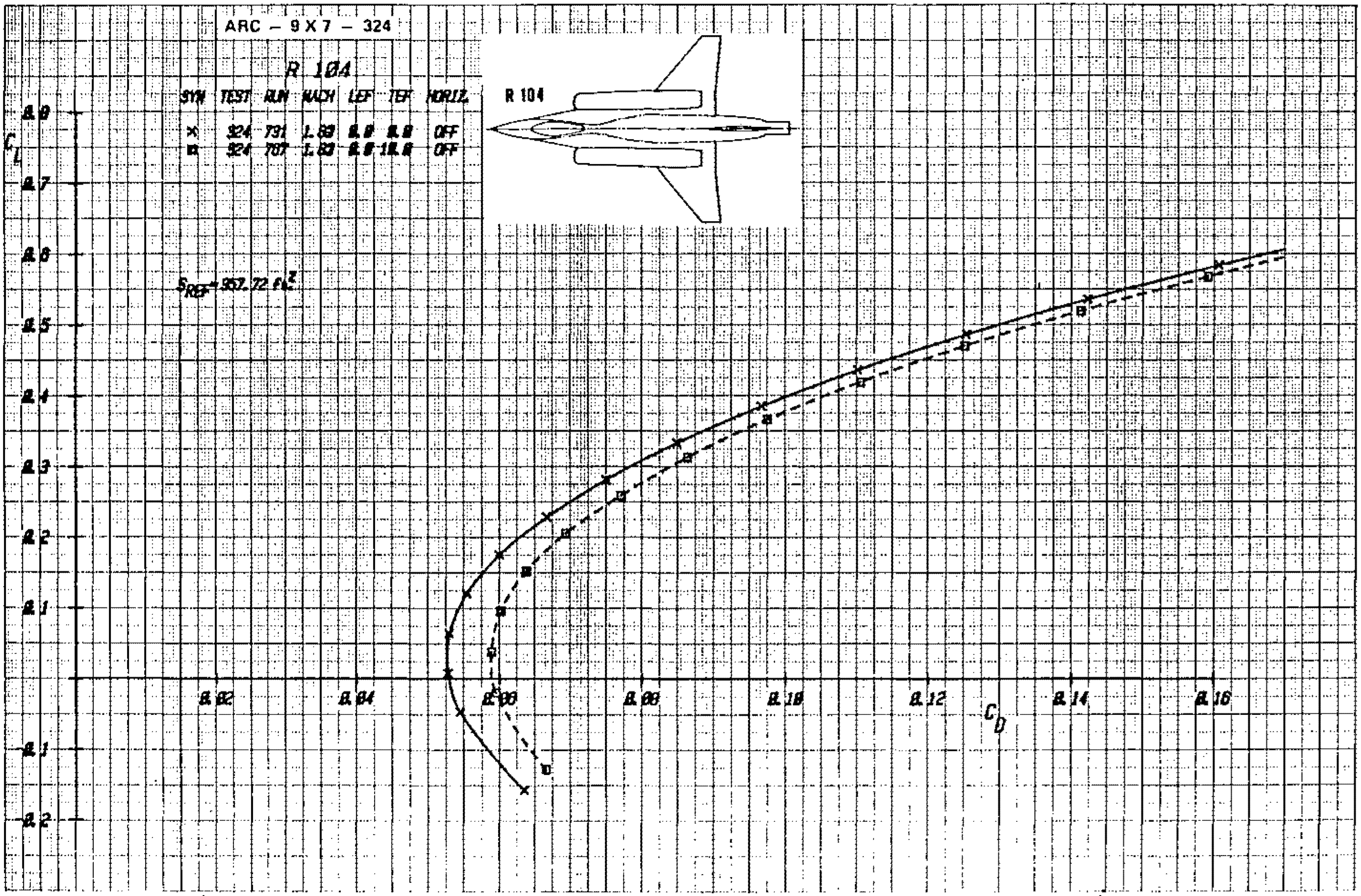

Figurel-57bEffect of Wing Trailing-Edge Flap Deflection on Drag with Canard Off, (Expanded Drag Scale), Mach = 1.8

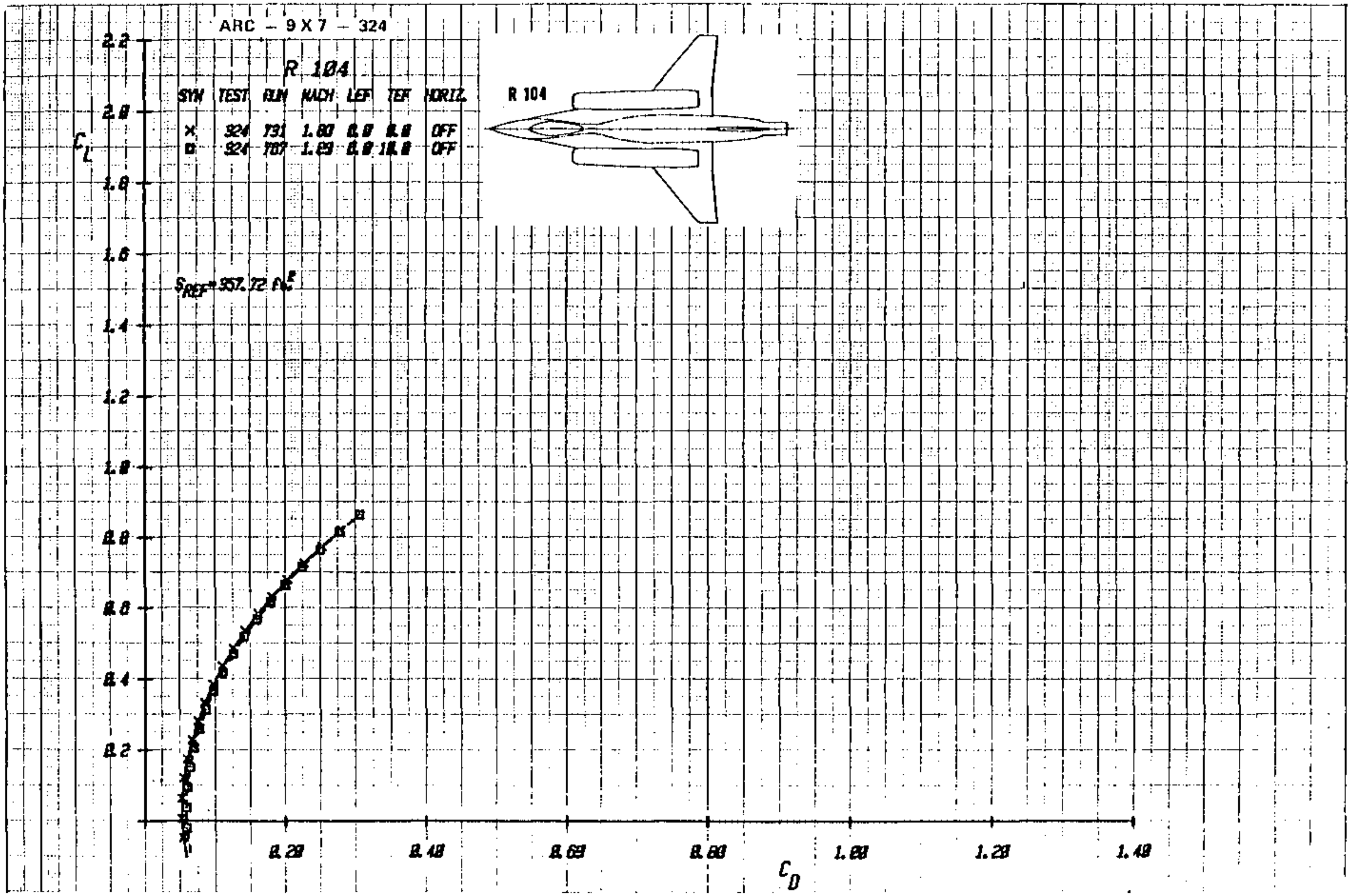

Figure1-57cEffect of Wing Trailing-Edge Flap Deflection on Drag with Canard Off,
Mach = 1.8

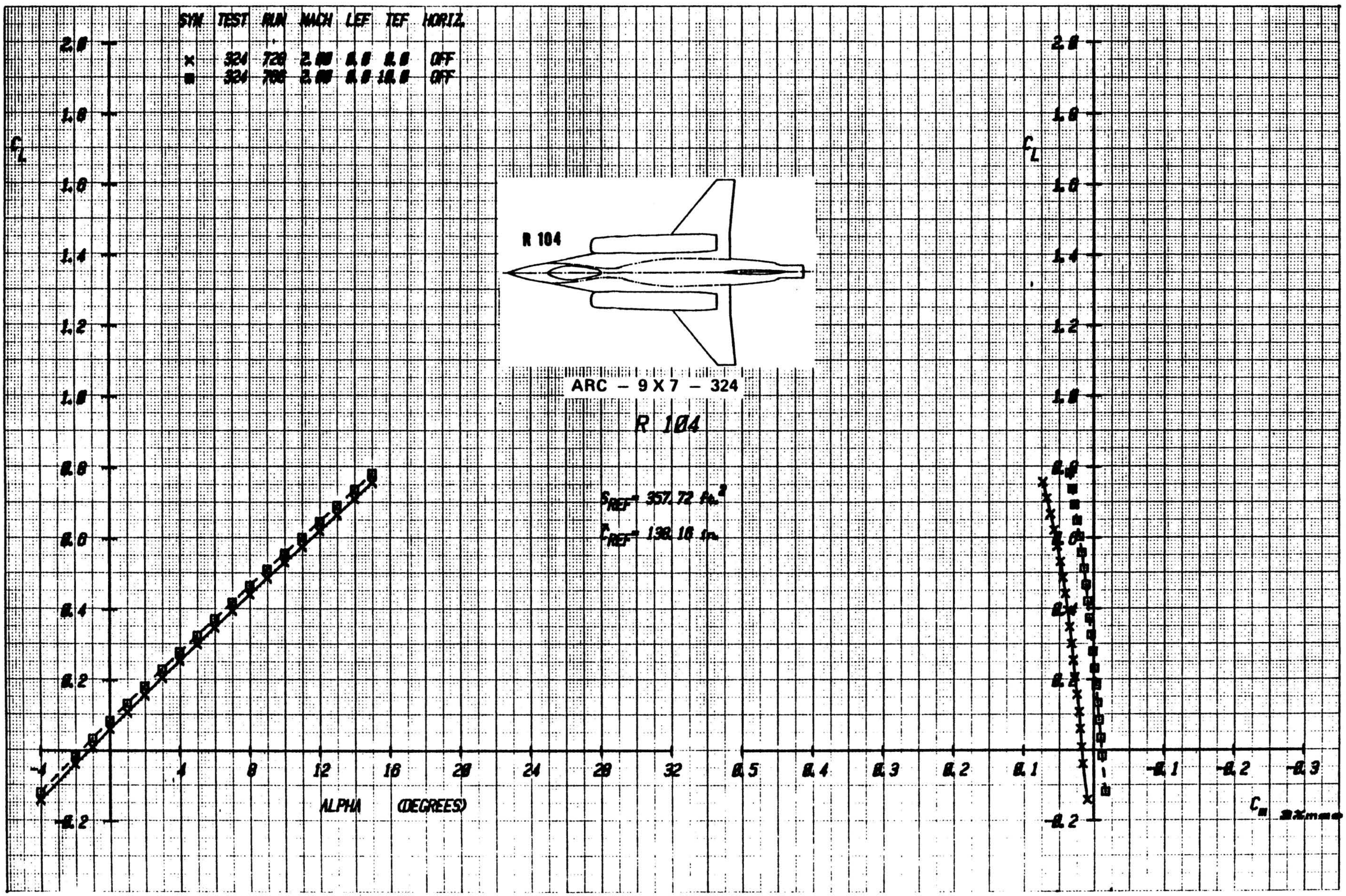

Figure1-58aEffect of Wing Trailing-Edge Flap Deflection on Lift and Moment with Canard Off, Mach = 2.0

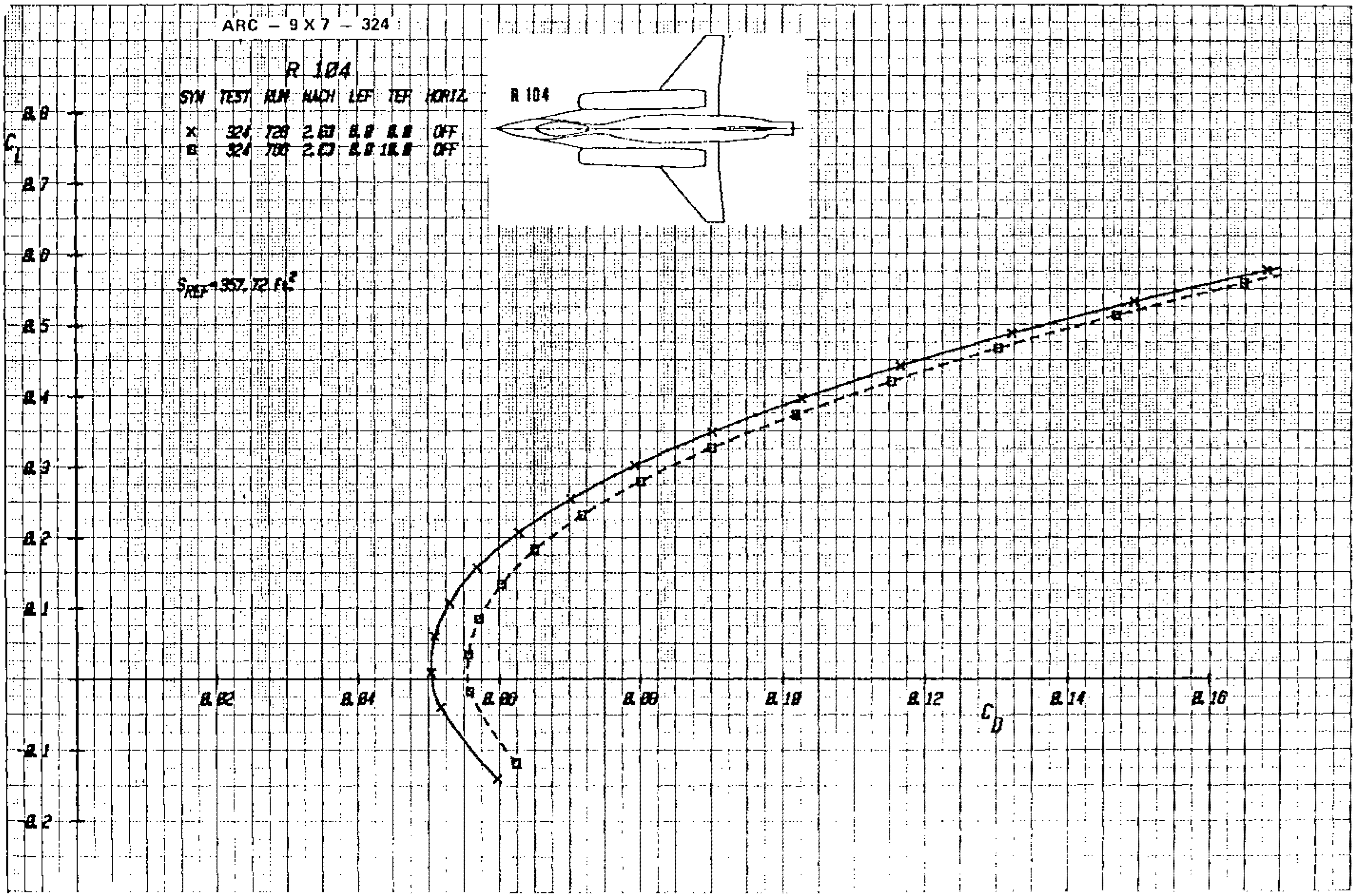

Figure1-58bEffect of Wing Trailing-Edge Flap Deflection on Lift and Moment with Canard Off, (Expanded Drag Scale), Mach = 2.0

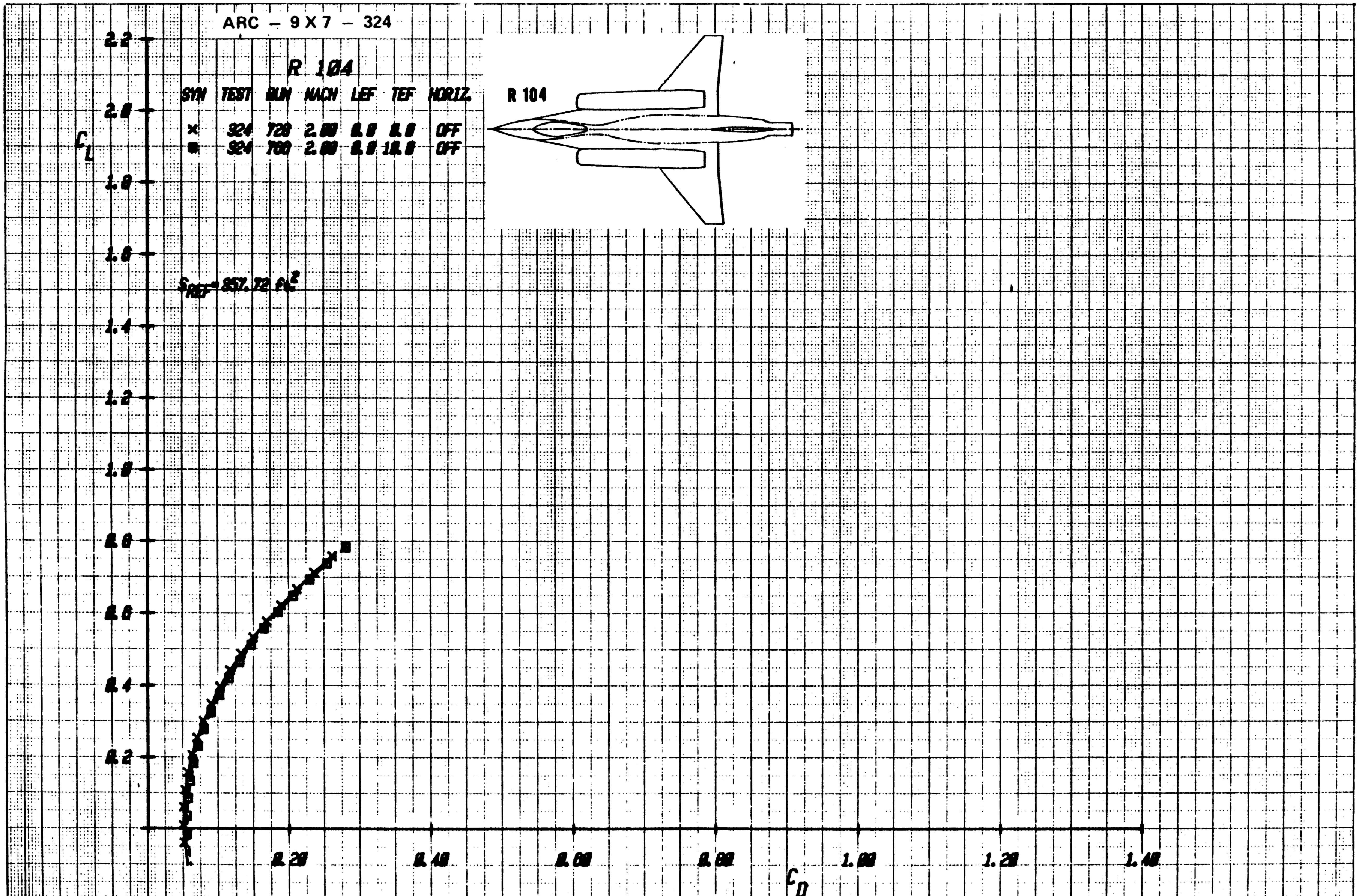

Figure1-58cEffect of Wing Trailing-Edge Flap Deflection on Drag with Canard Off, Mach = 2.0

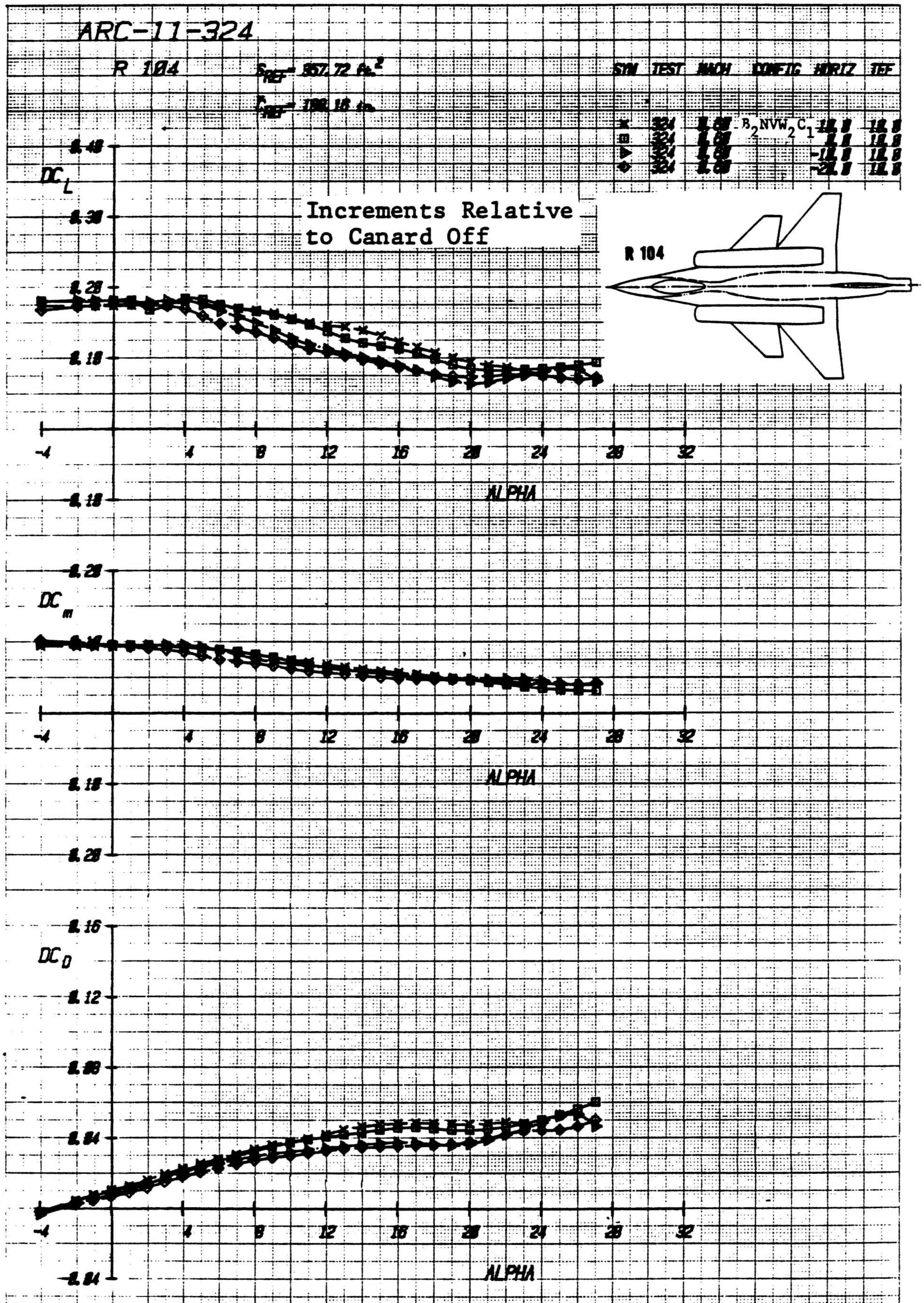

Figure 1-59 Incremental Effects of Canard Deflection with Wing Trailing-Edge Flap Deflected +10°, Mach = .6

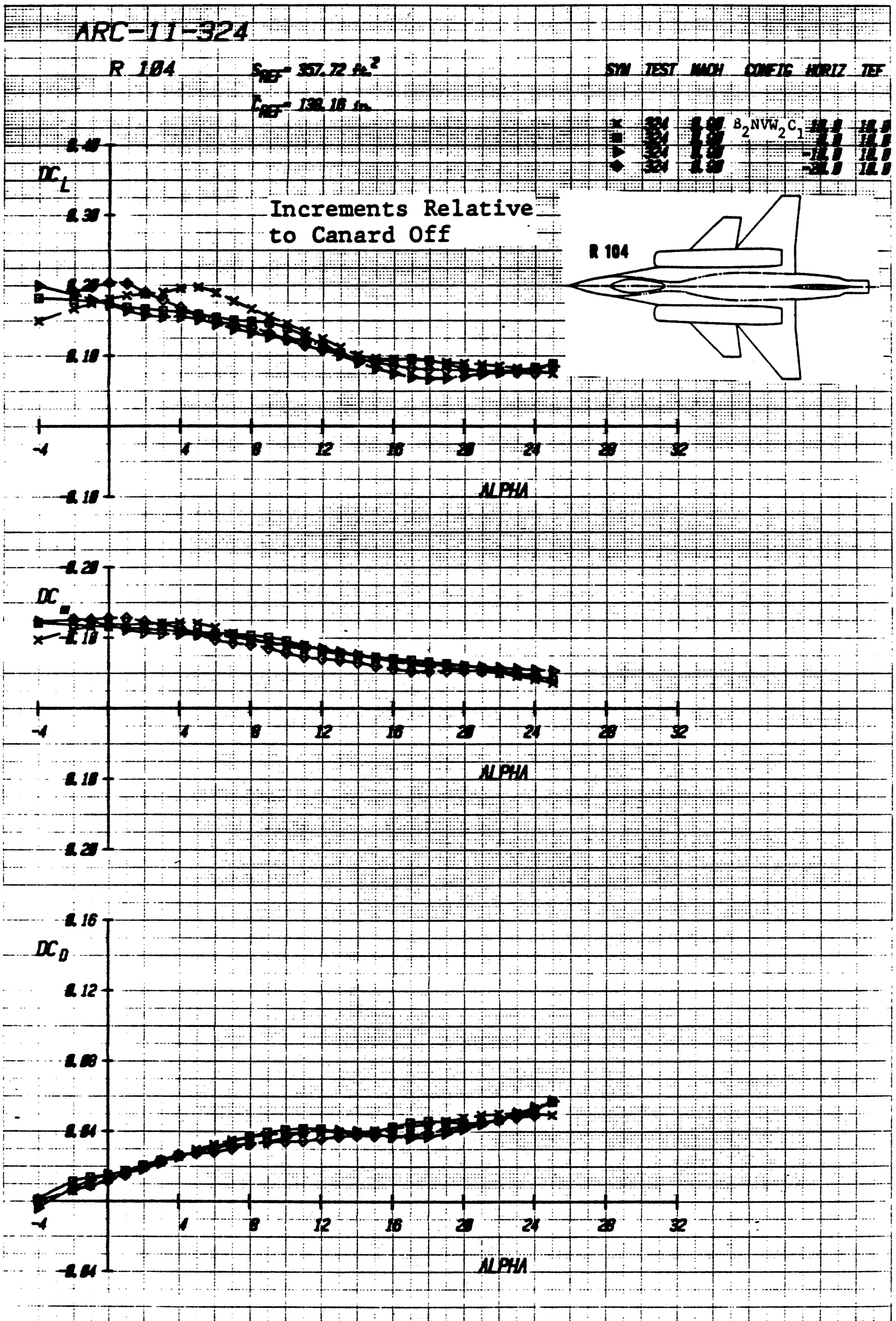

Figure 1-60 Incremental Effects of Canard Deflection with Wing Trailing-Edge Flap Deflected +10°, Mach = .9

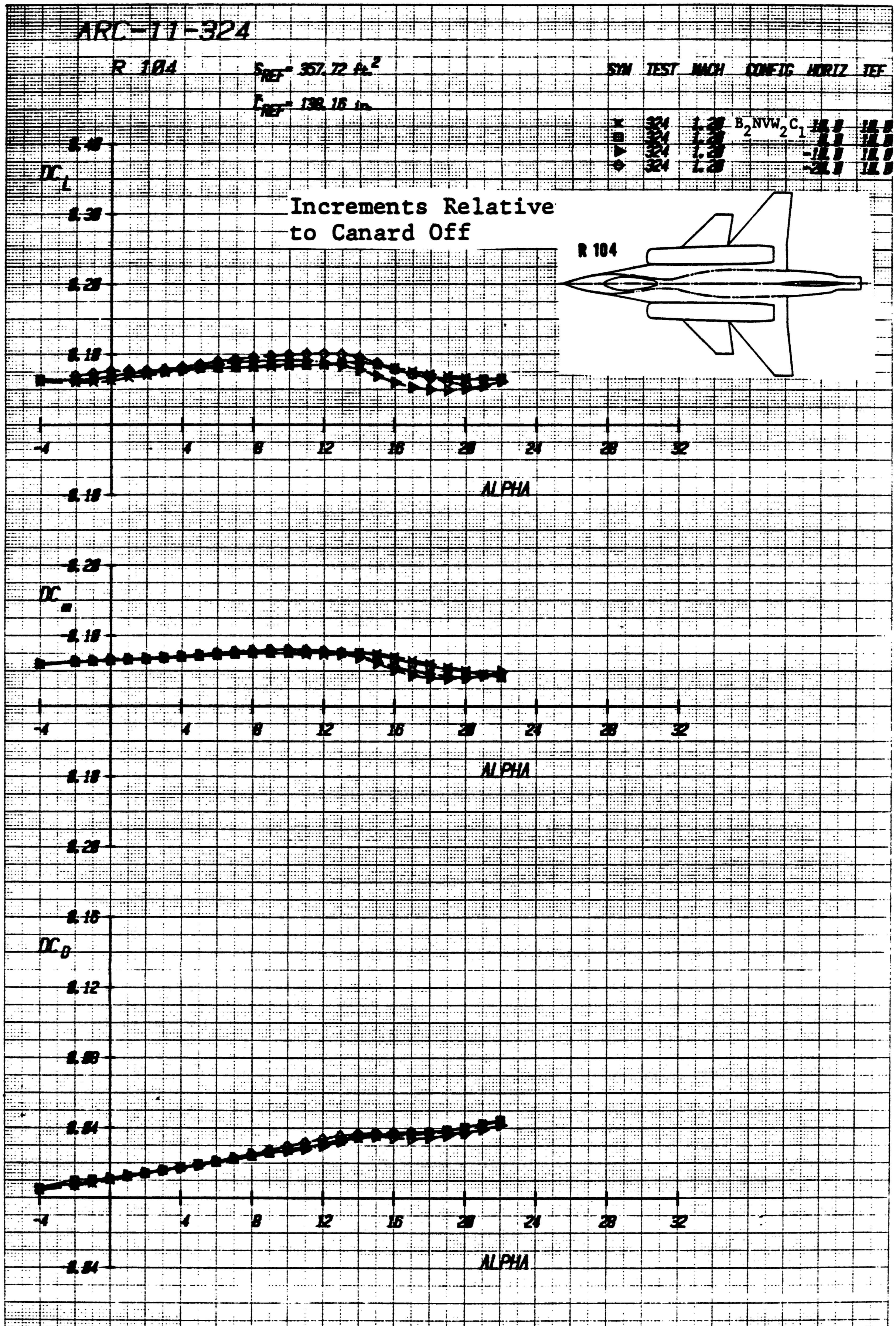

Figure 1-61 Incremental Effects of Canard Deflection with Wing Trailing-Edge Flap Deflected +10°, Mach = 1.2

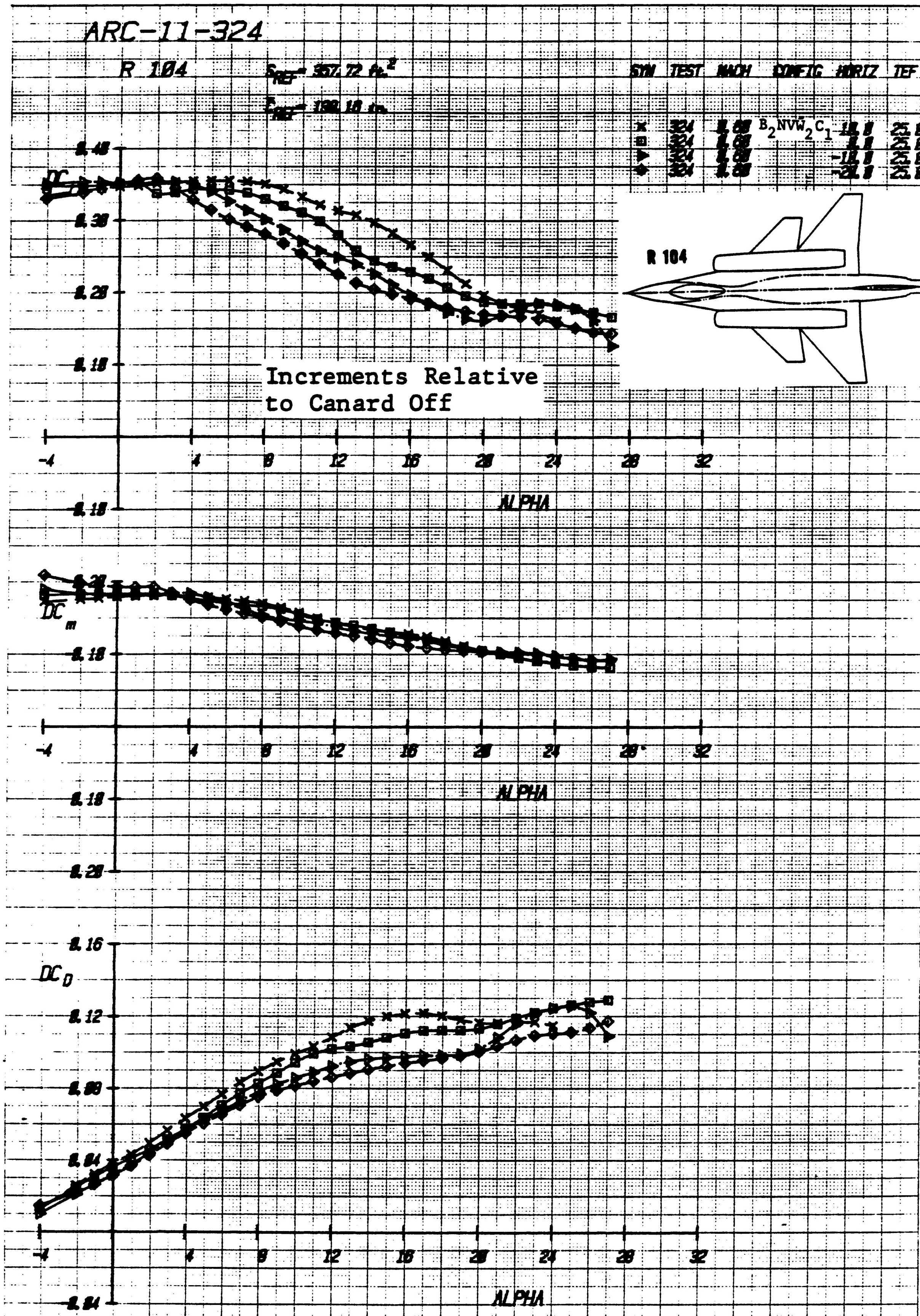

Figure 1-62 Incremental Effects of Canard Deflection with Wing Trailing-Edge Flap Deflected +25°, Mach = .6

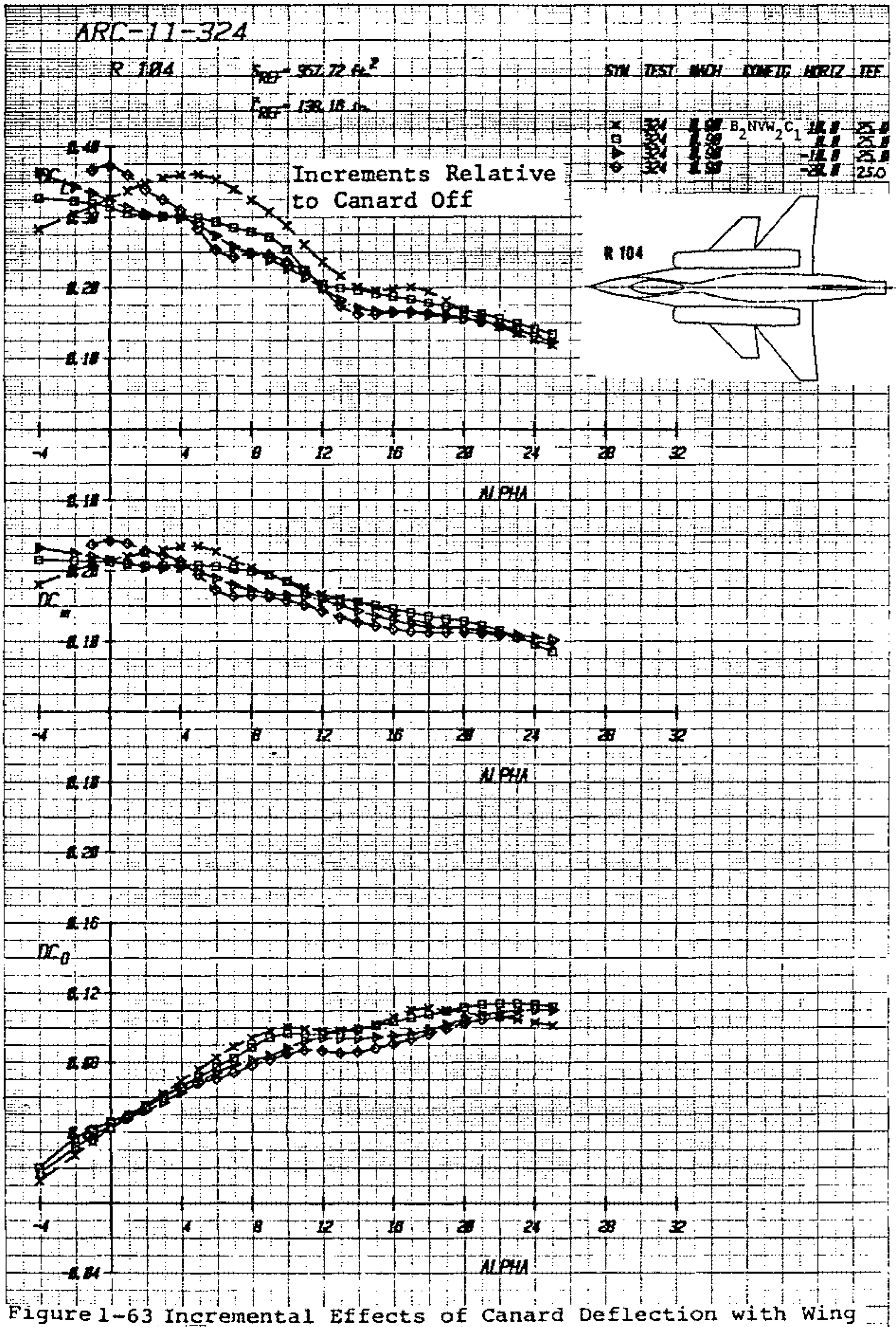

Figure 1-63 Incremental Effects of Canard Deflection with Wing Trailing-Edge Flap Deflected +25°, Mach = .9

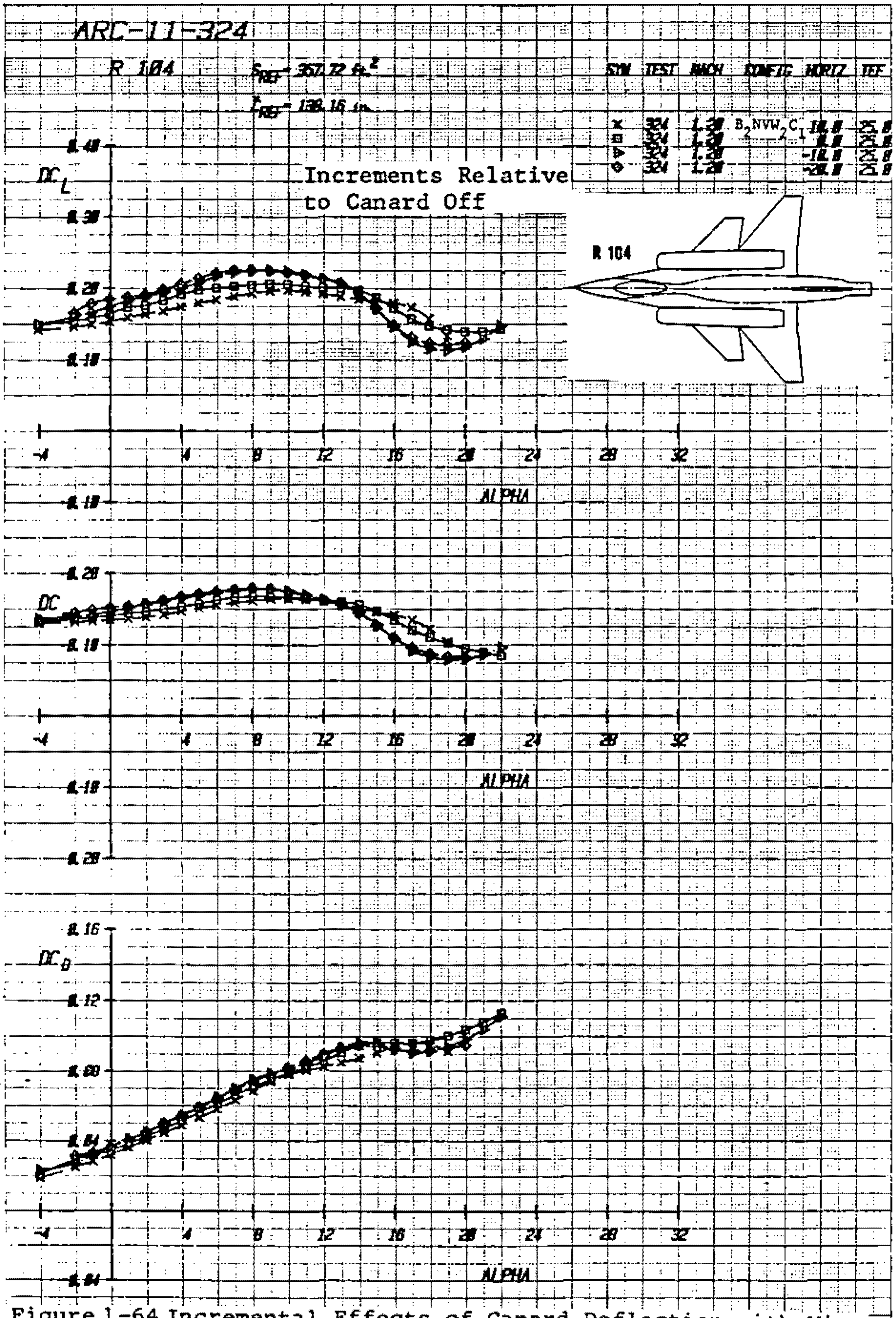

Figure 1-64 Incremental Effects of Canard Deflection with Wing Trailing-Edge Flap Deflected +25°, Mach = 1.2

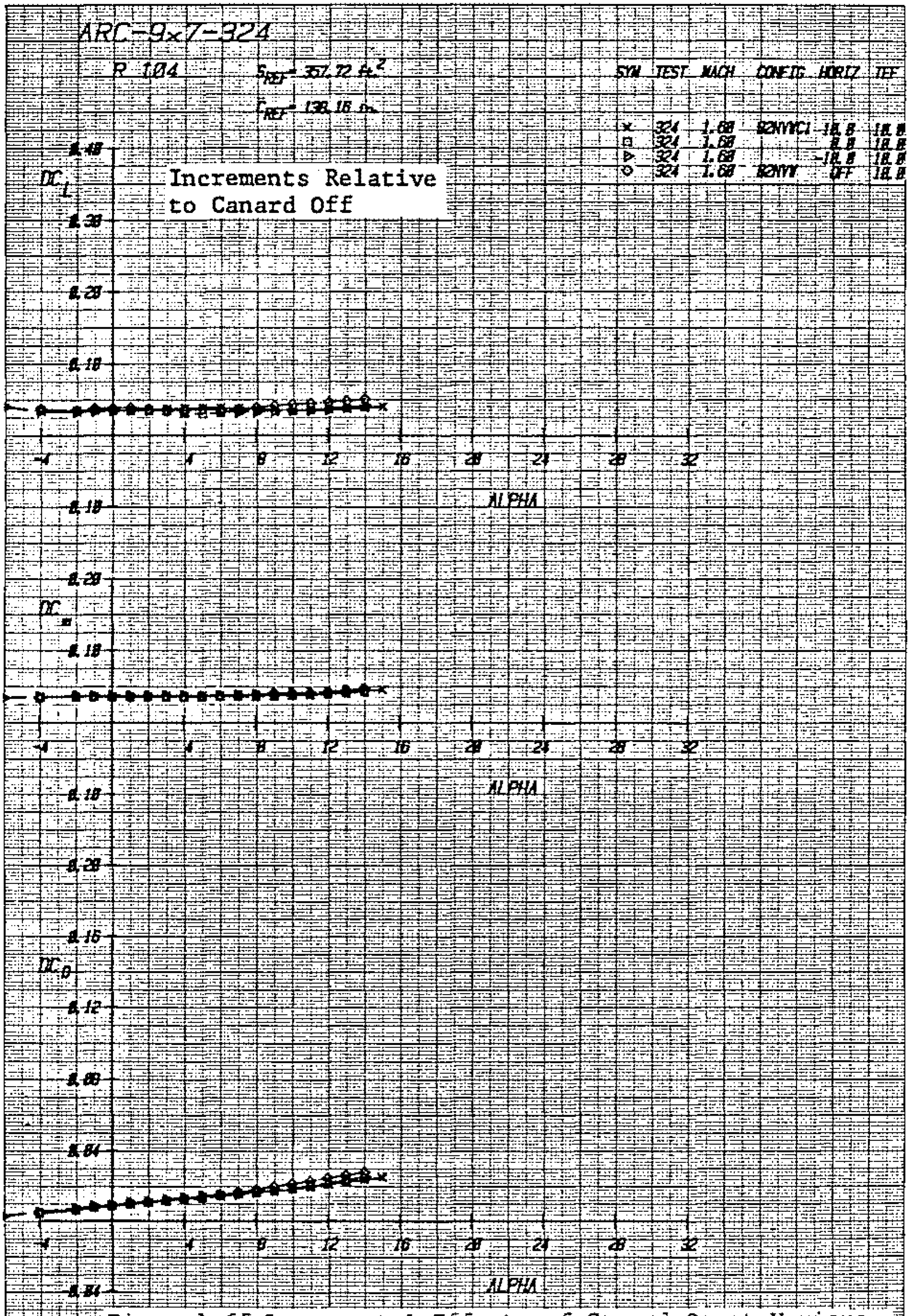

Figure 1-65 Incremental Effects of Canard On at Various Deflections and Off, with Wing Trailing-Edge Flap Deflected +10°, Mach = 1.6

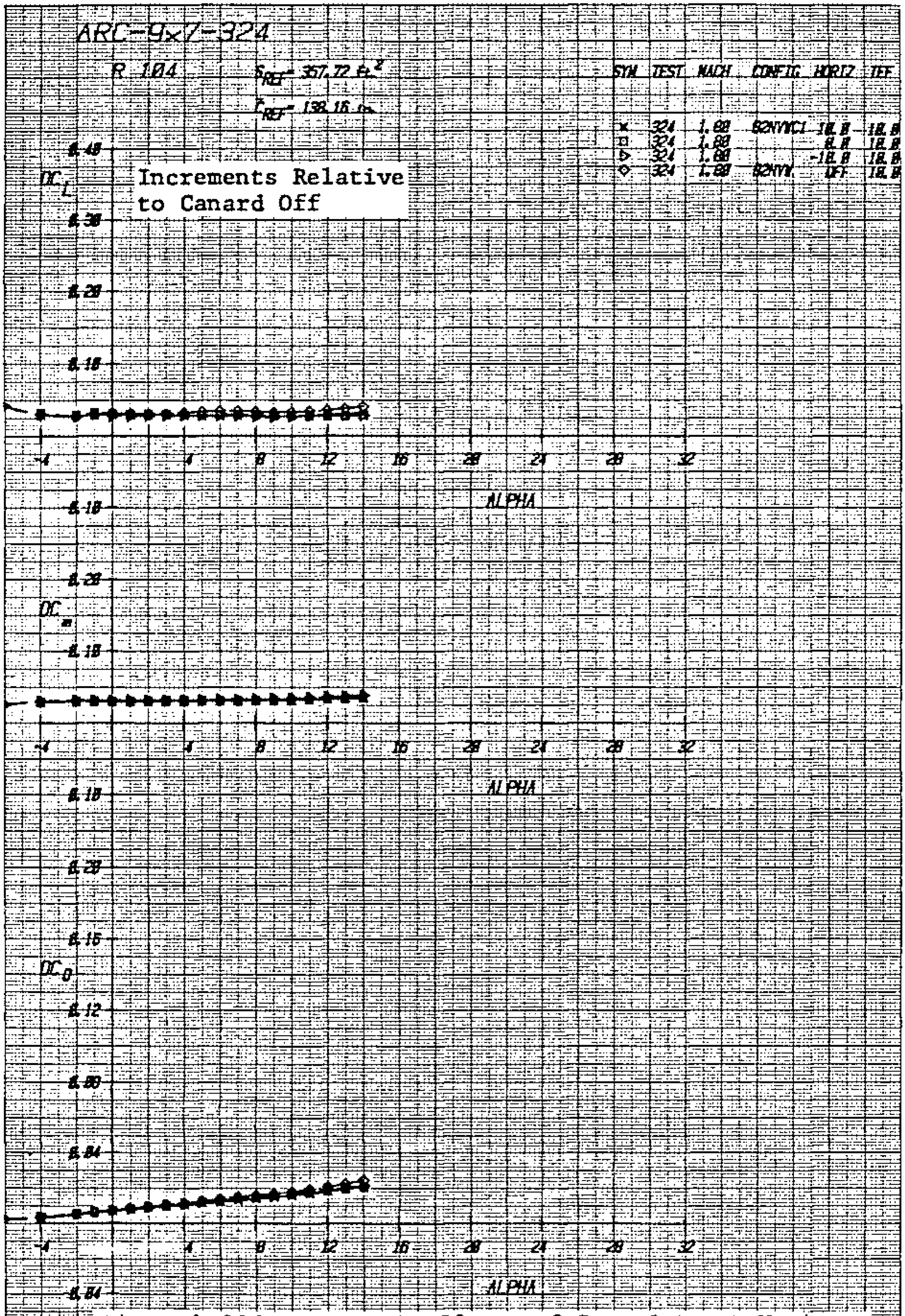

Figure 1-66 Incremental Effects of Canard On at Various Deflections and Off, with Wing Trailing-Edge Flap Deflected +10°, Mach = 1.8

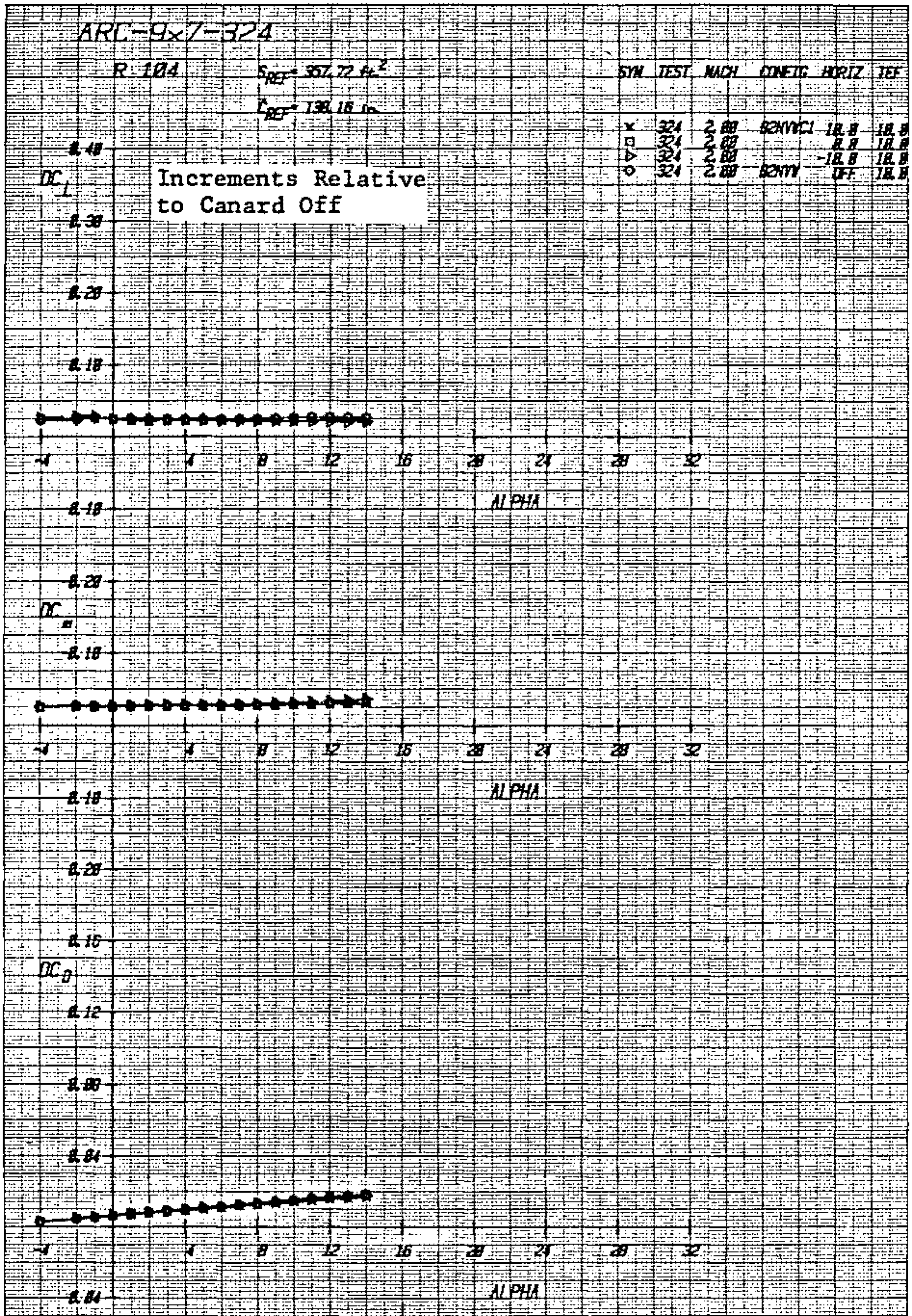

Figure1-67 Incremental Effects of Canard On at Various Deflections and Off, with Wing Trailing-Edge Flap Deflected +10°, Mach = 2.0

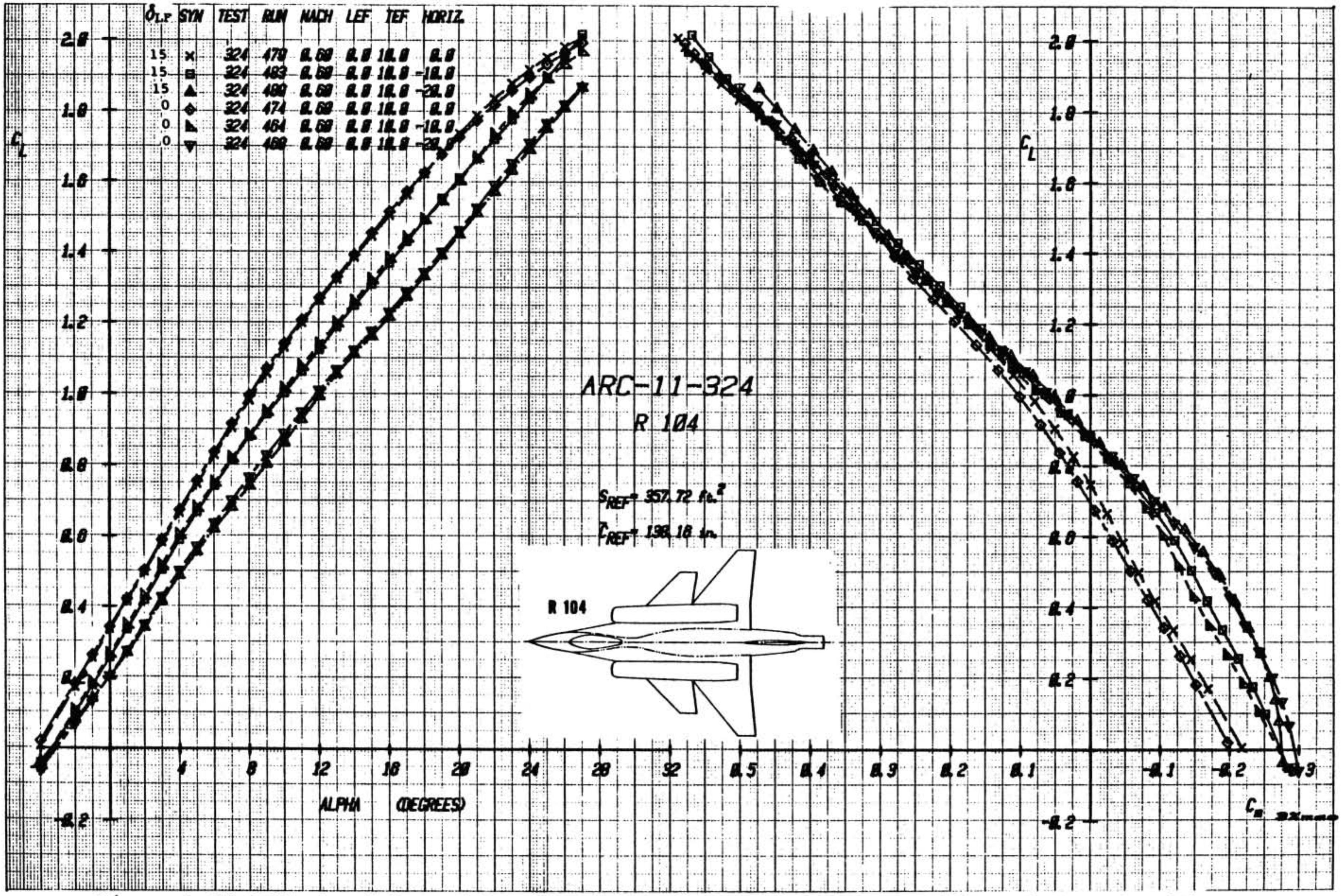

Figure1-68aEffect of Canard Leading-Edge Flap Deflection on Lift and Moment with Wing Trailing-Edge Flap Deflected +10°, Mach = .6

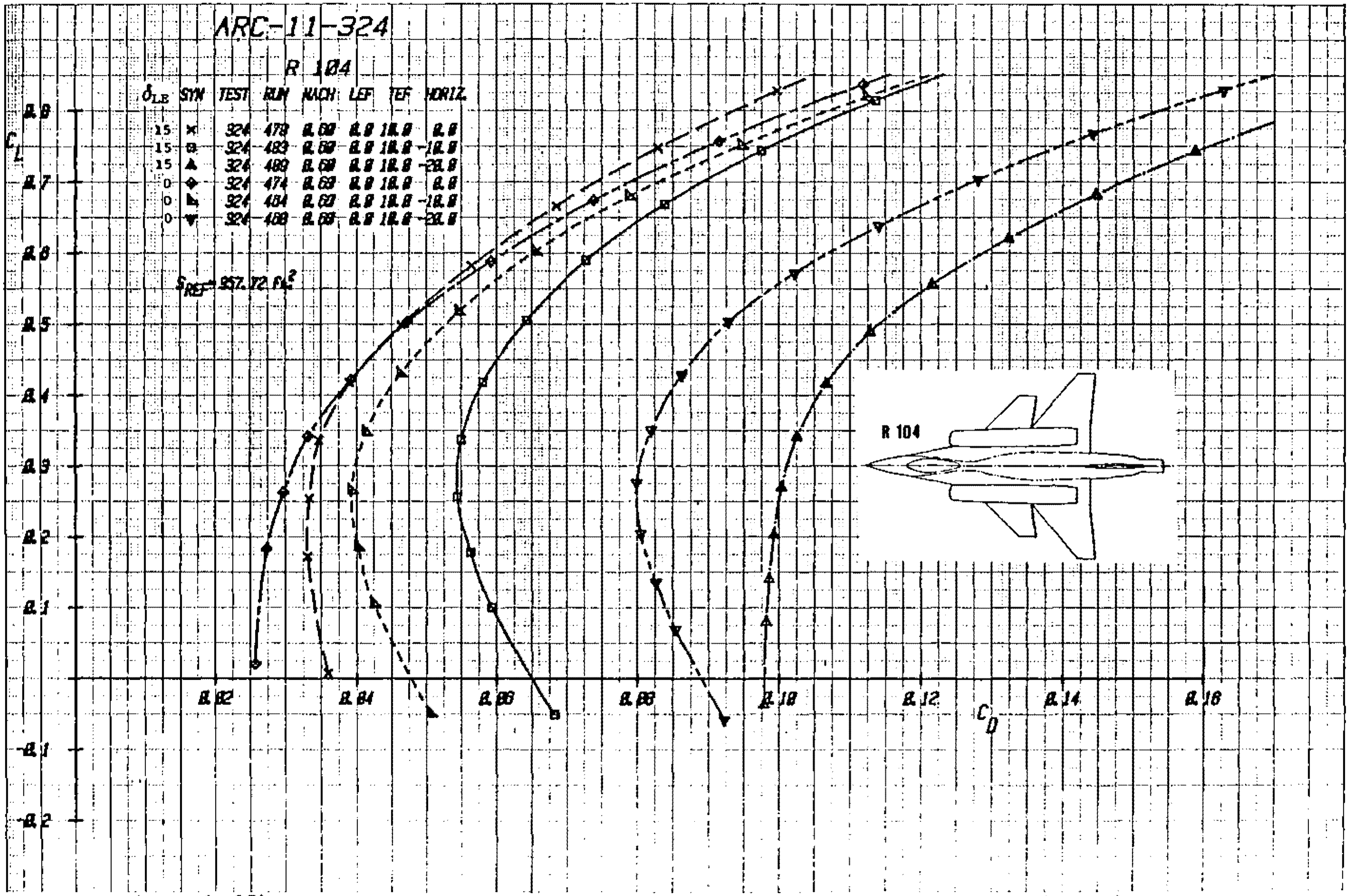

Figure1-68b Effect of Canard Leading-Edge Flap Deflection on Drag with Wing Trailing-Edge Flap Deflected +10°, Mach = .6

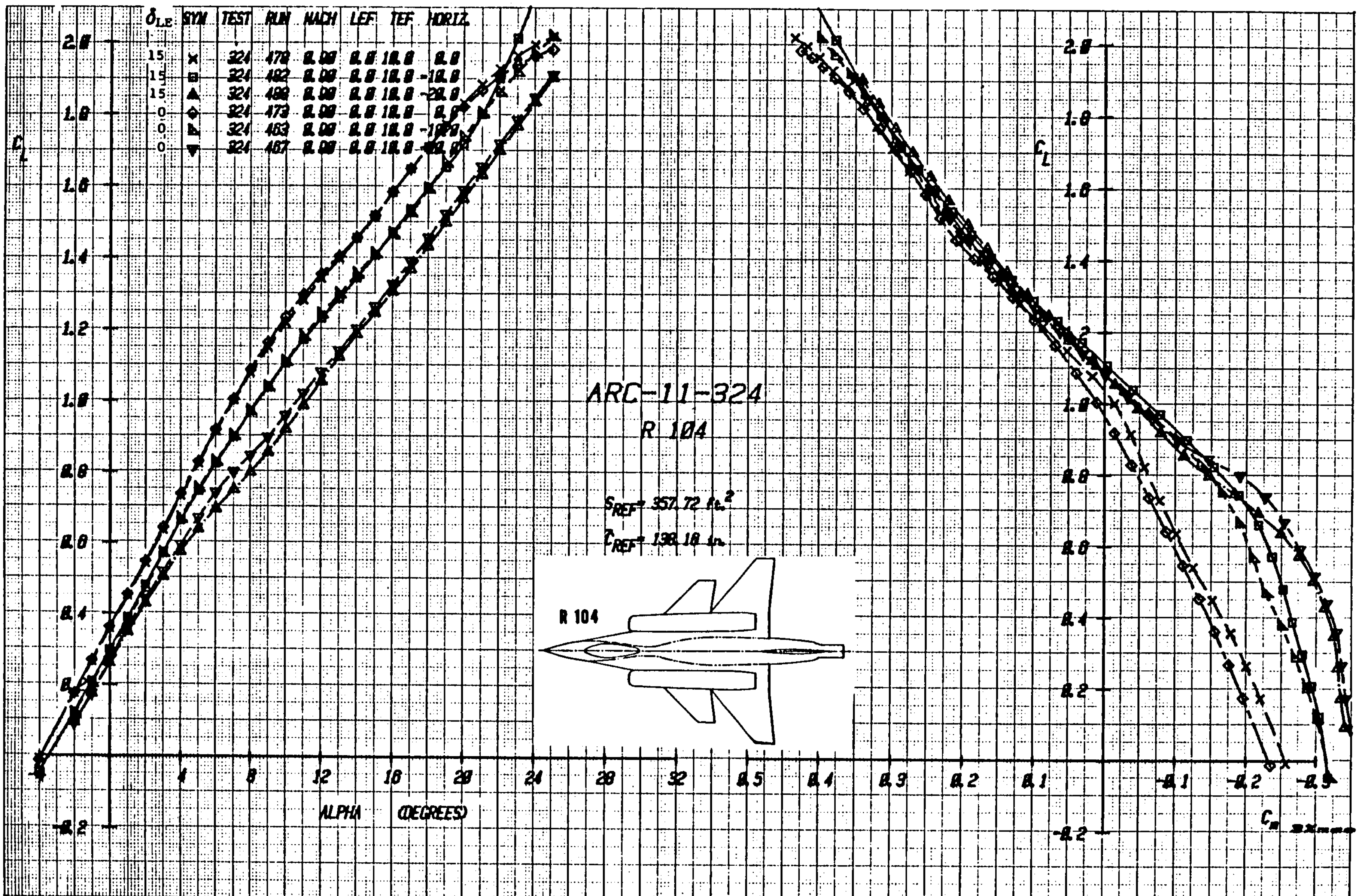

Figure1-69aEffect of Canard Leading-Edge Flap Deflection on Lift and Moment With Wing Trailing-Edge Flap Deflected +10°, Mach = .9

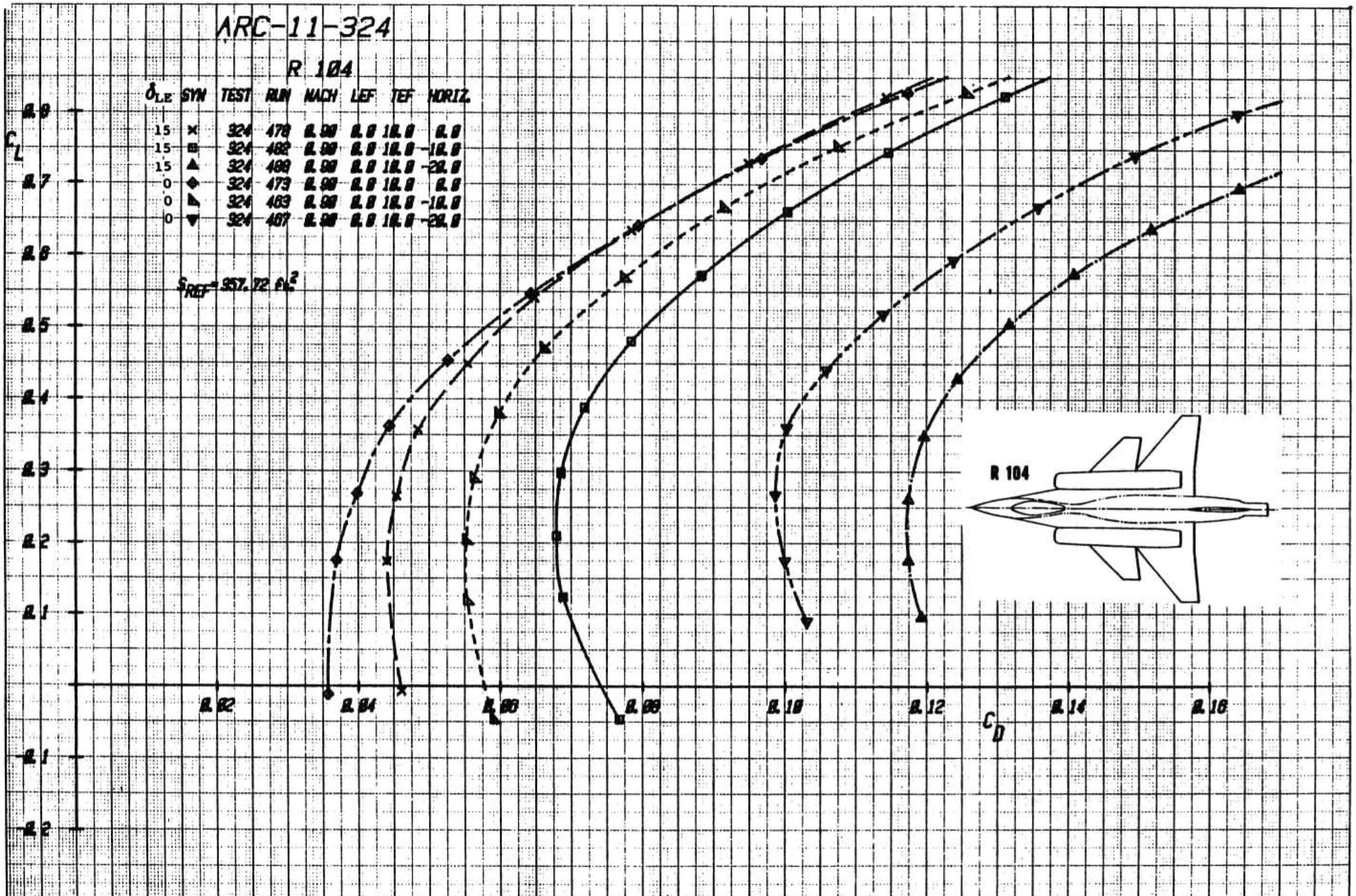

Figurel-69bEffect of Canard Leading-Edge Flap Deflection on Drag With Wing Trailing-Edge Flap Deflected +10°, Mach = .9

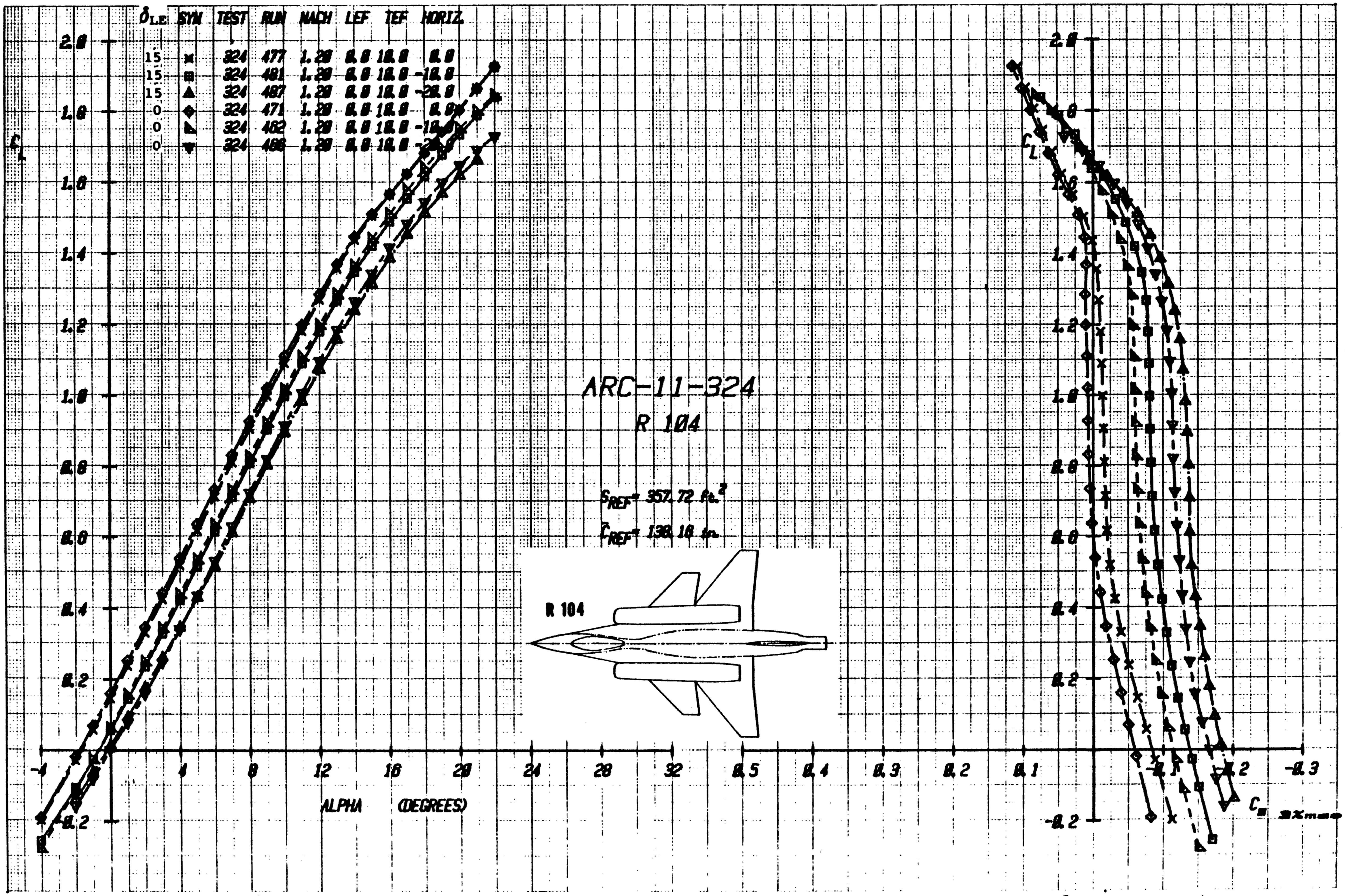

Figure1-70a Effect of Canard Leading-Edge Flap Deflection on Lift and Moment With Wing Trailing-Edge Flap Deflected +10°, Mach = 1.2

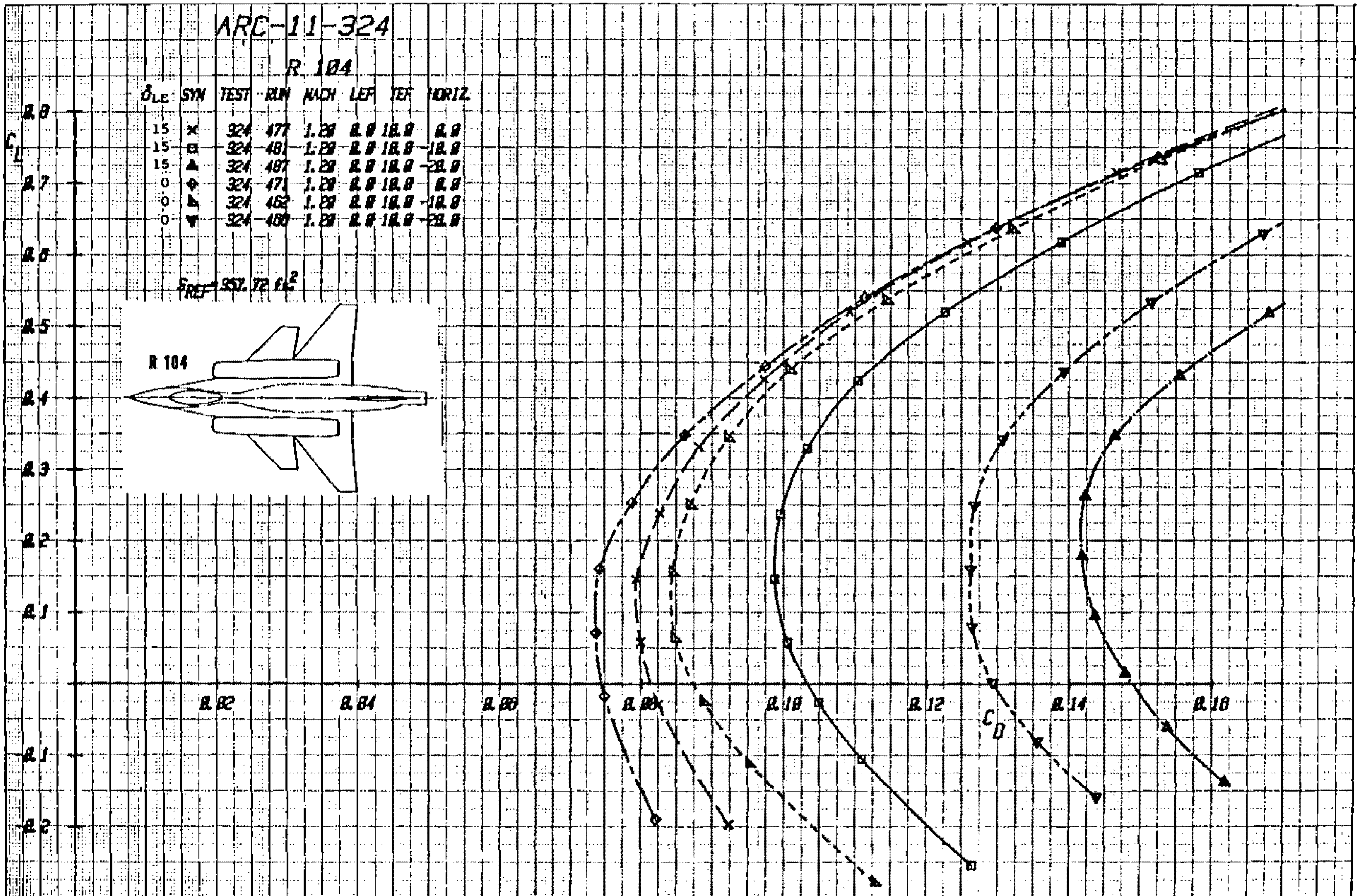

Figure1-70bEffect of Canard Leading-Edge Flap Deflection on Drag With Wing Trailing-Edge Flap Deflected +10°, Mach = 1.2

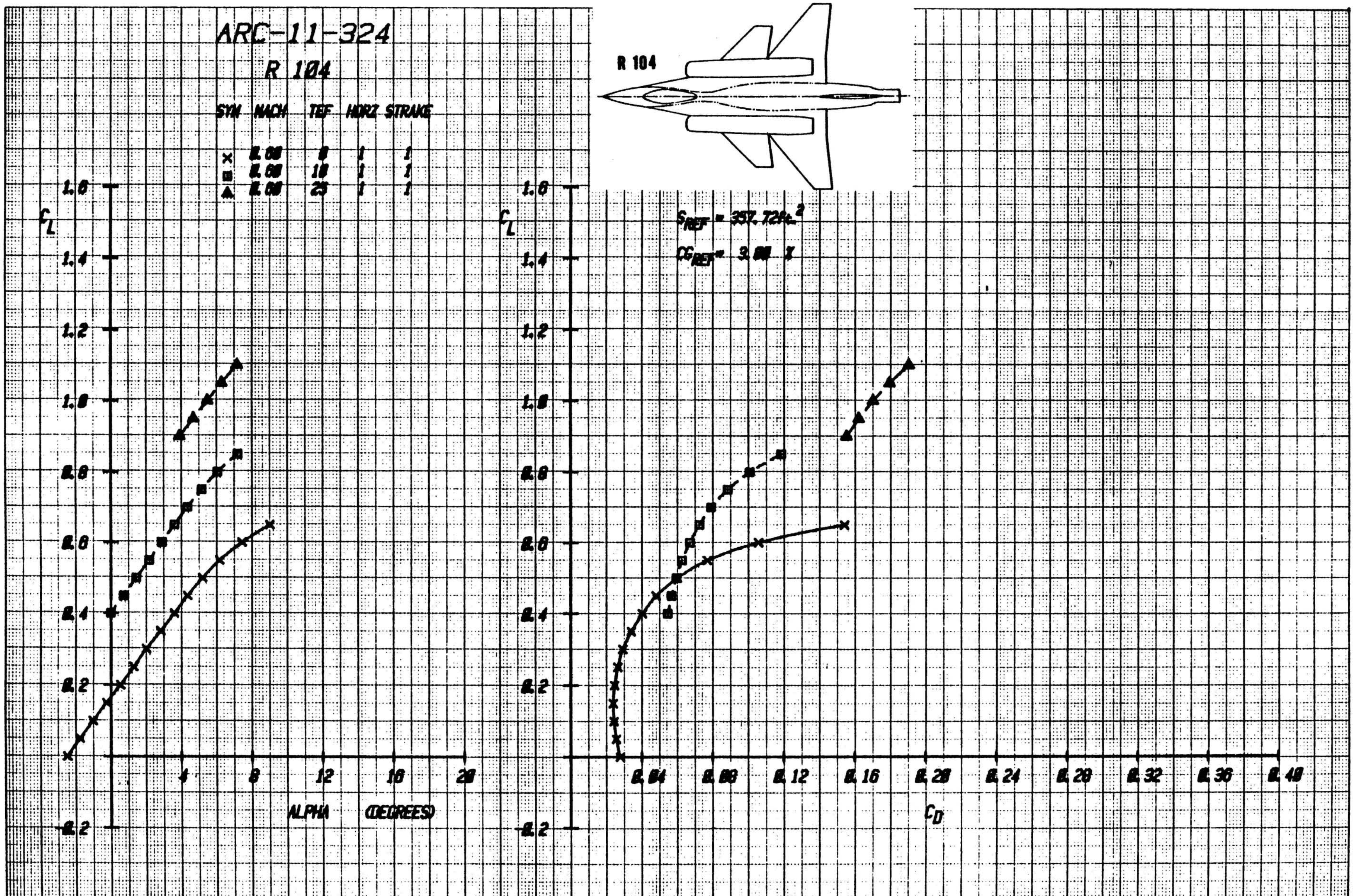

Figure 1-71 Trimmed Lift and Drag for Baseline R104 Configuration Using Canard and Trailing-Edge Flap Deflections, Mach = .6

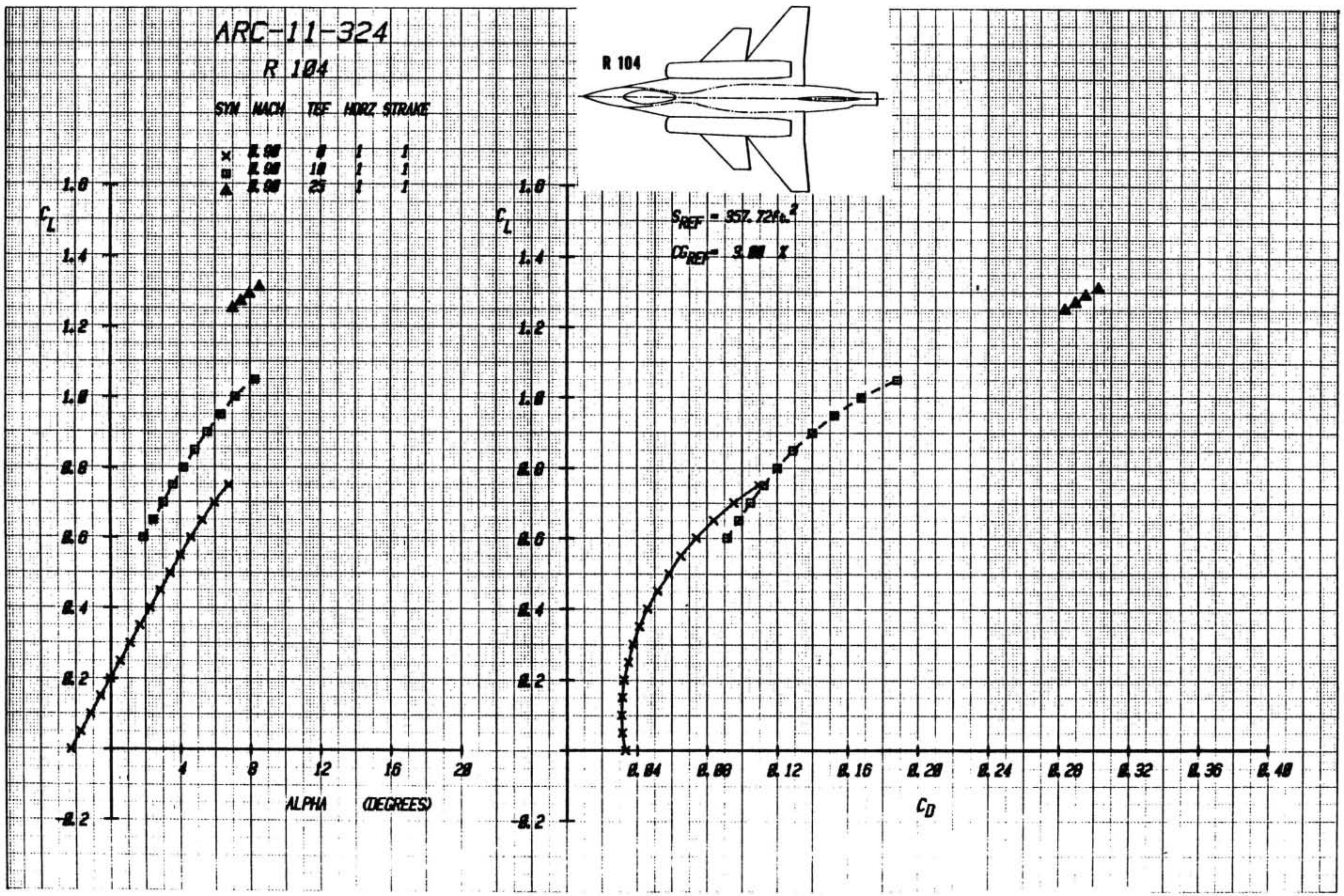

Figure1-72 Trimmed Lift and Drag for Baseline R104 Configuration Using Canard and Trailing-Edge Flap Deflections, Mach = .9

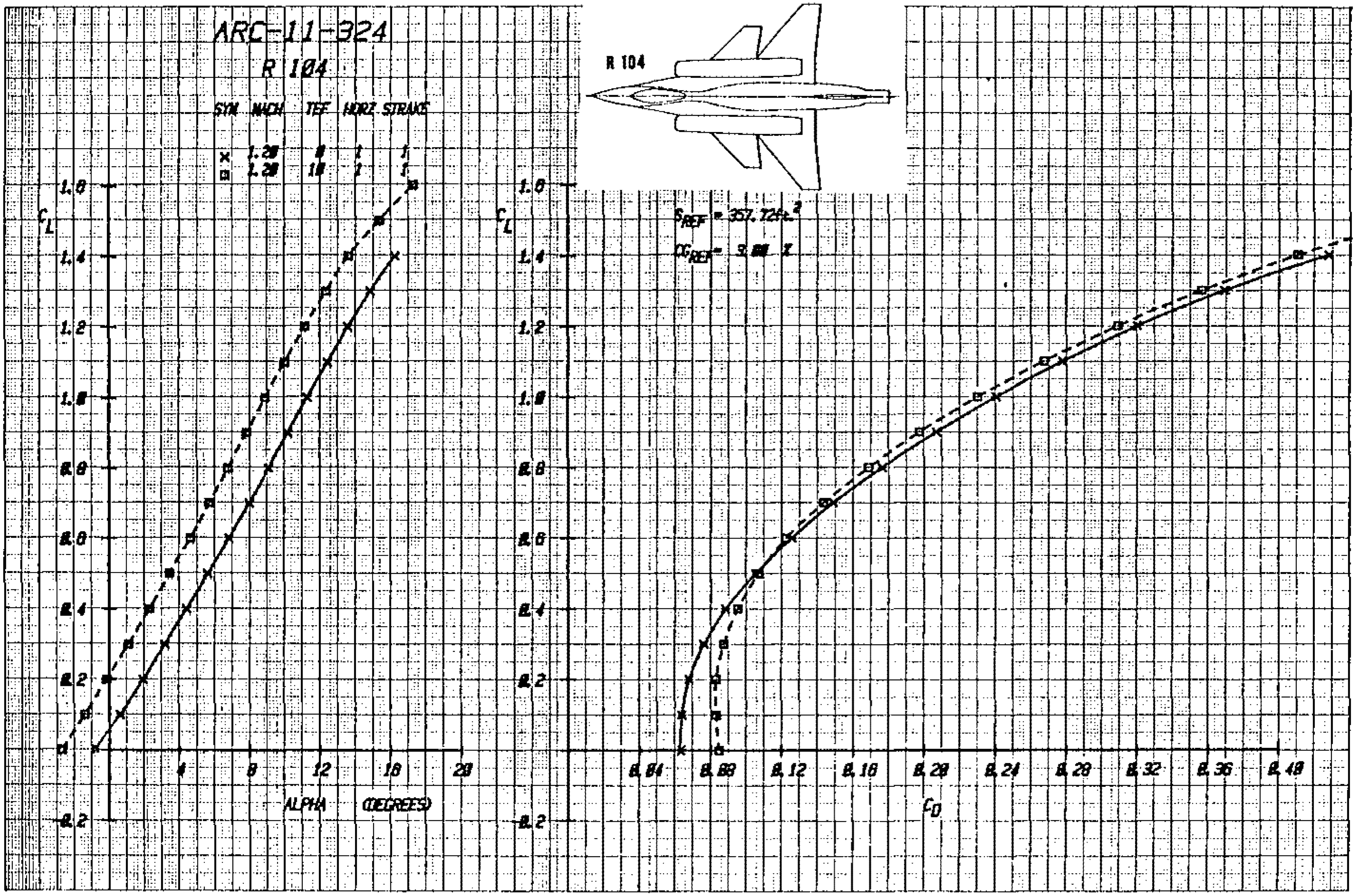

Figure 1-73 Trimmed Lift and Drag for Baseline R104 Configuration Using Canard and Trailing-Edge Flap Deflections, Mach = 1.2

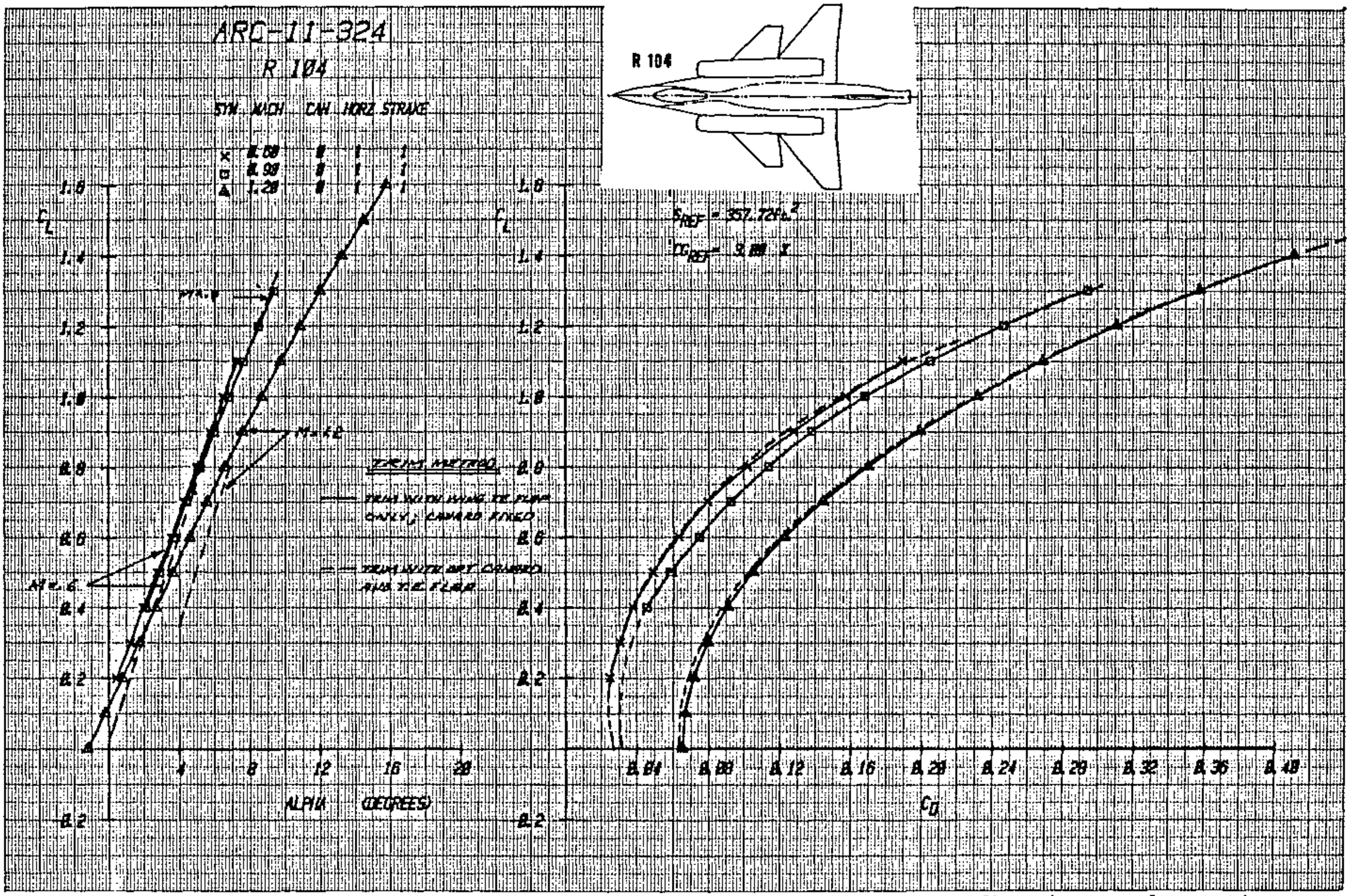

Figure 1-74 Trimmed Lift and Drag with Wing Trailing-Edge Flap Deflections and Baseline Canard Undeflected

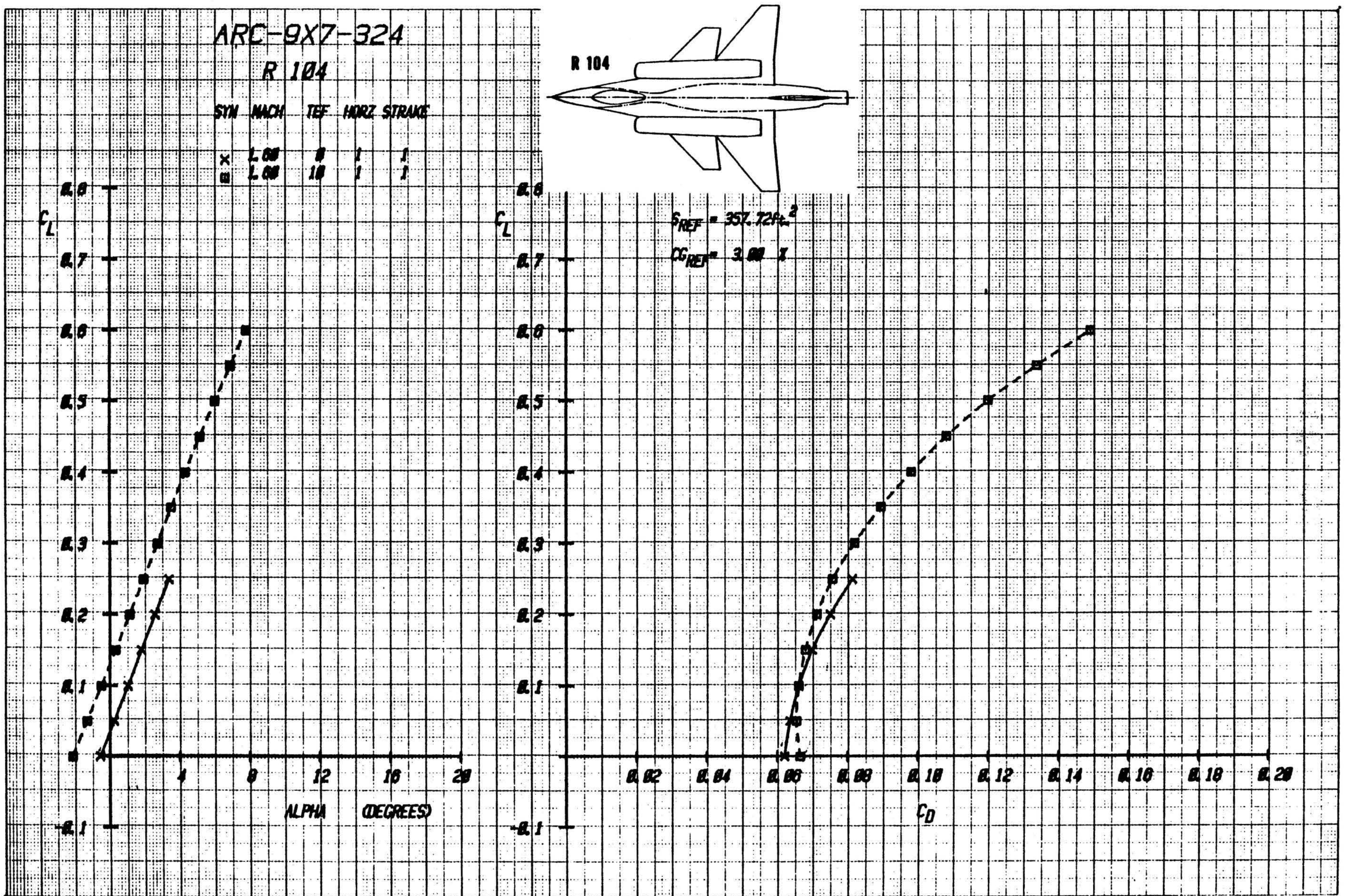

Figure 1-75 Trimmed Lift and Drag for Baseline R104 Configuration Using Canard and Trailing-Edge Flap Deflections, Mach = 1.6

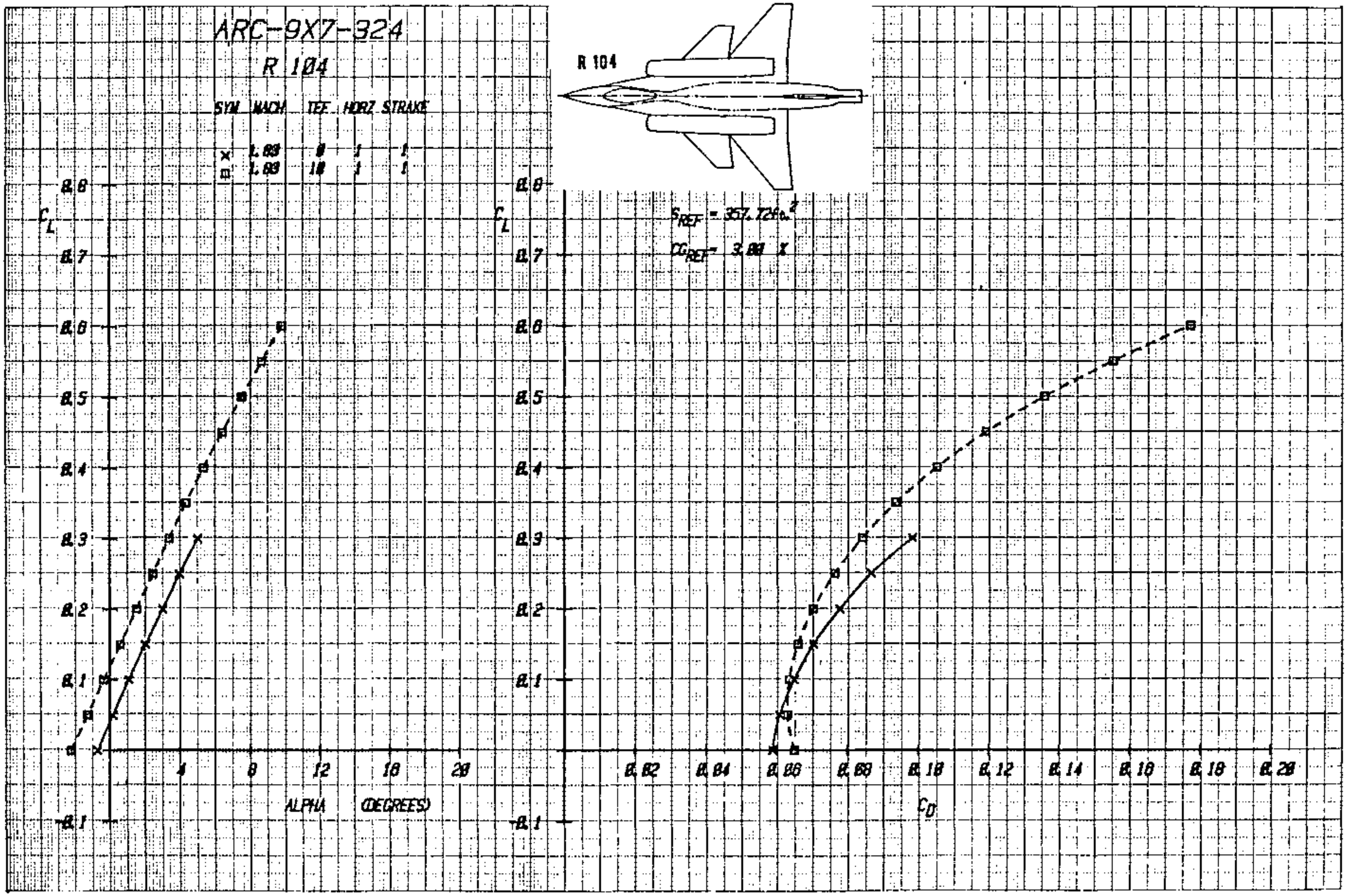

Figure 1-76 Trimmed Lift and Drag for Baseline R104 Configuration Using Canard and Trailing-Edge Flap Deflections, Mach = 1.8

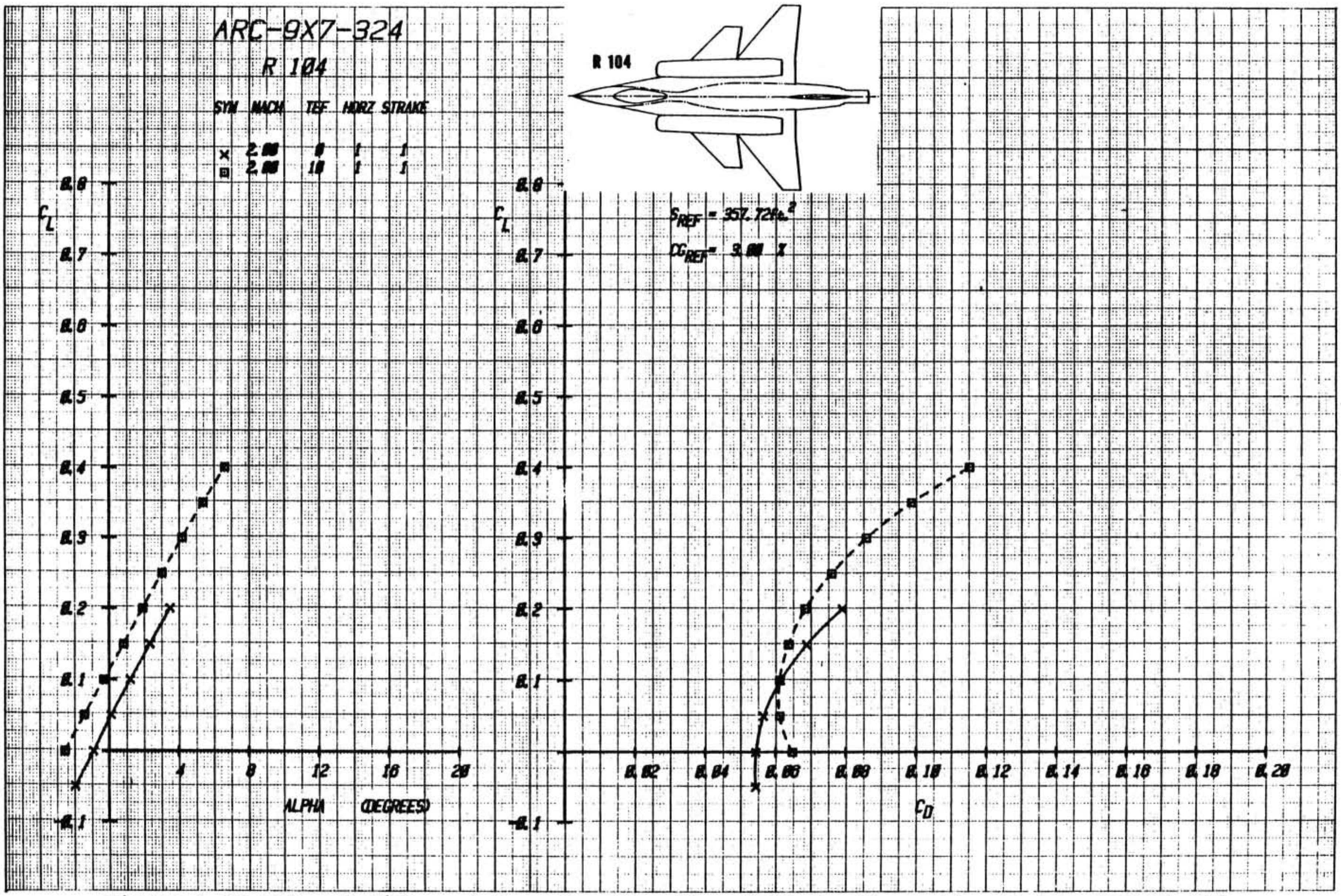

Figure 1-77 Trimmed Lift and Drag for Baseline R104 Configuration Using Canard and Trailing-Edge Flap Deflections, Mach = 2.0

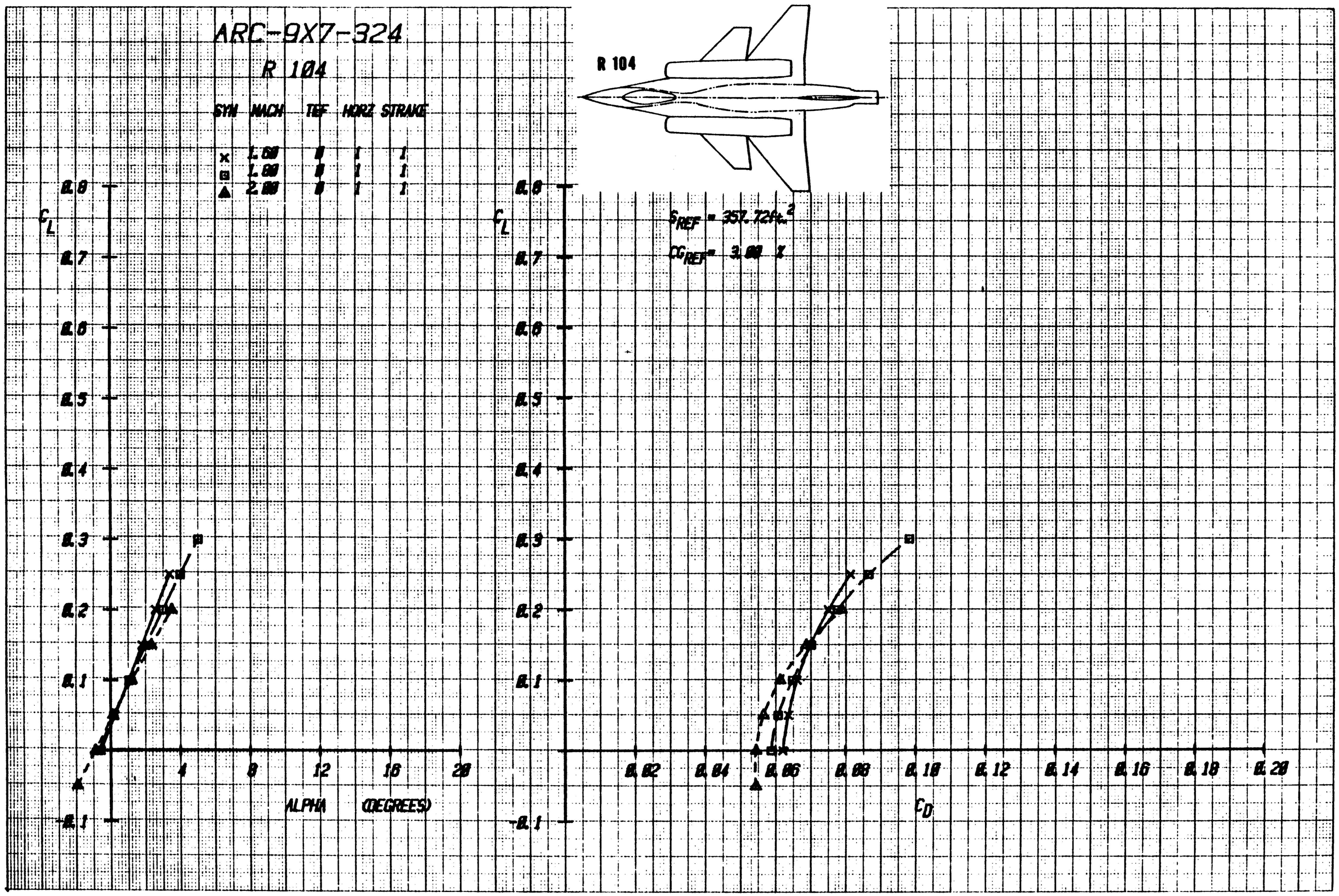

Figure 1-78 Trimmed Lift and Drag for Baseline R104 Configuration with Wing Trailing-Edge Flap Undeflected, Various Mach Numbers.

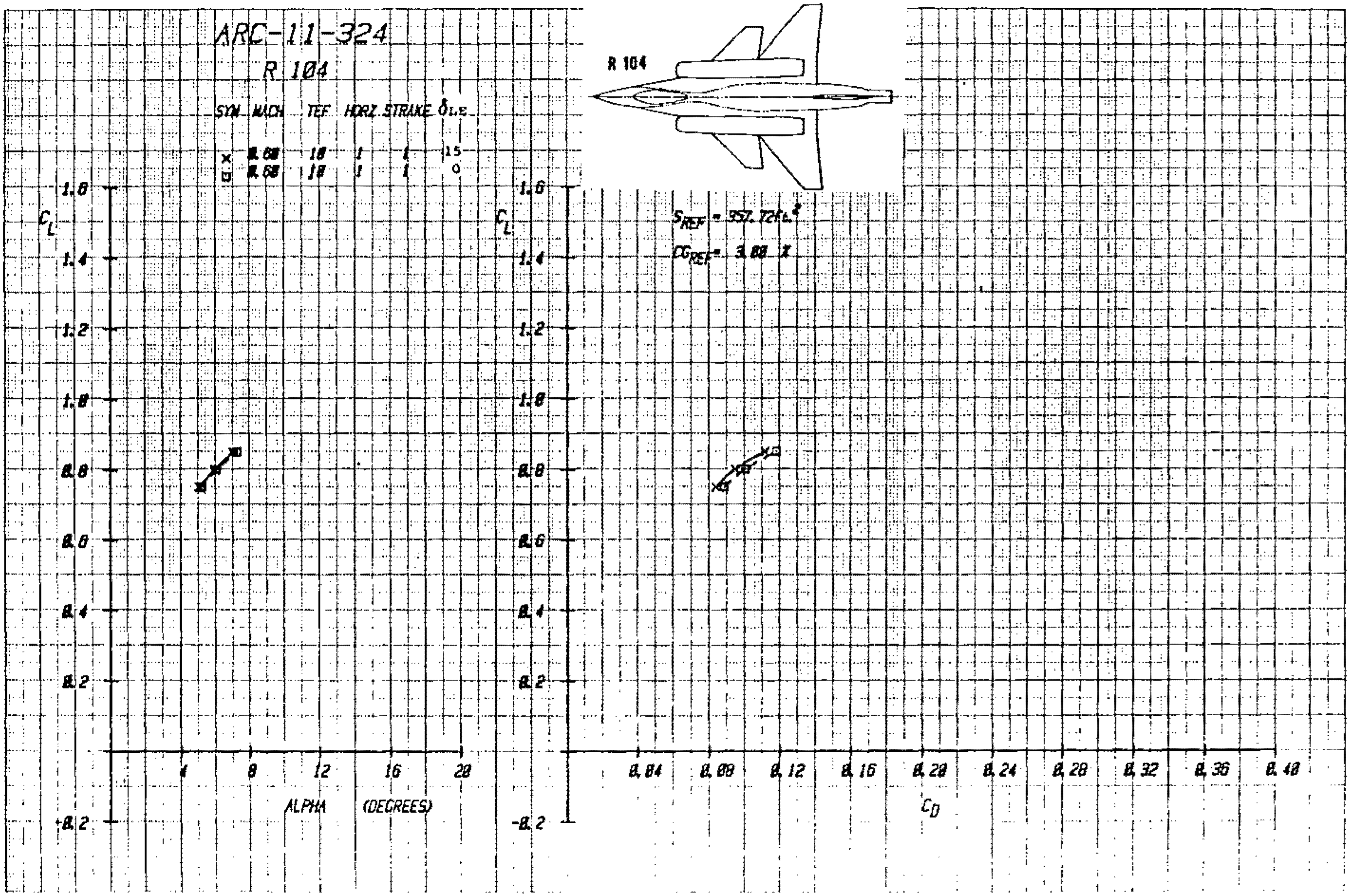

Figure 1-79 Trimmed Lift and Drag with Canard Leading-Edge Flap Deflected and Wing Trailing-Edge Flap Deflected +10°, Mach = .6

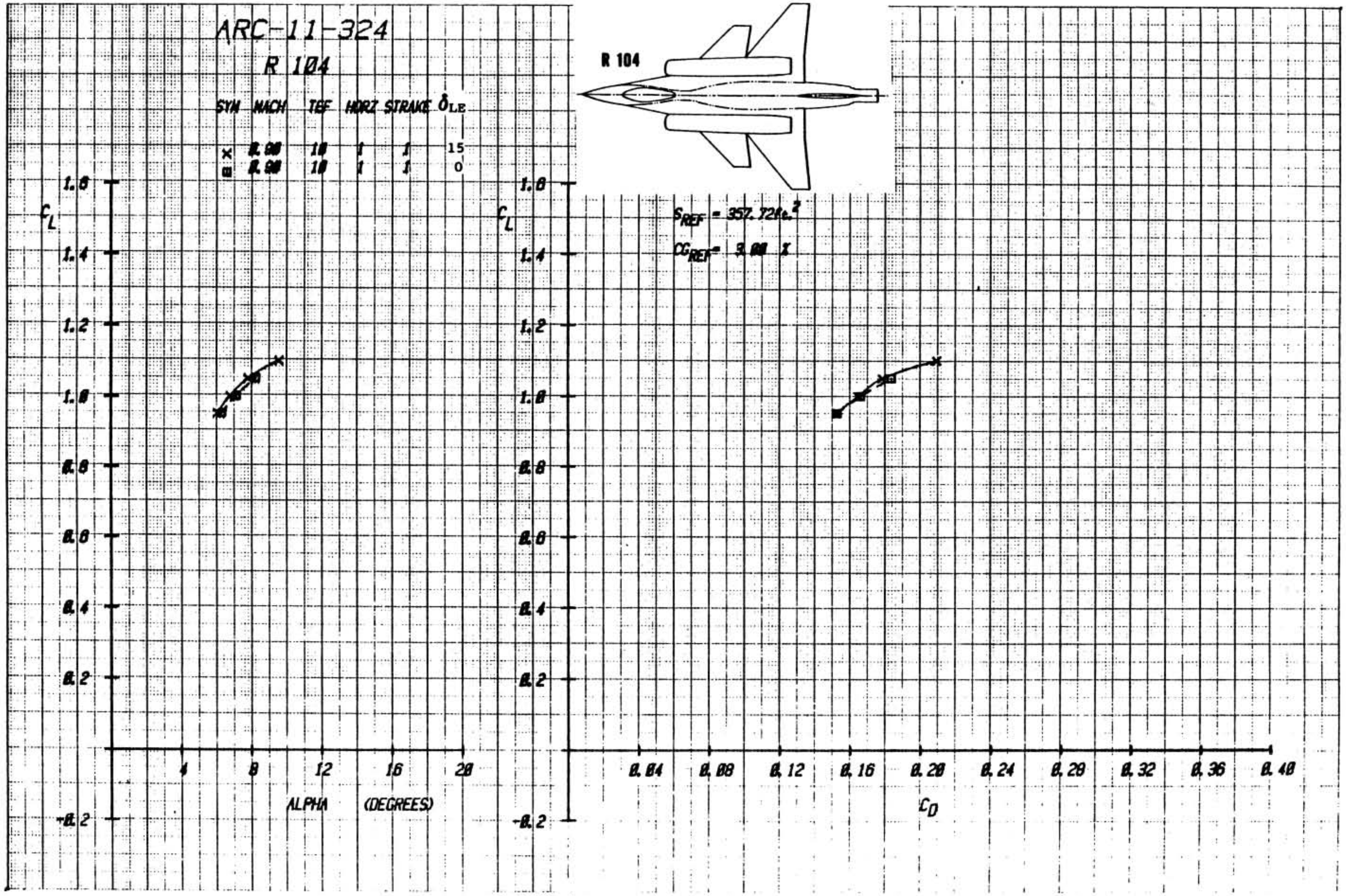

Figure 1-80 Trimmed Lift and Drag With Canard Leading-Edge Flap Deflected and Wing Trailing-Edge Flap Deflected +10°, Mach = .9

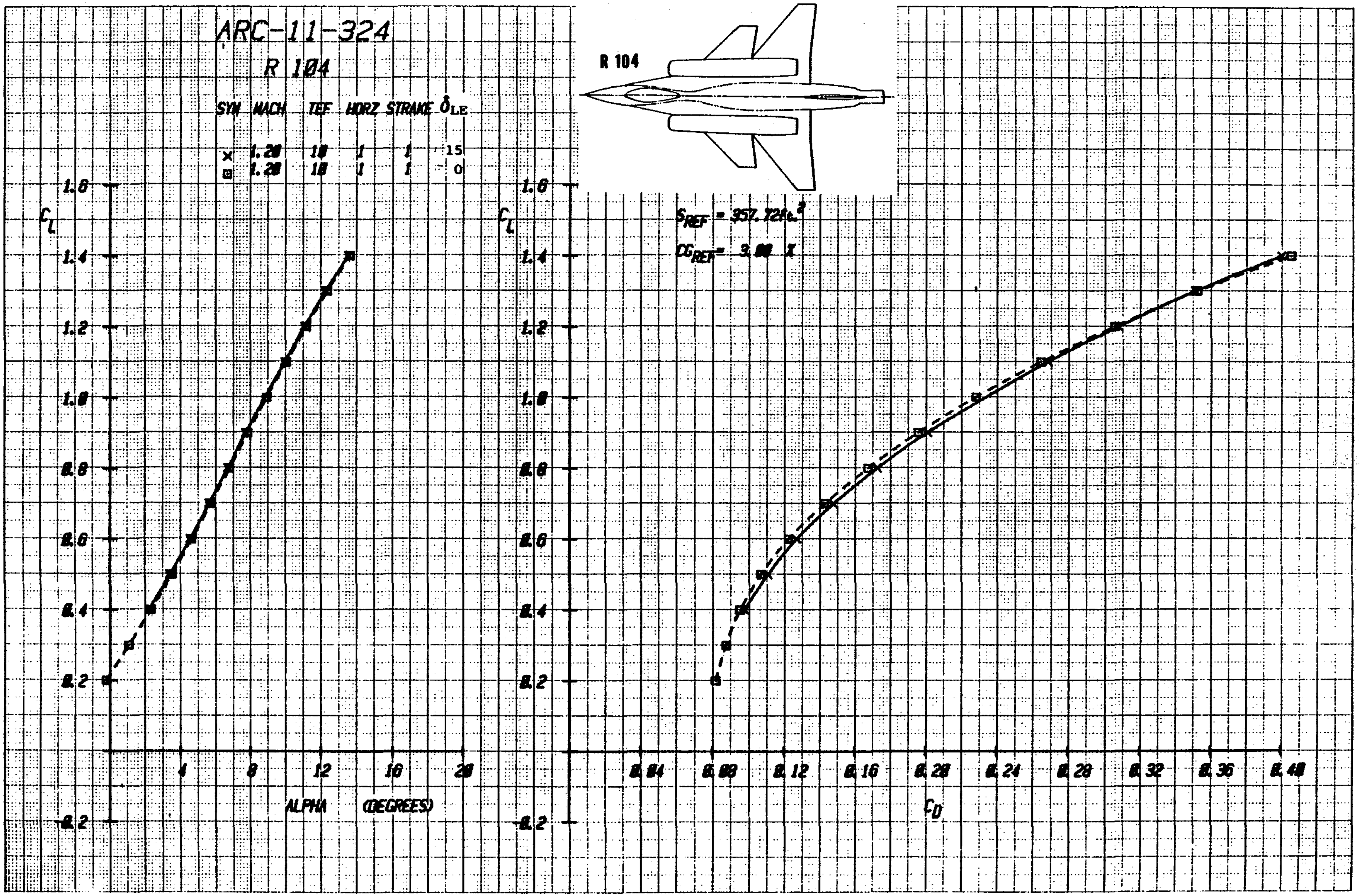

Figure 1-81 Trimmed Lift and Drag With Canard Leading-Edge Flap Deflected and Wing Trailing-Edge Deflected +10°, Mach = 1.2

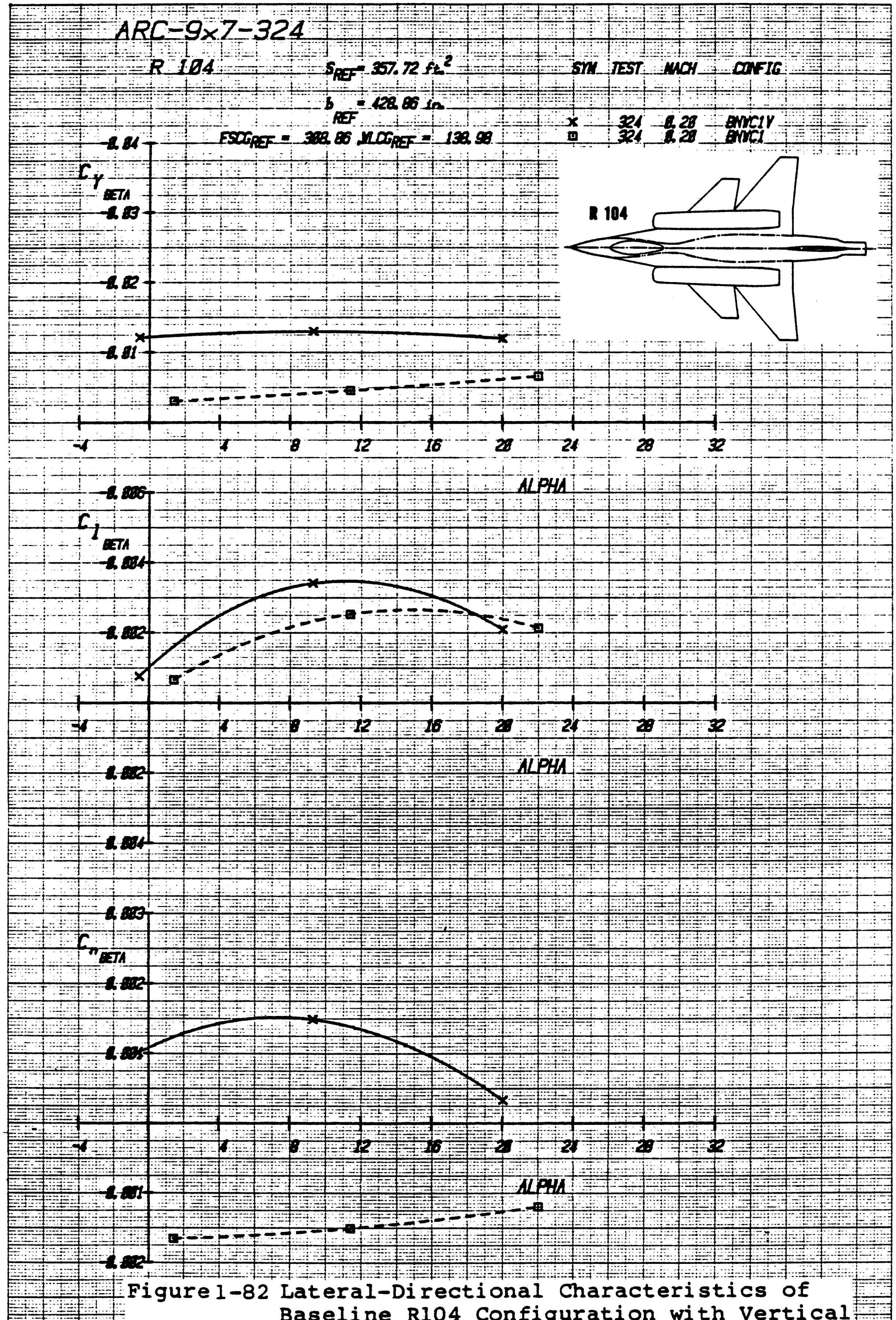

Figure 1-82 Lateral-Directional Characteristics of Baseline R104 Configuration with Vertical Tail On and Off, Mach = .2.

ARC-12-327

R104

Sidewash Gradient

M = 0.2

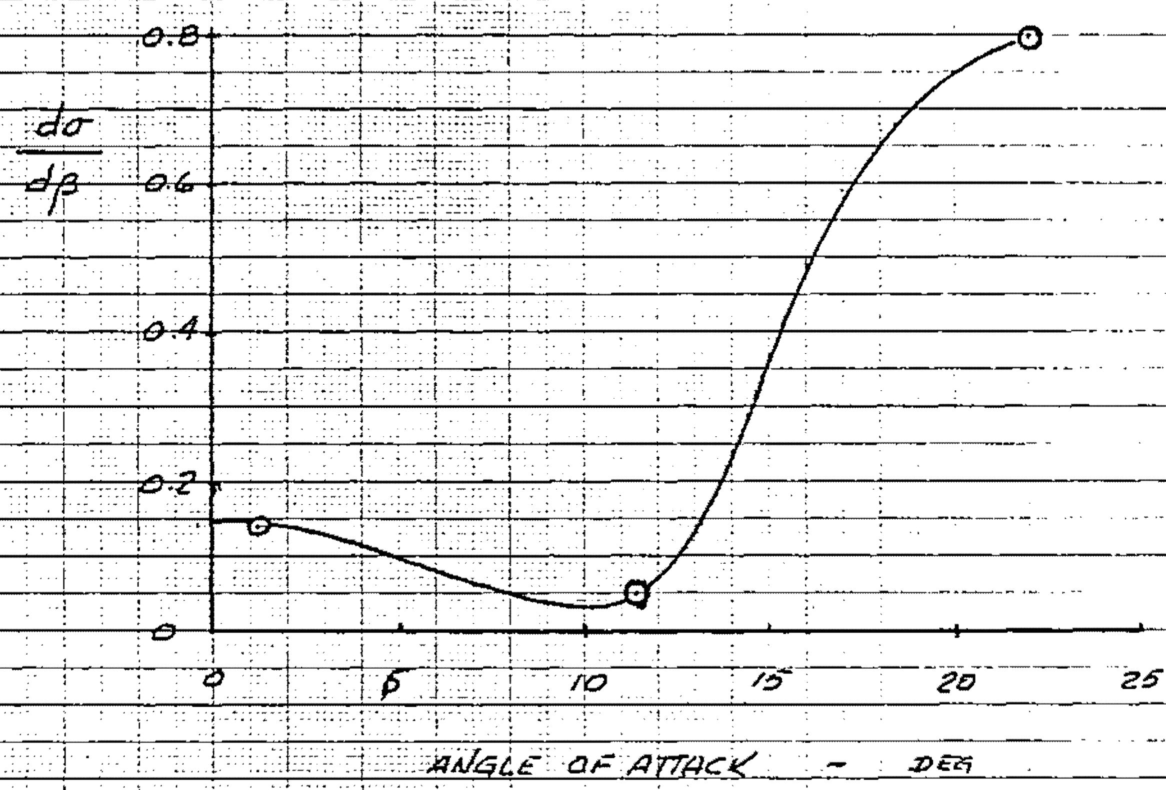

Figure 1-83 Sidewash Gradient Variation with Angle of Attack for Baseline R104 Model Configuration, M = .2

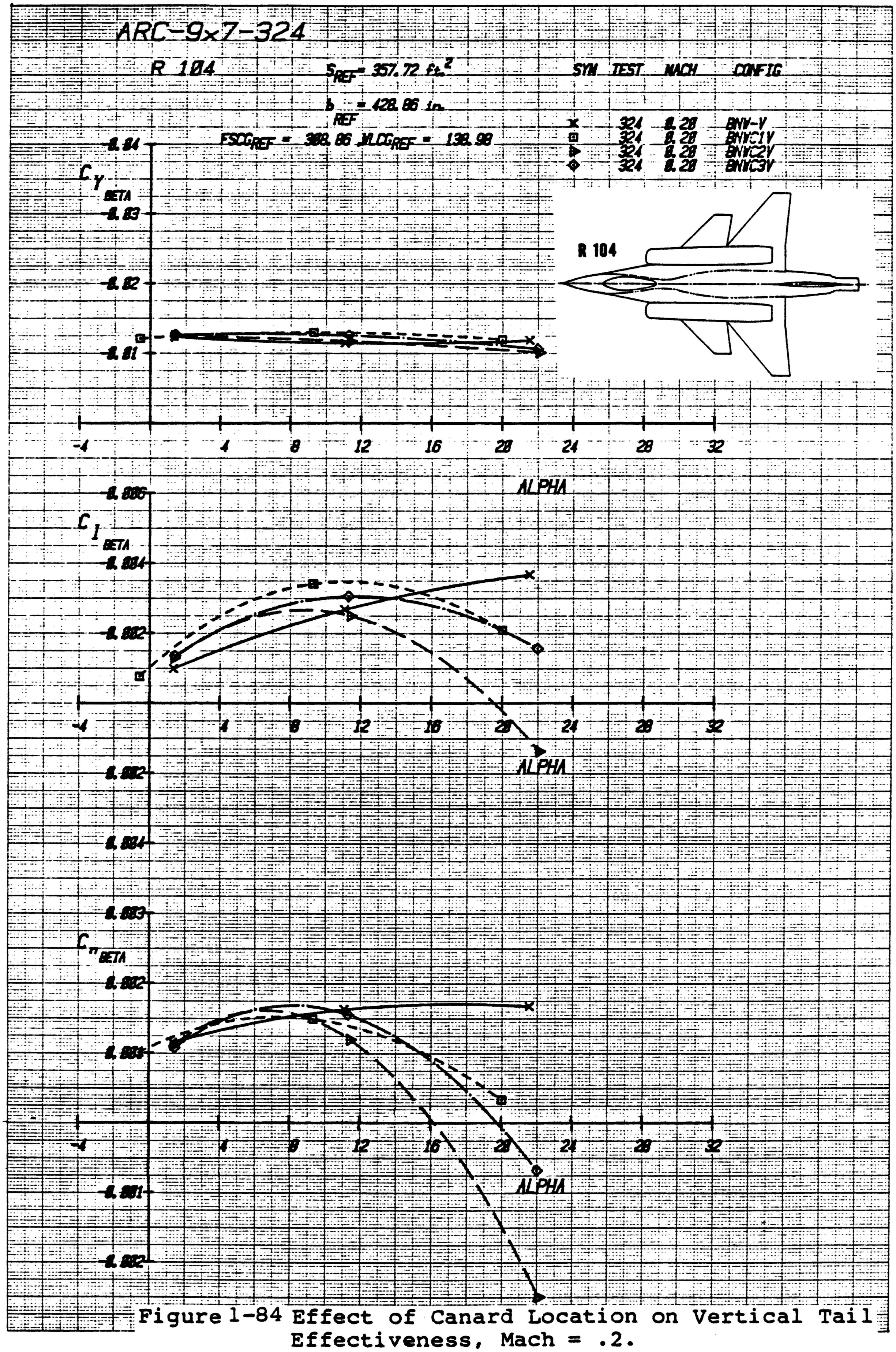

Figure 1-84 Effect of Canard Location on Vertical Tail Effectiveness, Mach = .2.

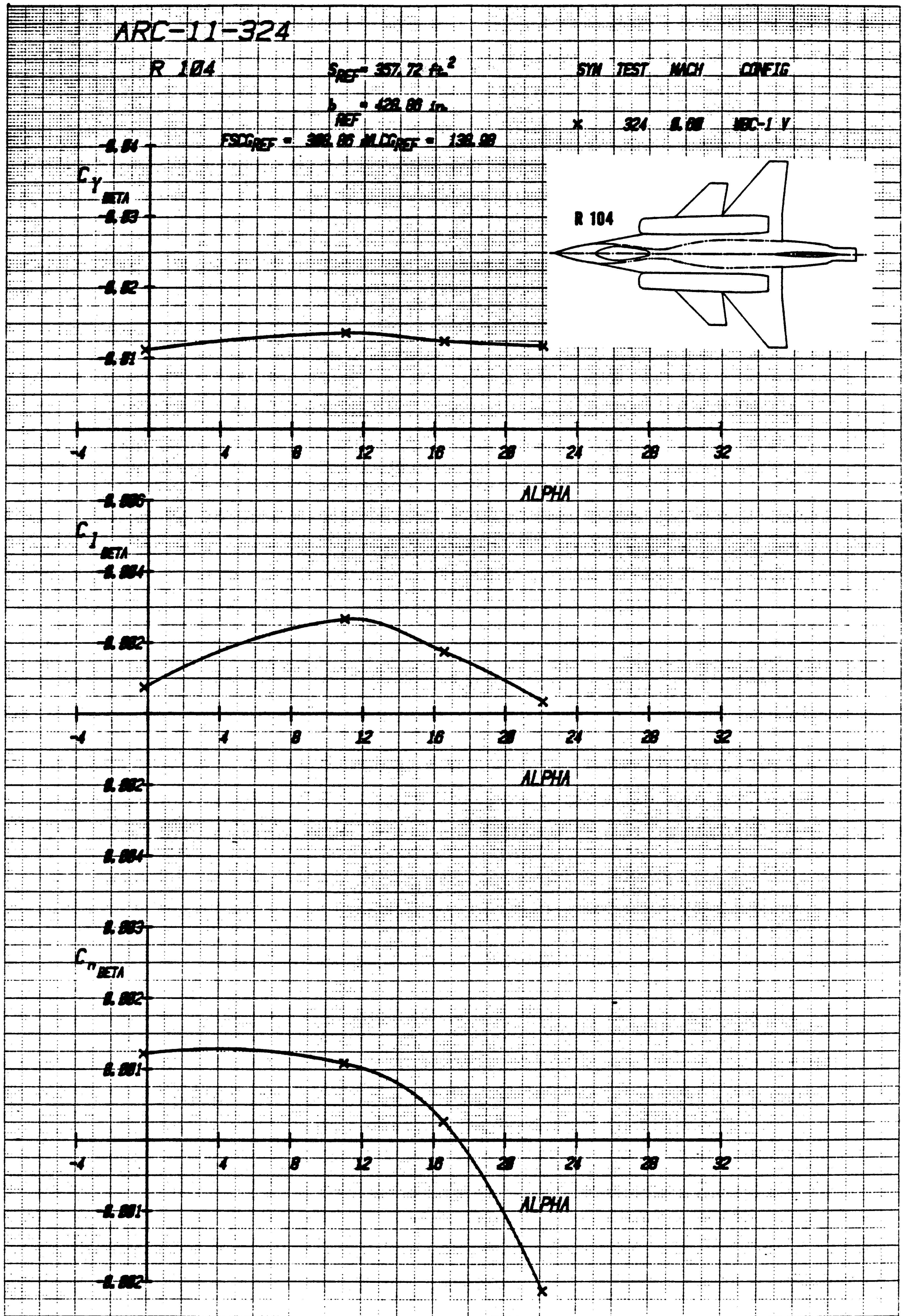

Figure 1-85 Lateral-Directional Characteristics of Baseline R104 Model Configuration, M = .6

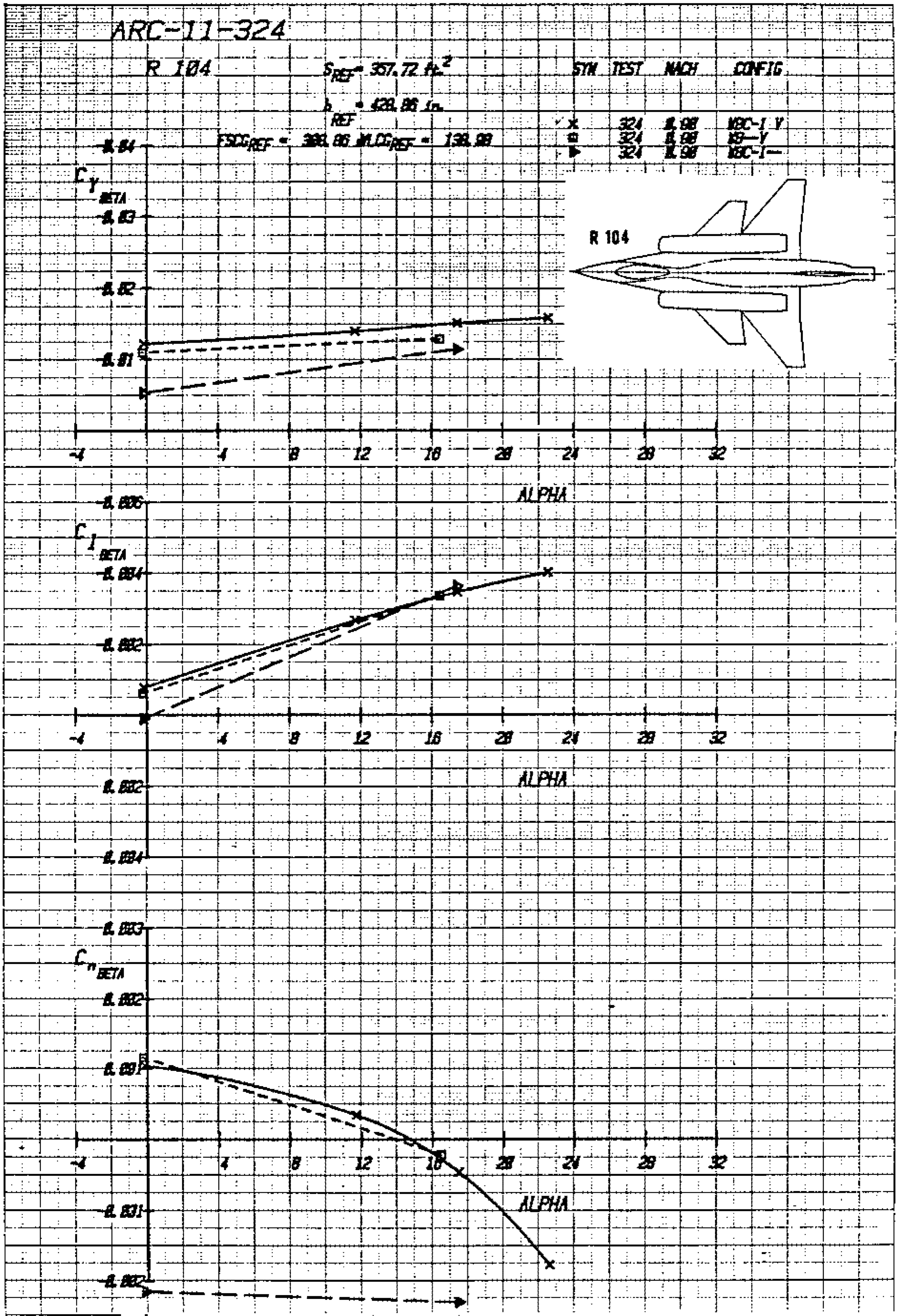

Figure 1-86 Comparison of Lateral-Directional Characteristics of Baseline R104 Model Configuration, with Canard Removed, and with Vertical Tail Removed, M = .9

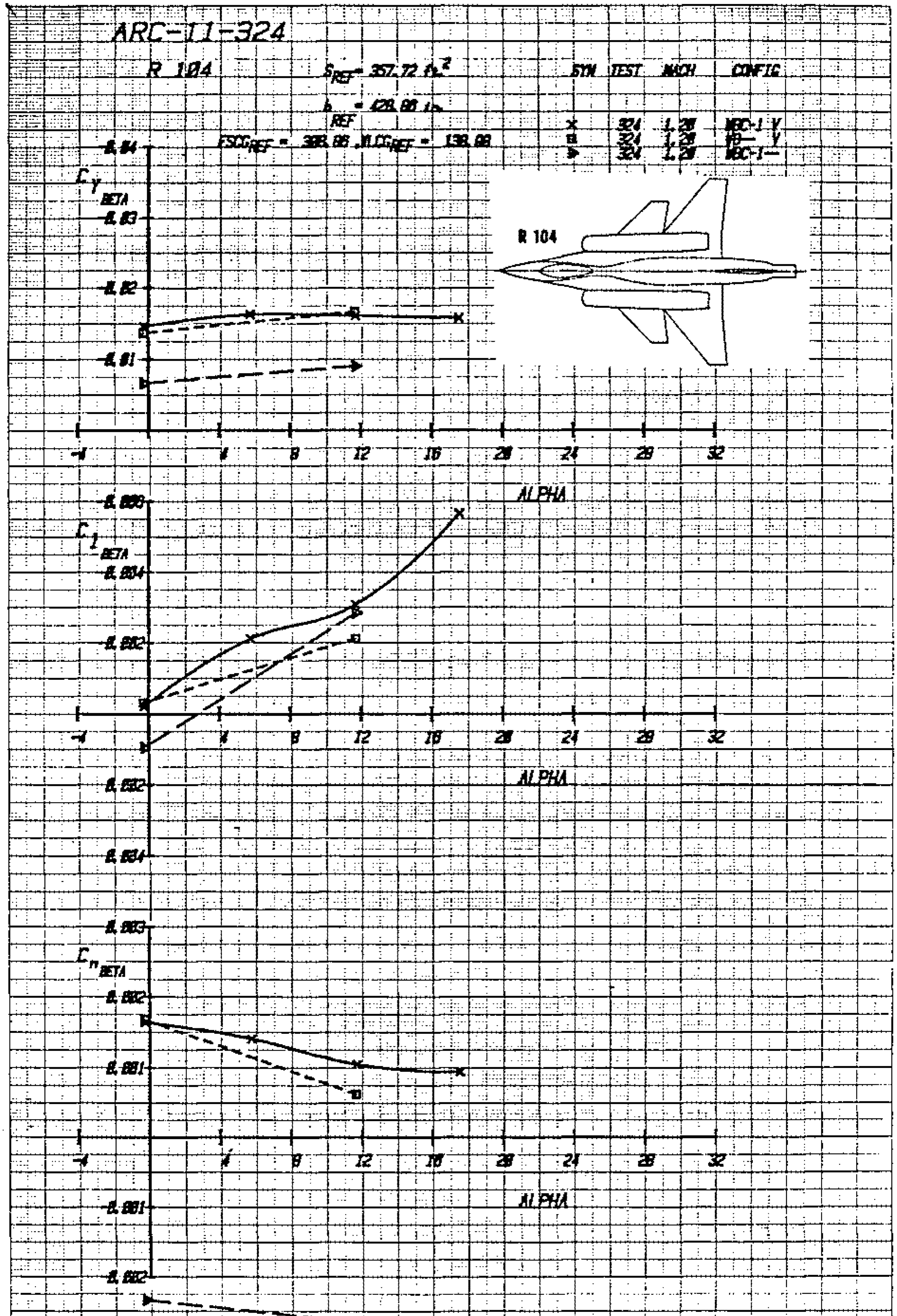

Figure 1-87 Comparison of Lateral-Directional Characteristics of Baseline R104 Model Configuration, with Canard Removed, and with Vertical Tail Removed, M = 1.2

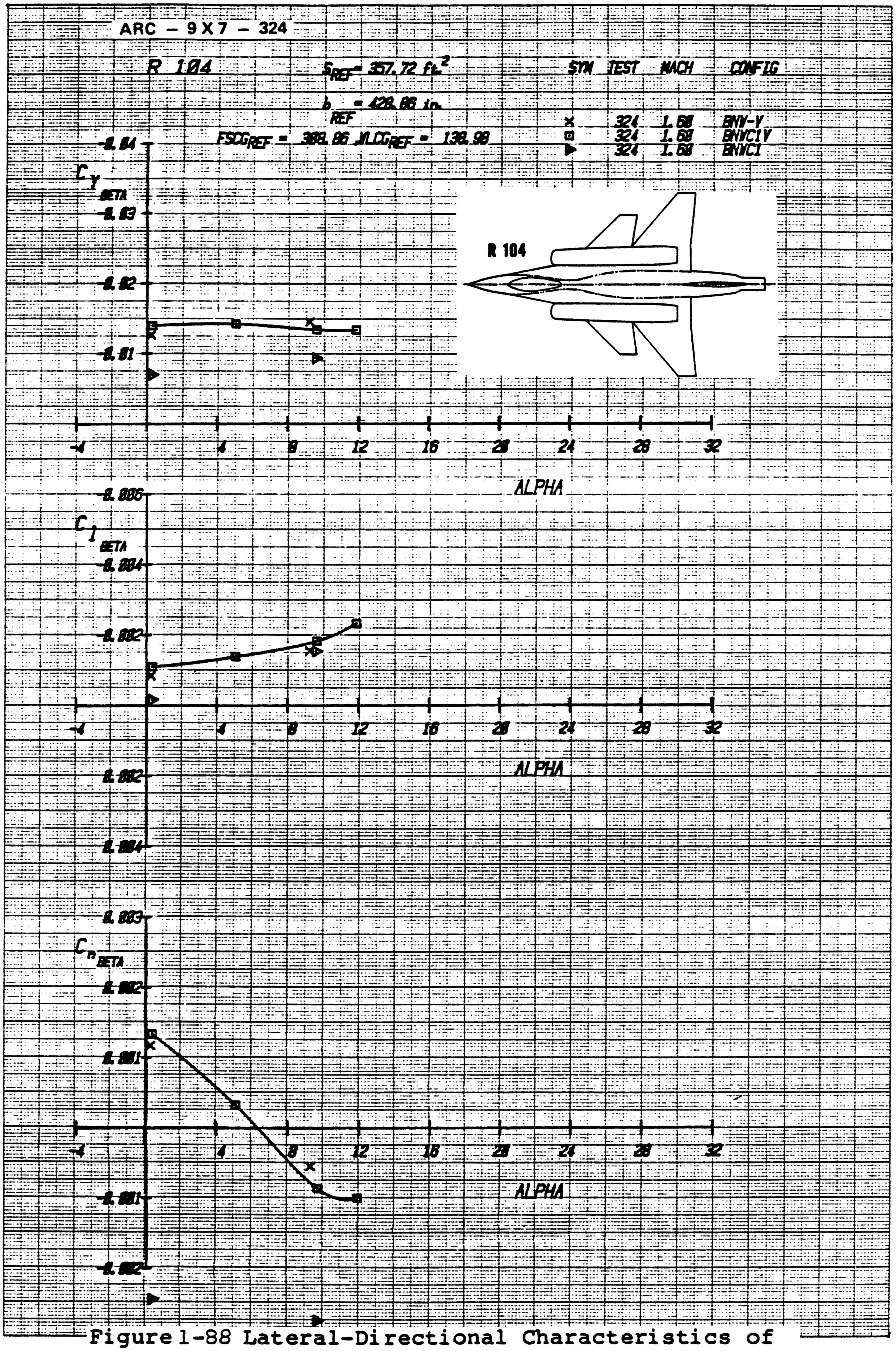

Figure 1-88 Lateral-Directional Characteristics of Baseline R104 Configuration, Mach = 1.6.

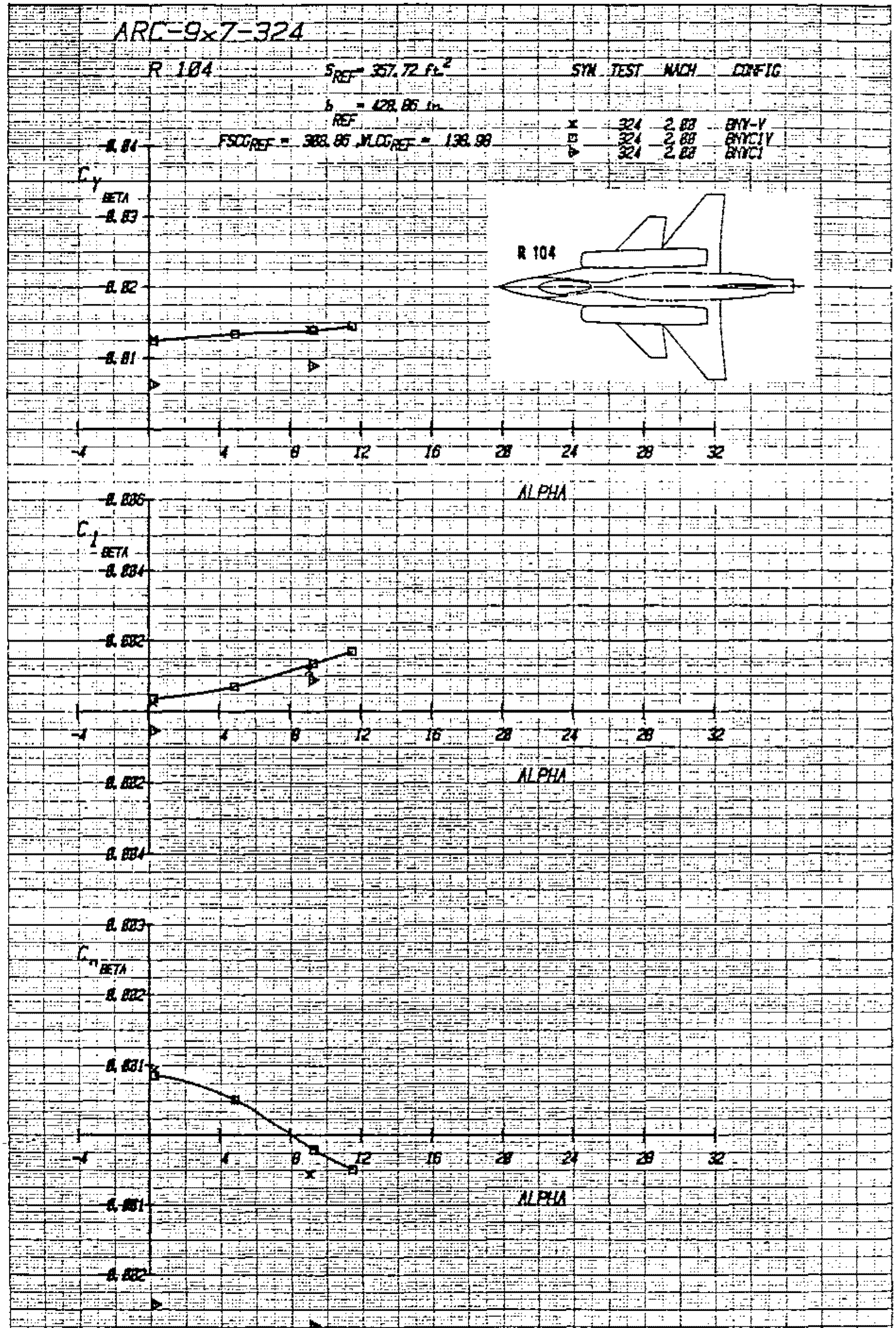

Figure 1-89 Lateral-Directional Characteristics of Baseline R104 Configurations, Mach = 2.0.

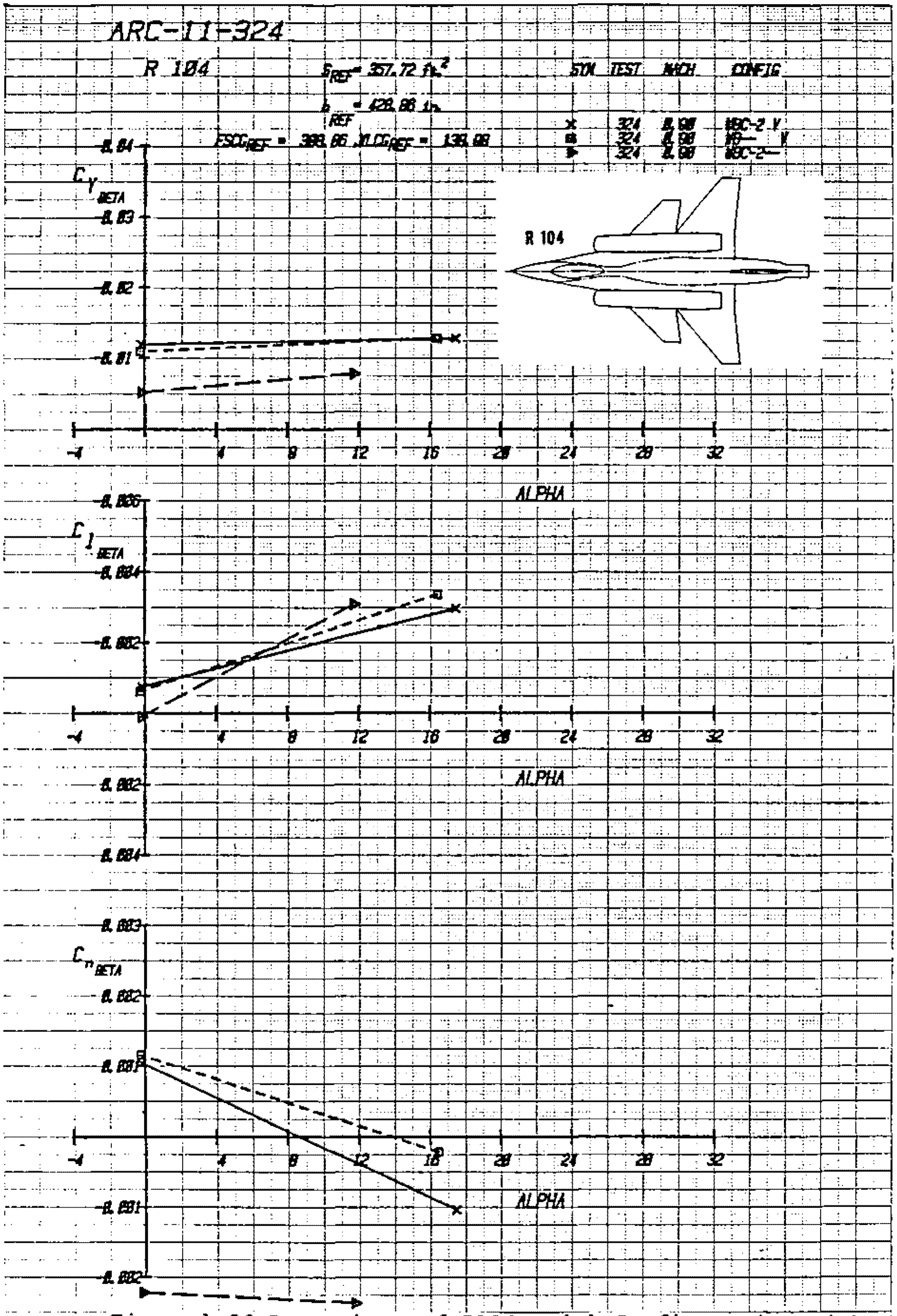

Figure 1-90 Comparison of R104 Model Configuration with Canard in Forward Location C_2, with Canard Removed, and with Vertical Tail Removed, M = .9

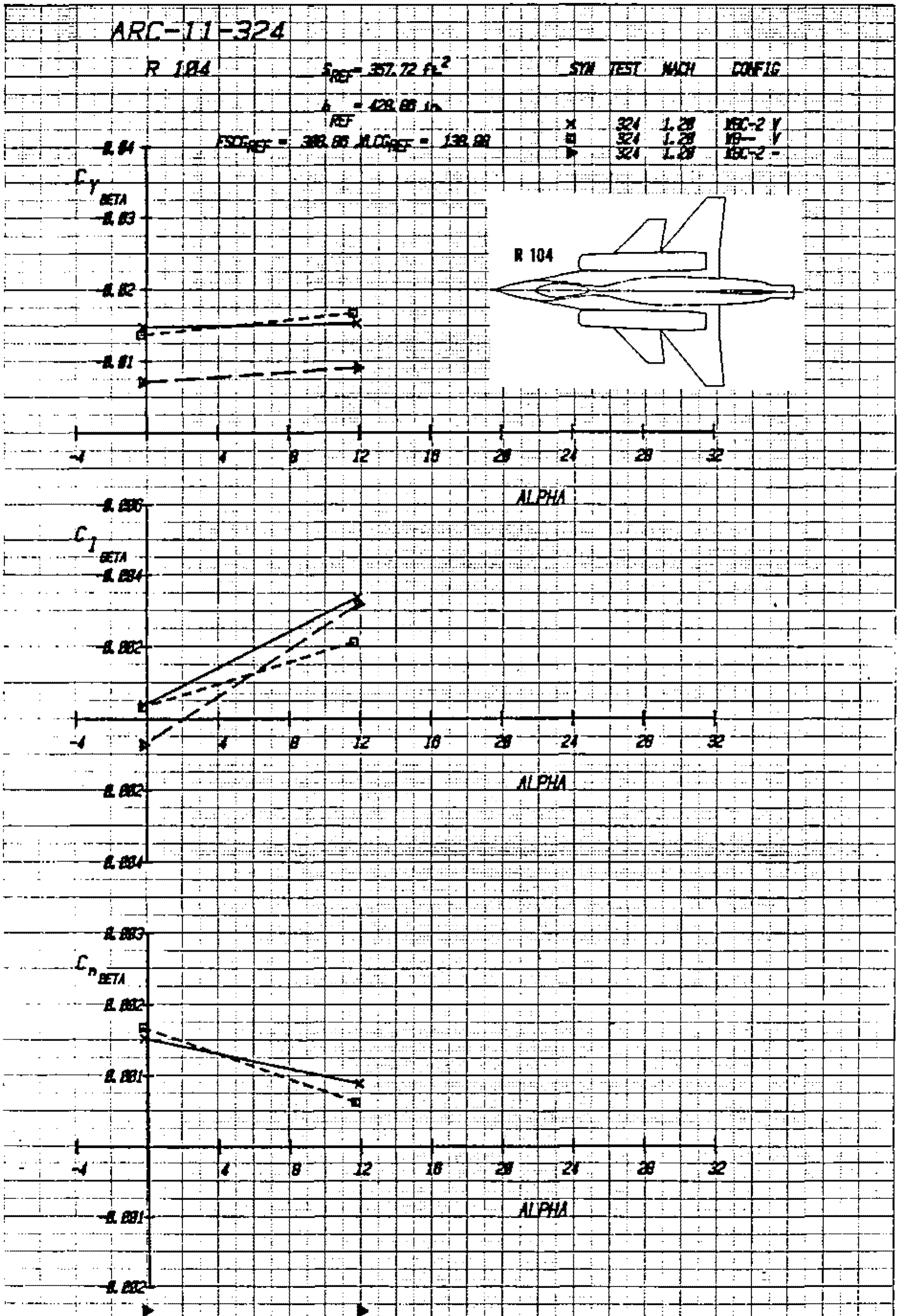

Figure 1-91 Comparison of R104 Model Configuration with Canard in Forward Location C_2, with Canard Removed, and with Vertical Tail Removed, M = 1.2

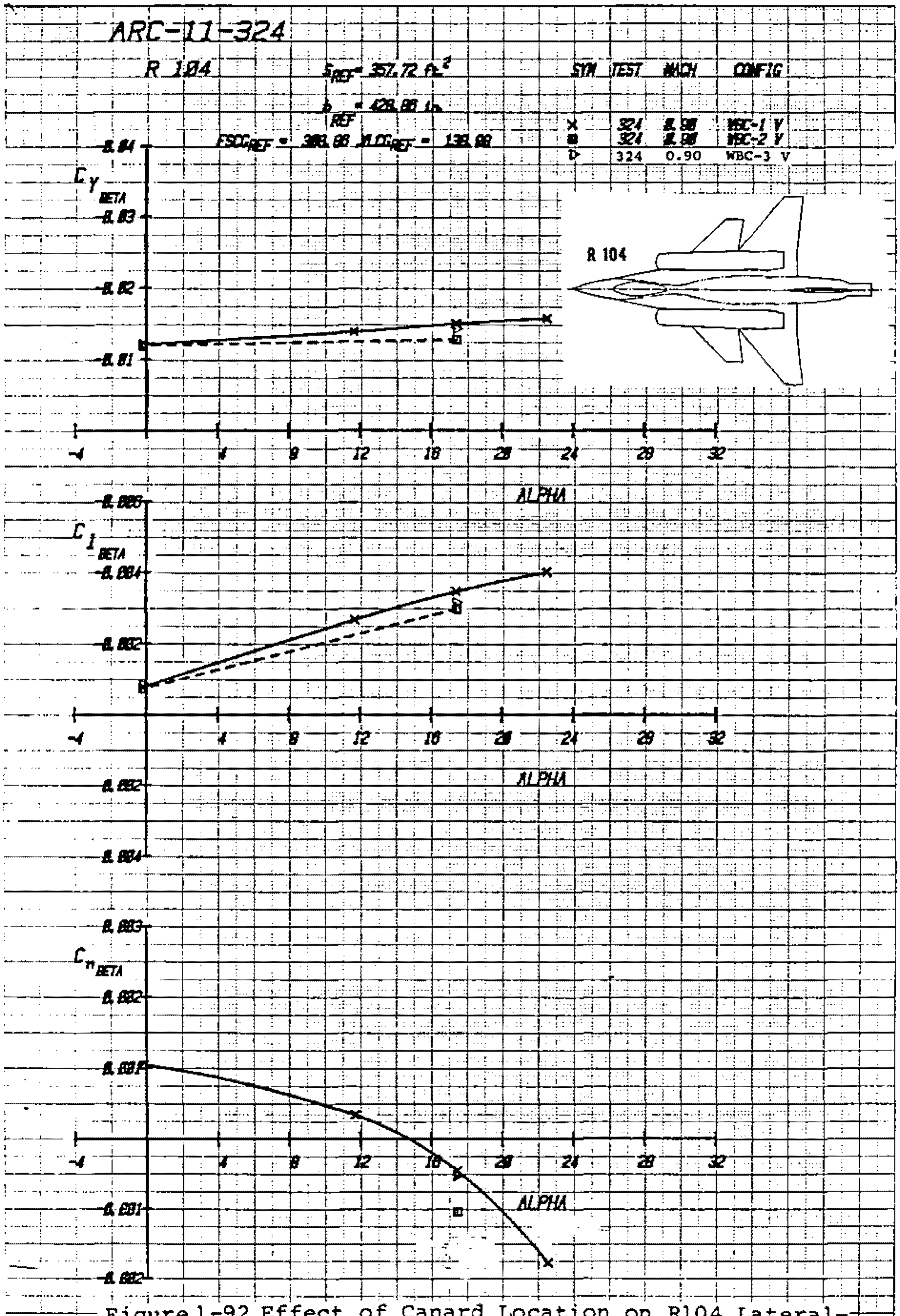

Figure 1-92 Effect of Canard Location on R104 Lateral-Directional Characteristics, M = .9

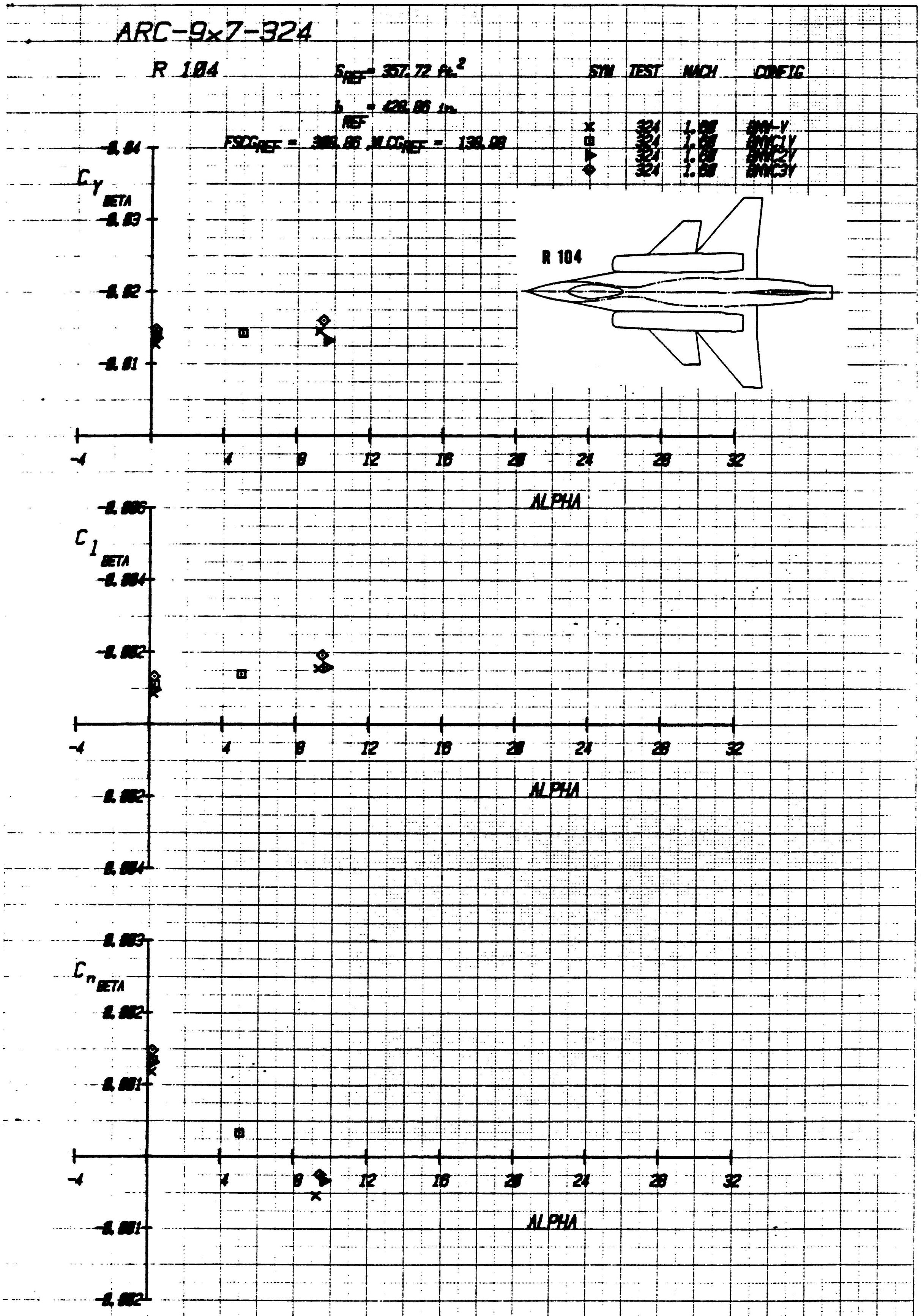

Figure 1-93 Effect of Canard Location on Vertical Tail Effectiveness, Mach = 1.6.

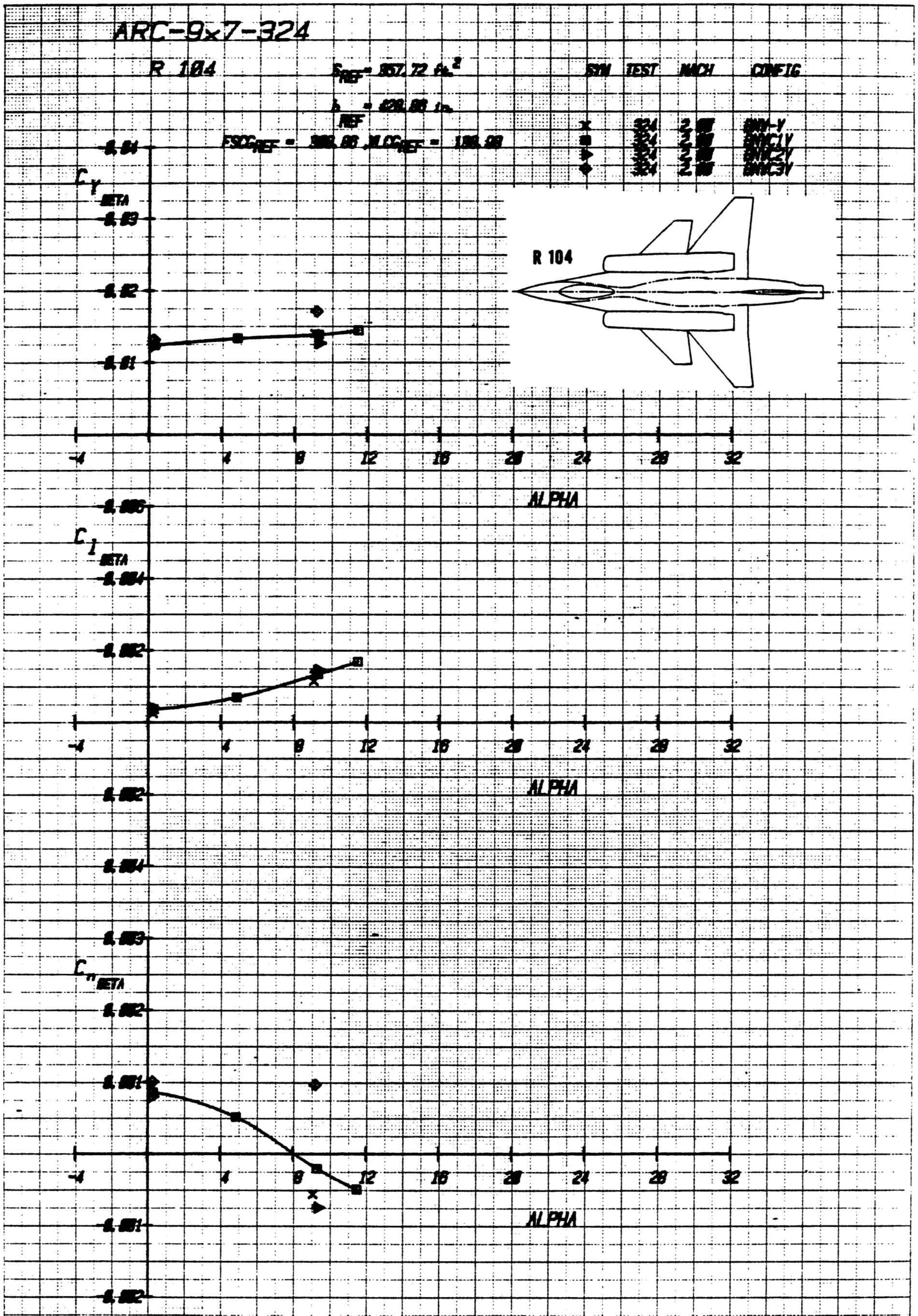

Figure 1-94 Effect of Canard Location on Vertical Tail Effectiveness, Mach = 2.0.

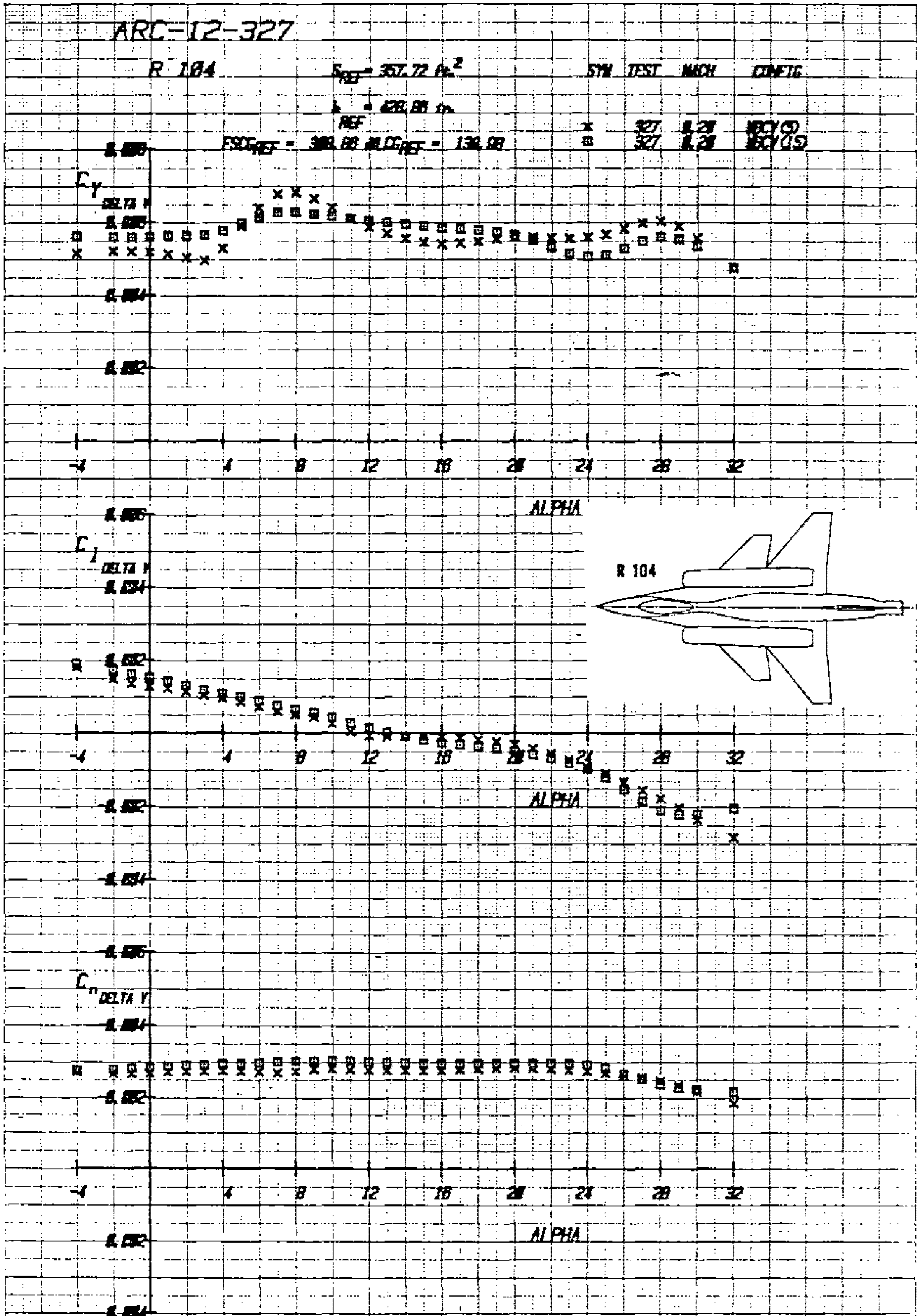

Figure 1-95 Directional Control Effectiveness for Baseline R104 Configuration With δ_{VT} at +5° and +15°, Mach = .2.

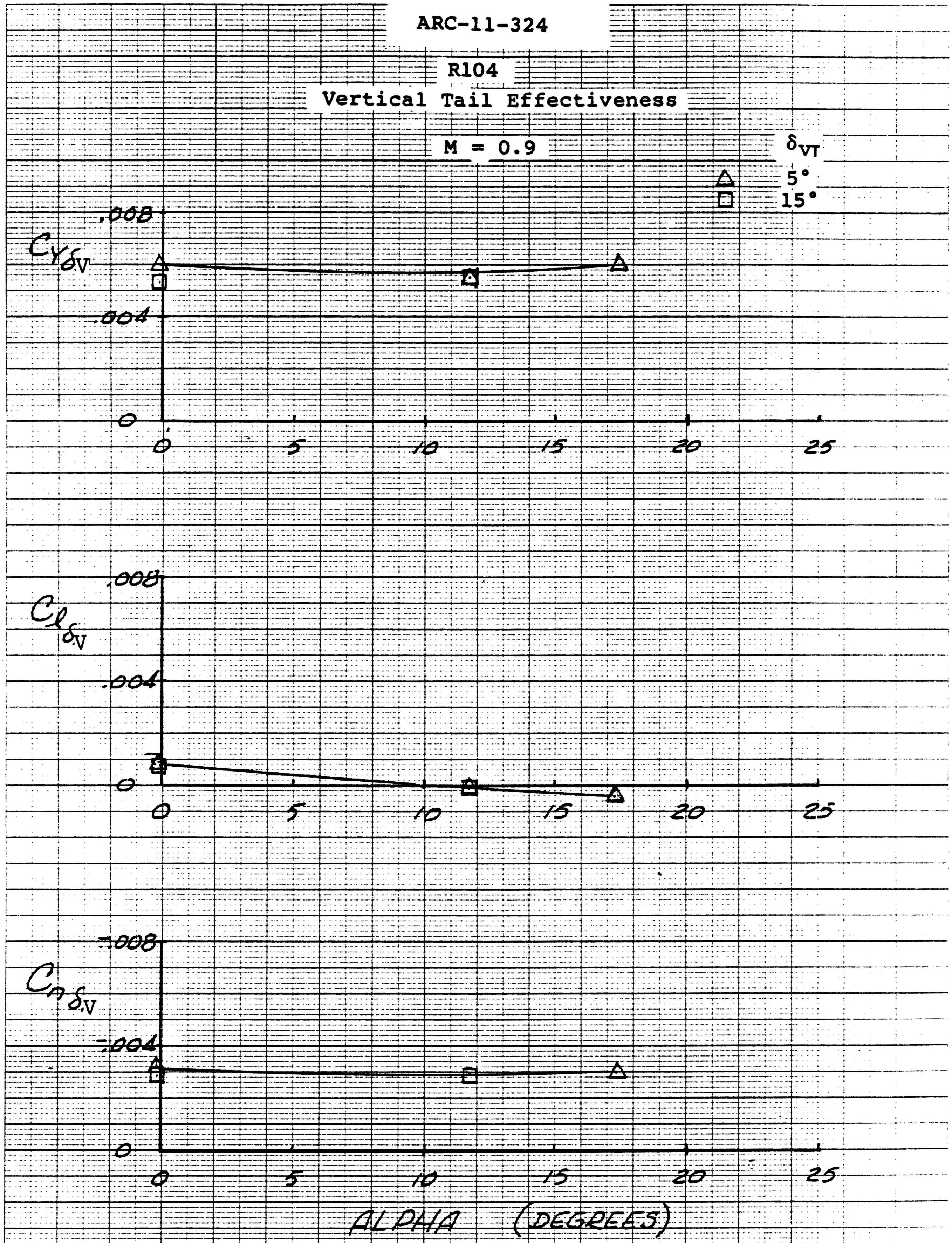

Figure 1-96 Variation in Vertical Tail Effectiveness with Tail Deflection and Angle of Attack, M = .9

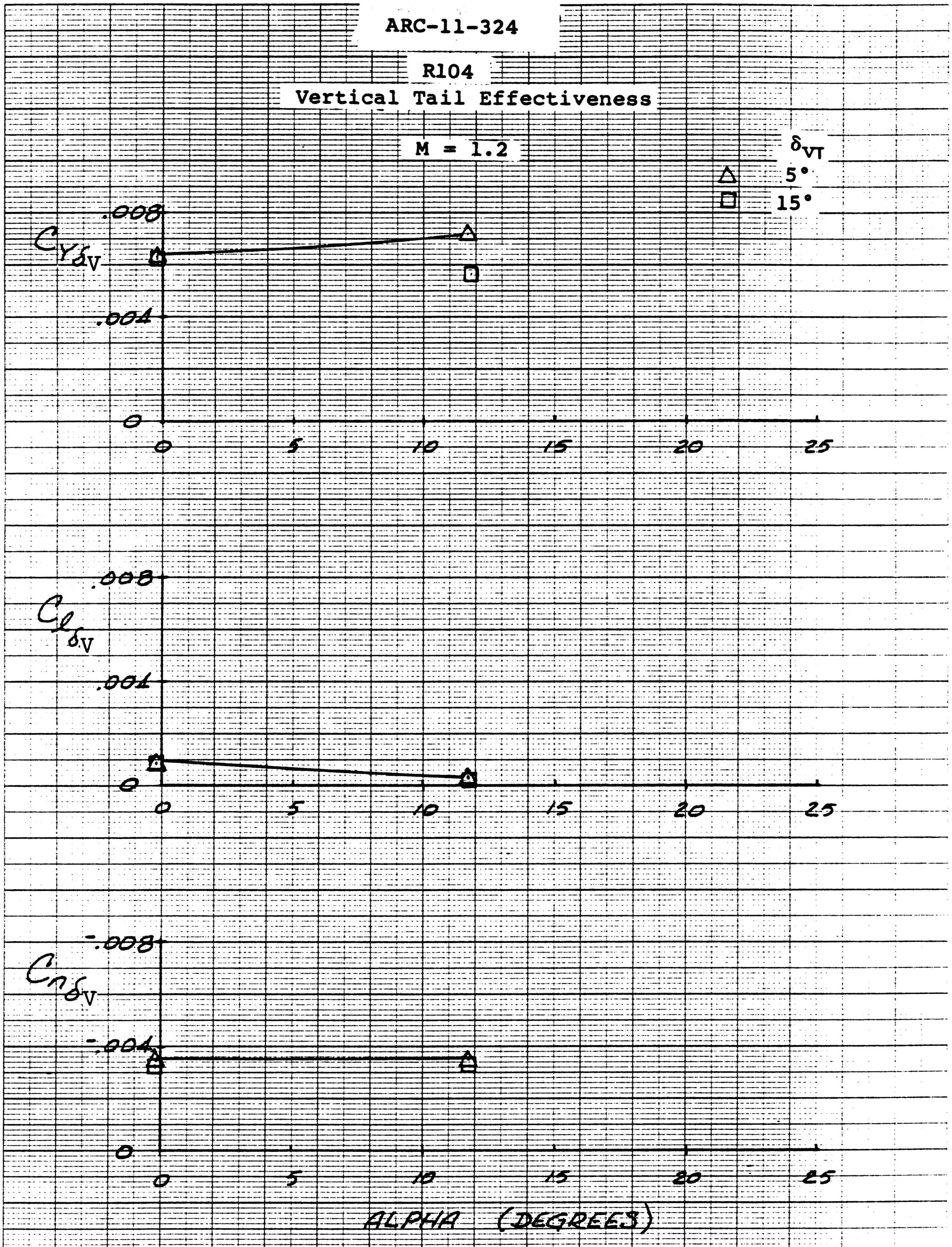

Figure 1-97 Variation in Vertical Tail Effectiveness with Tail Deflection and Angle of Attack, M = 1.2

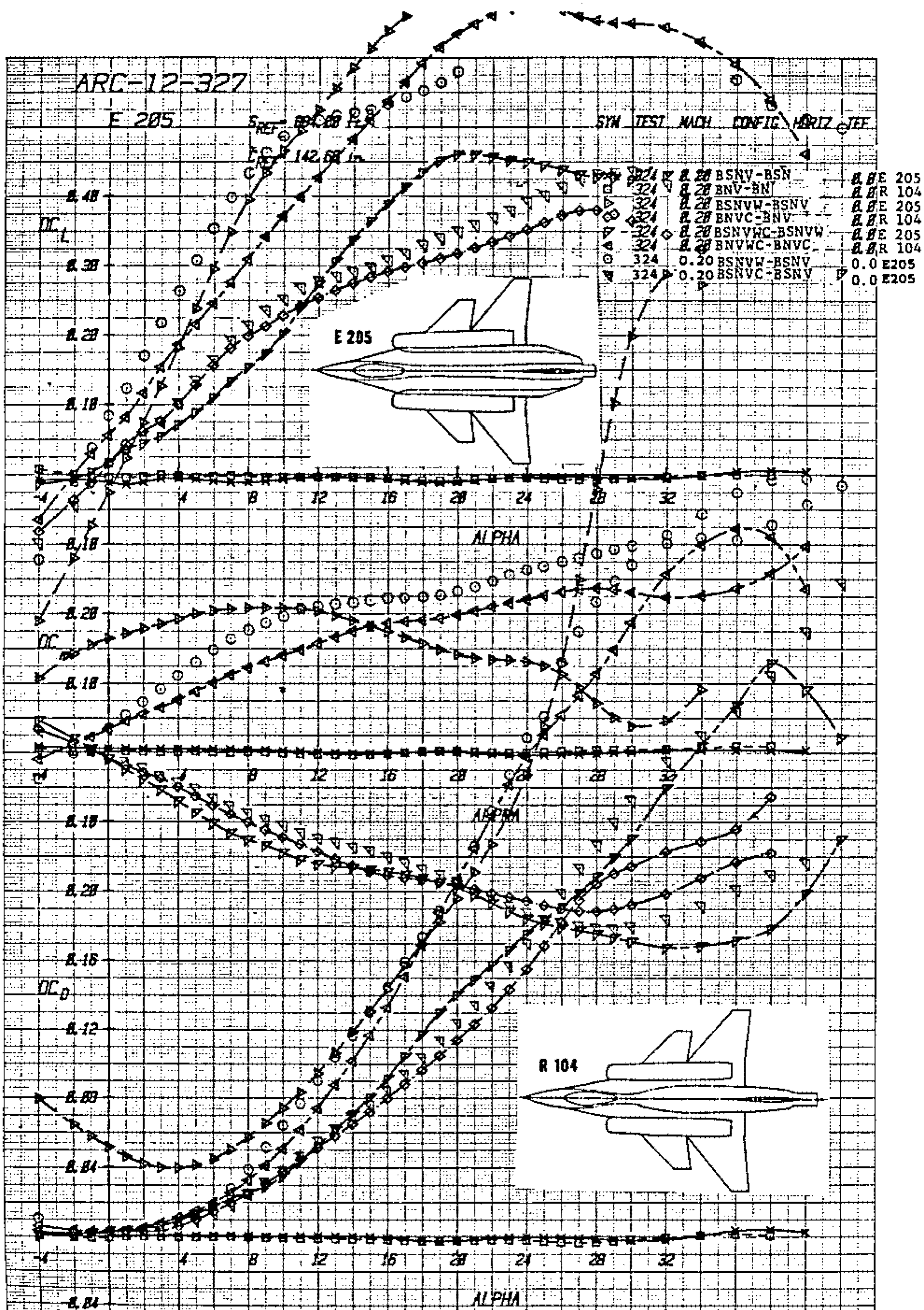

Figure 2-1 Comparison of E205 and R104 Lift, Drag, and Pitching Moment Increments for Vertical Tail, Wing, and Canard, M = .2

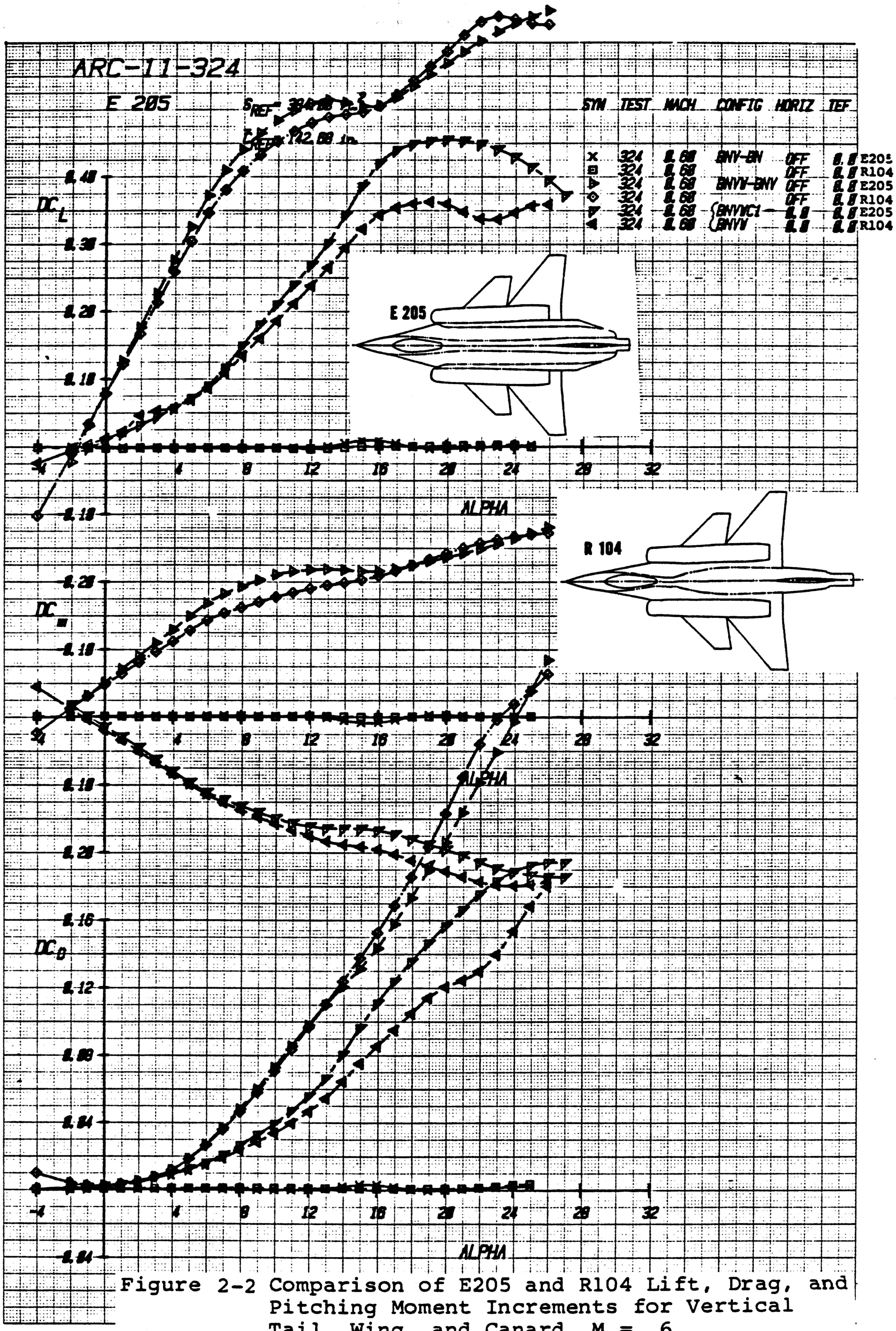

Figure 2-2 Comparison of E205 and R104 Lift, Drag, and Pitching Moment Increments for Vertical Tail, Wing, and Canard, M = .6

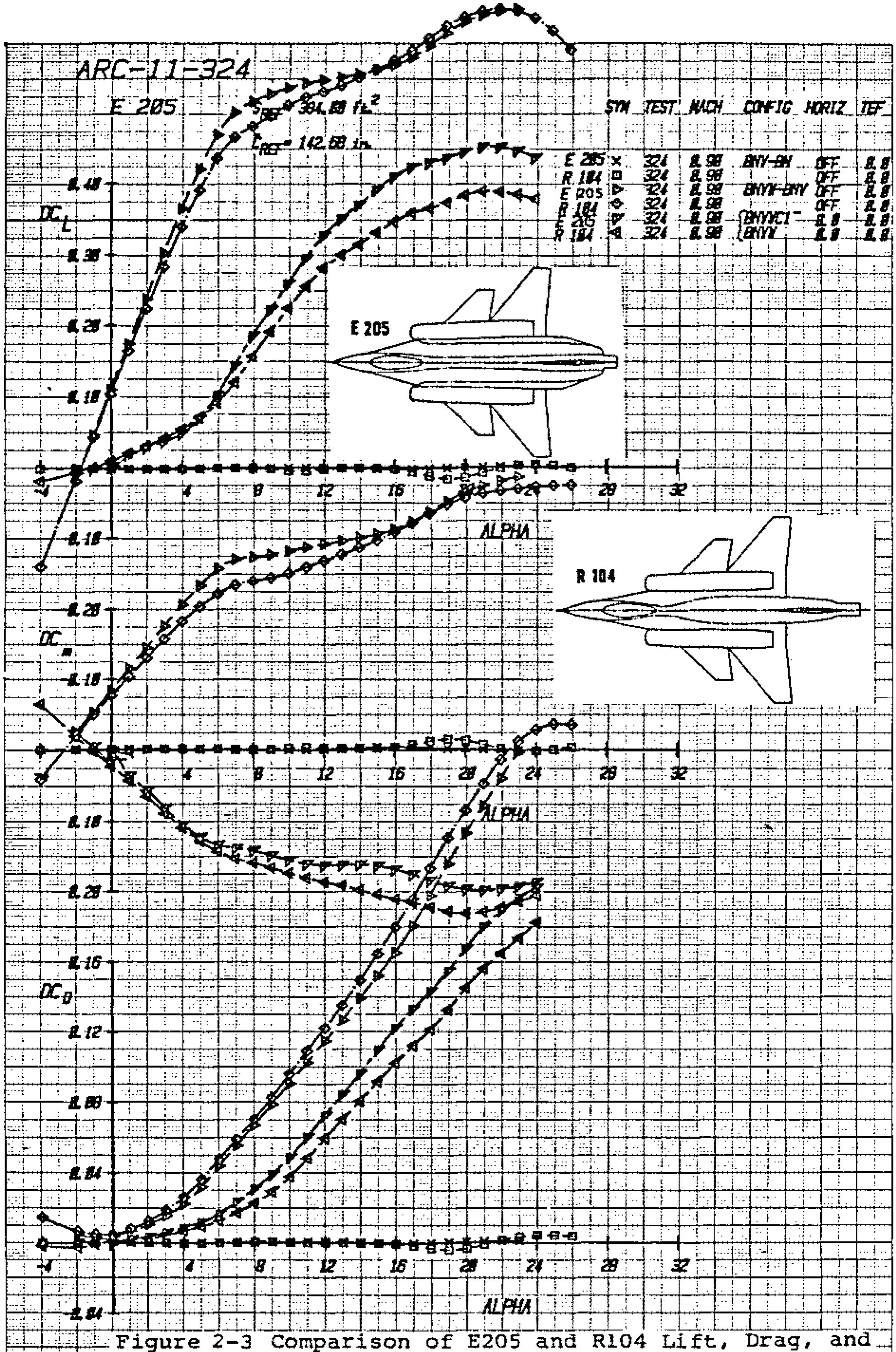

Figure 2-3 Comparison of E205 and R104 Lift, Drag, and Pitching Moment Increments for Vertical Tail, Wing, and Canard, M = .9

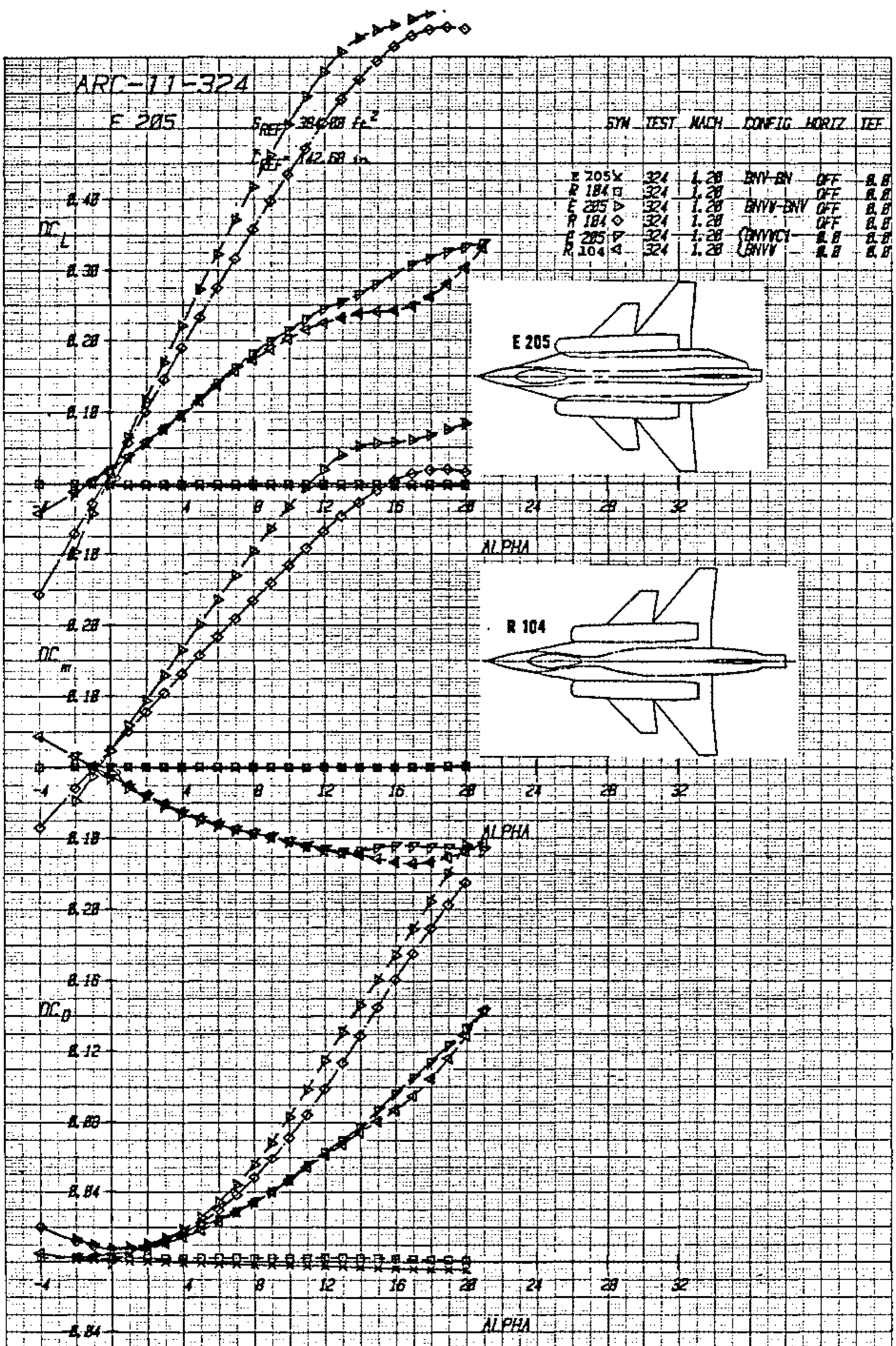

Figure 2-4 Comparison of E205 and R104 Lift, Drag, and Pitching Moment Increments for Vertical Tail, Wing, and Canard, M = 1.2

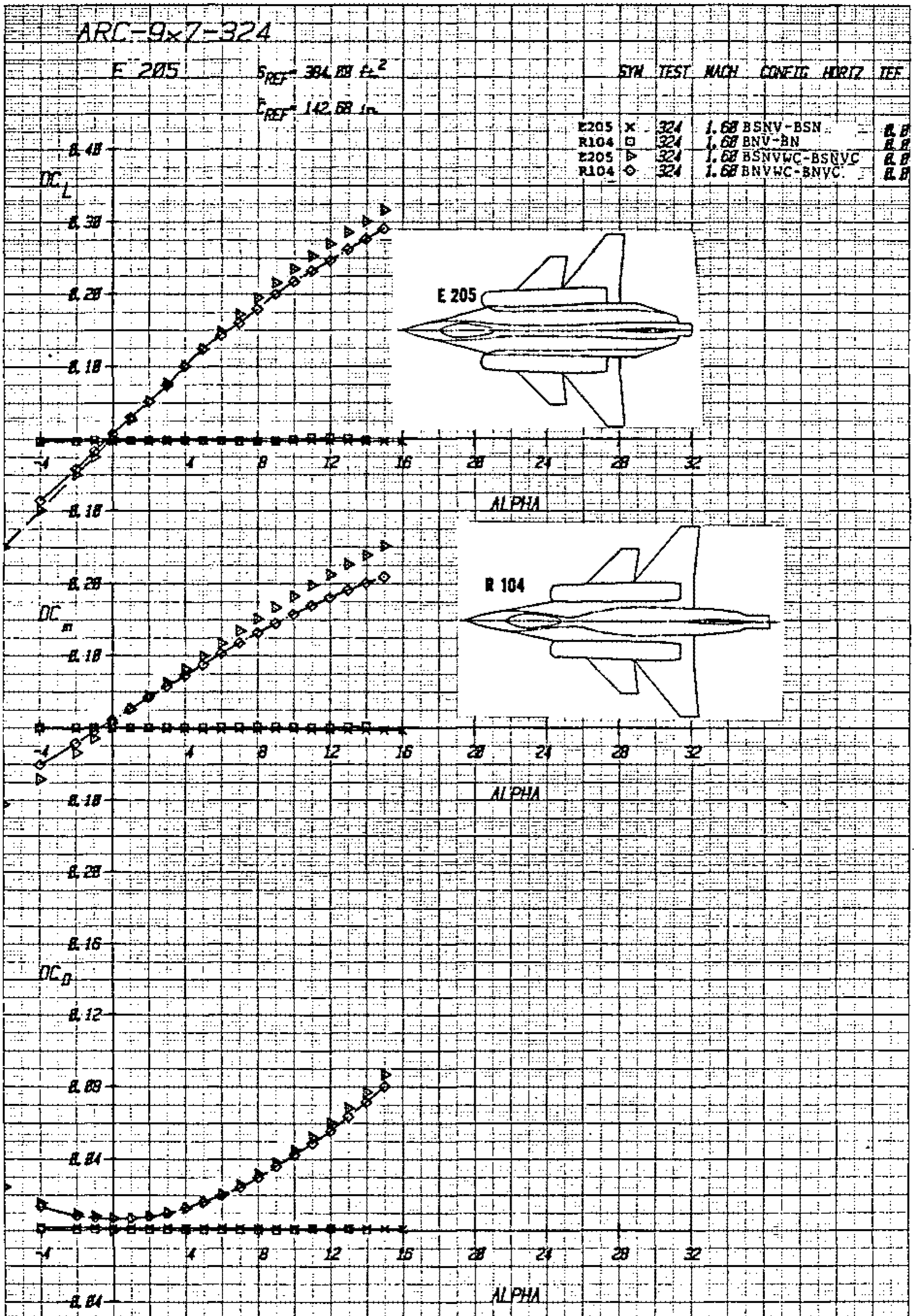

Figure 2-5 Comparison of E205 and R104 Lift, Drag, and Pitching Moment Increments for Vertical Tail, Wing, and Canard, M = 1.6

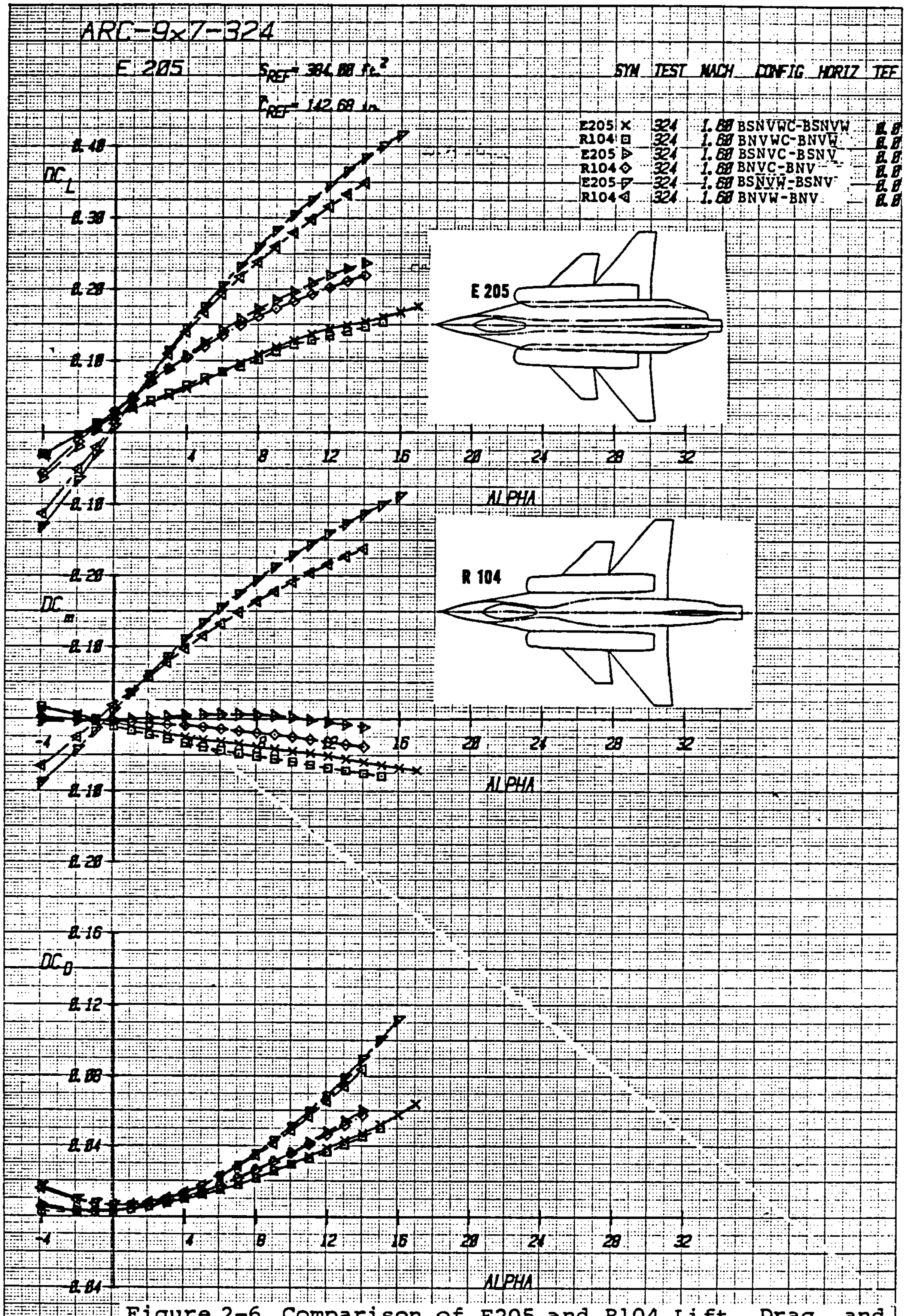

Figure 2-6 Comparison of E205 and R104 Lift, Drag, and Pitching Moment Increments for Vertical Tail, Wing, and Canard (continued), M = 1.6

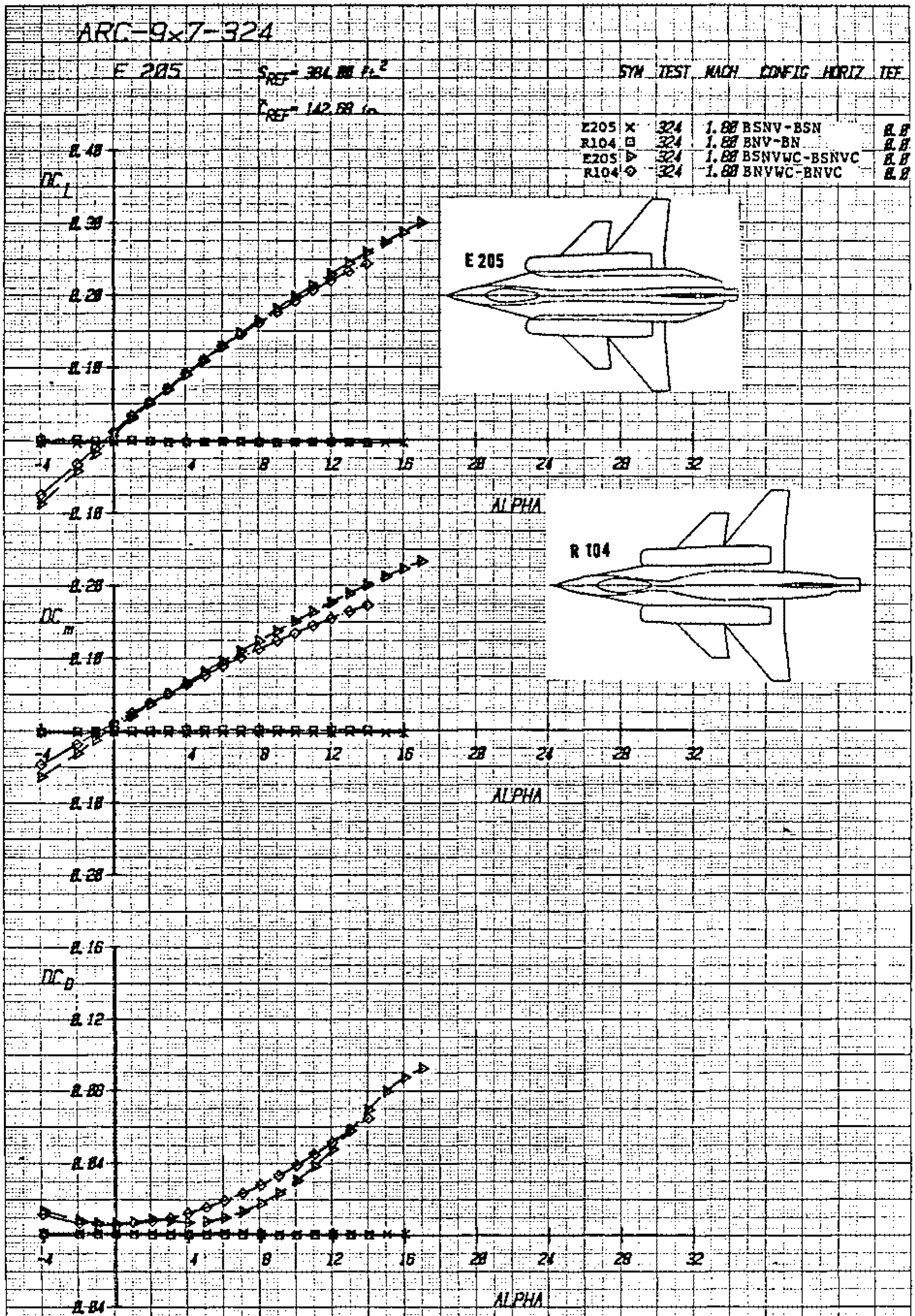

Figure 2-7 Comparison of E205 and R104 Lift, Drag, and Pitching Moment Increments for Vertical Tail, Wing, and Canard, M = 1.8

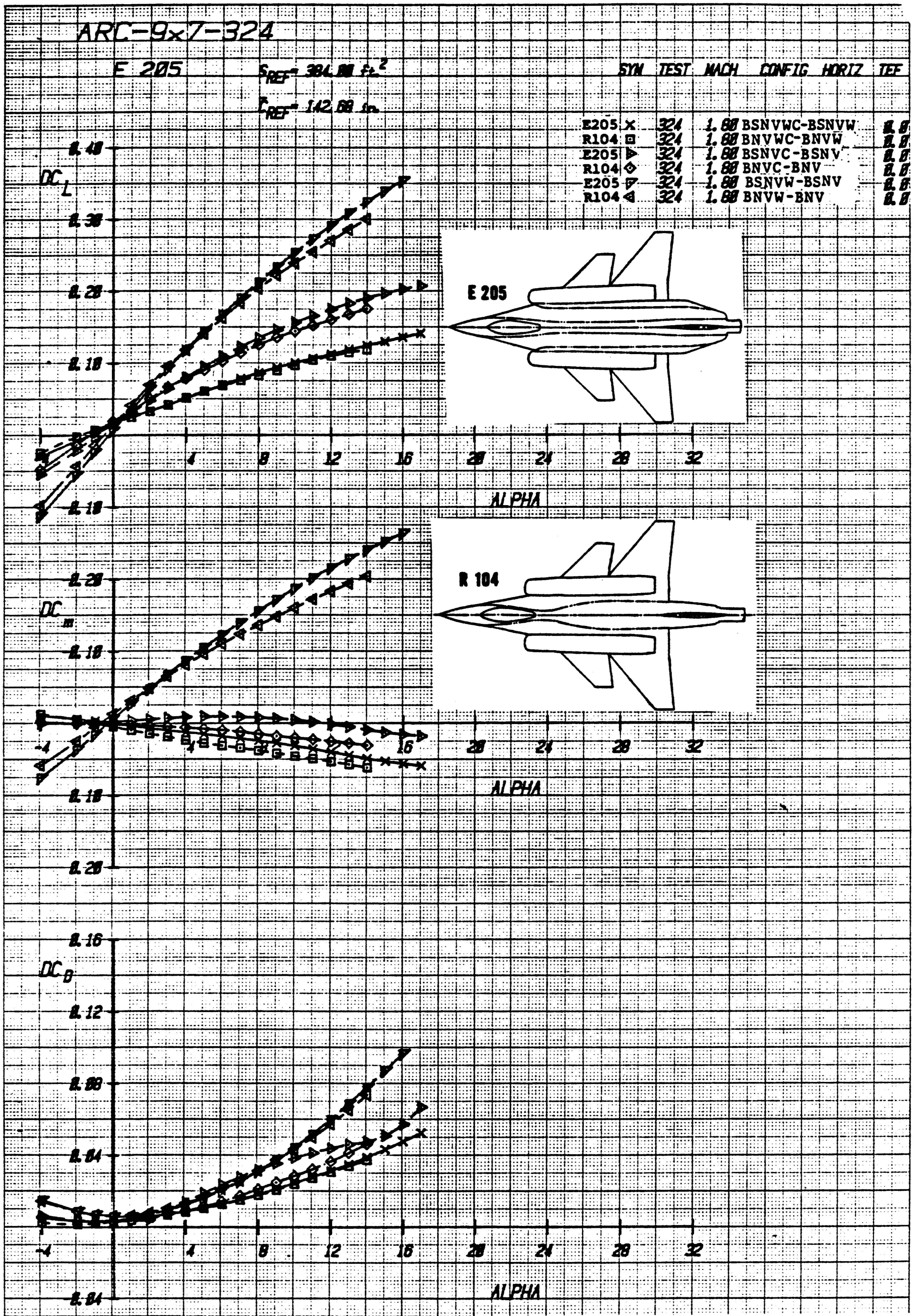

Figure 2-8 Comparison of E205 and R104 Lift, Drag, and Pitching Moment Increments for Vertical Tail, Wing, and Canard (continued), M = 1.8

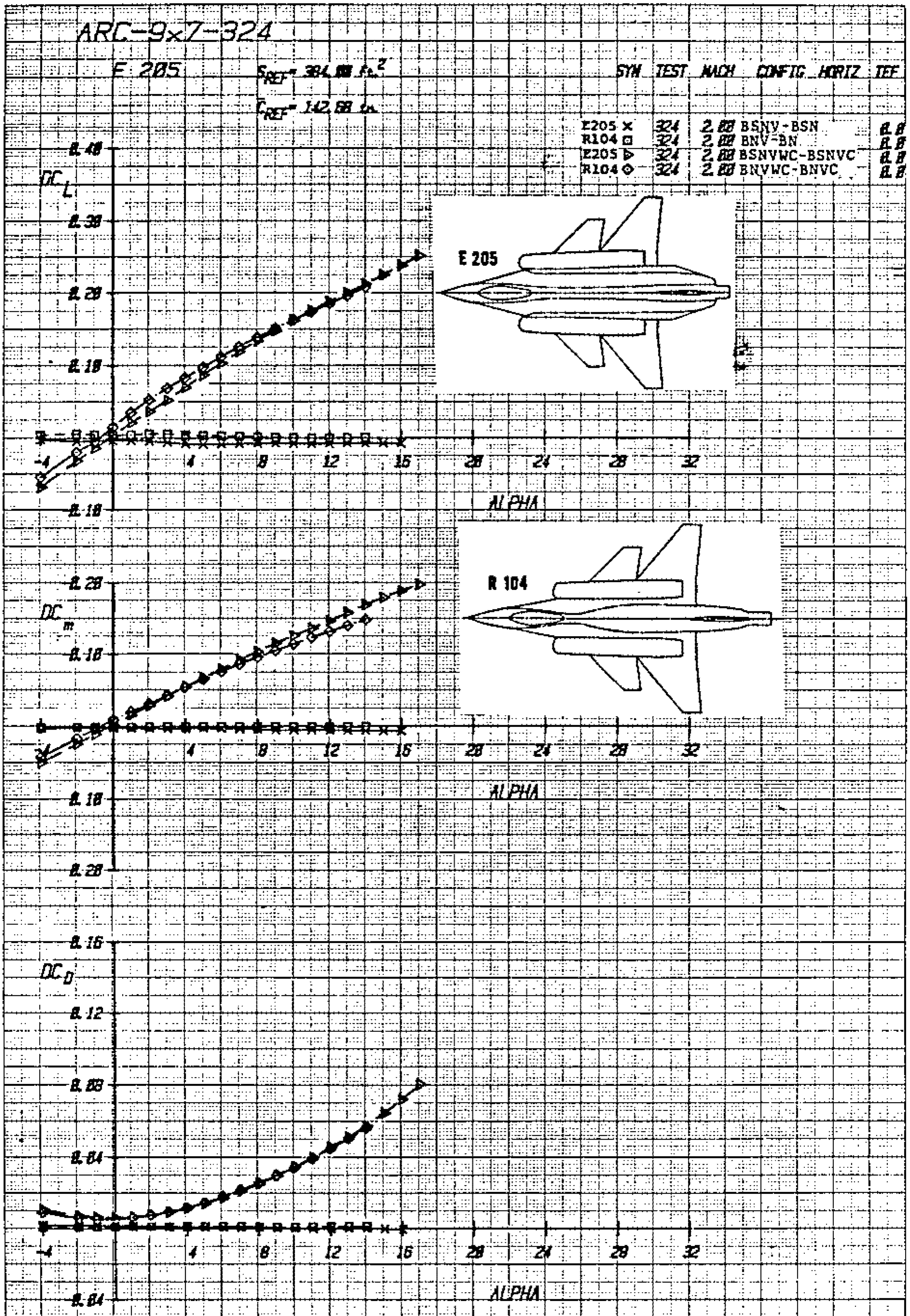

Figure 2-9 Comparison of E205 and R104 Lift, Drag, and Pitching Moment Increments for Vertical Tail, Wing, and Canard, M = 2.0

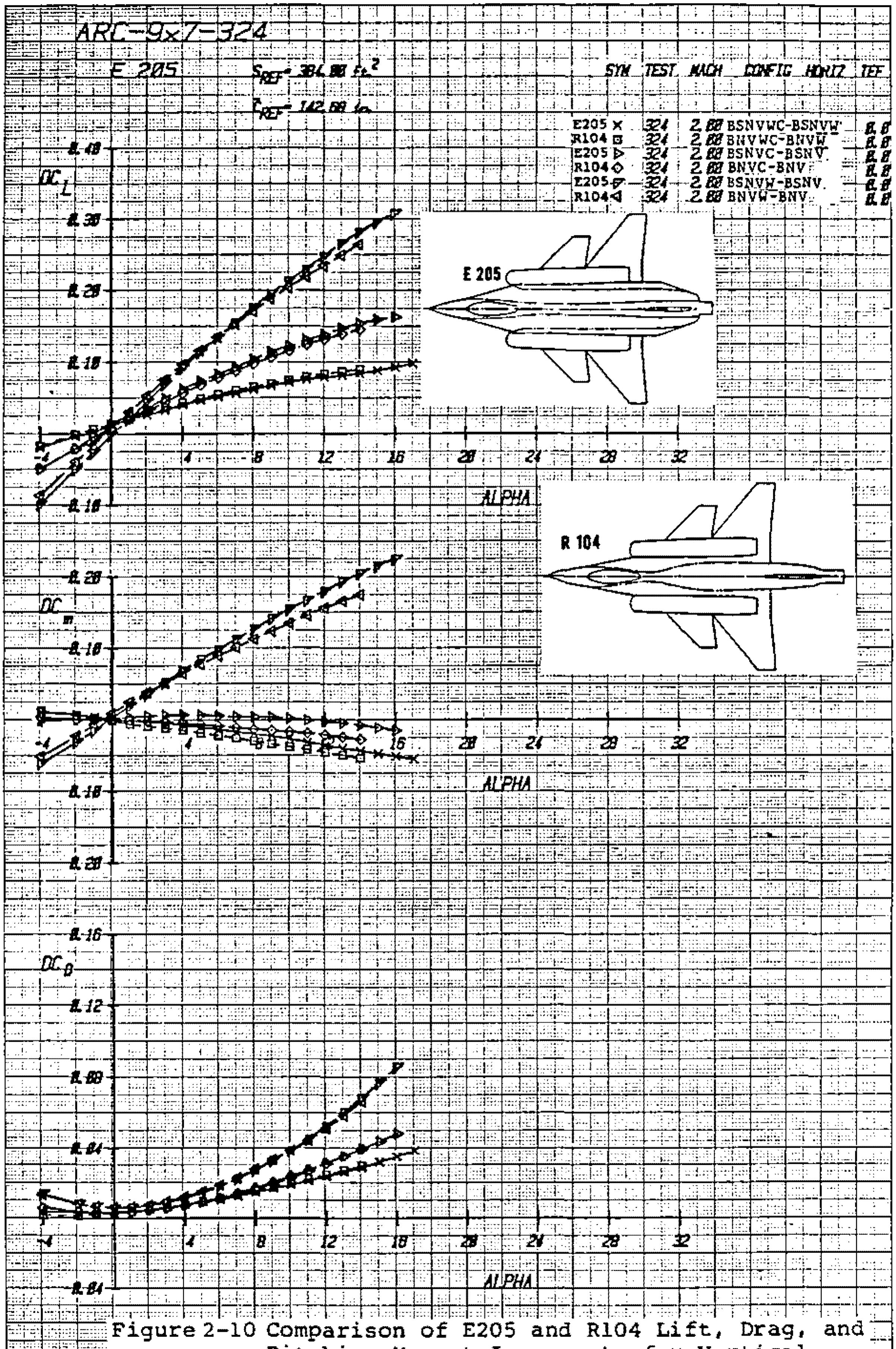

Figure 2-10 Comparison of E205 and R104 Lift, Drag, and Pitching Moment Increments for Vertical Tail, Wing, and Canard, (continued), M = 2.0

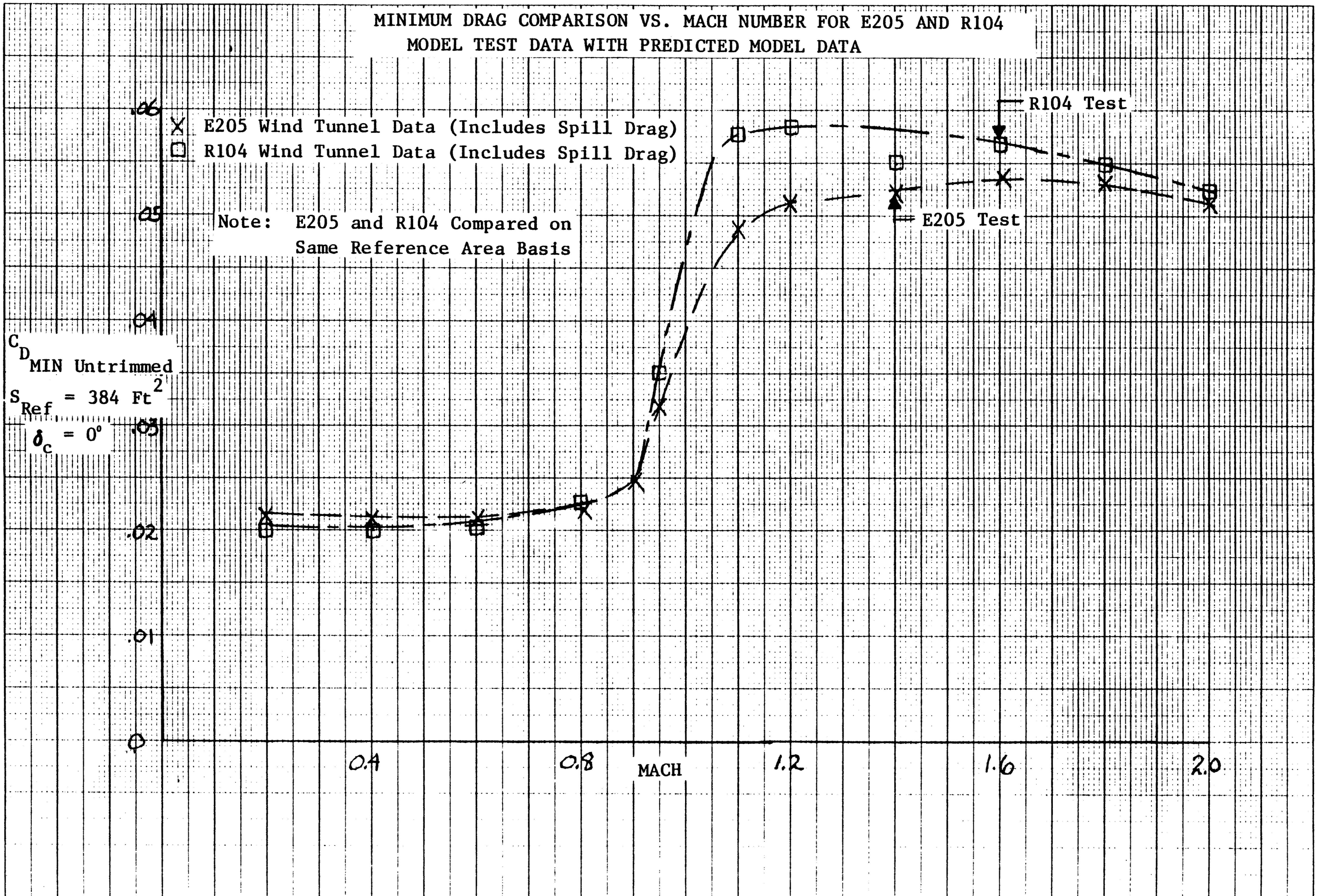

Figure 2-11 Comparison of Minimum Drag Vs. Mach Number for E205 and R104 Wind Tunnel Models

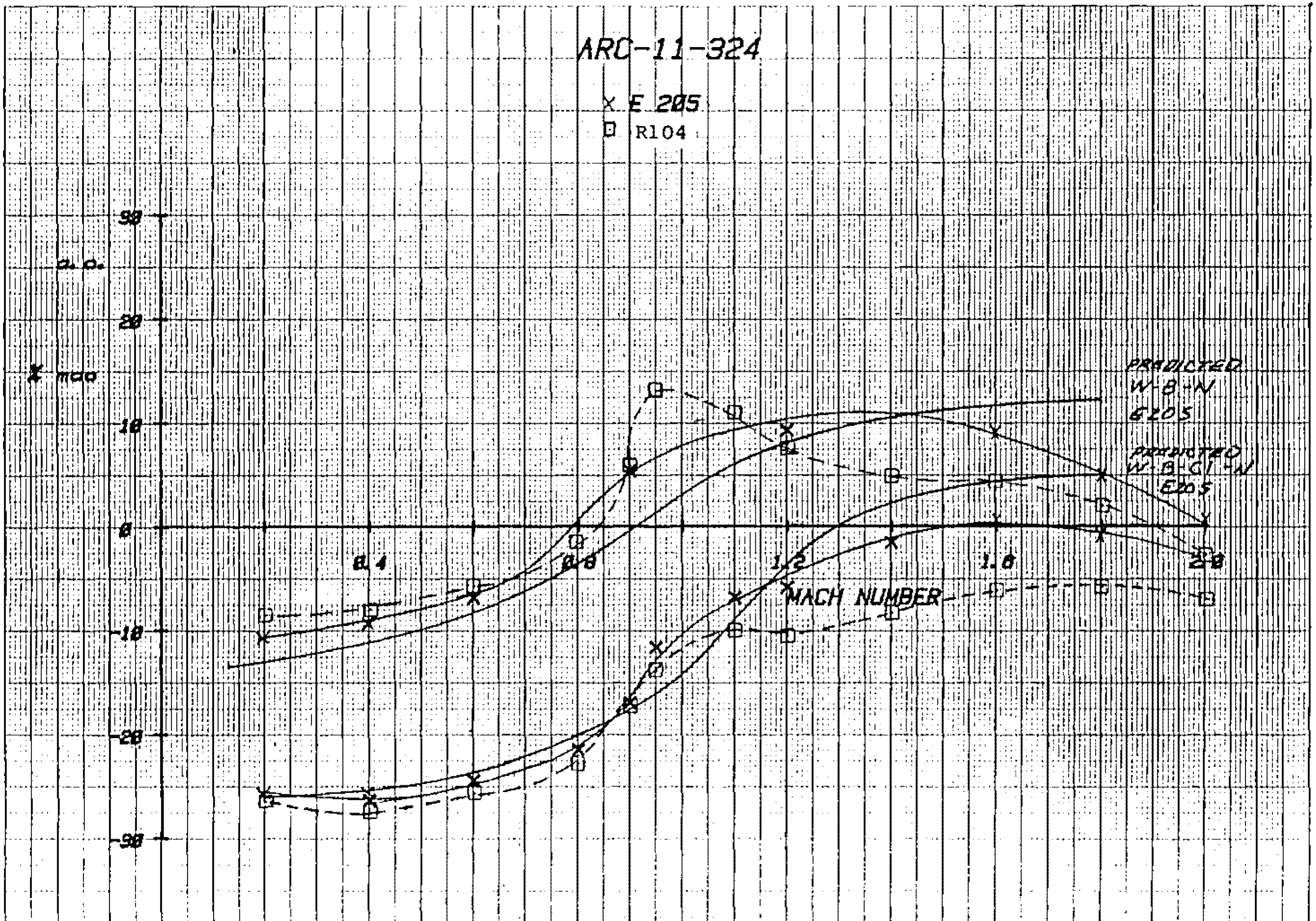

Figure 2-12 Comparison of Aerodynamic Center for E205 and R104

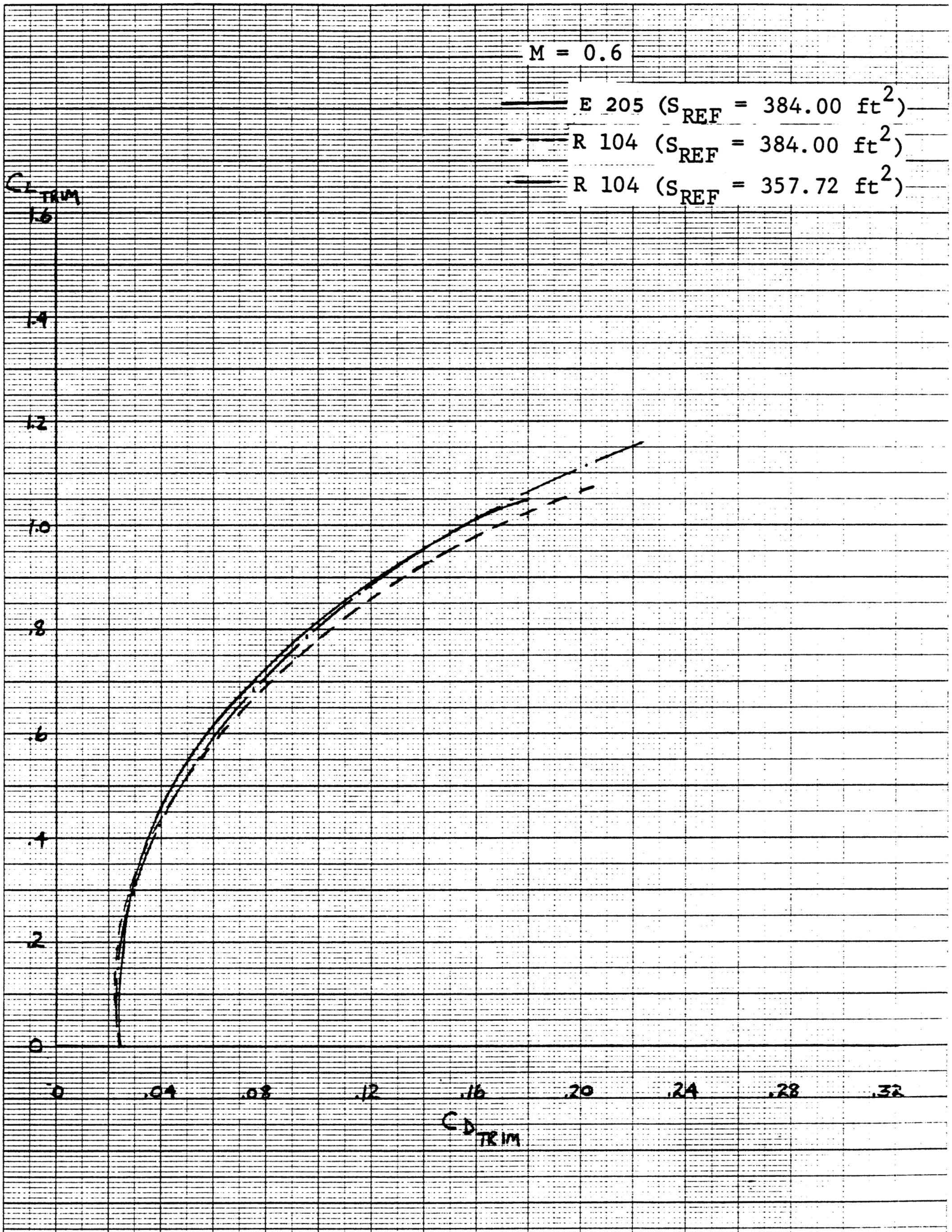

Figure 2-13 Comparison of Trimmed Envelope Polars (Unpowered) for the R104 and E205 Configurations, Mach = .6

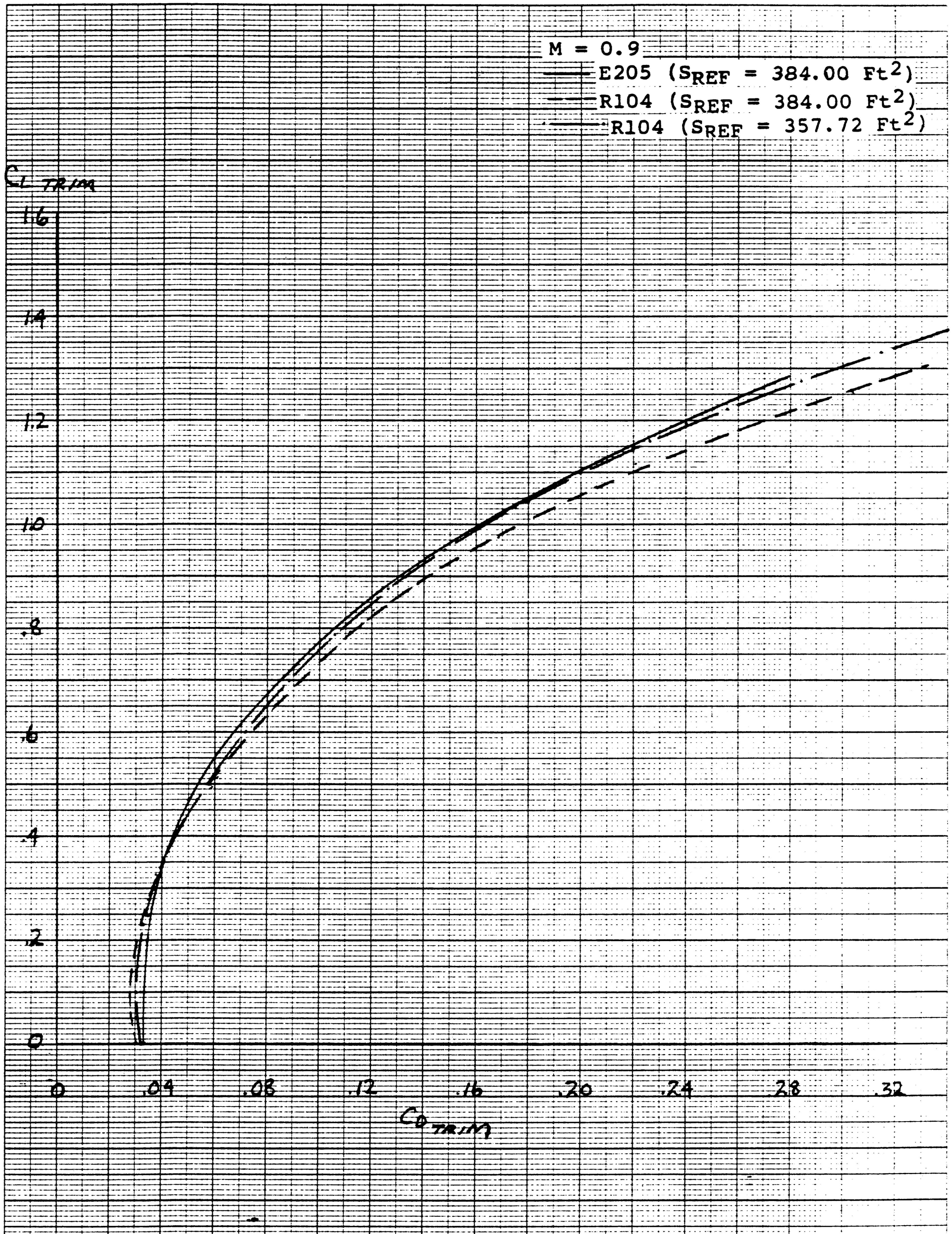

Figure 2-14 Comparison of Trimmed Envelope Polars (Unpowered) for the R104 and E205 Configurations, Mach = .9

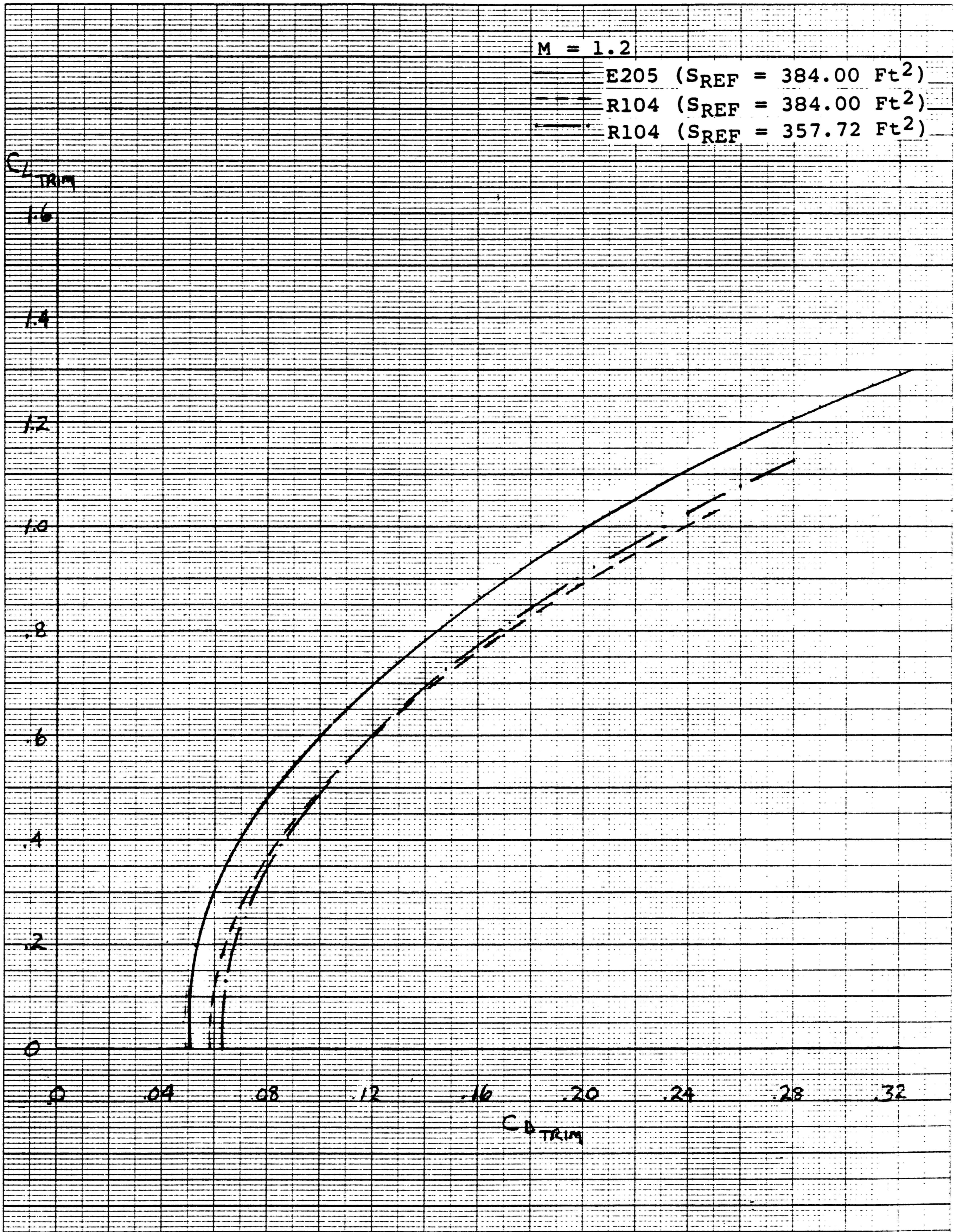

Figure 2-15 Comparison of Trimmed Envelope Polars (Unpowered) for the R104 and E205 Configurations, Mach = 1.2

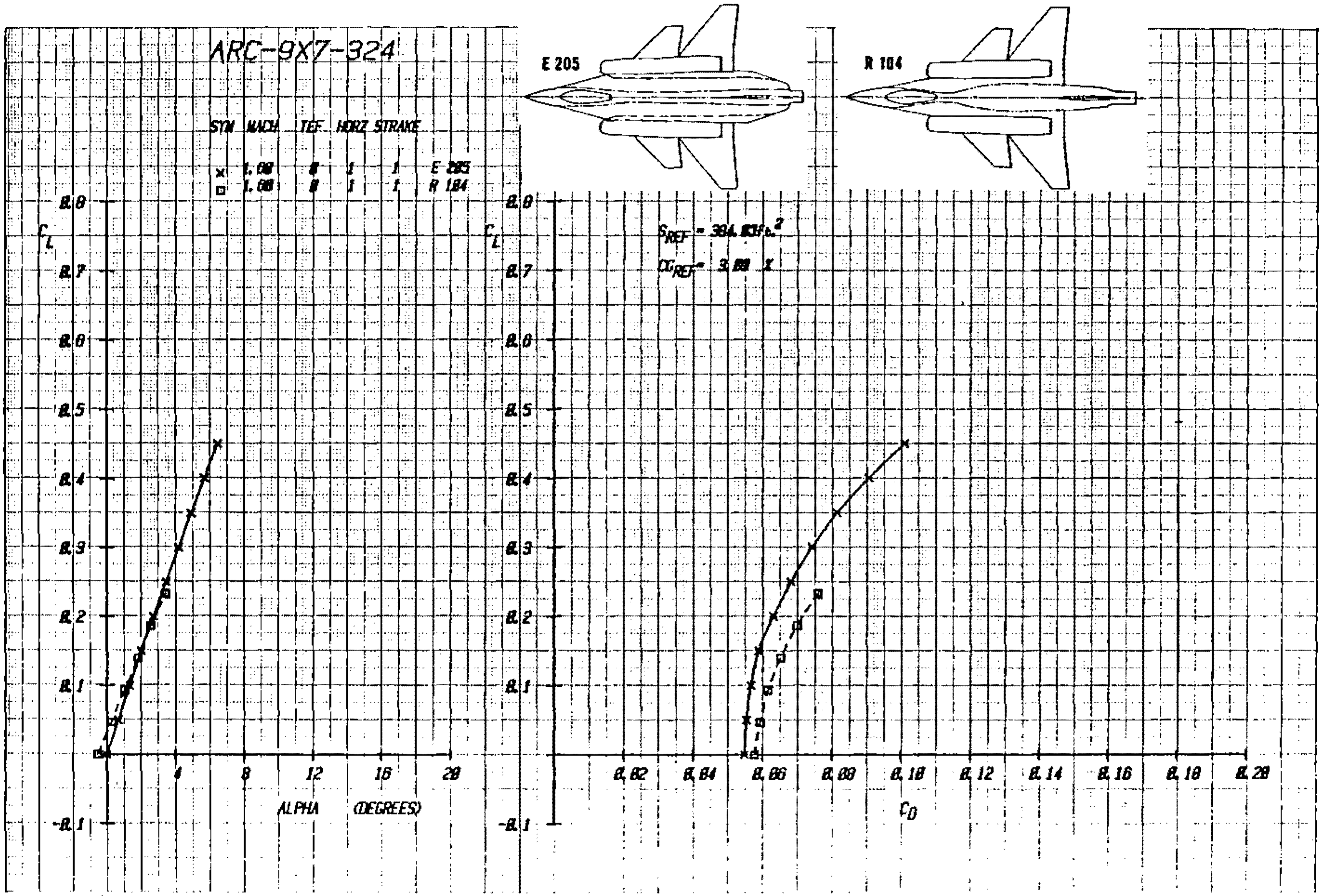

Figure 2-16 Trimmed Lift and Drag Comparison for E205 and R104 Baseline Configurations with Varying Canard Deflections and Wing Trailing-Edge Flap Undeflected, Mach = 1.6

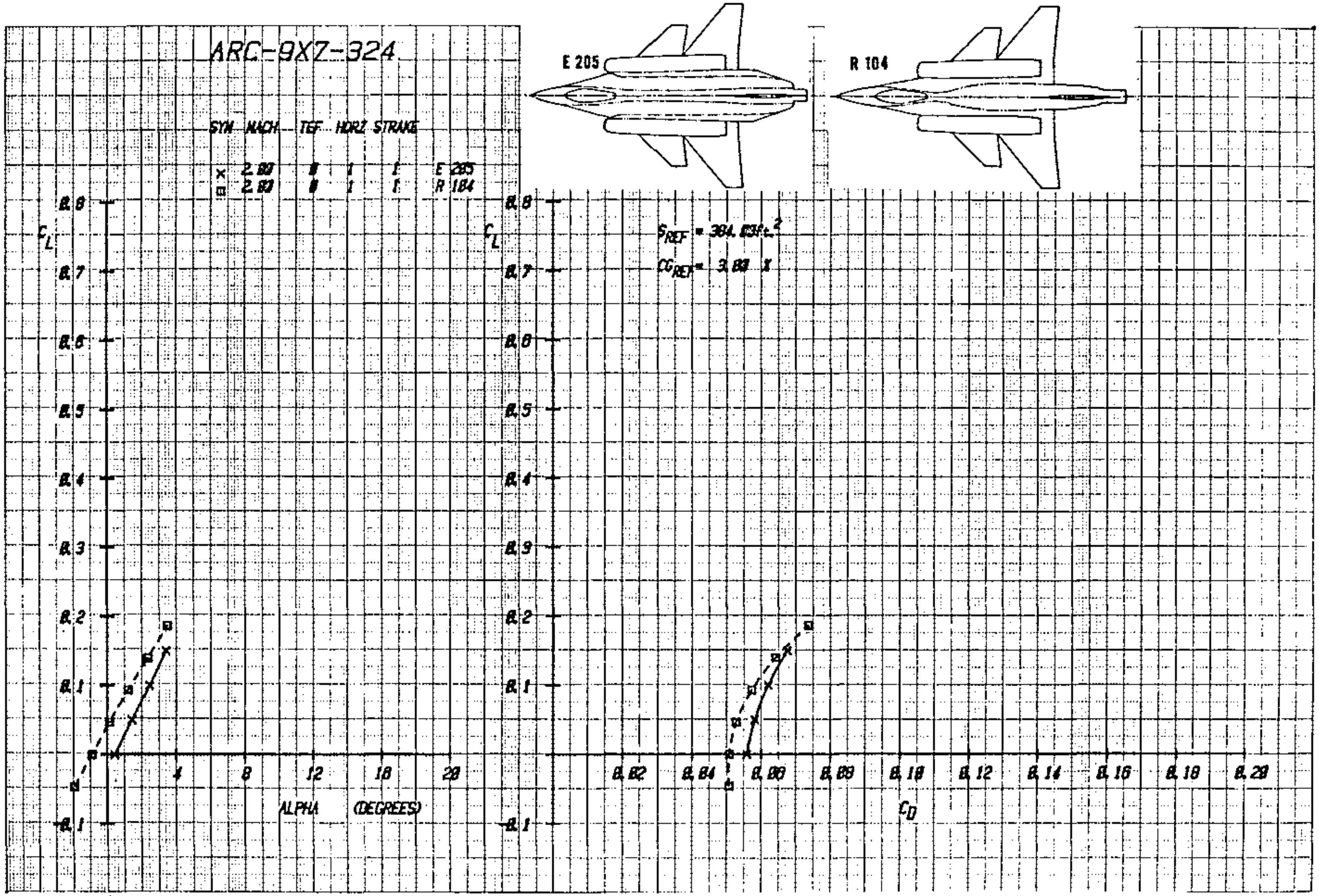

Figure 2-17 Trimmed Lift and Drag Comparison for E205 and R104 Baseline Configurations with Varying Canard Deflections and Wing Trailing-Edge Flap Undeflected, Mach = 2.0

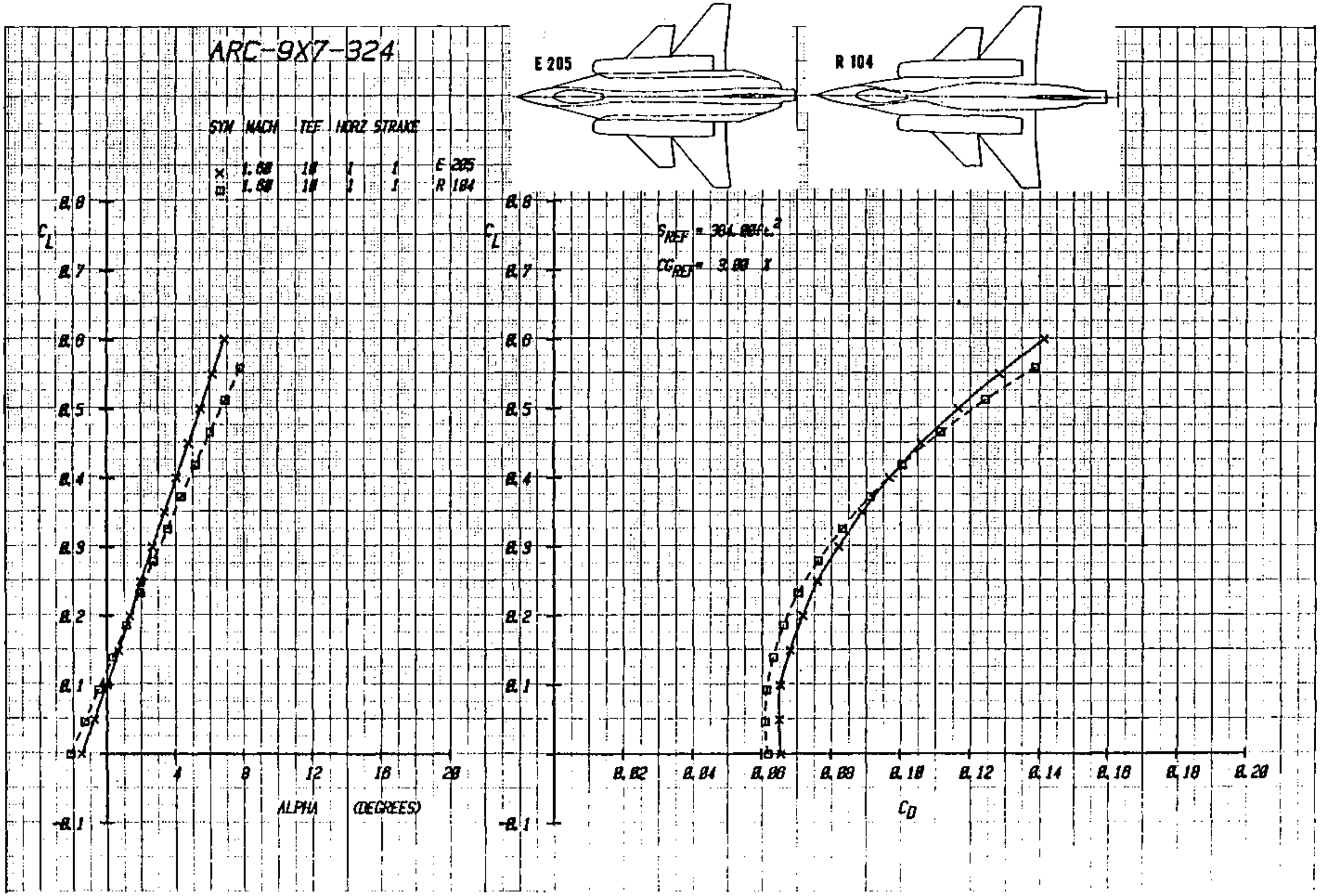

Figure 2-18 Trimmed Lift and Drag Comparison for E205 and R104 Baseline Configurations with Varying Canard Deflections and Wing Trailing-Edge Flap Deflected +10°, Mach = 1.6

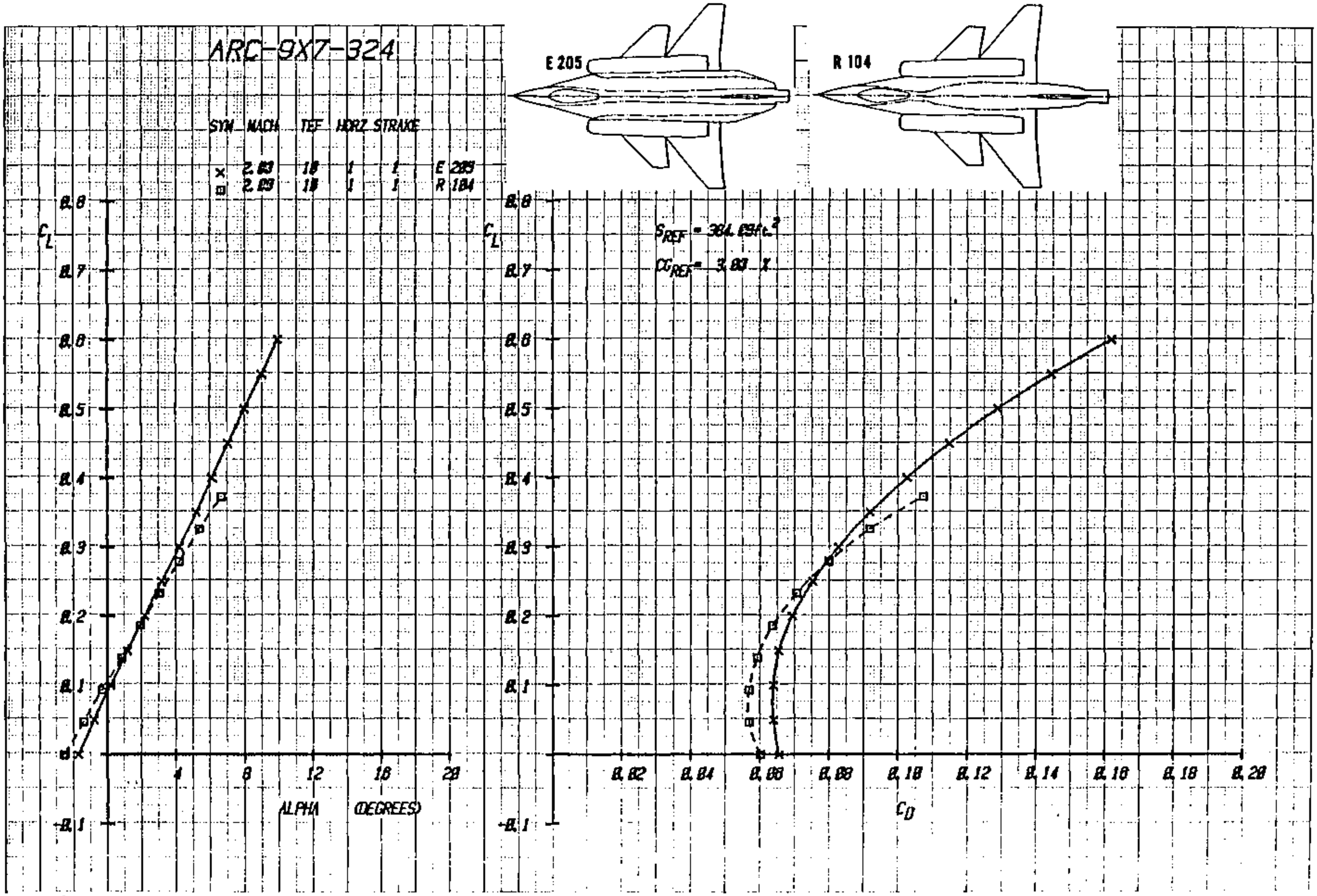

Figure 2-19 Trimmed Lift and Drag Comparison for E205 and R104 Baseline Configurations with Varying Canard Deflections and Wing Trailing-Edge Flap Deflected +10°, Mach = 2.0

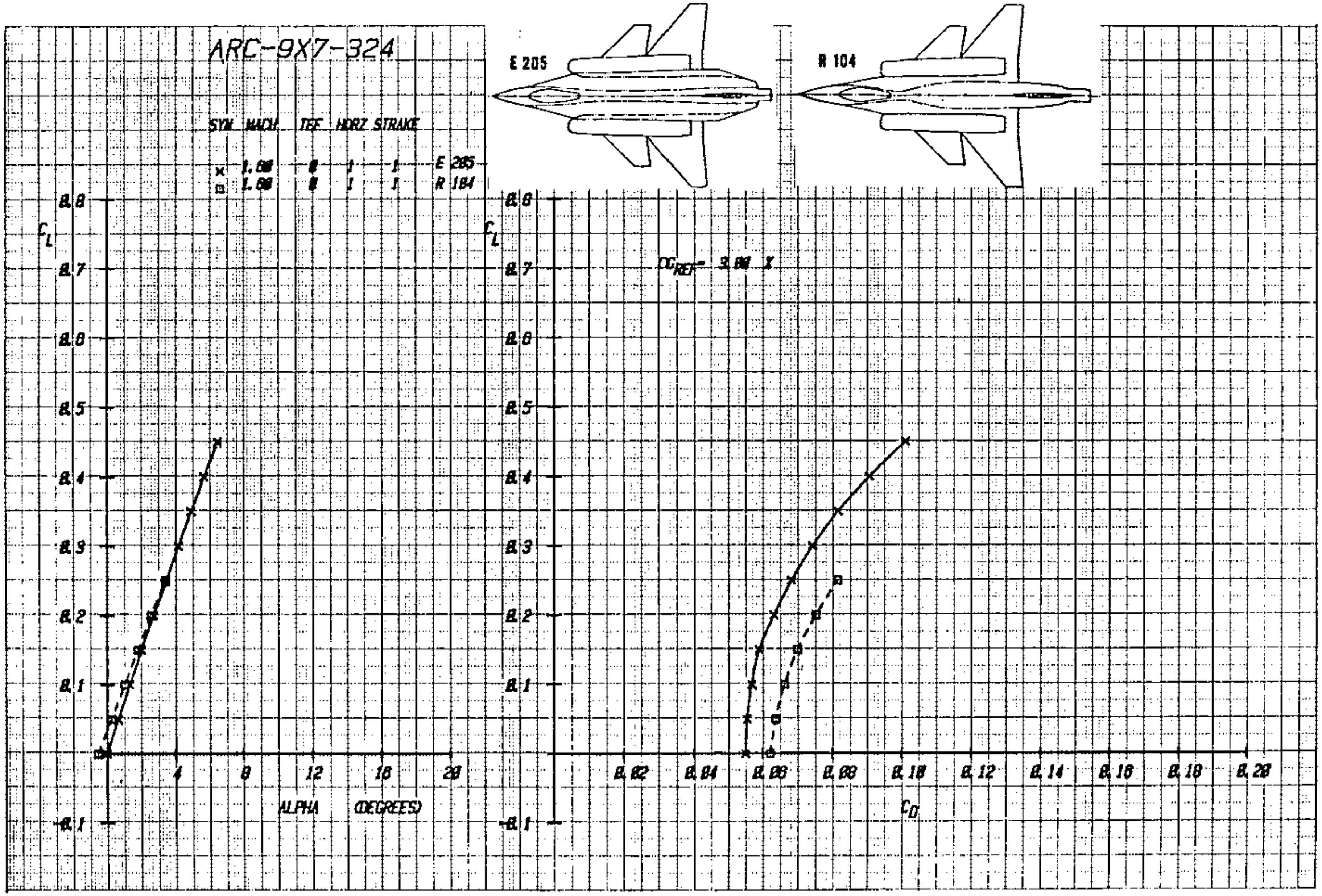

Figure 2-20 Comparison of Canard-Trimmed Lift Curves and Drag Polars for E205 and R104, $\delta_F = 0°$, ($S_{REF} = 384\ ft^2$), $M = 1.6$

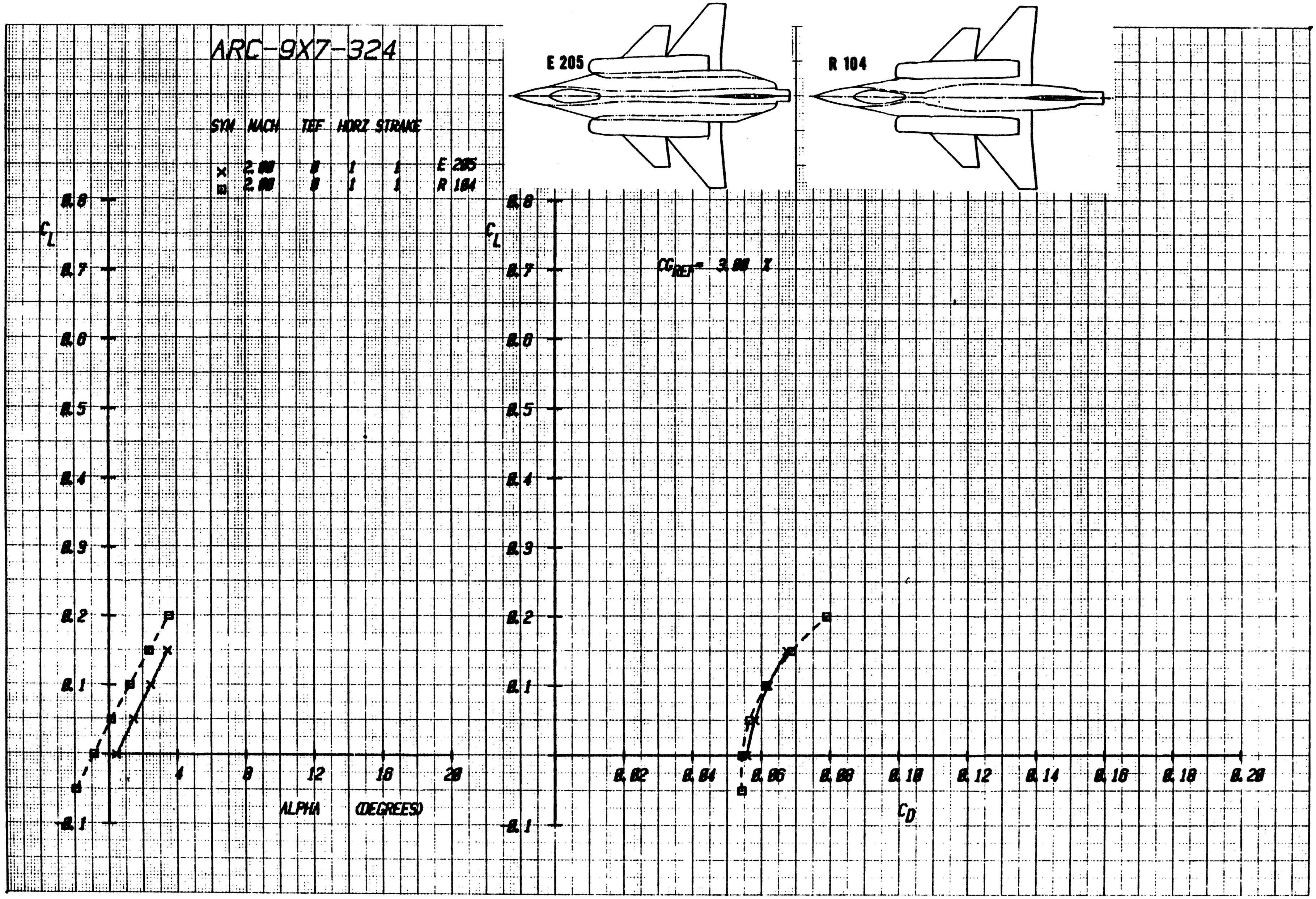

Figure 2-21 Comparison of Canard-Trimmed Lift Curves and Drag Polars for E205 and R104, $\delta_F = 0°$, ($S_{REF} = 384$ ft^2), M = 2.0

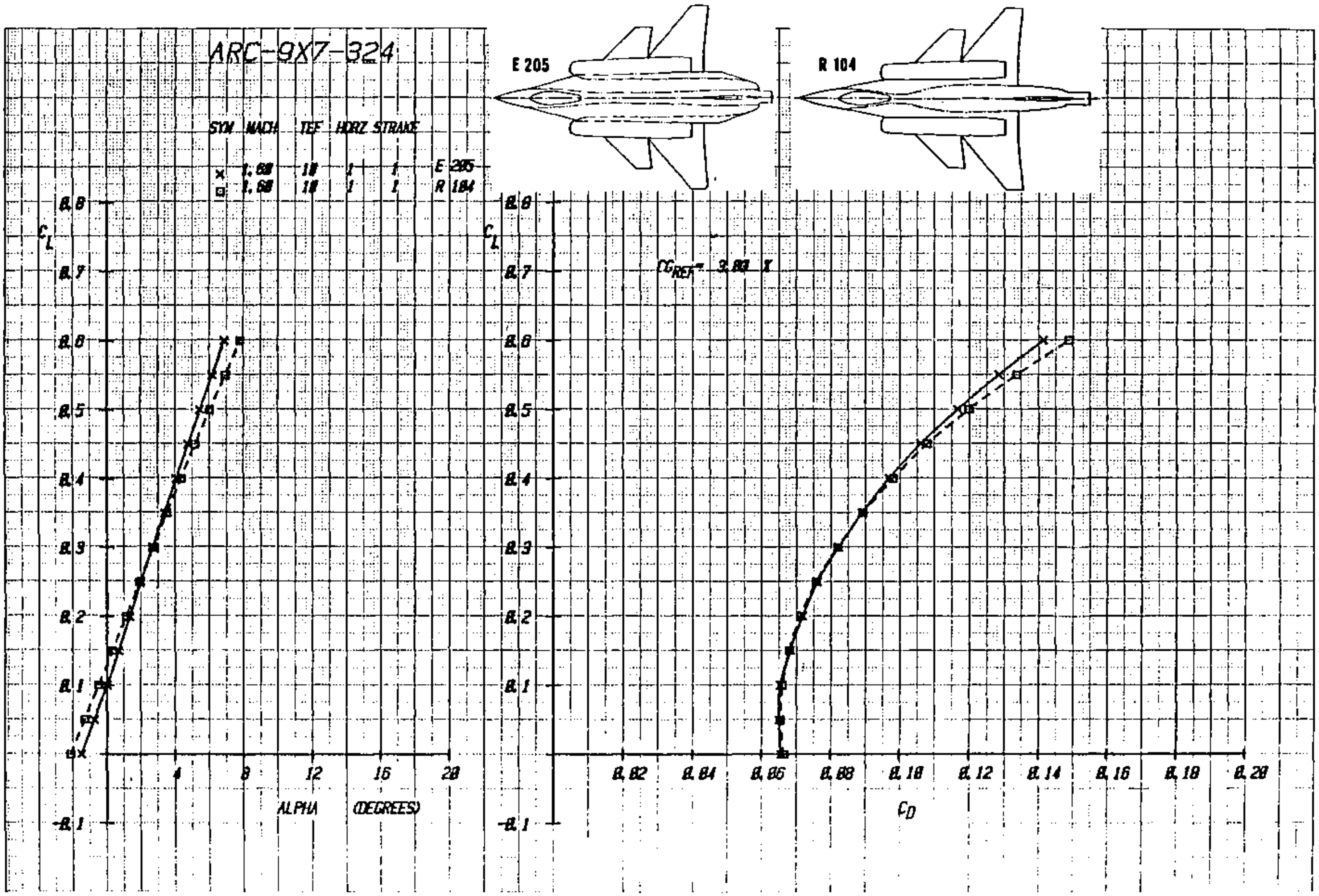

Figure 2-22 Comparison of Canard-Trimmed Lift Curves and Drag Polars for E205 and R104, $\delta_F = 10°$, ($S_{REF} = 384$ ft^2), M = 1.6

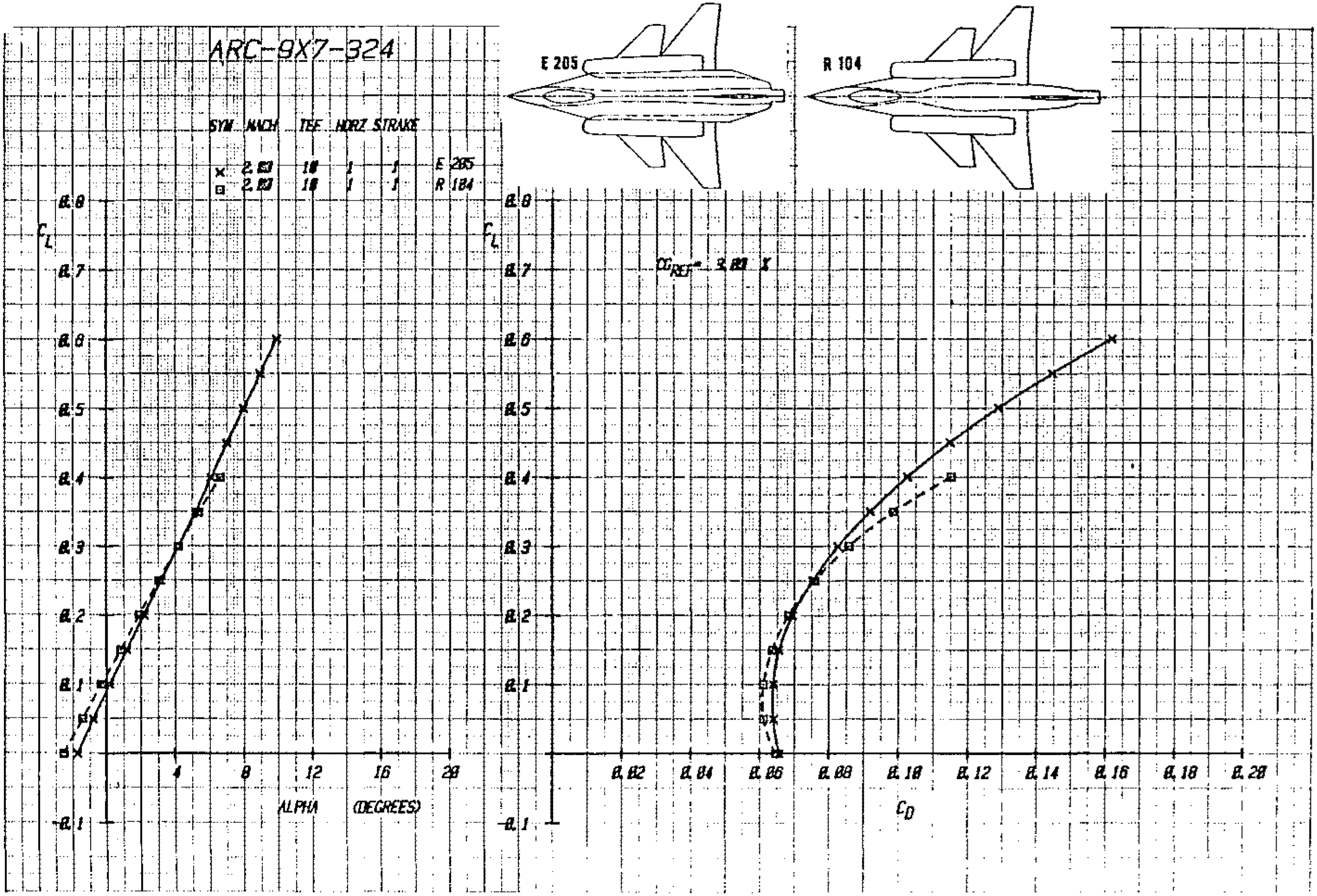

Figure 2-23 Comparison of Canard-Trimmed Lift Curves and Drag Polars for E205 and R104, $\delta_F = 10°$, ($S_{REF} = 384\ ft^2$), M = 2.0

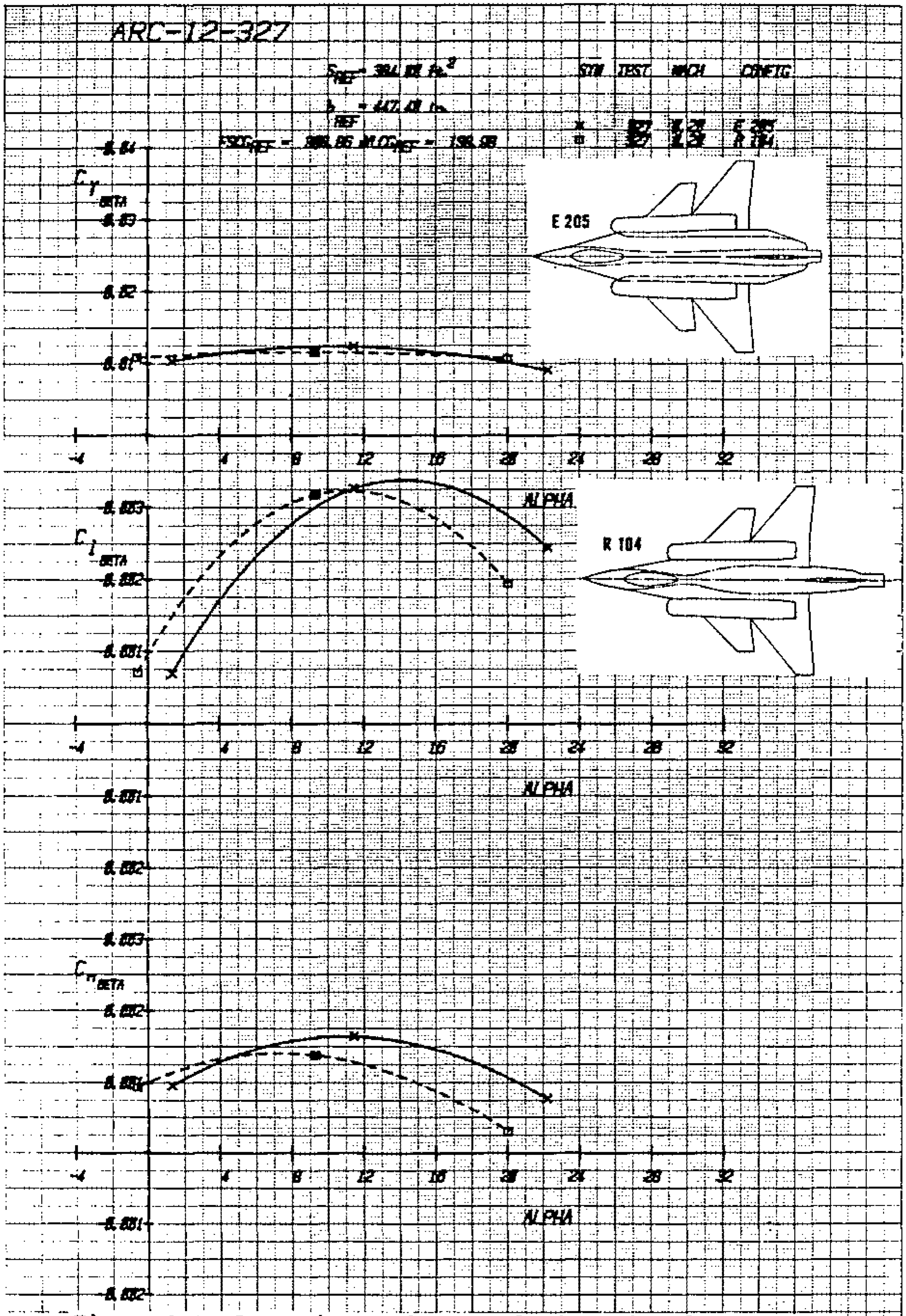

Figure 2-24 Comparison of Lateral-Directional Characteristics for E205 and R104 Configurations, Mach = .2.

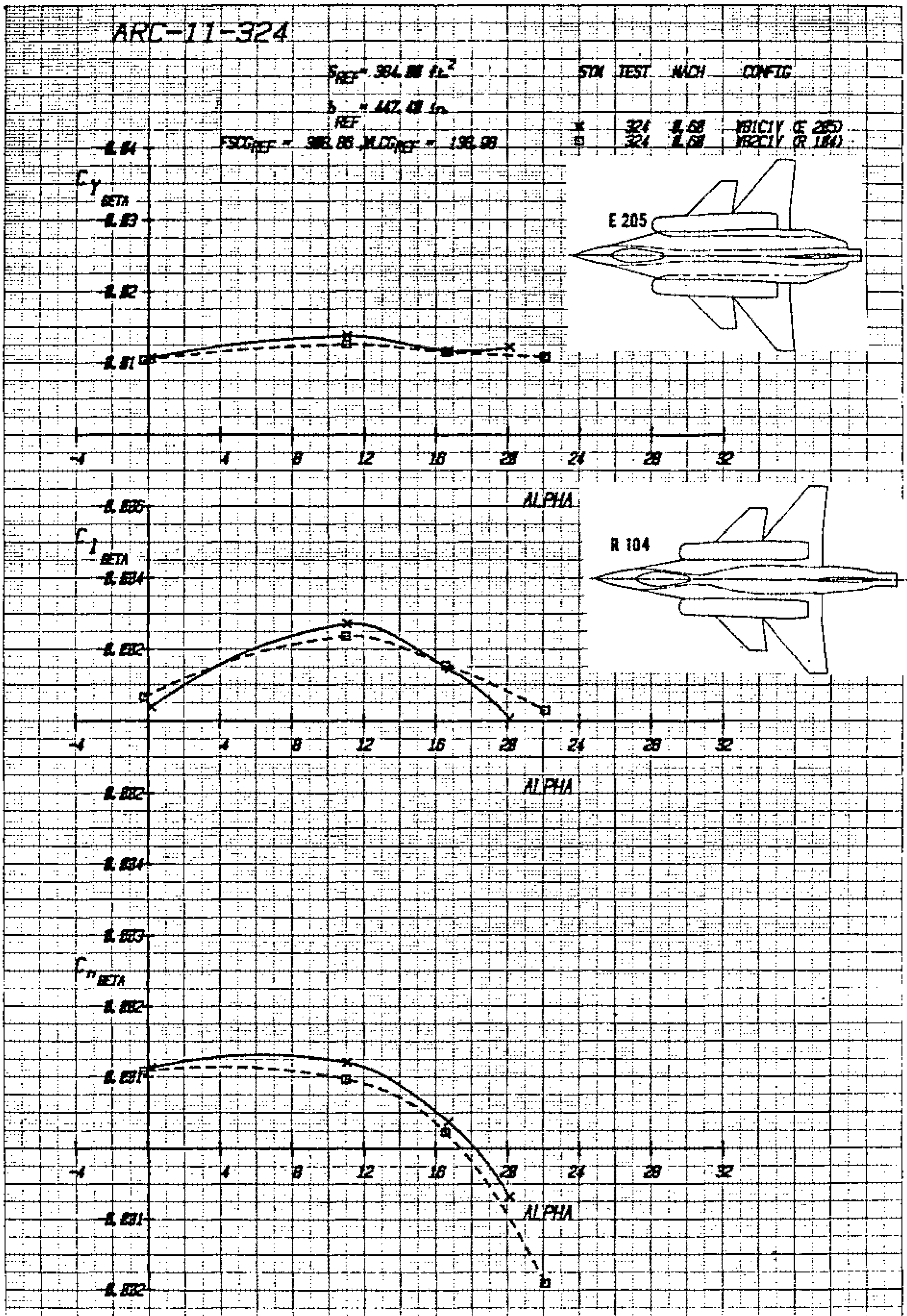

Figure 2-25 Comparison of Lateral-Directional Characteristics for E 205 and R 104 Configurations, Mach = .6

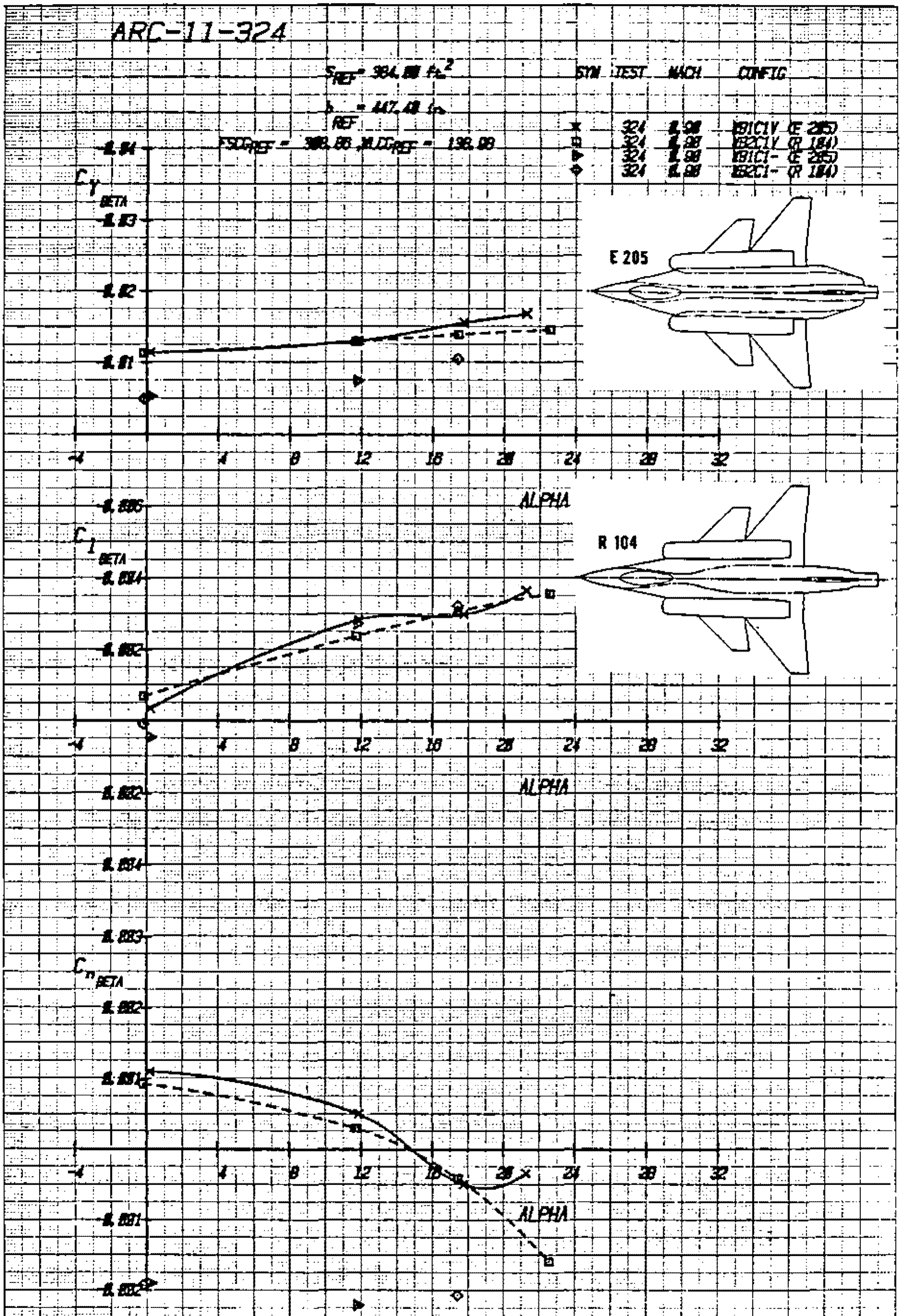

Figure 2-26 Comparison of Lateral-Directional Characteristics for E 205 and R 104 Configurations, Mach = .9

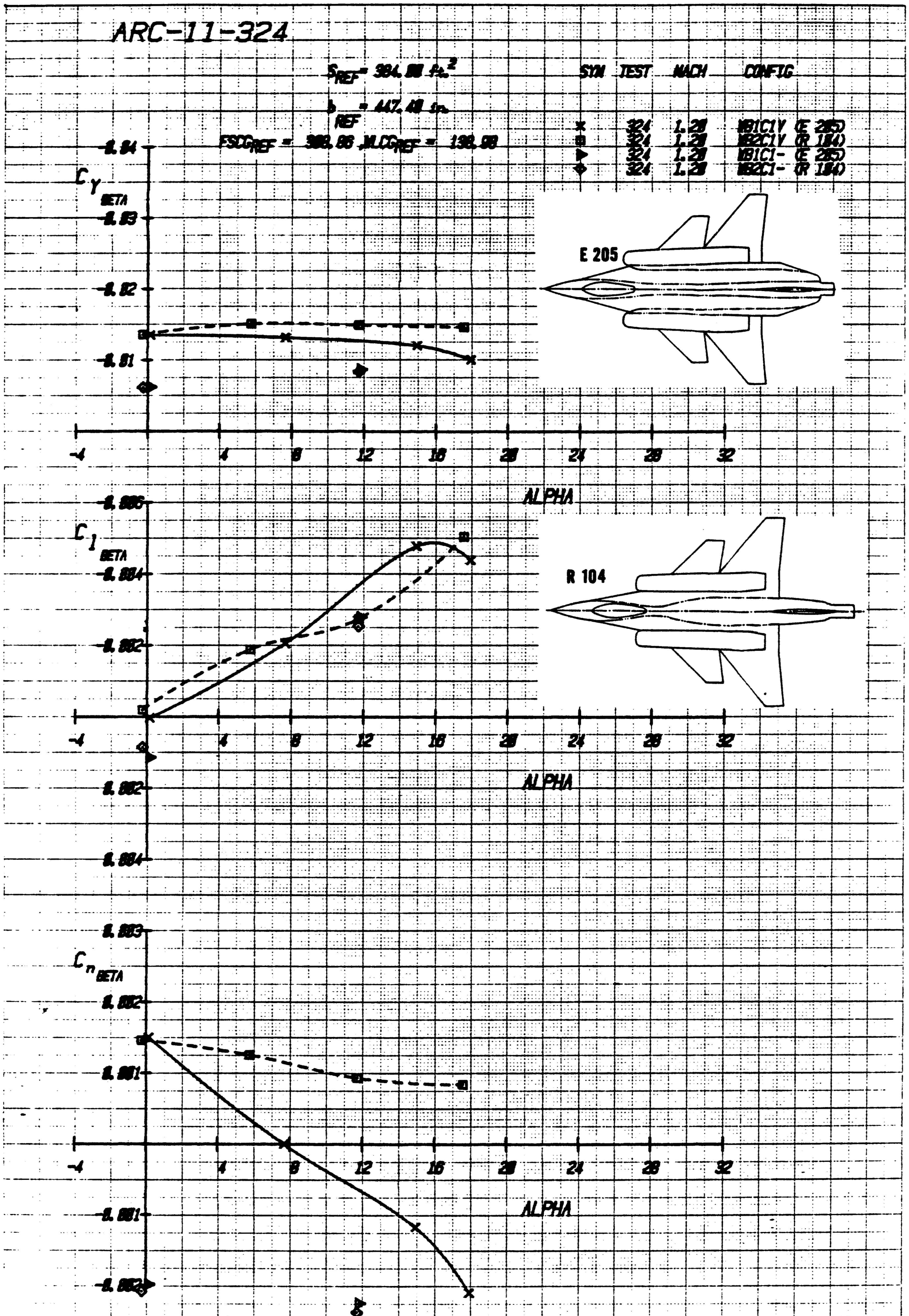

Figure 2-27 Comparison of Lateral-Directional Characteristics for E 205 and R 104 Configurations, Mach = 1.2

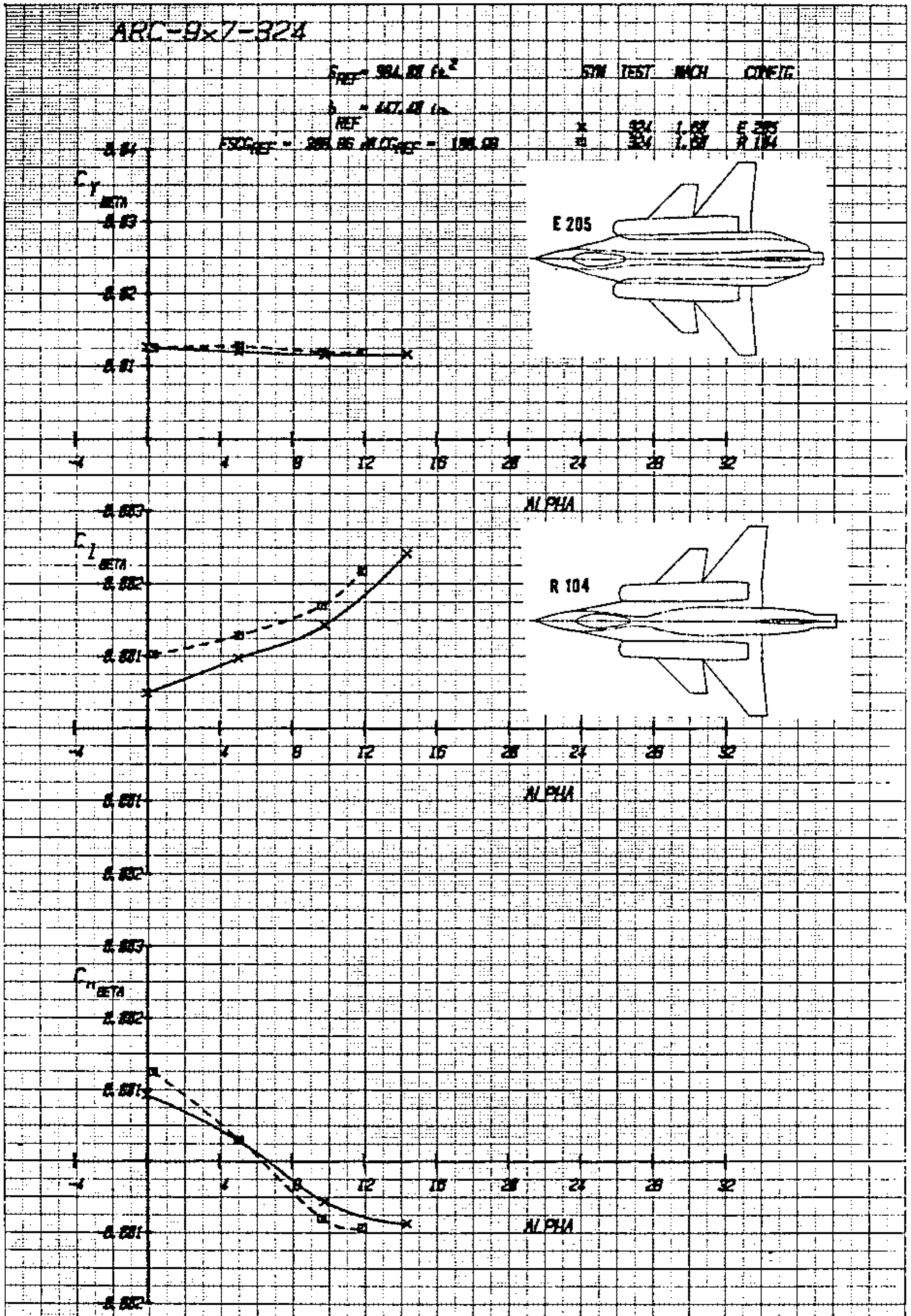

Figure 2-28 Comparison of Lateral-Directional Characteristics for E205 and R104 Configurations, Mach = 1.6.

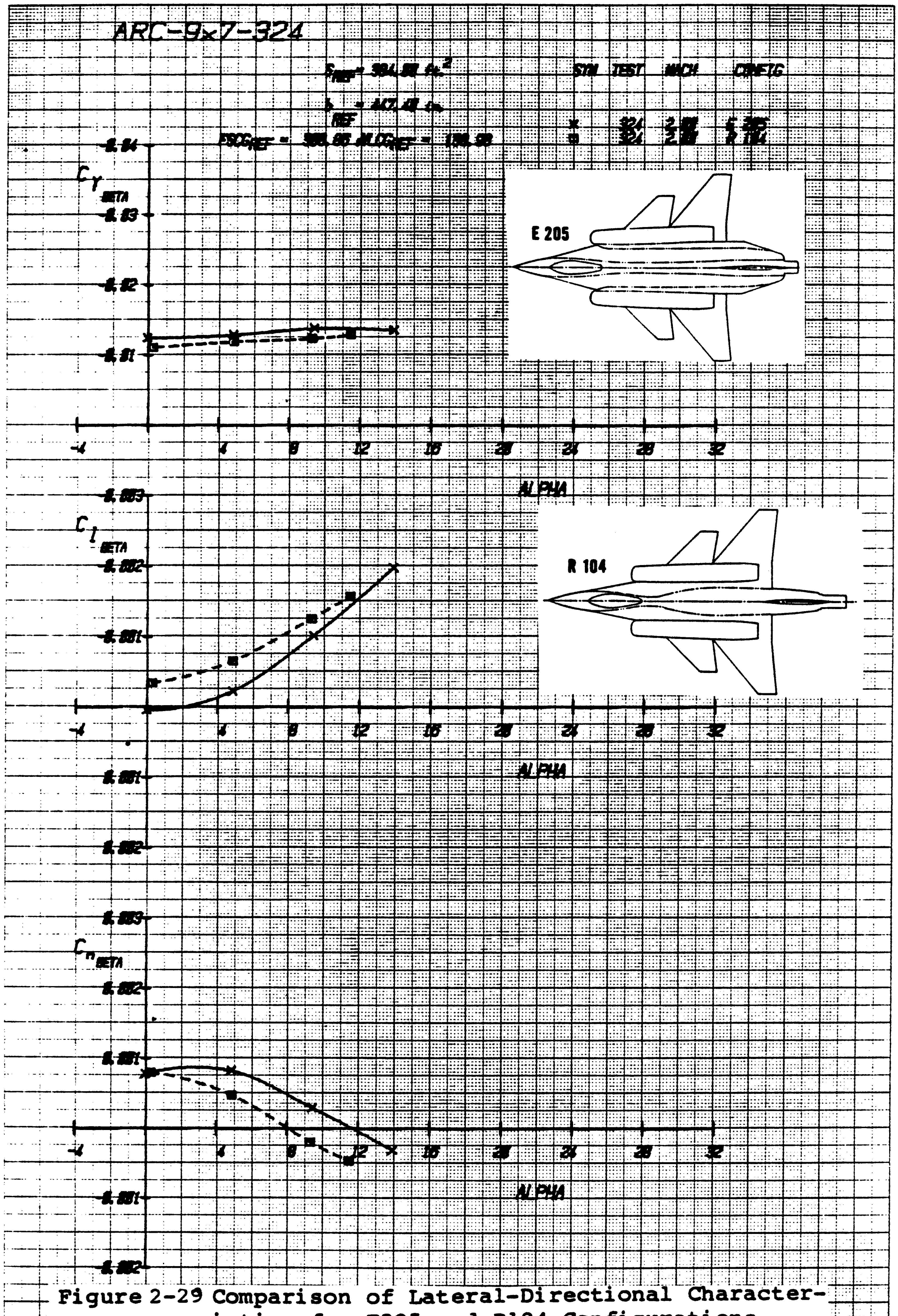

Figure 2-29 Comparison of Lateral-Directional Characteristics for E205 and R104 Configurations, Mach = 2.0.